β, β'-π-EXTENDED PORPHYRINS: EXPLORATION OF FUNCTIONALIZATION AND AROMATIC CHARACTER

Courtney Taylor Cooper

Dissertation Prepared for the Degree of

DOCTOR OF PHILOSOPHY

UNIVERSITY OF NORTH TEXAS

July 2023

APPROVED:

Hong Wang, Major Professor
Molly Atkinson, Committee Member
Thomas R. Cundari, Committee Member
Francis D'Souza, Committee Member
LeGrande Slaughter, Chair of the Department of Chemistry
John Quintanilla, Dean of the College of Science
Victor Prybutok, Dean of the Toulouse Graduate School

Cooper, Courtney Taylor. *β, β'-π-Extended Porphyrins: Exploration of Functionalization and Aromatic Character*. Doctor of Philosophy (Chemistry), July 2023, 305 pp., 47 tables, 114 figures, 21 schemes, numbered chapter references.

Seventeen new dithiophenyl- and napthodithiophenyl- fused porphyrins were synthesized; from these an additional 7 porphyrin oligomers were also synthesized. Additionally freebase 2,7-dimethoxytriphenylene fused porphyrin was also synthesized from a freebase precursor. Aromatic indices NICS and AICD were used to evaluate these new molecules.

ACKNOWLEDGEMENTS

I would like to first thank Dr. Hong Wang for her guidance and encouragement during my time as her student. She helped me grow personally and professionally. I would also like to express my thanks to my dissertation defense committee members Dr. Hong Wang, Dr. Molly Atkinson, Dr. Thomas Cundari, Dr. Francis D'Souza, and Dr. Ronald Smaldone. I appreciate the help that my collaborators Dr. Vladmir Nesterov, Dr. Hongjun Pan, Dr. Sergei Vinogradov, Dr. Francis D'Souza, Ros Paul and Ajyal Alsaleh have provided me with my research projects. I would also like to thank the University of North Texas, the Department of Energy and the National Science Foundation for funding the research discussed in this dissertation.

Achieving my Ph.D. would not have been possible without the support of my friends and colleagues, especially Stacey, Kaitlyn, Austen, Jacob, Catherine, Autumn, Jacqkis, Ting, Jose, Spenser, and Saad. They helped support my emotional and mental health through several difficult times during my Ph.D. and I greatly appreciate them. I would also like to thank Heather Vidaurri, Autumn Arvidson, Bonnie Davidson, and Joy Curtis for all their help.

My deepest gratitude goes to my husband, John Cooper, who has supported me throughout my graduate studies and has always been my foundation. I would also like to mention my late father, Perry Stewart, who was unable to see me complete my degree; he always encouraged me to push myself and I attribute the completion of this dissertation to him. I also greatly appreciate the rest of my family who helped support me during some rough times.

TABLE OF CONTENTS

Page

LIST OF TABLES

Page

LIST OF FIGURES

Page

LIST OF SCHEMES

Page

CHAPTER 1

INTRODUCTION

1.1 Porphyrin Introduction

Porphyrins are a group of heterocyclic aromatic macrocycle made up of four pyrrolic units linked together by methine bridges. The word “porphyrin” had once been a catch-all phrase that described polypyrrole macrocycles such as porphyrins, phthalocyanines, corroles, and porphyrazines. The name porphyrin comes from the Greek word *porphura* which was given due to the vivid red and purple colors of theses macrocycles. This intense color is a result of high molar absorptivity within the electromagnetic spectrum’s visible region. Commonly known examples of porphyrin derivatives found in nature include chlorophyll, protoporphyrin IX, vitamin B_{12}, and hemoglobin. Porphyrins and their derivatives are known to have a diverse set of functions in nature, such as oxygen/energy transport and storage, and metabolic functions.

The versatility demonstrated by porphyrins has attracted researchers to develop synthetic methods to synthesize and functionalize porphyrins within the last century. Functionalized porphyrins have a wide range of applications in fields such as: chemistry, material science, medicine, and geology. [1] Examples of practical applications of porphyrins include its ability to function as a photocatalyst for organic transformations, a dye for dye-sensitized solar cell, or photosensitizer in photodynamic therapy. As a result of porphyrin versatility, the development and study of new porphyrins continues to be an area of active research.

The work of this dissertation includes the synthesis and characterization of new dithiophenyl-fused porphyrin derivatives. In this introduction we provide a general overview of

the porphyrin structure, nomenclature, electronic properties, and synthetic methodology relevant to the work in this dissertation.

1.1.1 Structure and Naming Conventions

Porphine (Figure 1.1) is the name of the unsubstituted, and therefore simplest, porphyrin known although rarely—if ever—encountered. Porphyrins have twelve positions that can be substituted, so developing a system of naming was important. Hans Fischer was the first to develop a systematic naming system for porphyrins. [2] In Fischer's numbering system (Figure 1.2) three types of carbons were specified: alpha, beta, and *meso*-carbons. α-Carbons (blue) are attached to one of the four nitrogen atoms present, one of the eight β-carbons (green) in the pyrrole ring, and to a *meso*-position (pink). Meso-carbons are commonly numbered utilizing Greek lower case letters α–δ.

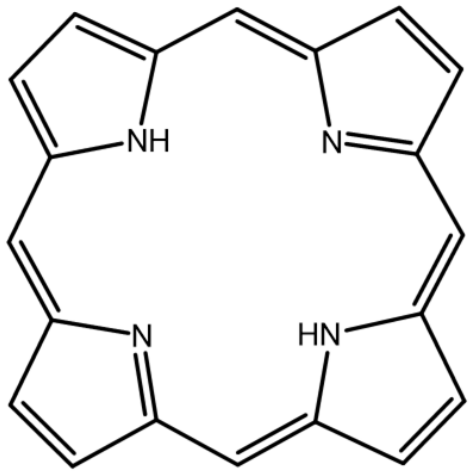

Figure 1.1: Structure of porphine

Fischer's naming convention only works well for simple porphyrins like porphine. To aptly name substituted porphyrins, many porphyrin chemists utilize the IUPAC nomenclature system [3] from 1979. In the IUPAC nomenclature labels the carbon atoms from 1-20 starting

with an α-carbon continuing to a β-carbon until all carbons are labelled. Nitrogen atoms are then labelled as 21-24; the order of these nitrogen atoms depend on which α-carbon is listed as C_1. The benefit of utilizing IUPAC nomenclature in porphyrins is that we can consider that 5,10,15, and 20 always be the *meso* positions and all beta positions are 2,3,7,8,12,13,17, and 18 when naming new porphyrin compounds.

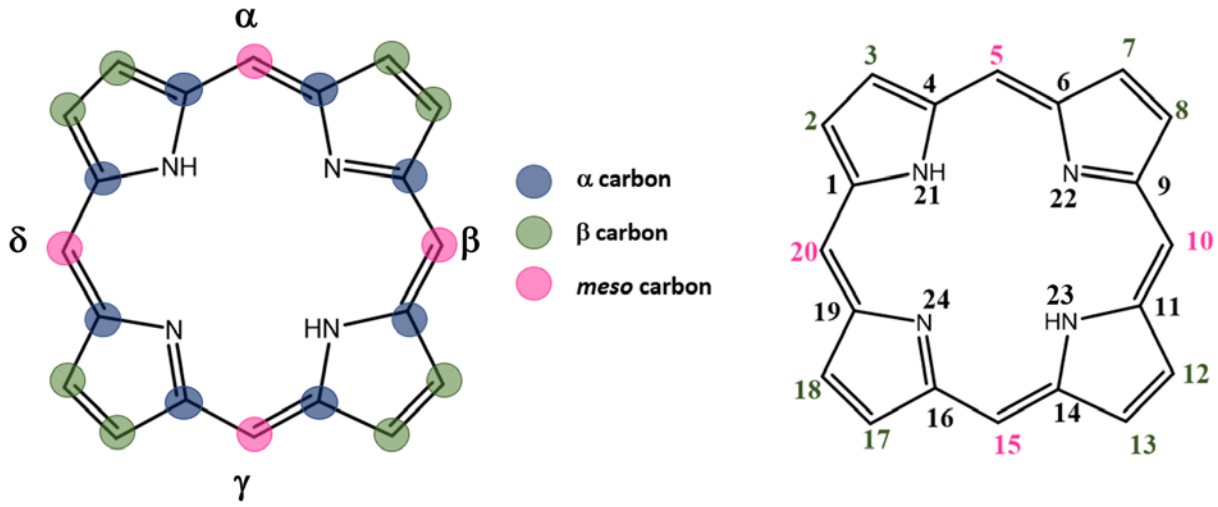

Figure 1.2: Fischer nomenclature (left) and IUPAC nomenclature (right) systems.

IUPAC nomenclature for porphyrins can become large and a way to overcome this is combining IUPAC with commonly used names. A frequently encountered case for this would be fused porphyrin systems.

To understand how to label fused porphyrins it is important to start with simple systems first. [4] In the case of fused polycyclic arenes the molecule should be oriented so that the greatest number of rings lie in a horizontal row; numbering begins at the most counterclockwise position that is *not* involved in fusion of the top ring furthers to the right. Numbering continues in a clockwise direction around the exterior. Bridgeheads fusing two rings together are not numbered – these are referred to be a "face" and instead are labelled with the

preceding number followed by a letter, starting with '*a*.' In the case of fused rings with a benzene present, the prefix *benzo*- is used. Trivial names of compounds also exist and tend to be used as parent structures; examples of common names included in this dissertation are triphenylene and naphthalene.

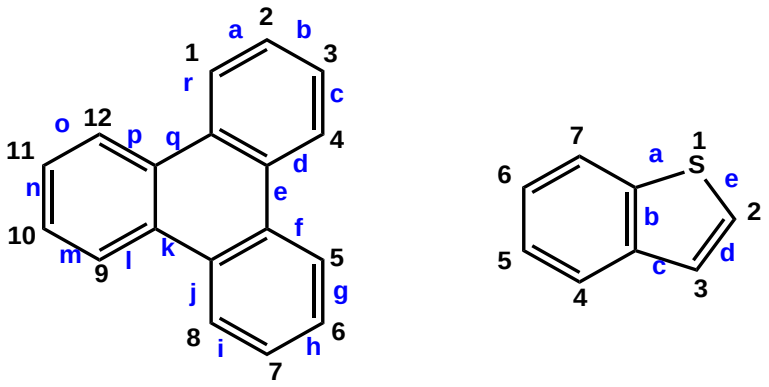

Figure 1.3: Fused ring example of triphenylene and benzo[b]thiophene with appropriate numbering in black and faces labeled in blue.

Heterocycles have a higher priority than arenes and are considered the parent chain. Heteroatoms are assigned priority based on descending order of groups in the periodic table and an ascending order of atomic number within each group. [4]

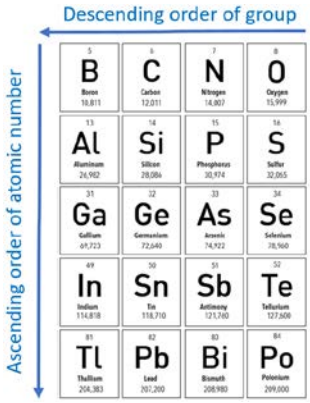

Figure 1.4: Order of priority when naming heterocycles.

Fused porphyrin systems are encountered frequently and will be a main focal point of

this dissertation. Porphyrins with cyclic hydrocarbons utilizing IUPAC rules for fused compounds and have the porphyrin as the parent. Many of the porphyrins have fused rings involving both the *meso*- and *beta*- carbons. The fused ring is numbered as a substituent of the lowest possible position on the porphyrin ring. A simple example of this is when a benzene ring is fused directly to the porphyrin core (Figure 1.5); when numbering the benzene ring the carbons not fused directly to the porphyrin core are labelled as 2^n where n = the number of carbon atoms between the two bridges. However, an easier way to name this porphyrin would be benzo[b]porphyrin in which the benzene ring is fused to the '*b*' face of the porphyrin.

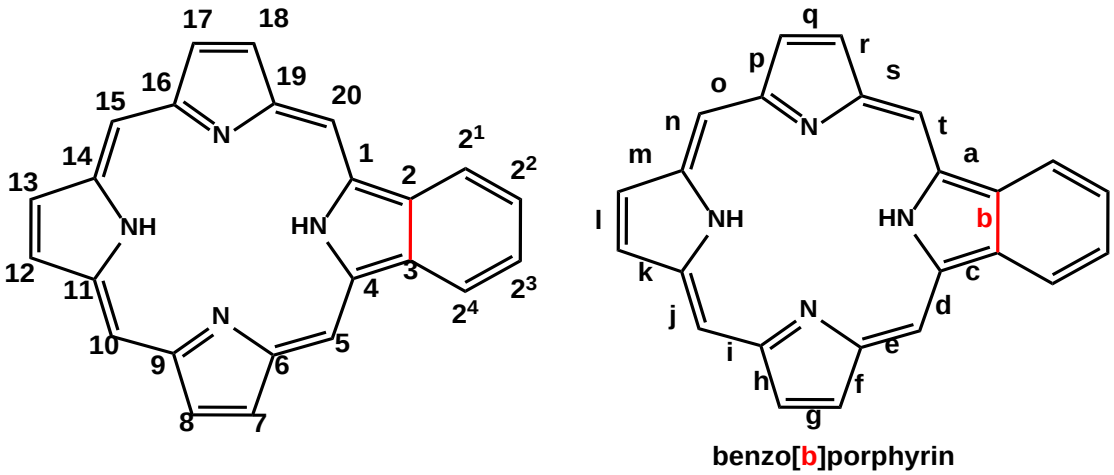

Figure 1.5: Fused porphyrin numbering (left) and faces labeled a-t (right).

1.1.2 Optical and Electronic Properties

Porphyrins are known for their vivid colors and the ability to absorb in the visible and ultraviolet region of the electromagnetic spectrum. Porphyrins have rich optical and electronic properties. Depending on the functionalization of the porphyrin core, porphyrins have exhibited paramagnetism, luminescence, photosensitivity, and even semiconductivity. [5]

Porphyrins often show strong Soret, B, band around 400-500 nm and weaker Q bands

occurring in the 500-700 nm region. While there are four Q bands for free base porphyrins, metalated porphyrins only show two Q bands due to decreased symmetry.

Martin Gouterman's four-orbital model is a well-accepted theoretical model to interpret the electronic transitions of porphyrins in the absorption spectroscopy. Gouterman developed the model based on the extended Hückel calculations. [6] These calculations identified two HOMOs and two LUMOs which are energetically separated from all the other π molecular orbitals. The two HOMOs were found to be nearly degenerate, while the LUMOs were degenerate. Based on these orbitals, the B and Q bands of the UV-Vis were assigned. The Q-bands correspond to the transition from $S_0 \rightarrow S_1$ and the B-band corresponds to the transition from $S_0 \rightarrow S_2$.

Gouterman theoretical model explains three broad classes of porphyrins: normal, hypso, and hyper. Normal porphyrins are described by the four-orbital model and are most frequently seen with freebase or Zn/Mg metalated porphyrins. Hypsoporphyrin spectra have B and Q bands which are blue-shifted; these are typically a result of late transition metals in the porphyrin core such as Co(II), Ni(II), Pd(II), and Cu(II). Hyperporphyrins have B and Q bands which are red shifted; they also show an extra absorption band with a wavelength greater than 320 nm. Gouterman discussed two specific types of hyperporphyrins: p-type and d-type. P-types typically involve lower-valent p block elements that have a lone pair. D-types typically have d electron counts of six or higher. Most of the porphyrins discussed in this dissertation will exhibit normal UV-Vis based on the four-orbital model.

1.2 Synthetic Methodology

Porphyrins have been synthesized through various reported methodologies such as, but

not limited to, the use of: monopyrroles, dipyrromethanes, and a,c-biladienes. [7] However, in this dissertation, only the synthesis of porphyrins via monopyrrole tetramerization will be discussed. In particular, the synthetic methodologies that generate aryl-porphyrins will be explored. The first reported synthesis of porphine was reported by Rothemund [8] in 1936 when pyrrole was reacted with gaseous formaldehyde in methanol. The reaction time for the reaction varied depending on whether the solution was kept at room temperature—several weeks— or under reflux—15 to 25 h—and generated porphine in low yields.

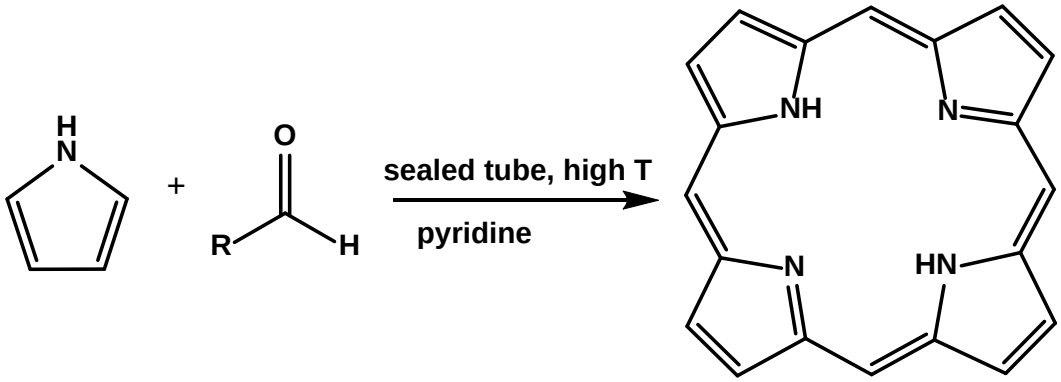

Scheme 1.1: Rothemund synthesis of porphin, where R= H.

Rothemund also synthesized porphine in pyridine in a sealed tube under nitrogen and heated it in a water bath for 30 h (Scheme 1.1) still with a low yield. Rothemund postulated that his one-pot synthesis would work for other aldehydes as well. A limitation of this methodology was that it required milligram scales.

1.2.1 Synthesis of Substituted Porphyrins

Rothemund experimented with other aldehydes in the synthesis of *meso*-substituted porphyrins. However, these conditions were harsh and unable to be scaled up. Adler-Longo [9] et al (Scheme 1.2) improved the reaction conditions by reacting equimolar pyrrole and

aldehydes in refluxing acetic or propionic acid under aerobic conditions instead of the sealed tube. These conditions were milder than the one proposed by Rothemund and allowed for substituted benzaldehydes to be reacted with pyrrole to generate various *meso*-substituted aryl-porphyrins.

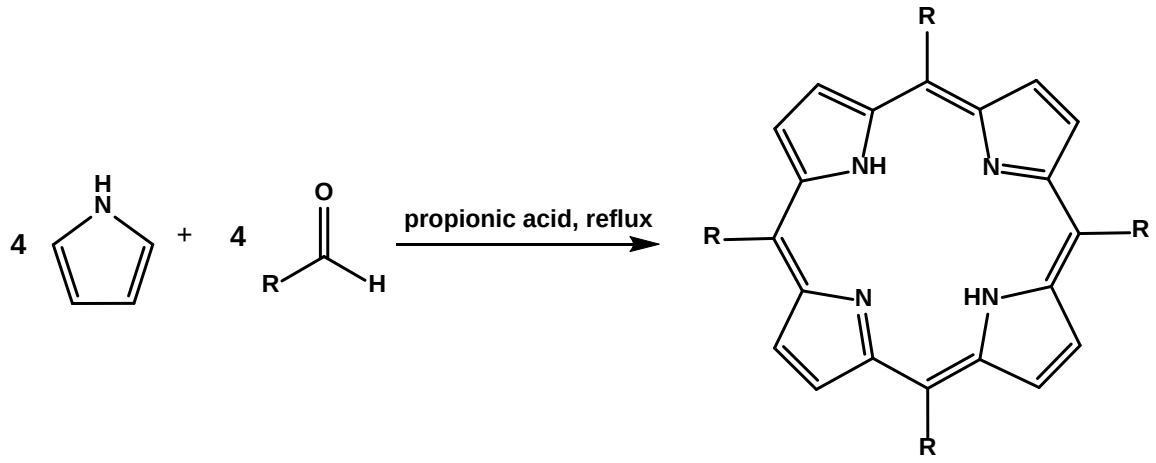

Scheme 1.2: Adler-Longo synthesis of substituted porphyrins where R= H, alkyl, or aryl groups.

The Adler-Longo method increased the porphyrin yield to around 20%. Another benefit of this method is that it can be scaled up and has successfully synthesized aryl-substituted porphyrins on a gram scale. A problem with this methodology is the tar-like impurity and various undesirable aldehyde-pyrrole byproducts that make purification challenging.

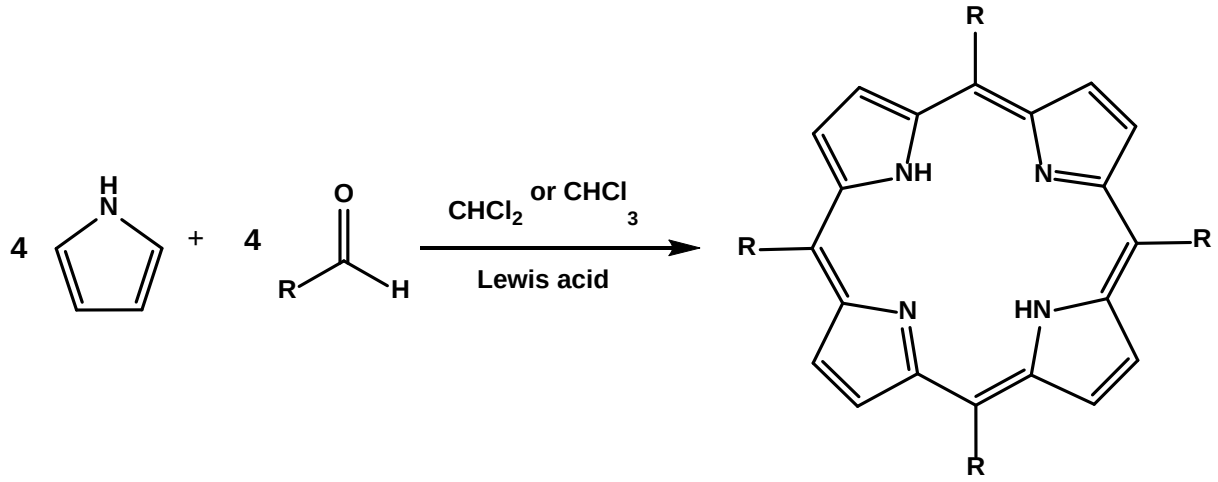

Scheme 1.3: Lindsey synthesis of substituted porphyrins, where R= H, alkyl, or aryl groups.

Lindsey [10] et al eliminated the use of a mild acid as the reaction medium by using chlorinated solvents and a Lewis acid catalyst (Scheme 1.3). By utilizing a two-step and highly diluted solution in this methodology, Lindsey reported porphyrin yields of 30-40%. In the first step the pyrrole and aldehyde are stirred at room temperature in a chlorinated solvent like chloroform or dichloromethane in the presence of a Lewis acid like boron trifluoride. The second step is the oxidation of the porphyrinogen with 2,3-dichloro-5,6-dicyanobenzoquinone (DDQ) at reflux for 1h. This methodology has a milder set of conditions than those reported either of the Rothemund or Alder-Longo syntheses which extend the scope of aryl aldehydes. Although it can be synthesized on a gram scale, the Lindsey method does not allow for industrial commercialization due to the elevated level of chlorinated solvents required.

All three of the porphyrin syntheses discussed in this section built upon each other and through these studies valuable information about porphyrin synthesis has been obtained. These methodologies found that the yield of the porphyrin produced was dependent on several factors: oxidant and acid catalyst used, condensation time, presence of water, and the concentration of pyrrole, aldehyde, and acid present.

The synthesis of 5,10,15,20-tetrakis(isopropylphenyl)porphyrin used in this work was prepared using the Alder-Longo method in which a 1:1 ratio of pyrrole and isopropylbenzaldehyde were added to propionic acid and refluxed for two hours (Scheme 1.4). The solution was then allowed to cool, and air bubbled through the solution overnight to oxidize to the target porphyrin in ~22% yields.

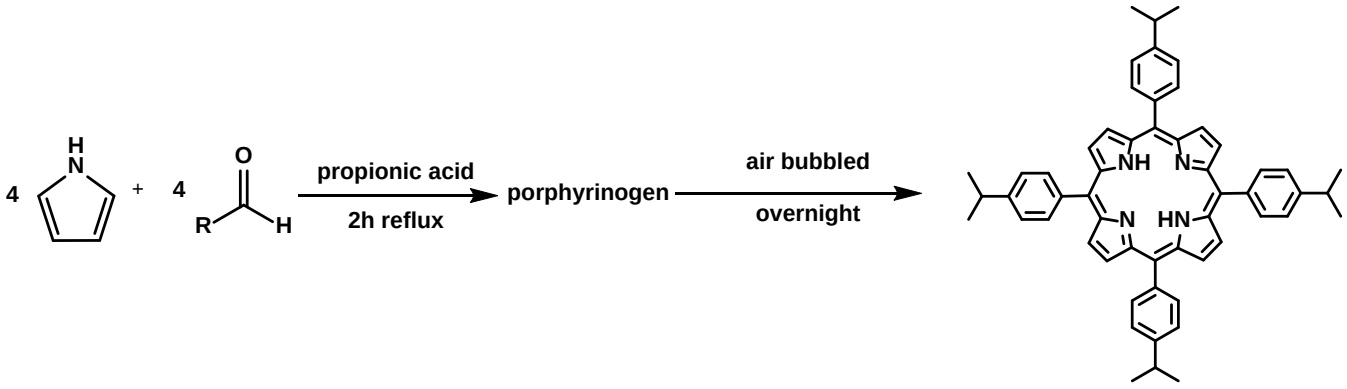

Scheme 1.4: The synthesis of 5,10,15,20-tetrakis(isopropylphenyl)porphyrin.

1.2.2 Synthesis of π-Extended Porphyrins

There are multiple ways to functionalize the porphyrin core at either the *meso*- or *beta*-positions. [7, 11] Prefunctionalization and post functionalization are the two common synthetic procedures to extend the porphyrin core. Prefunctionalization occurs when the pyrrole or aldehyde are functionalized prior to the synthesis of the porphyrin. A traditional way of prefunctionalization is the use of functionalized benzaldehydes to substitute the *meso* positions of the porphyrin. Examples of prefunctionalization at the beta position include the fusion of a benzene or anthracene [12] to the pyrrole moiety, as shown in Figure 1.6, via retro-Diels-Alder, isoindole condensation [13] or oxidative aromatization.

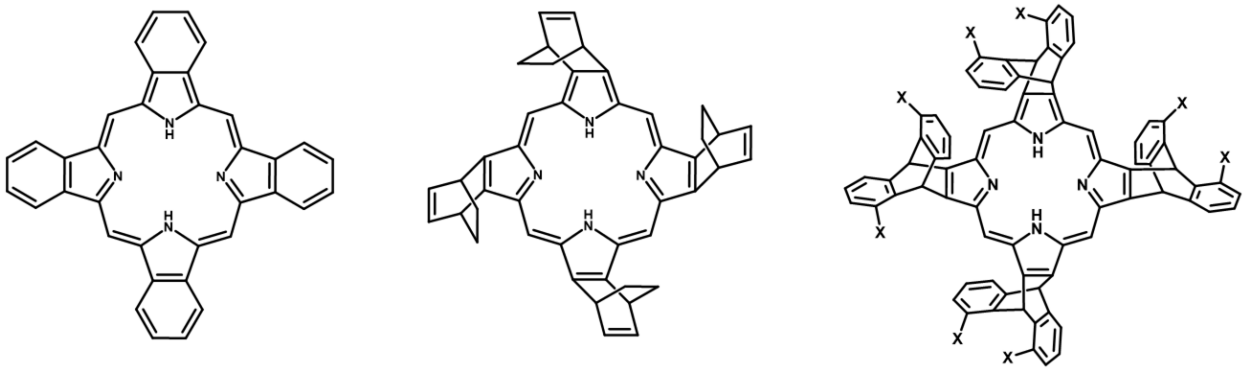

Chem. Soc. Rev., 2013, 42, 3302 ***J. Chem. Soc., Perkin Trans. 1***, 1997, 3161-3166

Figure 1.6: Prefunctionalized porphyrins on all *beta* positions.

Prefunctionalization on the beta positions is generally “all or nothing” in which all eight of the beta positions are functionalized or none of them are.

Post-functionalization [11,13] occurs when functional groups are substituted onto the core *after* the porphyrin synthesis. There are two types of post-functionalization: 1) core-functionalization and 2) peripheral functionalization. In core functionalization the porphyrin core is directly functionalized at the *meso*- or *beta*- positions whereas peripheral functionalization involves utilizing peripheral substituents, labeled as R in Figure 1.7, to introduce the functional group.

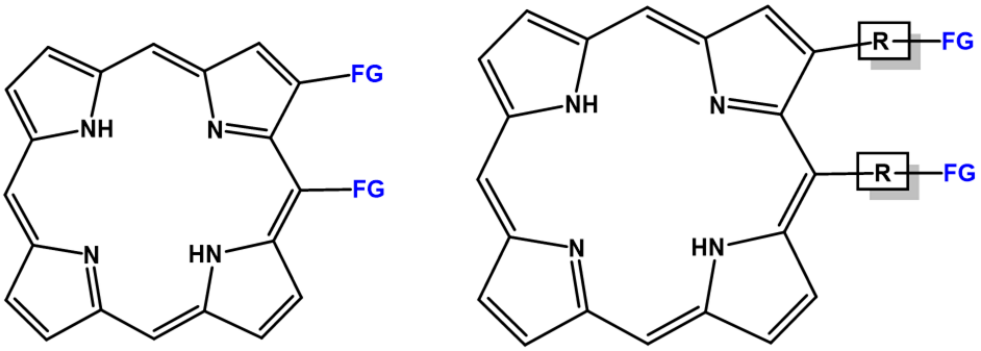

Figure 1.7: Generalized examples of the two classes of post-functionalization: core-functionalization (left) and peripheral functionalization (right).

Peripheral functionalization can occur on the *meso*- or *beta* positions by using organometallic reactions such as but not limited to: Suzuki, Sonogashira, and Heck reactions.

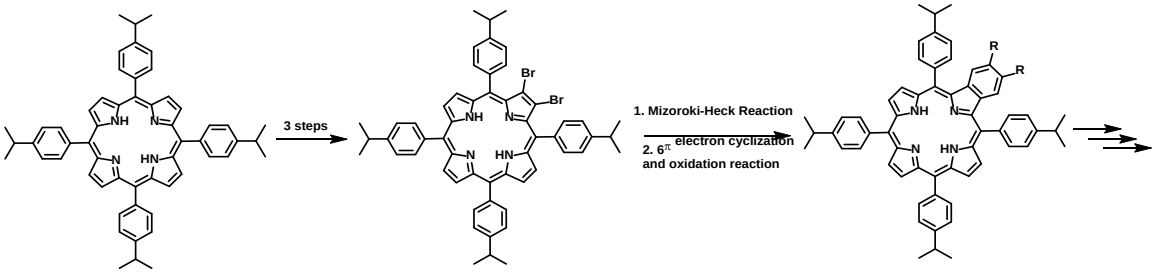

Scheme 1.5: Synthetic methodology for functionalization of monobenzoporphyrins developed by our group.

Previous work by our group [14] provided a method to functionalize two or more *beta*-positions on the porphyrin via a Heck-based reaction. The peripheral functionalization of only two beta positions on novel porphyrins synthesized in this dissertation are depicted in Scheme 1.5. Further functionalization of these porphyrins and a previously triphenylene fused derivative will be discussed in later chapters.

1.3 Aromaticity and Reactivity

Aromaticity occurs in cyclic molecules which exhibit delocalization of electrons over multiple atoms. Aromatic molecules tend to have higher stabilization energy and more uniform bond lengths. For a molecule to be aromatic it must be cyclic, planar, conjugated and has a Hückel number of π electrons defined by 4n+2. A common aromatic macrocycle which fits these criteria are porphyrins which contain a total of twenty-six π-electrons (n=6).

Gouterman's four-orbital theory was mentioned earlier to explain the absorption spectra of porphyrins; however, it can also be used to explain the aromaticity of porphyrins. Gouterman utilized Hückel LCAO-MO approach [7] which showed that individual atomic p_z orbitals overlap to create a set of π-orbitals. A system containing conjugated π-orbitals allows for electrons to move around freely and generate a magnetic current and a destabilizing effect on the molecule. In cases such as benzene, this makes the molecule less chemically reactive.

A unique feature of porphyrins is the presence of two potential delocalization pathways. The delocalization pathways of freebase porphyrins, one shown in Figure 1.8 Delocalization pathway of freebase porphyrin proposed by Vogel in red and the delocalization pathway of metalloporphyrin in blue. in red, are defined by an [18]-annulene derivative [15] system containing two isolated double bonds with eighteen π-electrons present.

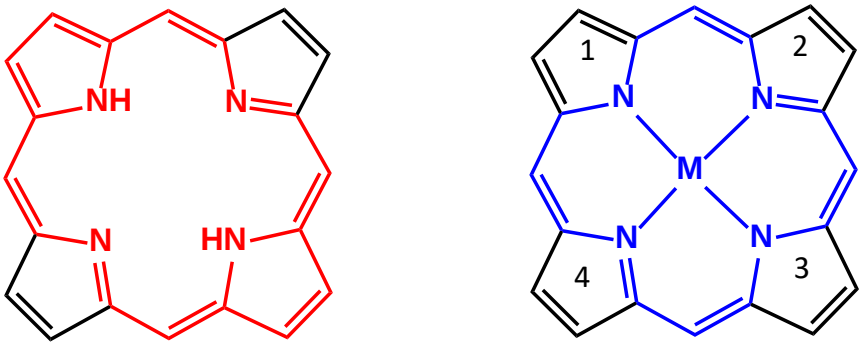

Freebase Porphyrin Metalloporphyrn

Figure 1.8: Delocalization pathway of freebase porphyrin proposed by Vogel in red and the delocalization pathway of metalloporphyrin in blue.

The presence of the two isolated double bonds on the porphyrin core are not involved in the macrocycle's aromaticity and therefore behave chemically more like an alkene. In fact, bromination of at one or both isolated double bonds can occur using NBS in chloroform. Our work reduces the starting porphyrin into a chlorin derivative prior to bromination to ensure only two bromines are added instead of four (Scheme 1.6).

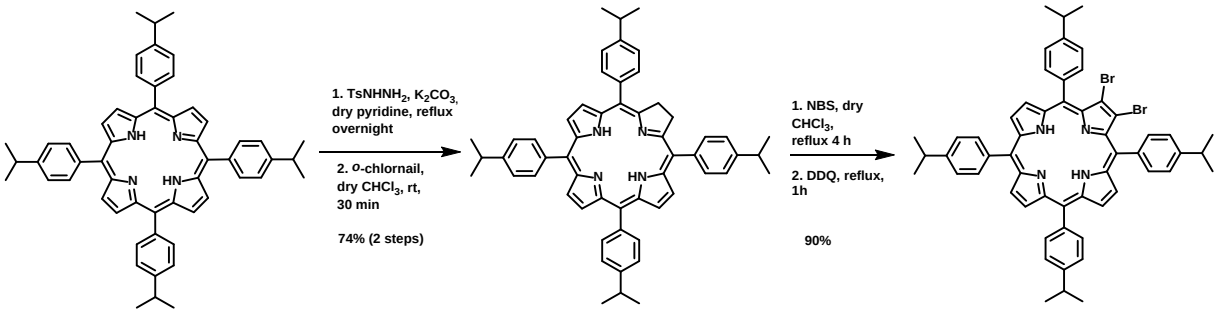

Scheme 1.6: Synthesis of 2,3-dibromo-5,10,15,20-tetrakis(isopropylphenyl)porphyrin.

The most reactive site on the porphyrin is the four *meso*- positions. This may seem odd considering the delocalization pathway shown above as the *meso*-positions are part of the aromaticity. However, it is important to remember that the delocalization pathway of a porphyrin is considered to be a diaza[18]-annulene. Sondheimer[16] had shown that [18]-annulene does conform to Hückel's rule, *but* it also displays a high reactivity as a result of its

conformational flexibility. Therefore, it is not surprising that porphyrins exhibit similar reactivity.

Metalloporphyrins experience a different delocalization pathway, shown in blue in Figure 1.8. To better understand why, we must look at studies done by Krygowski [17] et al which explored global and local aromaticity. Instead of using the popular [18]-annulene depiction, Kyrogwski divided the porphyrin into a macrocyclic internal cross, isolating the four pyrrole rings.

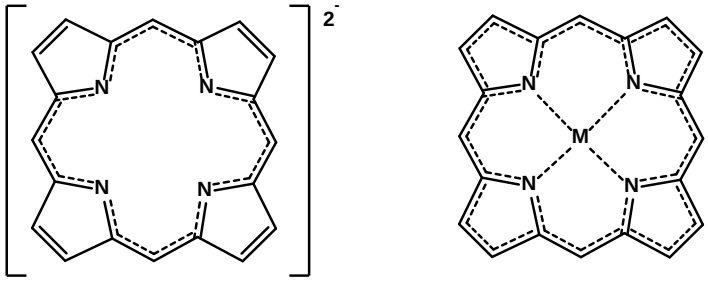

Figure 1.9: Krygowski's dianion depiction of the internal cross pathway (left) and aromatization of metalloporphyrins (right).

Utilizing HOMA and NICS, which will be discussed in the next section, Krygowski found that pyrrole rings 1 and 3 are more aromatic than pyrrole rings 2 and 4. This is rather important as it shows that the NH groups are not inert bridging groups as depicted in the diaza[18]annulene pathway. However, when we count the number of π-electrons there are only sixteen π-electrons, four of which come from the NH group. This means that the porphyrin would require an overall 2^- charge for the eighteen π-electron pathway the diaza[18]annulene has. As a result, the internal cross delocalization pathway of the porphyrin must be considered a dianion. This would then allow for the insertion of metals into the porphyrin core. Upon metal complexation the two types of pyrrole rings become closer in aromaticity generating the

delocalization on the right in Figure 1.9 showing that all the π-electrons participate in the aromatic system.

Characterization of aromaticity can be difficult as there are little experimental procedures which can determine how aromatic a compound is. Many aromaticity indices are computational and can be broken down into three categories: 1) evaluating molecular geometry, 2) assessing magnetic properties related to ring currents, and 3) calculation of the degree of energy stabilization.

The first category consists of evaluating ring planarity and bond length alteration via Harmonic Oscillator Model of Aromaticity (HOMA) [17, 18] developed by Kruszewski and Krygowski as a geometrical aromaticity index. This computational methodology is based on Equation 1.1 below.

$$\mathrm{HOMA} = 1 - \frac{a}{n}\sum_{i-l}^{n}(R_{opt} - R_i)^2 \qquad \text{(Equation 1.1)}$$

An empirical constant, α, is chosen such that HOMA index is equal to 1 for an aromatic molecule with equalized bond lengths. HOMA would be equal to 0 for molecules with alternating bond lengths. R_i indicates the bond length of the *i*-th bond and *n* denotes the number of bonds with π-electrons. R_{opt} is calculated using the deformation energy. Krygowski had used this method to explain the internal cross pathway that metalloporphyrins have. However, this dissertation will not discuss HOMA index beyond this point.

The second category looks at the magnetic current generated from mobile π-electrons and is one of the few methods that experimental methodology can be used, namely ^{1}H Nuclear Magnetic Resonance (NMR). NMR introduces an applied magnetic field (B_o) that is perpendicular to the plane of the molecule. [19]

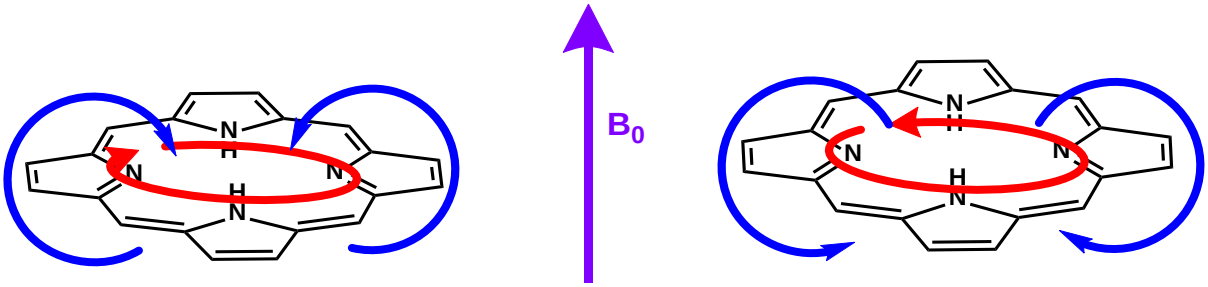

Figure 1.10: Applied magnetic field (purple arrow) depicting aromatic (left) and antiaromatic (right) ring current. Red arrows indicate the direction of the ring current, and the blue arrows indicate the induced magnetic field.

The introduction of the applied magnetic field results in the delocalization of π-electrons in the molecule and the ring generates its own magnetic field. Outside of the ring, the magnetic field generated runs in the same direction as the externally applied magnetic field; whereas the magnetic field generated inside the ring runs in the opposite direction. Protons that are on the outside of the ring (*meso*- and *beta*- protons) are shifted downfield because of a deshielding effect because of the applied magnetic field and the magnetic field generated by the ring running in the same direction. The internal two N-H porphyrins are shifted upfield because of shielding effects resulting in the opposite directions of the applied magnetic field and the magnetic field generated inside of the ring.

A second method that falls under this category is Nucleus Independent Chemical Shifts (NICS) [20] which is a computational method that provides a quantitative assessment by calculating aromaticity using quantum chemical calculations of magnetic shielding. In using NICS, a molecule can be determined to be either aromatic, nonaromatic or antiaromatic based on whether there is diatropic current or paratropic current present. Negative values indicate diatropic current and positive values show paratropic current for a compound to be considered nonaromatic it must fall close to zero. This method has been the most frequently used to study

porphyrin aromaticity.

A final method that looks at magnetic current are current density maps such as Anisotropy Current Induced Density (AICD). [21] This is a pictorial view of ring currents within a cyclic compound but there is no way to separate the delocalized electrons from the total electron density. It does, however, give a good look into the global aromaticity of a molecule and the direction of the current density.

The third category for characterizing aromaticity will not be explored in depth in this dissertation as it primarily looks at the following calculations: heat of formation, bond energy, and thermodynamic stability metrics. However, this paper will explore the use of a variation of the NICS method and AICD to explore the aromatic character of novel benzodithiophenyl-fused porphyrin monomers and oligomers.

Chapter 2 of this dissertation focuses on synthetic method development to fuse a naphthodithiophene to 5,10,15,20-tetrakis(isopropylphenyl)porphyrin. Chapter 3 will focus on the design and synthesis of freebase and metalated porphyrin oligomers derived from naphthodithiophene-fused porphyrins. Chapter 4 will be further exploration of triphenylene-fused porphyrins as a synthetic precursor to build up conjugated porphyrin oligomers. Chapter 5 will provide an overall conclusion of my dissertation work and future direction.

1.4 References

[1] a) Borisov, S. M.; Nuss, G.; Klimant, I. *Anal Chem* **2008**, *80* (24), pp 9435–9442; b) Kumar, S.; Choudhuri, I.; Pathak, B. *J Mater Chem C Mater* **2016**, *4* (38), pp 9069–9077; c) Aratani, N.; Osuka, A.; Cho, H. S.; Kim, D. *Journal of Photochemistry and Photobiology C: Photochemistry Reviews* **2002**, *3* (1), pp 25–52; d) Hisaki, I.; Hiroto, S.; Kim, K. S.; Noh, S. B.; Kim, D.; Shinokubo, H.; Osuka, A. *Angewandte Chemie - International Edition* **2007**, *46* (27), pp 5125–5128; e) Czernuszewicz, R. S. *J Porphyr Phthalocyanines* **2000**, *4* (4), 426–431; f) Solonenko, D.; Gasiorowski, J.; Apaydin, D.; Oppelt, K.; Nuss, M.;

Keawsongsaeng, W.; Salvan, G.; Hingerl, K.; Serdar Sariciftci, N.; Zahn, D. R. T.; Thamyongkit, P. *Journal of Physical Chemistry C* **2017**, *121* (39); g) Szliszka, E.; Czuba, Z. P.; Domino, M.; Mazur, B.; Zydowicz, G.; Krol, W. *Molecules* **2009**, *14* (2), pp 738–754.

[2] a) Fischer, H. & Orth, H. (1937) *Die Chemie des Pyrrols*, vol. 11.1, Akademische Verlagsgesellschaft, Leipzig; b) Fischer, H. & Stern, A. (1940) *Die Chemie des Pyrrols*. vol. 11.2, Akademische Verlagsgesellschaft, Leipzig.

[3] Moss, G. P. *Eur J Biochem* **1988**, *178* (2), 277–328.

[4] a) Brothers, P. J.; Senge, M. O. *In Fundamentals of porphyrin chemistry: A 21st century approach*; John Wiley & Sons, Incorporated, 2022; Vol. 1, pp 24–27; b) Moss, G. P. *Pure & Appl. Chem.,* Vol. 70, No. 1, pp 143-216, 1998; c) Rasmussen, S. C. *ChemTexts* **2016**, *2* (4), pp 1–13; d) International Union of Pure and Applied Chemistry, *J. Am. Chem. Soc.* 1960, 82, 21, pp 5545-5574.

[5] a) Finikova, O. S.; Cheprakov, A. V.; Vinogradov, S. A. *Journal of Organic Chemistry* **2005**, *70* (23), pp 9562–9572; b) Xiang, N.; Liu, Y.; Zhou, W.; Huang, H.; Guo, X.; Tan, Z.; Zhao, B.; Shen, P.; Tan, S. *Eur Polym J* **2010**, *46* (5), pp 1084–1092; c) Crossley, M. J.; Burn, P. L. *J. Chem. Soc. Chem. Commun.* 1991, pp 1569-1571; d) Jiang, J.; Spies, J. A.; Swierk, J. R.; Matula, A. J.; Regan, K. P.; Romano, N.; Brennan, B. J.; Crabtree, R. H.; Batista, V. S.; Schmuttenmaer, C. A.; Brudvig, G. W. *Journal of Physical Chemistry C* **2018**, *122* (25), pp 13529–13539.

[6] a) Gouterman M.; *Optical Spectra and Electronic Structure of Porphyrins and Related Rings*; Academic Press, Incorporated, 1978; Vol. 3, pp 47-51; b) Gouterman M.; *Optical Spectra and Electronic Structure of Porphyrins and Related Rings*; Academic Press, Incorporated, 1978; Vol. 3, pp 89-127; c) Gouterman, M. *Spectra of Porphyrins**; 1961; Vol. 6; d) Gouterman, M.; Wagnière, G. H.; Snyder, L. C. *Spectra of Porphyrins Part II. Four Orbital Model*; 1963; Vol. 11; e) Wamser, C. C. *JACS Au* 2022, 2, pp 1543-1560; f) Brothers, P. J.; Senge, M. O. *In Fundamentals of porphyrin chemistry: A 21st century approach*; John Wiley & Sons, Incorporated, 2022; Vol. 2, pp 513-516, pp 517-525, and pp 525-528.

[7] a) Laha, J. K.; Dhanalekshmi, S.; Taniguchi, M.; Ambroise, A.; Lindsey, J. S. *Org Process Res Dev* **2003**, *7* (6), pp 799–812; b) Smith, K. M. *New Journal of Chemistry* **2016**, *40* (7), pp 5644–5649; c) Steiner, E.; Fowler, P. W. *ChemPhysChem* 3 (1): pp 3758-3772.

[8] a) Rothemund, P. *J. Am. Chem. Soc* **1935**, No. II; b) Rothemund, P. *J. Am. Chem. Soc* **1936,** *157* (6), pp 625–627.

[9] a) Adler, A. D.; Longo, F. R.; Shergalis, W. *J Am Chem Soc* **1964**, *86* (15), pp 3145–3149; b) Adler, A. D.; Longo, F. R.; Finarelli, J. D. *Journal of Organic Chemistry*, 1966, 32 (1), 476.

[10] Lindsey, J. S.; Schreiman, I. C.; Hsu, H. C.; Kearney, P. C.; Marguerettaz, A. M. *Journal of Organic Chemistry* **1987**, *52*, 827–836.

[11] a) Vicente, M.; Smith, K. *Curr Org Synth* **2014**, *11* (1), pp 3–28; b) Carvalho, C. M. B.; Brocksom, T. J.; Thiago de Oliveira, K. *Chem Soc Rev* **2013**, *42* (8), pp 3302–3317; c) Vicente, M. G.; Smith, K. *Curr Org Chem* **2005**, *4* (2), 139–174.

[12] Yamada, H.; Kuzuhara, D.; Takahashi, T.; Shimizu, Y.; Uota, K.; Okujima, T.; Uno, H.; Ono, N. *Org Lett* **2008**, *10* (14), 2947–2950.

[13] a) Abdulaeva, I. A.; Birin, K. P.; Gorbunova, Y. G.; Tsivadze, A. Y.; Bessmertnykh-Lemeune, A. *J Porphyr Phthalocyanines* **2018**, *22* (8), pp 619–631; b) Hiroto, S.; Miyake, Y.; Shinokubo, H. *Chem Rev* **2017**, *117* (4), 2910–3043; c) Donatoni, M. C.; Vieira, Y. W.; Brocksom, T. J.; Rabelo, A. C.; Leite, E. R.; De Oliveira, K. T. *Tetrahedron Lett* **2016**, *57* (27–28), pp 3016–3020; d) Chen, Y. J.; Lee, G. H.; Peng, S. M.; Yeh, C. Y. *Tetrahedron Lett* **2005**, *46* (9), 1541–1544; e) Tanguy, L.; Hetru, O.; Langlois, A.; Harvey, P. D. *J. Org. Chem.* 2019, 84, 6, pp 3590–3594; f) Morisue, M.; Kawanishi, M.; Nakano, S. *J Polym Sci A Polym Chem* **2019**, *57* (24), pp 2457–2465; g) Shultz, D. A.; Gwaltney, K. P.; Lee, H. *Journal of Organic Chemistry* **1998**, *63* (12), pp 4034–4038; h) Morisue, M.; Ohno, N.; Saito, G.; Kawanishi, M. *Journal of Organic Chemistry* **2022**, *87* (5), pp 3123–3134.

[14] a) Jinadasa, R. G. W.; Fang, Y.; Kumar, S.; Osinski, A. J.; Jiang, X.; Ziegler, C. J.; Kadish, K. M.; Wang, H. *Journal of Organic Chemistry* **2015**, *80* (24), 12076–12087; b) Deshpande, R.; Jiang, L.; Schmidt, G.; Rakovan, J.; Wang, X.; Wheeler, K.; Wang, H. *Org Lett* **2009**, *11* (19), 4251–4253.

[15] Vogel, B. E. Pure & Appl. Chern., Vol. 65, No. 1, pp. 143-152, 1993; b) Vogel, B. E. *Angew. Chem*. *Int. Ed*., 27, 1988, No. 3, pp 406-409.

[16] a) F. Sondheimer, R. Wolovsky, and Y. Amiel, *J. Am. Chem. Soc.*, **84**, 274 (1962); b. F. Sondheimer and R. Wolovsky, *J. Am. Chem. Soc.*, **84**, 260 (1962); c) F. Sondheimer, *Acc. Chem. Res.*, **5**, 81 (1972).

[17] a) Krygowski, T. M.; Szatylowicz, H.; Stasyuk, O. A.; Dominikowska, J. *Chem. Rev.* 2014, 114, 12, pp 6383-6422; b) Cyrañski, M. K.; Krygowski, T. M.; Wisiorowski, M.; Van Eikema Hommes, N. J. R.; Von Ragué Schleyer, P. *Angewandte Chemie - International Edition* **1998**, *37* (1–2), 177–180; c) Cyrañski, M. K.; Krygowski, T. M. Tetrahedron, 32 (5), pp 1713-1722.

[18] a) Dobrowolski, J. C. *ACS Omega* **2019**, *4* (20), pp 18699–18710; b) Brothers, P. J.; Senge, M. O. *In Fundamentals of porphyrin chemistry: A 21st century approach*; John Wiley & Sons, Incorporated, 2022; Vol. 2, pp 552-553; Krygowski, T. M. *J. Chem. Inf. Comput. Sci.* 1993, 33, 1, pp 70–78.

[19] a) Brothers, P. J.; Senge, M. O. *In Fundamentals of porphyrin chemistry: A 21st century approach*; John Wiley & Sons, Incorporated, 2022; Vol. 2, pp 553-555; b) Becker, E.D.; Bradley, R.B. *The Journal of Chemical Physics* 31 (5), pp 1413-1414; c) Ellis, J.; Jackason, A.H; Kenner, G.W; Lee, J. Tetrahedron Letters, 1960, 2, pp 23-27; d) Gershoni-Poranne, R.; Stanger, A. ***Chem. Soc. Rev.***, 2015,**44**, pp 6597-6615.

[20] a) Chen, Z.; Wannere, C. S.; Corminboeuf, C.; Puchta, R.; Von, P.; Schleyer, R. *Chem. Rev.* 2005, 105, 10, pp 3842-3888; b) Von, P.; Schleyer, R.; Maerker, C.; Dransfeld, A.; Jiao, H.; Van, N. J. R.; Hommes, E. *J. Am. Chem. Soc.* 1996, 118, 26, pp 6317–6318.

[21] Geuenich, D.; Hess, K.; Köhler, F.; Herges, R. *Chem. Rev.*, 105, 10, 3758–3772.

CHAPTER 2

NAPHTHODITHIOPHENE-FUSED PORPHYRINS

2.1 Introduction

Linearly π-extended porphyrins such as benzoporphyrins [1] have been investigated in depth; similarly, β-extended porphyrins which incorporate naphthalene, anthracene, and other polycyclic aromatic hydrocarbons (PAH) have also been reported. [2] The incorporation of heteroatoms into a porphyrin system has also been documented as well. In these compounds a pyrrole is either replaced, oriented differently, or a new heteroatom is inserted elsewhere on the porphyrin. Most of the reported literature focus on either modifying the porphyrin core or expanding the core. [3]

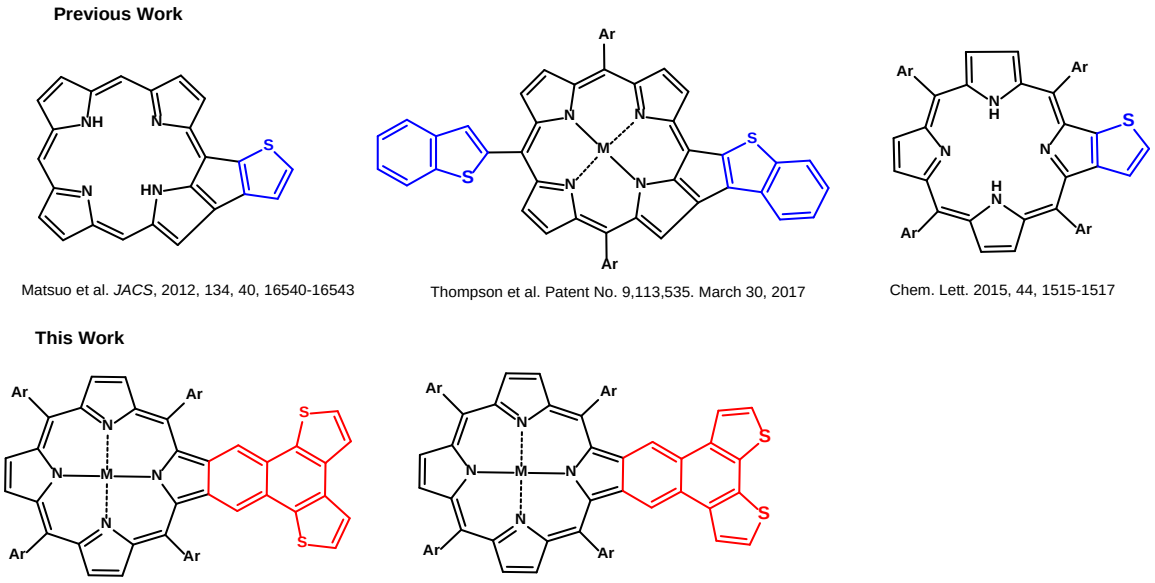

Figure 2.1: Porphyrins with thiophene moieties attached to the porphyrin.

Aromatic heterocycles linearly fused to porphyrins, however, have been rarely reported due to limited synthetic methodology. Those that have been mentioned predominately focus

on the inclusion of N-heterocycles [2,4] which show a variety of applications including but not limited to organic optical-electronics and biomedical applications. [3,5]

Thiophenes and their derivatives are another commonly featured aromatic heterocycles in porphyrin arrays [2,6] (Figure 2.1) due to their ability to act as a good electron donor. As a result of their ability to alter the charge carrier capacity they are widely used in both oligomeric and polymeric materials and for a variety of applications. [1,6,7] In almost all reported literature, the thiophene derivatives are placed either at the *meso*-position of the porphyrin or fused directly to the porphyrin core itself. It would be interesting to linearly extend the porphyrin with thiophene derivatives, which are expected to display novel electronic and photophysical properties.

2.2 Molecular Design and Synthesis

Our group has previously published a versatile approach to functionalizing benzoporphyrins. [8] Using this approach we have synthesized a new class of linearly π-extended napthodithiophene-fused porphyrins. The synthesis of napthodithiophene-fused porphyrins started with preparation of 2-vinylthiophene (Scheme 2.1) from a Wittig reaction with methyltriphenylphosphonium bromide, potassium carbonate, and 2-thiophenecarbaldehydes in refluxing dioxanes. 2-Vinylthiophene was successfully synthesized in 60% yield. 3-vinylthiophene was synthesized the same way with a similar yield.

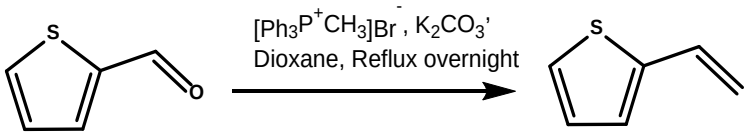

Scheme 2.1: Wittig reaction of 2-thiophenecarboxaldehyde to synthesize 2-vinylthiophene.

Dibromoporphyrin, 1 (Scheme 2.2), was reacted with 2-vinylthiophene via a Heck, 6π cyclization and aromatization cascade reaction to generate **2VTP** in 41% yield. **2VTP** is a compound in which a benzoporphyrin has two 2-vinylthiophenes attached to the benzene ring. To extend the π-conjugation further, we conducted an intramolecular Scholl reaction to yield **F2VTP**, however, in low yields (<15%). The low yield could be attributed to the reactivity of the 2- and 5- positions on the unsubstituted thiophene moiety, which led to formation of a polymer instead of a porphyrin monomer. To increase the yield of the intramolecular Scholl reaction, we decided to block the 5-positions of the attached thiophenes through bromination. By using a facile method, reported by Arsenyan and coworkers, [9] the thiophene moiety of **2VTP** was brominated by sonicating N-bromosuccinimide (NBS) and **2VTP** at room temperature for 30 seconds in DCM and **2vtBr** was generated in 86% yield. This new compound then underwent an intramolecular Scholl reaction to give **F2vtBr**, a naphtho[1,2-*b*:3,4-*b'*]dithiophene-fused porphyrin in 80% yield. To better understand this new class of porphyrins, Zinc analogues of **2VTP**, **2vtBr**, and **F2vtBr** were also prepared in high yields (<90%).

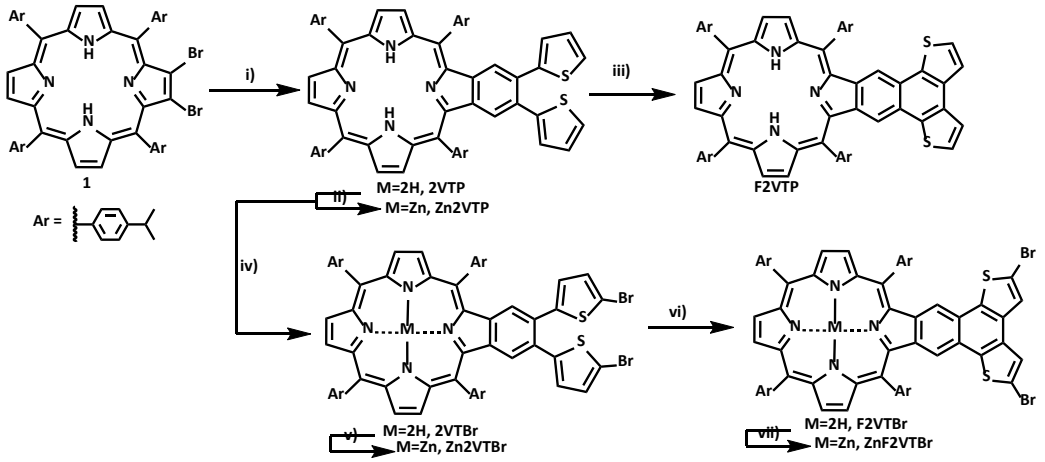

Scheme 2.2: Synthesis of 2VTP, F2VTP, 2VTBr and F2VTBr and zinc derivatives under the following conditions: i) 2.2eq K_2CO_3, 0.5 eq $Pd(OAc)_2$, 1.3 PPh_3, 1:1 DMF/xylenes, 10 eq 2-vinylthiophene, 90°C, 4 days. iii) and vi) 20 eq $FeCl_3$, 1 mL CH_3NO_2, 5 mL DCM, rt, 15 min. iv) 2eq NBS, DCM, sonicate for 30s at rt. ii), v), and vii) 10 eq $Zn(OAc)_2$, 3:1 $CHCl_3$/MeOH, reflux, 1h.

As mentioned previously, thiophenes derivatives have been incorporated into porphyrins due to their ability to alter electronic and optical properties. To look at how the location of the thiophene moiety attached may alter the properties these porphyrins, **3VTP** was designed and synthesized. Dibromoporphyrin (Scheme 2.3) was reacted with 3-vinylthiophene under the same conditions as for the synthesis of **2VTP** to generate **3VTP** in 58% yield. Subsequent intramolecular Scholl reaction afforded **F3VTP** in 70% yield. Interestingly, the yield for **F3VTP** is higher than that of **F2VTP**. We suspect that this is because **F3VTP** is obtained through coupling 2- positions of the two adjacent thiophenes and **F2VTP** through a C-C coupling at the 3-position. The different reactivity between 2- and 3-positions of thiophene accounts for the different yields of the coupling products, i.e., **F2VTP** and **F3VTP**. Zinc analogues for both **3VTP** and **F3VTP** were prepared in good yields.

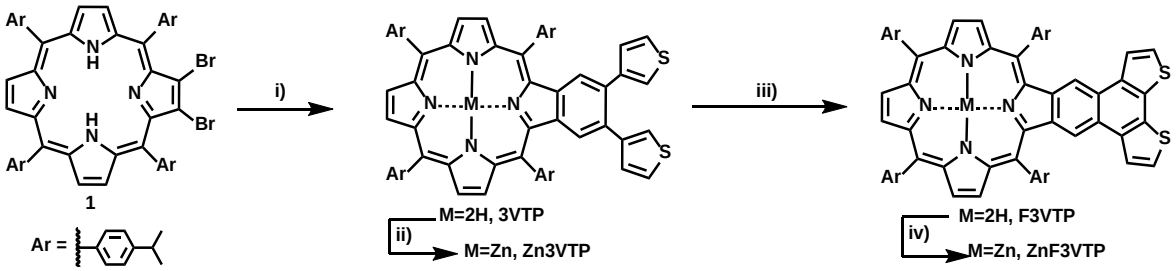

Scheme 2.3: Synthesis of 3VTP and F3VTP under the following conditions: i) 2.2eq K_2CO_3, 0.5 eq $Pd(OAc)_2$, 1.3 PPh_3, 1:1 DMF/xylenes, 10 eq 3-vinylthiophene, and heat at 90°C for 4 days. iii) 10 eq $FeCl_3$, 1 mL CH_3NO_2, 5 mL DCM, rt for 15 min. ii) and vi) 10 eq $Zn(OAc)_2$, 3:1 $CHCl_3$/MeOH, reflux for 1h.

2.3 Optical Properties

2.3.1 UV-VIS

Figure 2.2a shows the molar absorptivity of the synthesized freebase porphyrins in dichloromethane (DCM) and 2.2b shows the molar absorptivity for the Zinc-inserted analogues in 1,2-dichlorobenzene (DCB). The Soret of tetraphenylporphyrin (TPP) is known to be

approximately 420 nm. [10] **2VTP** and **3VTP** Soret bands were red shifted by 16 nm to 436 nm and 14 nm to 434 nm in DCM respectively. The Q bands red-shifted 10 nm and 14 nm respectively for the first two Q bands of **2VTP**. The brominated analogue **2vtBr** shows a similar Soret and Q band shift. The addition of the bromine atoms did not show impact on the UV-VIS spectra from 350-800 nm. The reason for this is not only due to the intensity of the Soret band but also because bromination of the thiophene shows a UV-VIS range under 250 nm. [11] **3VTP**, on the other hand, only has one visible Q band at 524 nm which shows a bathochromatic shift of 9 nm compared to TPP. Upon the insertion of Zinc into **2VTP** and **2VTBr** the absorption spectra show the expected two Q bands at 564 nm and 604 nm for **Zn2VTP** and at 566 nm and 601 nm for **Zn2VTBr**. **Zn3VTP** shows Q bands around 563 nm and 605 nm. Further fusing of the thiophene moieties to the benzene rings of **2VTP, 2vtBr,** and **3VTP** via the Scholl reaction produces similar bathochromatic shifts of 13 nm (**F2VTP** and **F2vtBr**) and 12 nm (**F3VTP**). The zinc anologues show a similiar trend and only two Q bands. **ZnF3VTP** shows Q bands at 572 nm and 616 nm while **ZnF2VTBr** has Q bands at 575 nm and 617 nm.

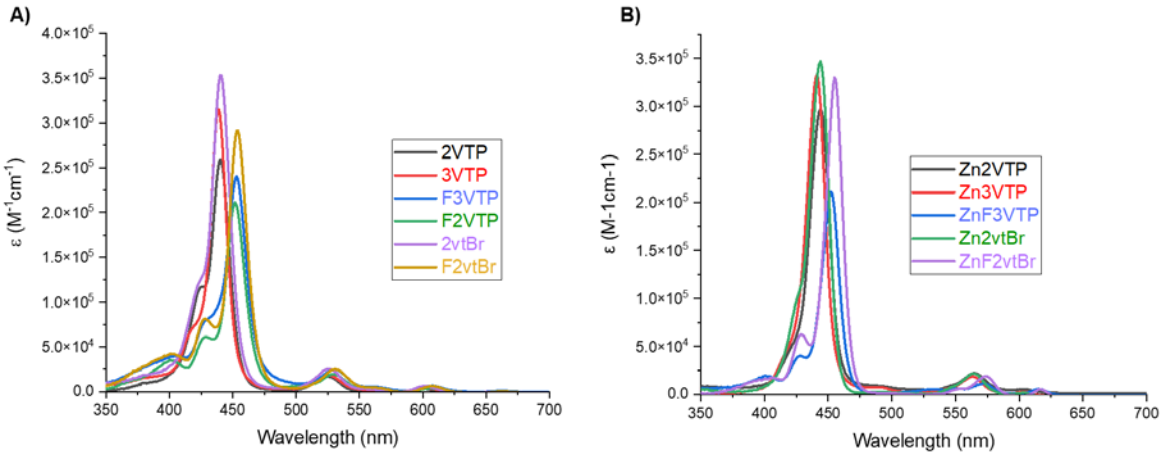

Figure 2.2: Absorptivity of a) Freebase Dithiophenyl-fused Porphyrins in DCM and b) Zn Analogues in 1,2-dichlorobenzene.

A Tauc plot was used to experimentally determine the energy band gaps. Tables for each compound are included in the experimental section (2.8.5). Bufaroosha had previously reported UV-VIS solution Tauc Plot calculations for **TPP**, **ZnTPP**, and **NiTPP**.[12] In order to calculate the optical band gap from solution UV-VIS spectroscopy, **Equation 2.1** shown below was used to determine the photon energy.

$$E = \hbar\nu = \hbar(2\pi f) = \frac{hc}{\lambda} = \frac{1240}{\lambda} \quad \text{(Equation 2.1)}$$

For this equation, $\hbar$ = 4.135667696...×10^{-15} eV·s and can be written as ħ = $\frac{h}{2\pi}$ in which h is Planck's constant. Frequency, ν, can be substituted for $\frac{c}{\lambda}$ so that the final equation 1 is derived. Once this is calculated, the UV-VIS absorbance can then be pluged in to determine the photon energy and calculate both an indirect (Equation 2.2) and a direct (Equation 2.3) Tauc relationship.

$$(\alpha h\nu)^{\frac{1}{2}} = \left(\frac{A}{E}\right)^{\frac{1}{2}} \quad \text{(Equation 2.2)}$$

$$(\alpha h\nu)^{2} = \left(\frac{A}{E}\right)^{2} \quad \text{(Equation 2.3)}$$

For both equations, A = experimental absorbance and E= photon energy calculated from Eq 2.1. Once the equations are plotted (Figure 2.3) one horizontal line can be drawn at the base of the spectra and another on the vertical slope of the porphyrin Soret band. Where these two lines meet, will indicate the energy band gap.

We found that the indirect relationship provides energy gaps that are in close agreement with those from the DFT calculated values (see Section 2.4 DFT Studies). For **2VTP** (2.68 eV), **F2VTP** (2.65 eV), and **ZnF3VTP** (2.62 eV) we see a difference of 0.01 eV for the experimental and computational energy band gap. There is a difference of 0.02 eV for **3VTP**

(2.67 eV) and **F2VTBr** (2.66 eV). Compounds **F3VTP** (2.66 eV) and **2VTBr** (2.68 eV) experimentally and computationally obtained the same energy band gap. **Zn3VTP** (2.66 eV) has a 0.03 eV difference and **ZnF2vtBr** (2.61 eV) has a difference of 0.04 eV. **Zn2VTP** (2.66 eV) and **ZnF2vtBr** (2.66 eV) show a 0.08 eV difference.

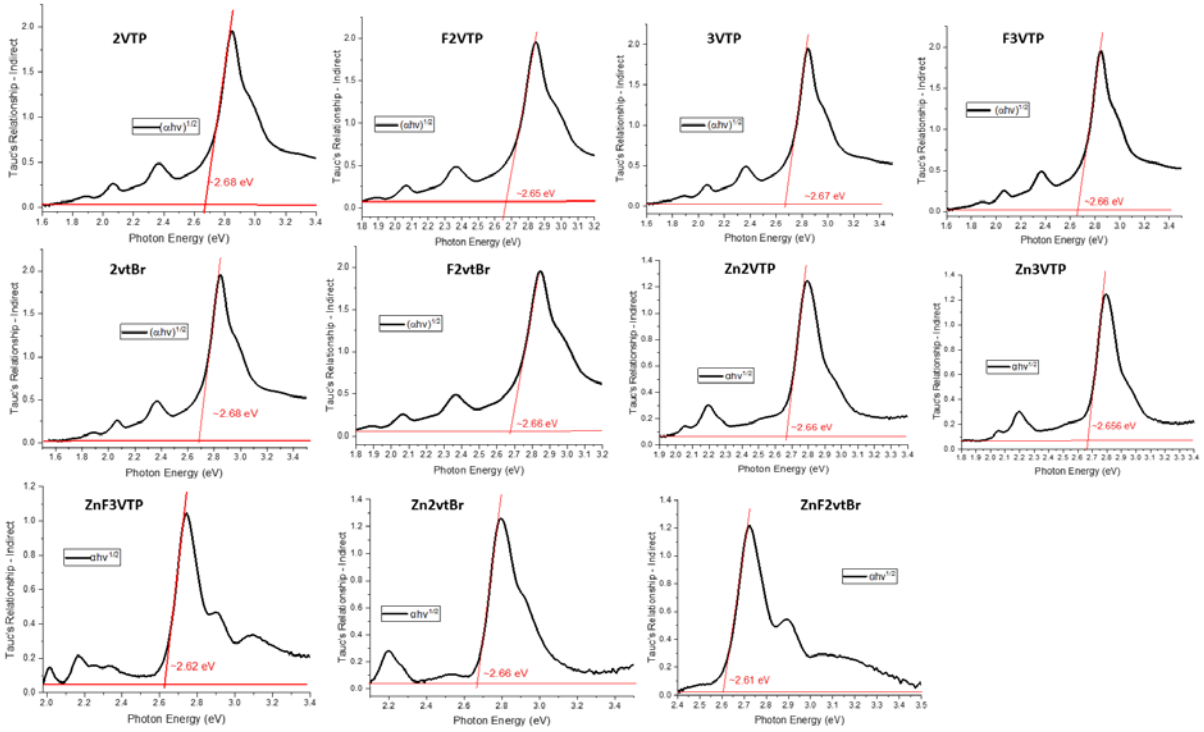

Figure 2.3: Plotted indirect relationship Tauc plot for all compounds.

2.3.2 Fluorescence Emission

The fluorescence emission spectra were obtained by our collaborator Dr. Sergei Vinogradov's group in dimethylformide (DMF). It was noted that the π-extended porphyrins show a similar pattern of two peaks for both the freebase and the zinc analogues from 600 to 800 nm. For all the monobenzoporphyrins the peak around 660 nm is the smaller of the two, while the peak around 730 nm is the larger one. The zinc inserted compounds were also obtained and show two fluorescence peaks around 620 nm and 680 nm with both peaks having

a lower intensity difference than their freebase analogues.

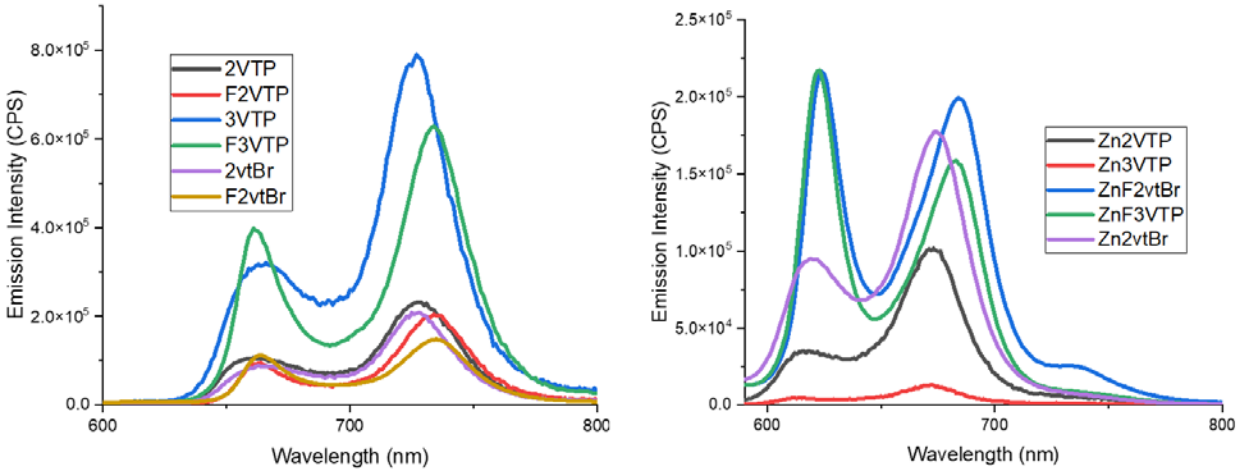

Figure 2.4: Fluorescence emission of all freebase dithiophenyl-fused porphyrins (a) and their Zinc analogues (b) in DMF.

Table 2.1: Fluorescence lifetimes of 2VTP, 3VTP, F2VTP, F3VTP, 2VTBr, and F2VTBr in dimethylformamide (DMF).

Compounds	τ_{avg} (ns)
2VTP	10.6
3VTP	10.2
F2VTP	13
F3VTP	12.1
2vtBr	10.4
F2vtBr	12.9
Zn2VTP	2.53
Zn3VTP	1.86

The fluorescence lifetimes (Table 2.1), also obtained by Dr. Sergei Vinogradov's group, were measured for **2VTP, 3VTP, F2VTP, F3VTP, 2VTBr, F2VTBr, Zn2VTP, and Zn3VTP** in DMF. **TPP** and **ZnTPP** have a reported fluorescence lifetime of 9.9 ns and 2.1 ns [13] respectively. The monobenzoporphyrins in this work have a longer average fluorescence lifetime of 10.6 ns, 10.2 ns, and 10.4 ns for **2VTP, 3VTP,** and **2VTBr**. Their fused analogues experience an even longer

fluorescence lifetime of 13 ns, 12.1 ns, and 12.9 ns for **F2VTP, F3VTP,** and **F2VTBr**. The fluorescence lifetime of **Zn2VTP** (2.53 ns) has a higher lifetime and **Zn3VTP** (1.86 ns) has a lower lifetime in comparison to ZnTPP.

2.4 DFT Studies

2.4.1 The HOMOs and LUMOs of Studied Compounds

To delve deeper into the optical and electronic properties of this novel class of β,β'-π-extended porphyrins, four computational studies were performed including DFT, TDDFT, AICD, and NICS-scan methodology. The basis set used for DFT calculations were B3LYP-6-31(d,p) level of theory; TDDFT level of theory used was B3LYP-6-31++(d,p) scrf iefpcm in dichlorobenzene. The aromaticity studies level of theory was B3LYP-6-31G* nmr=csgt for AICD and GIAO B3LYP/6-31g(d,p) for all NICS studies.

Figure 2.5 shows the calculated isodensity surfaces of **2VTBr**, **F2VTBr**, **2VTP**, **F2VTP**, **3VTP** and **F3VTP**. Both the HOMO and LUMO isodensity surfaces suggest little impact of the extended π-system of **2VTP, F2VTP, 2VTBr, 3VTP** and **F2VTBr** since the isodensity orbitals are predominately located on the porphyrin core, not the thiophene moieties. Unlike the others, **F3VTP** HOMO diagram experiences electron density on the porphyrin core and the thiophene moieties; its LUMO isodensity is only on the porphyrin core. The HOMO -1 of 2VTP and 2VTBr involve the fused benzene rings but not the thiophene moiety. Whereas **F2VTP**, **F2vtBr**, and **3VTP** show isodensity on the respective fused ring and the thiophene moieties. For the monobenzoporphyrins, the isodensity of the LUMO +1 is located on the porphyrin core and on the fused benzene ring but not on the thiophene moieties. For the fused analogues the

isodensity is distributed to the porphyrin core, the fused benzene rings, and a small portion on the thiophene moiety.

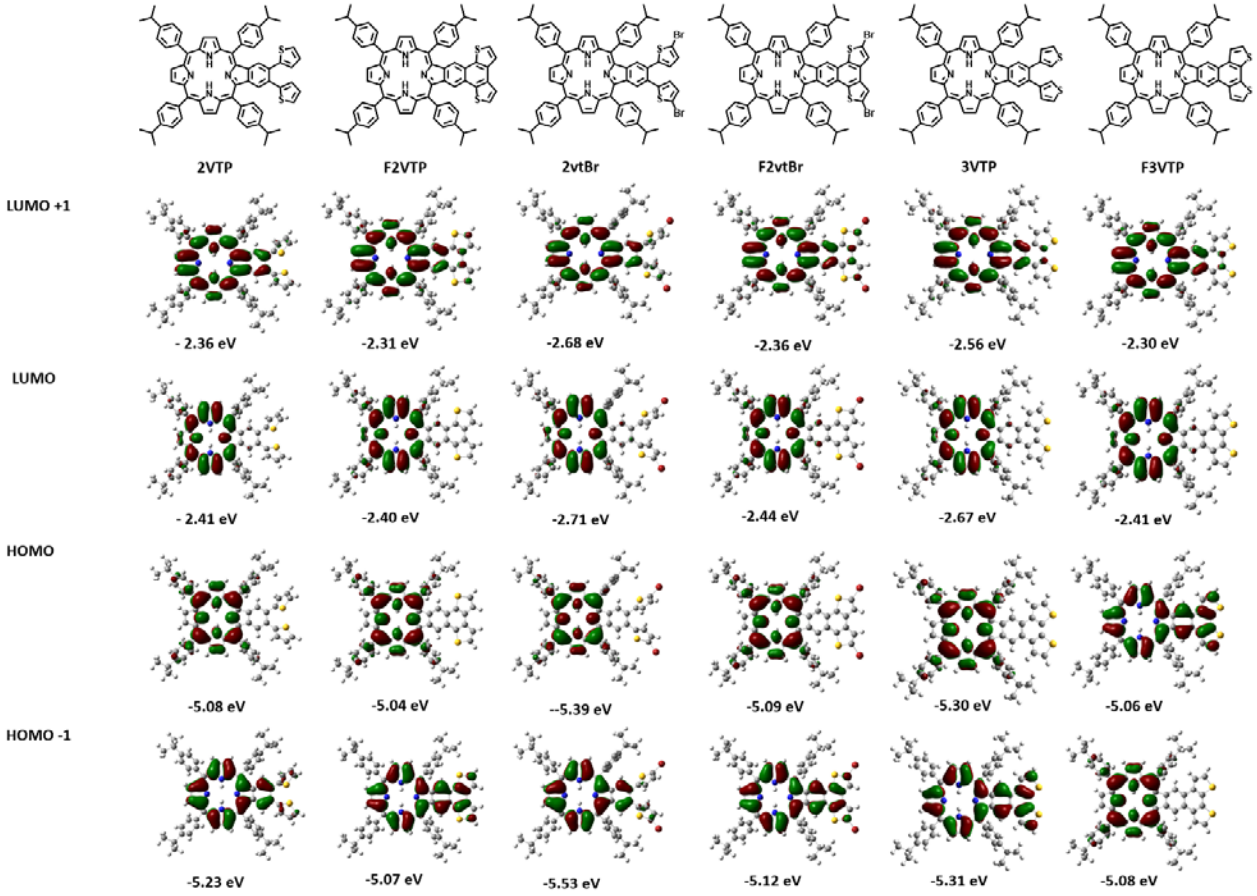

Figure 2.5: HOMO-1 to LUMO +1 isodensity surfaces for all freebase porphyrins.

Figure 2.6 shows the DFT calculations for the zinc inserted porphyrins. For the monobenzoporphyrins and the naphthoporphyrins most of the isodensity is on the porphyrin core; however, very minor isodensity is found on the benzene rings and none on the thiophene moieties. The HOMO involves not only the porphyrin core but all the way to the thiophene moieties as well for **ZnF2VTBr, Zn3VTP,** and **ZnF3VTP**. LUMO +1 shows the porphyrin core and the benzene fused rings having isodensity for **Zn2VTP, Zn3VTP** and **ZnF3VTP**. Similarly, the brominated porphyrins **Zn2VTBr** and **F2VTBr** show the involvement of the porphyrin core, the

benzene, and the naphthalene rings, and the thiophene moieties. These DFT calculations suggest that even slight changes in the structure can affect the electronic properties.

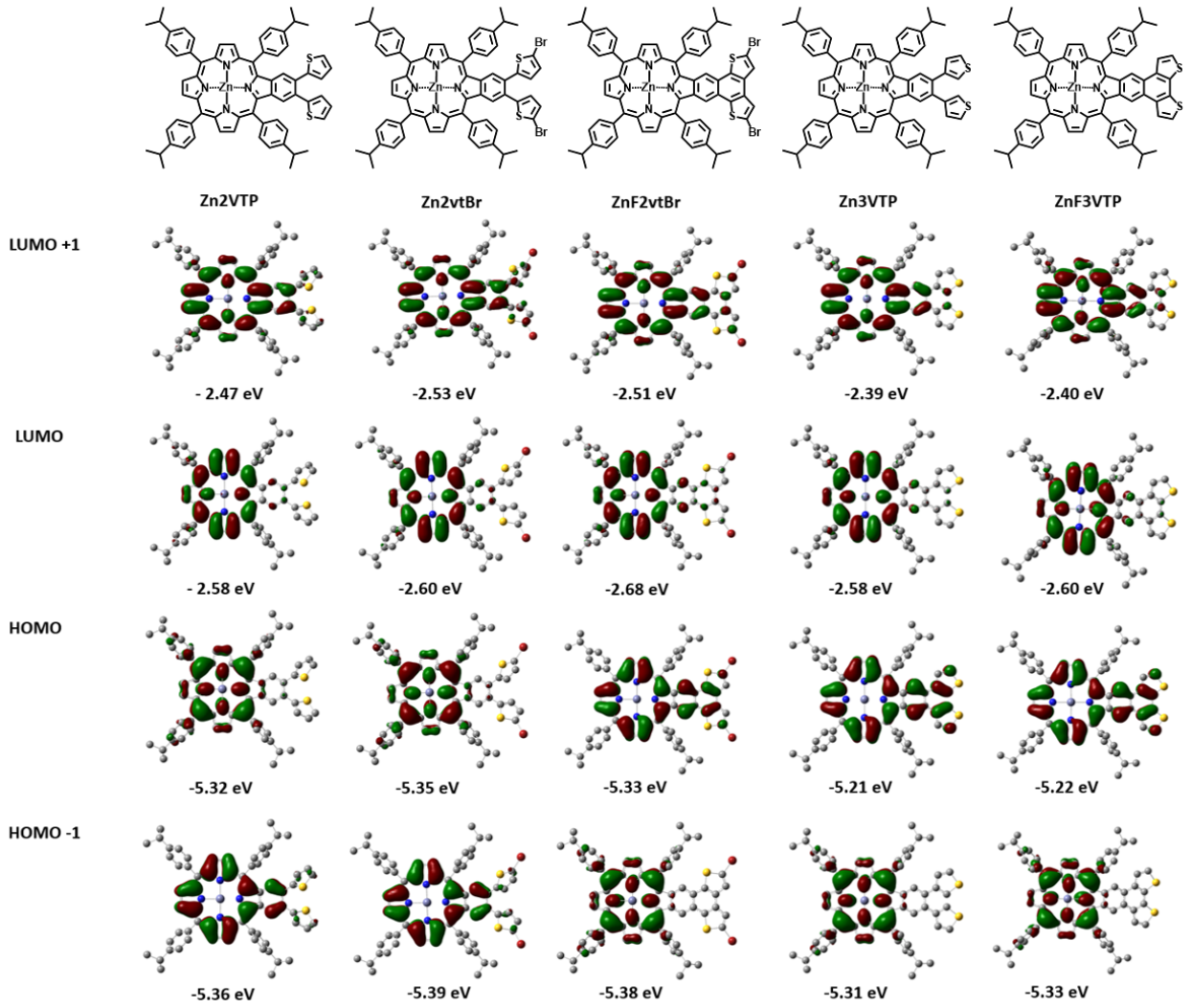

Figure 2.6: HOMO-LUMO isodensity surfaces and energy levels for the synthesized Zinc porphyrins

In Figure 2.7, little difference in the energy gap was observed when comparing **3VTP, F3VTP** and **F2VTBr** and their zinc derivatives. **Zn2VTP** and **Zn2VTBr** on the other hand have a larger energy gap than their freebase analogues. Overall, as mentioned in section 2.3.1, the DFT calculated energy gaps agree with those of the experimentally determined by the Tauc plots for both the free base and the zinc porphyrins with a maximum ΔE of 0.08 eV.

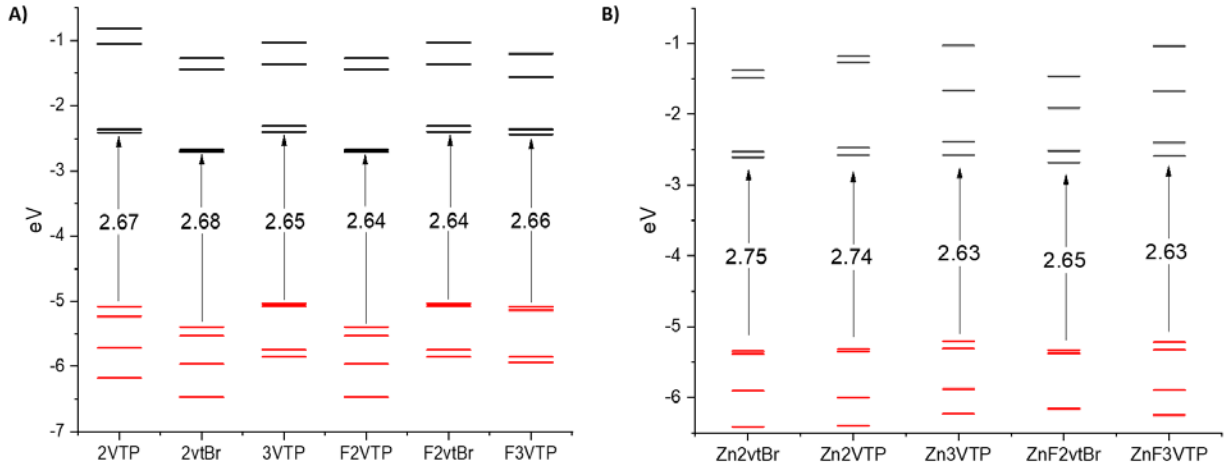

Figure 2.7: Computationally calculated energy level diagrams for A) free base porphyrins and B) zinc porphyrins.

2.4.2 TDDFT Calculations

Figure 2.8 shows the overlaid spectra of experimentally obtained molar absorptivity spectra and the calculated oscillation strengths for each compound. A complete oscillator table can be found in the experimental section. For the monobenzoporphyrins **2VTP, 3VTP,** and **2VTBr** the HOMO/LUMO and HOMO/LUMO+1 transition predominately corresponds to the Q bands. The Q bands of **F2VTP** and **F3VTP** are a result of the transition between HOMO-1/LUMO and HOMO/LUMO whereas **F2VTBr** Q bands correspond to HOMO/LUMO and HOMO/LUMO+1. **Zn2VTP**, **Zn3VTP**, and **Zn2VTBr** have one Q band because of the HOMO/LUMO transition, but the second set of Q bands are attributed to different transitions: HOMO-1/LUMO+1 (**Zn3VTP**), HOMO-1/LUMO (**Zn2VTP**), and HOMO/LUMO+1 (**Zn2VTBr**). **ZnF3VTP** and **ZnF2vtBr** Q bands both arise due to the HOMO/LUMO and HOMO-1/LUMO transitions.

The Soret bands of **2VTP** and **3VTP** have a higher probability of HOMO-1/LUMO but also show only a difference of around 5% lower contribution from HOMO-2/LUMO+1 (**2VTP**) and HOMO/LUMO+1 (**3VTP**). **The** Soret band of **2VTBr** has only a 28.4% probability that it

corresponds to the HOMO-2/LUMO+1 but also contributions from HOMO-1/LUMO and HOMO-1/LUMO+1 at 20.4% and 18% respectively. A similar pattern was observed with the naphthodithiophenyl-fused porphyrins in which the Soret band has a higher probability from the HOMO-1/LUMO (**F2VTP** and **F2VTBr**) and HOMO-LUMO (**F3VTP**) transitions. There is a difference of, once again, 5% between the first and second highest contributing transitions HOMO/LUMO+1 (**F2VTP**) and HOMO-2/LUMO+1 (**F3VTP**). The Soret band for **Zn2VTP** and **Zn2vtBr** is a result of the HOMO-1/LUMO+1 transition whereas **Zn3VTP** is attributed to HOMO/LUMO+2. The **ZnF3VTP** Soret band corresponds to the HOMO-1/LUMO+1 transition and the Soret of **ZnF2VTBr** is a result of the HOMO/LUMO+1.

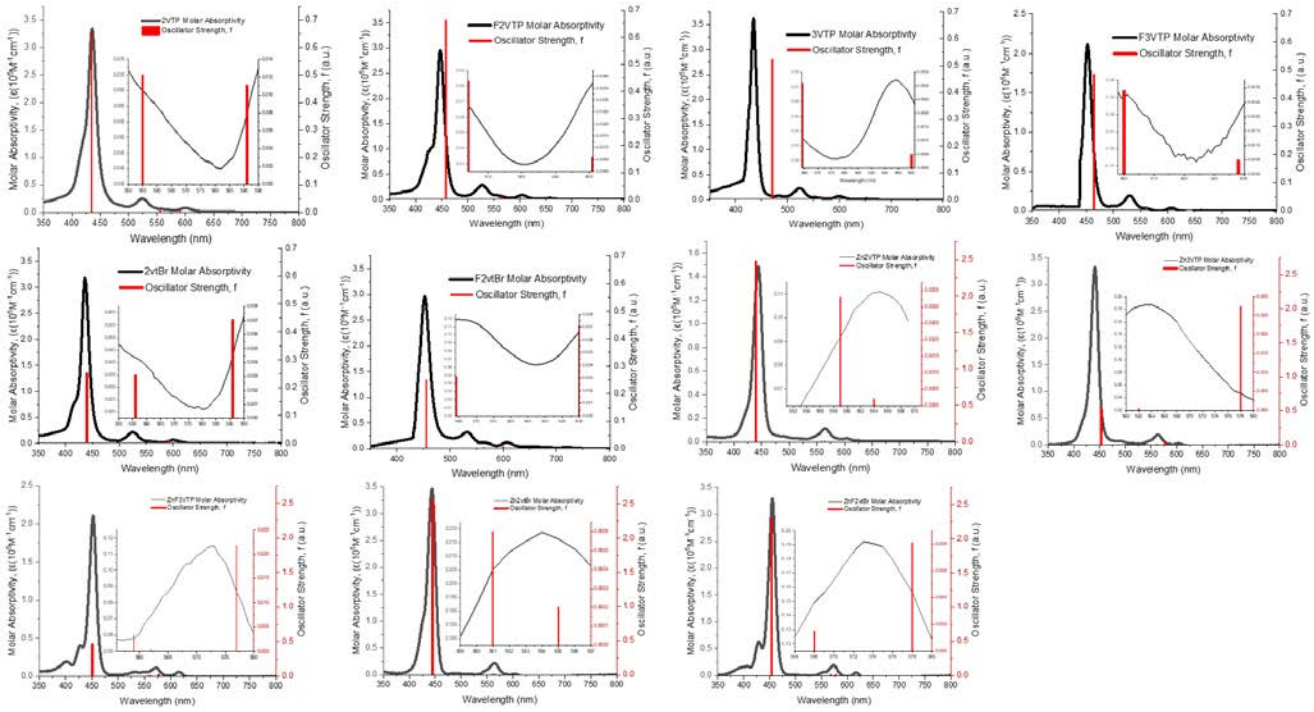

Figure 2.8: TDDFT Oscillator strength graph overlaid with the UV-VIS molar absorptivity of both free base and zinc dithiophenyl-fused porphyrins.

2.5 Aromaticity Studies

Common methods utilized in analyzing aromaticity include nucleus independent chemical shift (NICS), anisotropy current induced density (AICD), aromatic stabilization energies (ASE), and harmonic oscillator model of aromaticity. Of these aromaticity indices AICD and NICS were explored for this class of naphthodithiophene-fused porphyrins. AICD is a useful tool to visually analyze the global aromaticity of a compound but is limited in comparison to the others. NICS— in which a dummy atom is placed at the center of the molecule (NICS(0)) or 1Å (NICS(1)) above the molecule as a probe—is perhaps the most commonly reported in literature as it agrees well with other aromaticity indices. It is especially useful in determining aromatic, antiaromatic, and nonaromatic compounds as the chemical shielding value will either be negative, positive, or close to zero, respectively. However, there are also some problems utilizing this method: 1) in the case of NICS(0) and NICS(1), it is incapable of recognizing the source of the induced field or identify the individual contributions to said field, 2) magnetic information obtained is a local parameter and not a collective, and 3) the value obtained can be influenced by σ-effects. Ways to alleviate these issues is the incorporation of a scanning method introduced by Stanger [14] and the NICS-density maps introduced by Koch.[15] NICS-scan is useful as it has the potential to identify the individual aromatic contributions of each ring by aligning probes along an axis. When paired with other aromaticity indices, a more accurate analysis of a compound's aromaticity can be done. To our knowledge, there has been no NICS x-scan studies done on generic or expanded porphyrin systems. Therefore, in this dissertation, we will discuss our results from the NICS-scan method of the following $NICS_{\pi zz,}$ $NICS_{\pi zz}^{SOM}$ and $NICS_{\pi zz}^{NCS}$ in combination with AICD to analyze the aromaticity of the π-extended β,β'-

dithiophenyl-fused porphyrins.

All NICS and AICD computational studies were done using Gaussian16.[16] The optimal height for the NICS-x-scan was determined by placing the NICS probes above the center of the porphyrin from 1.0 to 2.0Å at intervals of 0.1Å above the molecular plane and scanned along the x-axis at 0.2Å intervals. It was found that around 1.6Å and above have similar shapes and therefore chosen to be our height for the remaining NICS studies, which will be referred to as $\mathrm{NICS}_{zz}^{1.6Å}$; this number is similar with Stanger[14], which reported a height of 1.7Å. Based on these results, the x-scan plots were done at a height of 1.6 Å above the molecular plane and across the x-axis. All NICS calculations were done with the GIAO-B3LYP/6-31g(d) basis set. The data from these calculations were then graphed on Origin software. AICD plots were done using B3LYP/6-31G* basis set in Gaussian16 and rendered in POVray software. Three NICS calculations were done: $\mathrm{NICS}_{zz}^{1.6Å}$ which was mentioned above, $\mathrm{NICS}_{\pi zz}^{SOM}$ in which we look at a sigma only model, and $\mathrm{NICS}_{\pi zz}^{NCS}$ natural chemical shielding (NCS) with natural bond orbital (NBO) calculations. The use of both NCS and SOM are used to determine the accuracy of $\mathrm{NICS}_{zz}^{1.6Å}$. As the $\mathrm{NICS}_{\pi zz}$ has the dummy atoms placed at a height greater than 1 Å away from the molecule to reduce the sigmatropic effects utilized both the methods which focus on the removal of sigmatropic effects if vital.

To determine the most aromatic regions of a compound, we look at the minima of the graphs as those are the areas of maximum diatropic current. Stanger [17] reported the initial NICS XY-scan for multiple small molecules, including benzene and naphthalene. Benzene showed a uniformly shaped plot with only one minimum and generates a current of -10, -11, and -15 ppm for π_{zz}, NCS, and SOM methods. Naphthalene is shown to have one minimum for

both $NICS_{\pi zz}$ and $NICS_{\pi zz}^{NCS}$ plots and two for $NICS_{\pi zz}^{SOM}$. If the aromatic character was a result of the two benzene rings generating their own current, then the expected NICS values of naphthalene should be doubled. However, that was not the case. This proved that the origin of diatropic current in naphthalene does not come because of two isolated benzenic ring currents, but instead a global current is shown involving both rings. This allows us to get an aromatic reference point for specific sections of our synthesized porphyrins.

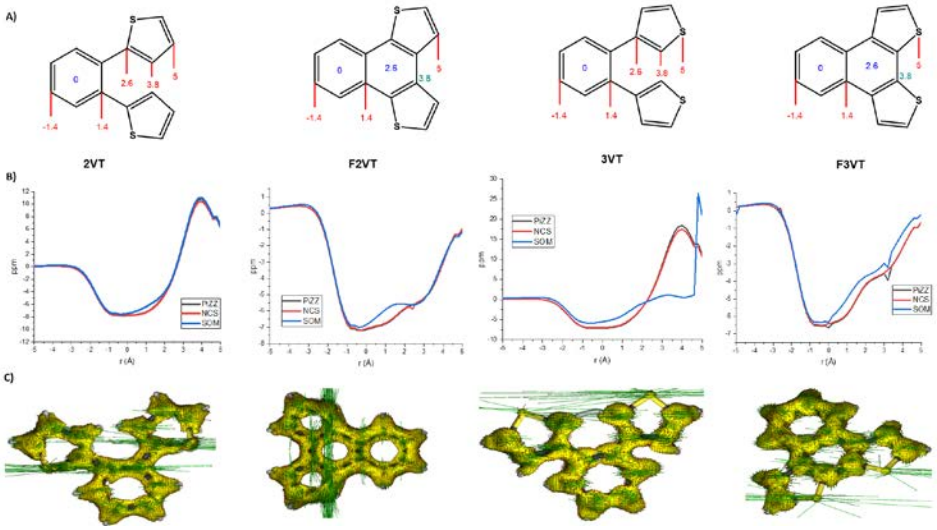

Figure 2.9: Aromaticity studies of fused unfused 1,2-di(thiophen-2-yl) and 1,3-di(thiophen-2-yl). a) Fused and unfused 1,2-di(thiophen-2-yl) and 1,3-di(thiophen-2-yl) structures; red indicates a dummy atom on the edge of a ring; blue indicates a dummy atom placed center of a ring and teal indicates a dummy atom over C-C bond; b) shows the plotted $NICS_{x\text{-}scan}$ studies using all three methodologies; c) shows the AICD plots.

To better understand the properties of these compounds, we first looked at the NICS-XY-scan[17] (Figure 2.9b) and AICD plots (Figure 2.9c) of the thiophene derivatives: 1,2-di(thiophen-3-yl)benzene (**3VT**), 1,2-di(thiophen-2-yl)benzene (**2VT**) and their fused analogues naphtho[2,1-*b:*3,4-*b'*]dithiophene (**F3VT**) and naphtho[1,2-*b:*3,4-*b'*]dithiophene (**F2VT**) respectively from a distance -5 to 5 Å. Both uncyclized compounds show nonaromatic character from approximately -5 to -2 Å, which is attributed to these dummy atoms being

outside of the benzene ring, before aromatic character begins from -1 to 2 Å. There is then a drastic increase in the antiaromatic characteristics from 3 to 5 Å. This can be attributed to the two thiophene rings not being in plane with each other.

All three methodologies show a similar shape and ppm values for **2VTP**. **3VTP** shows a similar shape for all three methods from -5 to -1 Å before the SOM calculations deviate from the other two particularly when it came to antiaromatic characteristics. Once the thiophene rings are fused to form the naphthalene moiety, the antiaromatic character disappears, which makes sense as the plane of aromaticity is extended by fusing the thiophene rings. Both **F3VTP** and **F2VTP** show nonaromatic regions from -5 to -2 Å and aromatic character from -1 to 3 Å. Figure 2.10a shows specific distances at which ppm were recorded and can be seen in the experimental section. AICD plots indicate that all four compounds display global aromaticity, however the sulfur atoms in **2VTP, 3VTP,** and **F3VTP** do not show aromatic current. **F2VTP** on the other hand shows full aromatic current along the entire molecule with sulfur atoms included. The geometric center, benzene moiety (ring 1), in **2VTP** ($\mathrm{NICS}_{\pi zz}^{NCS}$ -7.75 ppm) and **3VTP** ($\mathrm{NICS}_{\pi zz}^{NCS}$ -6.94 ppm) shows the strongest aromaticity. **F2VTP** ($\mathrm{NICS}_{\pi zz}^{NCS}$ -7.1 ppm) and **F3VTP** ($\mathrm{NICS}_{\pi zz}^{NCS}$ -6.4 ppm) aromatic studies show that ring 1 still has the stronger aromatic character compared to ring 2 ($\mathrm{NICS}_{\pi zz}^{NCS}$ -5.5 ppm and $\mathrm{NICS}_{\pi zz}^{NCS}$ -3.7 ppm respectively). The specific NICS distances at which ppm were recorded can be seen in the experimental section.

The geometric center of all compounds discussed in this chapter refers to the center of the porphyrin core. Figure 2.10b shows the NICS scans of the monobenzoporphyrins. All three NICS methods show a consistent shape and close ppm values. Since all compounds have negative ppm values, it can be concluded that there is diatropic current present within the

systems. **2VTP** has two minima at -28.4 ppm (-2 Å) and – 29.6 ppm (1 Å). **3VTP** also displays two minima at -30.2 ppm (-1.6 Å) and -32.4 ppm (1.8 Å). **2VTBr** only has one minimum which shows at -9.6 ppm (-1 Å). This area of diatropic current is drastically lower than that of either **2VTP** or **3VTP**. This could be a result of the electron-withdrawing properties of bromine pulling away the electron density of the thiophene moiety. As expected, in the case of **2VTP** and **3VTP,** the minimum on the positive axis tends to have more aromatic character due to the attachment of the benzene moiety fused to the porphyrin core. Furthermore, these plots demonstrate a lower-than-expected diatropic current of the benzene ring fused to the porphyrin of both **2VTP** ($\mathrm{NICS}_{\pi zz}^{\mathrm{NCS}}$ -4.22 ppm), **3VTP** ($\mathrm{NICS}_{\pi zz}^{\mathrm{NCS}}$ -1.93 ppm)**,** and to a much smaller scale **2VTBr** ($\mathrm{NICS}_{\pi zz}^{\mathrm{NCS}}$ -1.24 ppm). However, the AICD plots in Figure 11c show that each porphyrin has global aromaticity. This indicates that the local aromaticity of the benzene rings is compromised with the global aromaticity of the compounds.

It is interesting that different trends in terms of impact on aromaticity were observed for the fusion of isomeric heterocycles to porphyrin. The plot shapes derived from the NCS, SOM, and π_{zz} NICS methods are consistent with each other (Figure 2.10b). **F2VTP,** displaying two minima at -40 ppm (-1.6 Å) and -50 ppm (1.8 Å), showed a drastic increase in the aromatic character upon the fusion of the thiophene rings with the minima on the positive axis being more intense. **F3VTP** displays a similar shape and only a minimal change in diatropic current—two minima at -31.6 ppm (-1.8 Å) and -32.7 ppm (-1.8 Å)—as that of **3VTP**. The two minima are of almost equal intensity. Although **3VTP** shows stronger diatropic current compared to **2VTP**, the naphthodithiophene-fused **F2VTP** displays a stronger aromatic character than its **F3VTP** counterpart. This could be attributed to the **F2VT** (Figure 2.10c) showing a global current across

the entire molecule whereas **F3VT** has global aromaticity everywhere except the sulfur atoms and a stronger aromatic character in comparison. **F2VTBr** shows a difference in shape when compared to **2VTBr** as develops a second minima upon the C-C coupling and—although similar peaks within the spectra are still shown—a difference of ppm values for NCS and π_{zz} NICS methods compared to those of SOM. **F2VTBr** has a minimum at -14.1 ppm (-1.6 Å) and a more intense minimum at -20.1 ppm (2 Å). Both values show far more aromatic character than that of its monobenzoporphyrin analouge **2VTBr**.

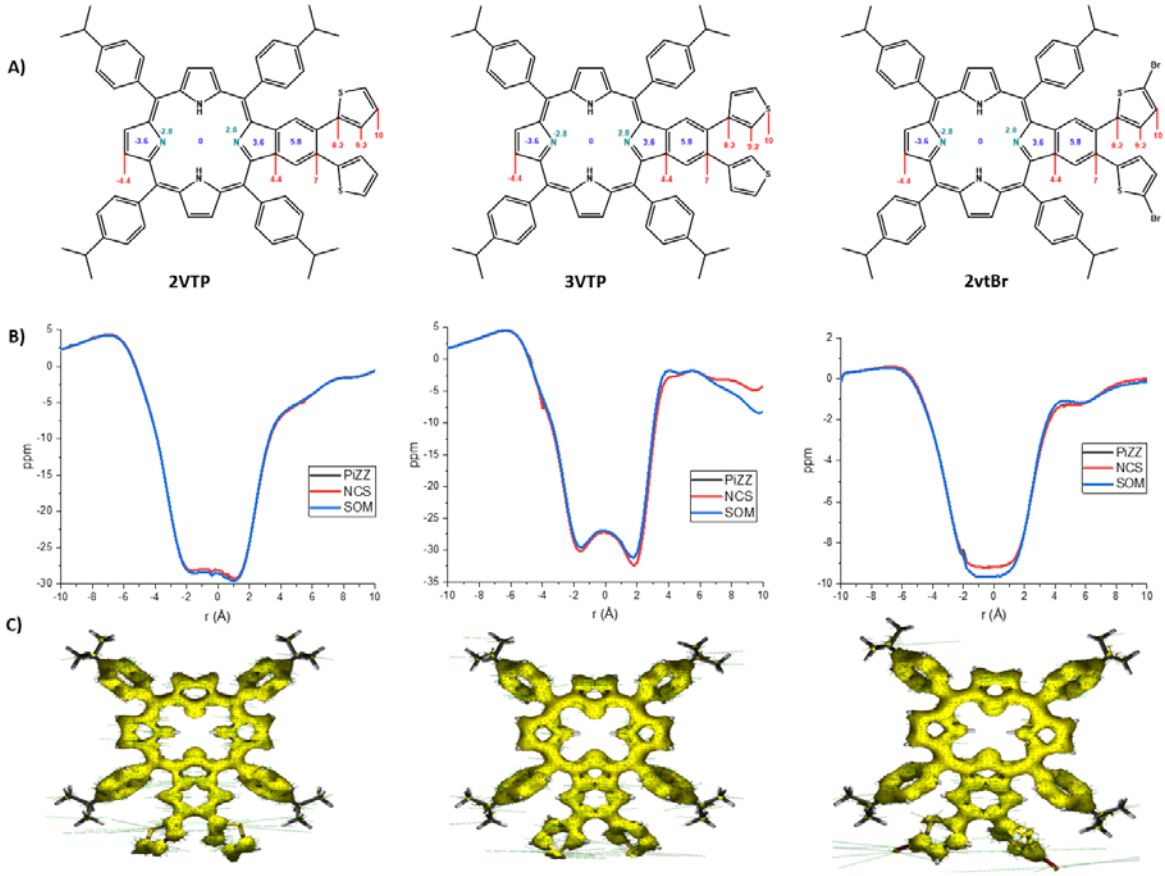

Figure 2.10: Aromaticity studies a) 2VTP, 3VTP, and 2VTBr; red indicates a dummy atom on the edge of a ring; blue indicates a dummy atom placed center of a ring and teal indicates a dummy atom over C-C bond; b) plotted NICS$_{xyscan}$ studies using all three methodologies; c) shows the AICD plots.

Like the monobenzoporphyrins, the plots for **F2VTP** ($NICS_{\pi zz}^{NCS}$ -15.9 ppm) and **F3VTP** ($NICS_{\pi zz}^{NCS}$ -9.16 ppm) also show a lower-than-expected diatropic current in the benzene ring

fused directly to the porphyrin core of both (ring 1, 5.8 Å) and to a much smaller extent for **F2VTBr**($NICS_{\pi zz}^{NCS}$ -6.29 ppm). A return of mild aromatic character can be seen for the benzene ring in which the thiophenes are fused to (ring 2, at 8.2 Å) in **F2VTP** ($NICS_{\pi zz}^{NCS}$ -11.9 ppm), **F2VTBr** ($NICS_{\pi zz}^{NCS}$ -4.16 ppm), and **F3VTP** ($NICS_{\pi zz}^{NCS}$ -7.05 ppm). However, the AICD plots in Figure 2.11c suggest that each porphyrin has global aromaticity throughout the conjugated system (excluding the thiophene moieties). These data indicate that the local aromaticity of ring 1 is still relinquished to the global aromaticity of the compounds even for the naphthodithiophene-fused porphyrins.

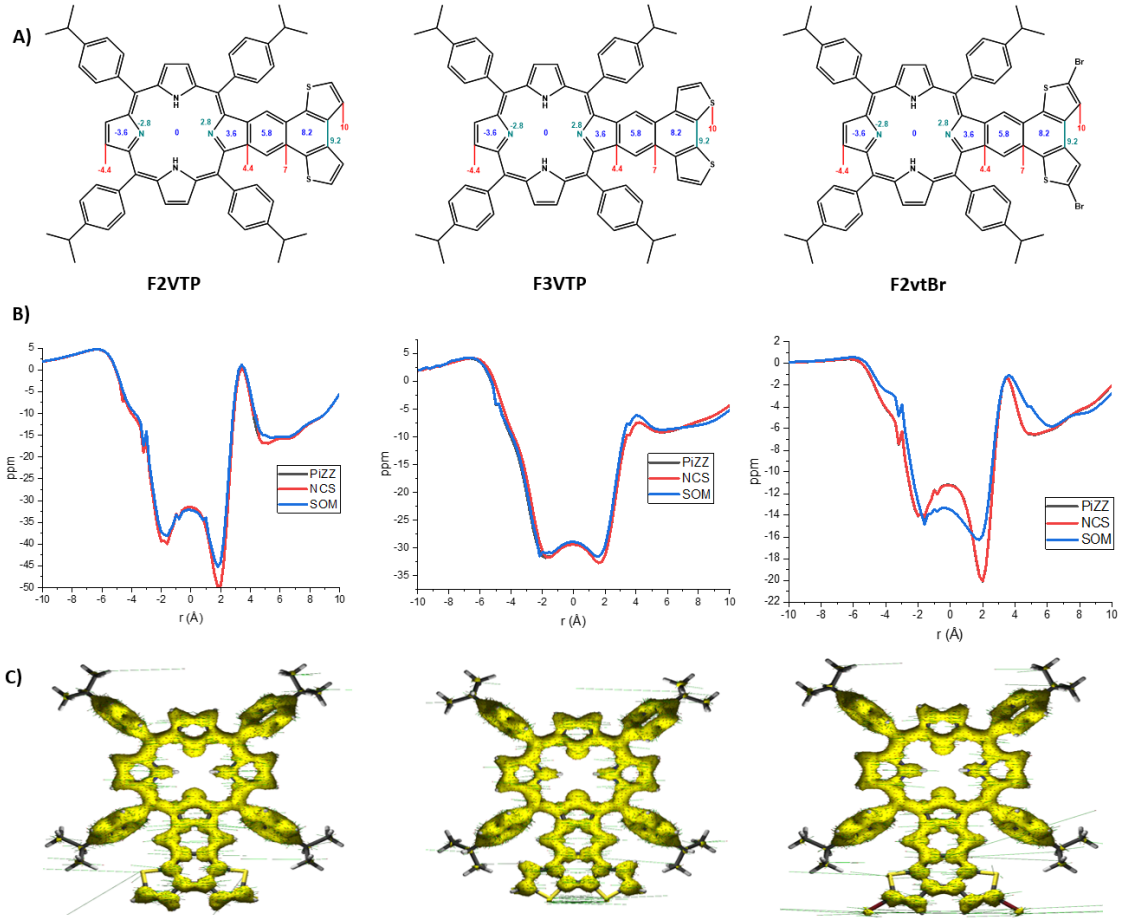

Figure 2.11: Aromaticity studies a) F2VTP, F3VTP, and F2VTBr; red indicates a dummy atom on the edge of a ring; blue indicates a dummy atom placed center of a ring and teal indicates a dummy atom over C-C bond; b) shows the plotted $NICS_{xyscan}$ studies using all three methodologies; c) shows the AICD plots.

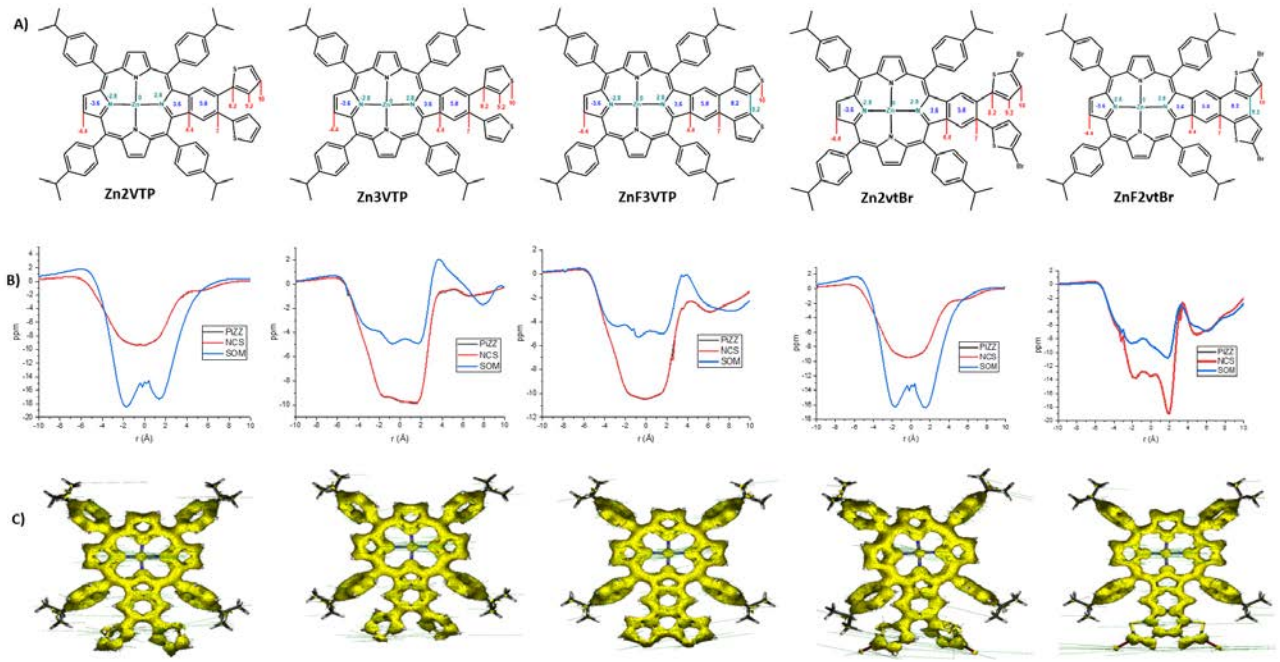

Figure 2.12: Aromaticity studies a) Zn2VTP, Zn3VTP, Zn2vtBr, ZnF3VTP, and ZnF2vtBr; red indicates a dummy atom on the edge of a ring; blue indicates a dummy atom placed center of a ring and teal indicates a dummy atom over C-C bond; b) shows the plotted $NICS_{xscan}$ studies using all three methodologies; c) shows the AICD plots.

All zinc porphyrins exhibit similar shapes for both the $\mathrm{NICS}_{\pi zz}^{\mathrm{NCS}}$ and $\mathrm{NICS}_{\pi zz}$ plots. **Zn2VTP** (-9.41 ppm), **Zn2VTBr** (-9.42 ppm) and **ZnF3VTP** (-10.4 ppm) give an almost uniform minimum. **Zn3VTP** shows three minima (-9.29, -9.73, and -9.83 ppm), at -1.6, 0, and 1.6 Å respectively, with only gradual intensities differences. **ZnF2VTBr** has two minima at -1.6 Å (-13.7 ppm) and 1.8 Å (-18.9 ppm). Unlike the freebase porphyrins, the $\mathrm{NICS}_{\pi zz}^{\mathrm{SOM}}$ plot for most of the zinc compounds do not share a similar shape as the other plots. Only **ZnF2VTBr** has similar minima shapes, but the aromatic character does decrease by about half. **Zn2VTP** and **Zn2VTBr** develop two minima. **Zn2VTBr** has equal intensity peaks at -1.6 Å (-16.2 ppm) and 1.6 Å (-16.3 ppm) whereas **Zn2VTP** has a more intense minimum at -1.8 Å (-18.4 ppm) and a second one at 1.4 Å (-17.3 ppm). **Zn3VTP** still has three minima at -2.8 (-3.76 ppm), -0.8 (-4.96 ppm), and 1.6 Å (-4.94 ppm). The intensities of these peaks are more pronounced compared to the other two

methods. **ZnF3VTP** develops four minima at -3 (-4.33 ppm), -1.4 (-4.74 ppm), -0.8 (-5.27 ppm), and 1.6 Å (-5.00 ppm) and more closely resembles **Zn3VTP**. The drastic differences between the $\mathrm{NICS}_{\pi zz}^{\mathrm{SOM}}$ plots to those of both $\mathrm{NICS}_{\pi zz}^{\mathrm{NCS}}$ and $\mathrm{NICS}_{\pi zz}$ only for the zinc-inserted porphyrins indicate that the zinc does not contribute to the aromaticity.

2.6 Crystal Structures

Figure 2.13 shows the X-ray crystal structures of **2VTP** (CCDC, 2210548) and **3VTP** (CCDC, 210550) that our collaborator Dr. Vladimir Nestrov resolved. The thiophenyl groups substituted do not affect the conformation of the macrocycle as both the porphyrin core and the fused benzene ring have a planar geometry. The crystal structures of naphthodithiophene-fused porphyrins (**F2VTP**, **F3VTP** and **F2VTBr)** are not available.

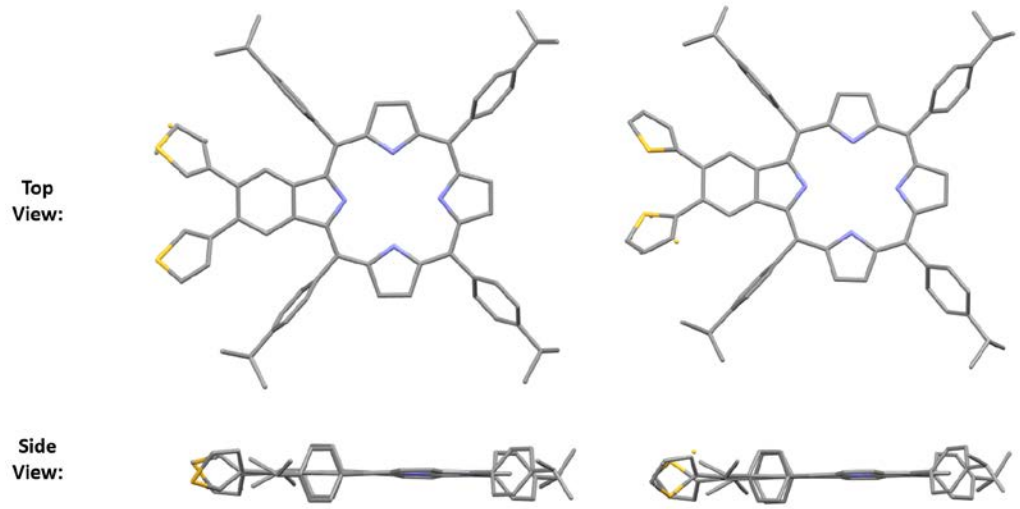

Figure 2.13: X-ray crystal structures of 2VTP (right) and 3VTP (left)

2.7 Conclusion

In this work synthetic methods were developed for the synthesis of a new class of π-extended porphyrins fused with napthodithiophenes through a Heck-based cascade reaction for **2VTP** and **3VTP**. Utilizing a sonication method with NBS, bromination at the 5-positions of

the thiophene was achieved to create **2VTBr**. An oxidative coupling reaction on each of these compounds, utilizing Scholl conditions, generated the naphthodithiophenes-fused porphyrins **F2VTP, F3VTP,** and **F2VTBr.** We have also synthesized the zinc analogues of these porphyrins and a total of eleven dithiophenyl-fused porphyrins were obtained. These compounds were experimentally characterized through UV-VIS absorption, steady state and time resolved fluorescence spectroscopy, differential pulse and cyclic voltammetry with the help of our collaborators. **F2VTP**, **F3VTP**, **F2VTBr**, **ZnF2VTBr**, and **ZnF3VP** showed broadening and bathochromatic shifts when compared to the precursor benzoporphyrins. This can be attributed to the extended π-conjugation. Fluorescence studies performed by our collaborator Dr. Sergei Vinogradov showed similar fluorescence emission patterns. The fluorescence lifetimes were found to be 0.7 ns, 0.3 ns, and 0.5 ns higher than that of TPP (9.9 ns) for **2VTP, 3VTP,** and **2VTBr** respectively. The naphthodithiophene-fused porphyrin analogues had even longer lifetimes (**F2VTP**, 13 ns; **F3VTP**, 12.1 ns; **F2vtBr**, 12.9 ns) compared to both their precursors and TPP. DFT calculations were also done to help characterize this new porphyrin class. Optimization and energy studies helped generate the HOMO-LUMO diagrams and the energy band gap, AICD and NICS were used to gauge global aromaticity across the macrocycle. These DFT calculations support the fluorescence data where the sulfur atoms are not involved in the frontier orbitals due to minimal electronic effects on the position of the thiophenes within the π-extended structures. This can be seen especially in the AICD which shows no current density present on the sulfur atom in any of the synthesized porphyrins. NICS studies demonstrated how even slight changes in the dithiophenyl-moieties influence the global aromaticity of the entire macrocycle. The characterization done on this class of porphyrins will

provide a useful template for further incorporation of aromatic heterocycles into β, β'-π-extended porphyrins.

2.8 Experimental Section

2.8.1 General Information

All reagents, including solvents, not specified below was purchased from Ambeed, Millipore-Sigma, Matrix-Scientific, and Fisher and—excluding DMF which was dried through a commercially available purification system—was used without further purification. All porphyrin products underwent purification on either a plug or column chromatography on silica gel. All reactions were monitored with UV-VIS and analytical thin-layer chromatography.

2.8.2 Synthesis and Characterization

Synthesis of 2-vinylthiophene and 3-vinylthiophene: A modified version of the reported synthesis [18] was done in which Potassium carbonate (32 mmol), and methyltriphenylphosphonium bromide (28 mmol) were added to a Schlenk flask and placed under vacuum and heated to 100°C overnight. The vacuum was released under an argon atmosphere to add anhydrous dioxane (20 mL) and the corresponding thiophenecarboxyaldehyde (18 mmol) was added and the flask was sealed and refluxed overnight. Then the reaction mixture was then run through celite with hexanes and undergone an aqueous work up, followed by a silica plug in hexanes. The products were isolated (50-60% yields).

Synthesis 2VTP and 3VTP: Dibromoporphyrin **1** (0.212 mmol), potassium carbonate (0.467 mmol), $Pd[OAc]_2$ (0.106 mmol), and triphenylphosphine (0.2763 mmol) was added to a

Schlenk flask and placed under argon and dissolved in dimethylformamide/xylenes (10 mL). The respective vinylthiophene (2.21 mmol) was then added and the mixture was degassed by four freeze-pump-thaw cycles. The solution was heated at 90°C for four days. A silica plug with toluene was done to remove excess Pd^0 and polymer before the solvent was removed under vacuum; the desired product was collected and recrystallized using dichloromethane/methanol.

2VTP

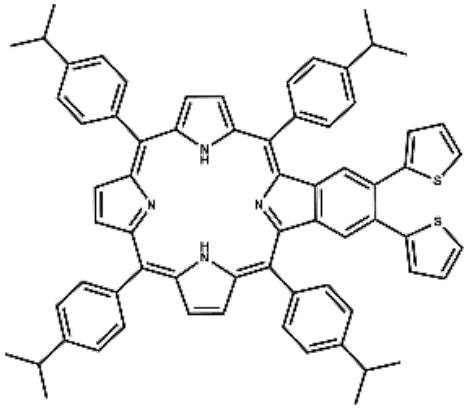

$C_{68}H_{60}N_4S_2$; purple crystalline solid; 41% yield; ^{1}H NMR (500 MHz, $CDCl_3$) δ 8.90 (d, *J* = 4.9 Hz, 2H), 8.83 (d, *J* = 4.9 Hz, 2H), 8.72 (s, 2H), 8.13 (dd, *J* = 14.5, 8.0 Hz, 8H), 7.63 (dd, *J* = 18.6, 7.9 Hz, 8H), 7.30 (s, 2H), 7.25 (d, *J* = 1.1 Hz, 1H), 7.24 (d, *J* = 1.1 Hz, 1H), 6.94 6.94 (dd, *J* = 5.2, 3.5 Hz, 2H), 6.80 (dd, *J* = 3.4, 1.2 Hz, 2H), 3.30 – 3.20 (m, 4H), 1.64 (s, *J* = 7.0 Hz, 6H) 1.49 (s, *J* = 7.0 Hz, 6H), -2.57 (s, 2H); ^{13}C NMR (500 MHz, $CDCl_3$) δ 149.22, 148.23, 139.82, 139.38, 134.66, 133.62, 127.29, 127.11, 126.68, 125.94, 125.83, 124.80, 34.29, 34.11, 24.29. UV/VIS (DCM): λ_{max} (log ε) = 436 (5.82), 525 (4.70), 562 (4.06), 600 (4.21), 656 (3.58) nm. HRMS (MALDI): m/z: calculated for $C_{68}H_{60}N_4S_2$: 996.425; found 996.424.

3VTP

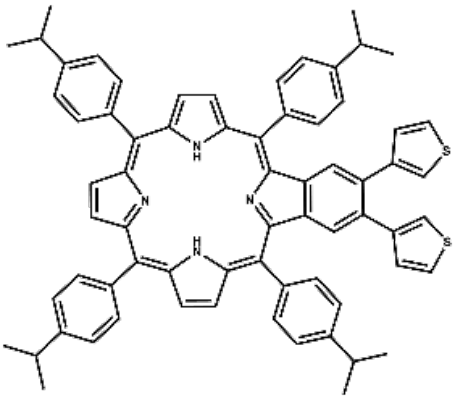

$C_{68}H_{60}N_4S_2$; purple, crystalline solid; 58% yield; ^{1}H NMR (500 MHz, $CDCl_3$) δ 8.90 (d, *J* = 4.8 Hz, 2H), 8.82 (d, *J* = 4.9 Hz, 2H), 8.72 (s, 2H), 8.13 (t, *J* = 7.8 Hz, 8H), 7.66 (d, *J* = 7.9 Hz, 4H), 7.61 (d, *J* = 7.9 Hz, 4H), 7.28 (s, *J* = 10.7 Hz, 2H), 7.15 (dd, *J* = 4.9, 3.0 Hz, 2H), 6.93 (dd, *J* = 3.1, 1.3 Hz, 2H), 6.71 (dd, *J* = 4.9, 1.2 Hz, 2H), 3.29 – 3.23 (m, 4H), 1.55 (s, 5H), 1.54 (s, 6H), 1.54 (s, 8H), 1.52 (s, 5H), -2.55 (s, 2H). ^{13}C NMR (126 MHz, $cdcl_3$) δ 134.65, 133.70, 132.94, 129.17, 126.57, 125.86, 124.80, 124.26, 122.90, 34.28, 34.11, 24.39, 24.30. UV/VIS (DCM): λ_{max} (log ε) = 434 (5.85), 522 (4.67), 557 (4.98), 599 (4.17), 649 (3.63) nm. HRMS (MALDI): m/z: calculated for $C_{68}H_{60}N_4S_2$: 996.425; found 996.425.

2VTBr

A modification of a previously reported methodology[42] to attach bromine to thiophene was used for our porphyrin system. 2VTP (0.05 mmol) and recrystallized N-bromosuccinimide (2 eq, 0.1 mmol) was dissolved in CH_2Cl_2 and sonicated for 30 sec before being quenched with triethylamine followed by an aqueous work up with deionized water. The desired product was collected and recrystallized using dichloromethane/methanol.

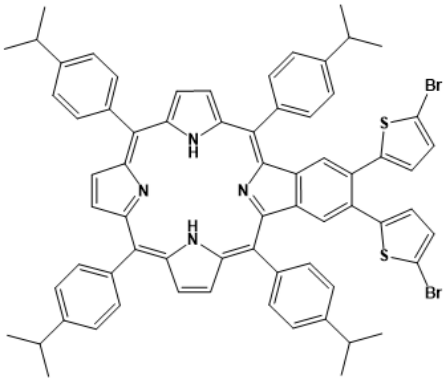

$C_{68}H_{58}N_4Br_2S_2$; purple crystalline solid; 86% yield; ^{1}H NMR (400 MHz, $CDCl_3$) δ 8.90 (d, *J* = 4.9 Hz, 2H), 8.83 (d, *J* = 4.9 Hz, 2H), 8.72 (s, 2H), 8.16 – 8.10 (m, 8H), 7.63 (dd, *J* = 18.6, 7.9 Hz, 8H), 7.31 (s, 2H), 7.25 (dd, *J* = 5.2, 1.2 Hz, 2H), 6.94 (dd, *J* = 5.2, 3.5 Hz, 2H), 6.80 (dd, *J* = 3.4, 1.2 Hz, 2H), 3.28 – 3.22 (m, 4H), 1.55 (s, 5H), 1.54 (s, 9H), 1.49 (s, 5H), 1.48 (s, 5H), -2.56 (s, 2H). ^{13}C NMR (126 MHz, $CDCl_3$) δ 149.21, 148.23, 143.75, 139.82, 139.39, 134.66, 133.62, 131.33, 127.29, 127.13, 126.68, 125.94, 125.83, 124.80, 121.14, 117.31, 34.29, 34.11, 24.29. UV/VIS (DCM): λ_{max} (log ε) = 436 (5.80), 524 (4.64), 563 (4.3.83), 600 (4.14), 653 (3.22) nm. HRMS (MALDI): m/z: calculated for $C_{68}H_{58}N_4Br_2S_2$: 1154.244; found 1154.243.

F2VTBr

Procedure**: 2VTBr** (0.0336 mmol) was dissolved in dry CH_2Cl_2. Ferric chloride (20 eq, 0.672 mmol) was dissolved in 1 mL nitromethane and added to the reaction solution slowly. It was allowed to react at room temperature for 20 min. Triethylamine was added to quench the reaction and was followed by an aqueous work up with deionized water. The desired product was collected and recrystallized using dichloromethane/methanol.

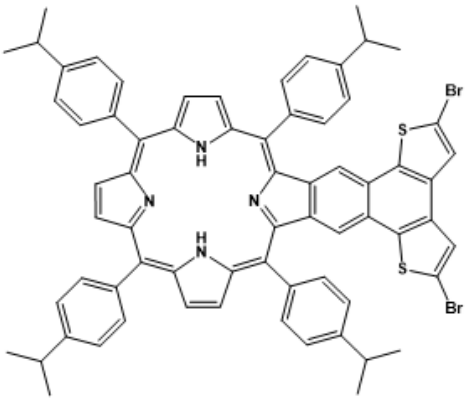

$C_{68}H_{56}N_4Br_2S_2$; purple crystalline solid; 90% yield; ^{1}H NMR (500 MHz, $CDCl_3$) δ δ 8.90 (d, *J* = 4.9 Hz, 2H), 8.80 (d, *J* = 5.0 Hz, 2H), 8.71 (s, 2H), 8.22 (d, *J* = 7.8 Hz, 5H), 8.16 (d, *J* = 7.8 Hz, 5H), 8.13 (s, 3H), 7.83 (d, *J* = 7.7 Hz, 6H), 7.75 (d, *J* = 5.1 Hz, 2H), 7.60 (dd, *J* = 18.7, 6.4 Hz, 10H), 3.52 – 3.47 (m, 2H), 3.30 – 3.25 (m, 2H), 1.73 (s, 8H), 1.72 (s, 6H), -2.36 (s, 2H). ^{13}C NMR (126 MHz, $CDCl_3$) δ 149.14, 148.21, 139.83, 139.42, 134.63, 133.71, 126.35, 125.23, 124.80, 123.01, 120.74, 116.47, 34.33, 34.11, 29.71, 24.40, 24.30, 1.03. UV/VIS (DCM): λ_{max} (log ε) = 450 (5.76), 530 (4.81), 573 (4.32), 606 (4.39), 658 (3.92) nm. HRMS (MALDI): m/z calculated for $C_{68}H_{56}N_4Br_2S_2$: 1152.228 and found 1152.227.

F2VTP

2VTP (0.0100 mmol) was dissolved in dry $CHCl_2$. Ferric chloride (0.2 mmol) was dissolved in 2mL nitromethane and added to the solution under argon and stirred at room temperature for 15 min. MeOH was added to quench the reaction and the solution was washed with 10% NaOH (aq) and deionized water before the residue was ran through a short plug before it was recrystallized with $CHCl_2$/MeOH (15% yield).

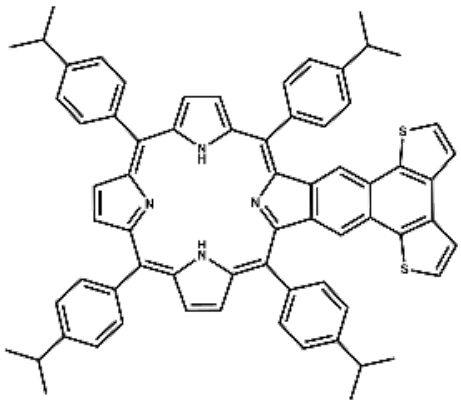

$C_{68}H_{58}N_4S_2$; purple, crystalline solid; m.p. > 300°C ^{1}H NMR (500 MHz, $CDCl_3$) δ 8.89 (d, *J* = 4.9 Hz, 2H), 8.79 (d, *J* = 4.8 Hz, 2H), 8.70 (s, 2H), 8.21 (d, *J* = 8.0 Hz, 4H), 8.15 (d, *J* = 8.0 Hz, 4H), 8.12 (s, 2H), 7.82 (d, *J* = 7.9 Hz, 4H), 7.73 (d, *J* = 5.2 Hz, 2H), 7.61 (d, *J* = 7.9 Hz, 4H), 7.57 (d, *J* = 5.2 Hz, 2H), 3.51 – 3.45 (m, 2H), 3.29 – 3.23 (m, 2H), 1.72 (s, 6H), 1.71 (s, 6H), 1.55 (s, 6H), 1.54 (s, 6H), -2.38 (s, 2H). ^{13}C NMR (126 MHz, $CDCl_3$) δ 149.13, 148.21, 139.86, 139.42, 136.79, 134.63, 133.71, 133.26, 127.76, 127.16, 126.34, 124.80, 122.96, 121.35, 120.72, 116.46, 34.32, 34.12, 24.39, 24.30. UV/VIS (DCM): λ_{max} (log ε) =449 (5.77), 527 (4.78), 564 (4.16), 605 (4.25), 657 (3.58) nm. HRMS (ESI): m/z calculated for $C_{68}H_{58}N_4S_2$: 994.4094; found 994.587.

F3VTP

3VTP (0.01 mmol) was dissolved in dry $CHCl_2$. Ferric chloride (mg, mmol) was dissolved in 2mL nitromethane and added to the solution under argon and stirred at room temperature for 14 min. MeOH was added to quench the reaction and the solution was washed with 10% NaOH (aq) and deionized water before the residue was ran through a short plug before it was recrystallized with $CHCl_2$/MeOH.

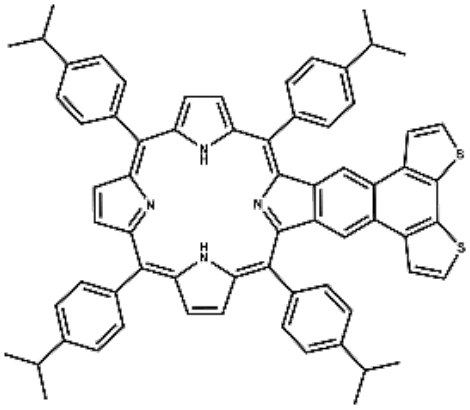

$C_{68}H_{58}N_4S_2$; purple, crystalline solid; 70% yield; ^{1}H NMR (500 MHz, $CDCl_3$) δ ^{1}H NMR δ δ 8.92 (d, *J* = 4.8 Hz, 2H), 8.81 (d, *J* = 4.8 Hz, 2H), 8.72 (s, 2H), 8.28 (s, 2H), 8.23 (d, *J* = 7.8 Hz, 4H), 8.16 (d, *J* = 7.9 Hz, 4H), 7.82 (d, *J* = 7.8 Hz, 4H), 7.60 (d, *J* = 5.9 Hz, 8H), 7.46 (d, *J* = 5.1 Hz, 2H), 3.49 – 3.45 (m, 2H), 3.30 – 3.25 (m, 2H), 1.74 (s, *J* = 7.0 Hz, 6H), 1.73 (s, 6H), 1.57 (s, *J* = 4.9, 2.1 Hz, 6H), 1.55 (s, 6H), -2.35 (s, 2H). ^{13}C NMR (126 MHz, $CDCl_3$) δ 148.95, 148.22, 140.45, 139.42, 135.43, 134.62, 133.89, 126.34, 125.78, 124.81, 123.55, 123.25, 121.45, 120.82, 116.23, 34.45, 34.12, 24.49, 24.31. UV/VIS (DCM): λ_{max} (log ε) = 446 (5.65), 529 (4.76), 572 (3.39), 608 (4.05), 652 (3.46) nm. HRMS (MALDI): m/z: calculated for $C_{68}H_{58}N_4S_2$: 994.4094; found 994.4086.

Synthesis of Zn(II) porphyrins

All of the above compounds were obtained by dissolving 0.01 mmol of porphyrin and $Zn(OAc)_2$ (10 eq, 0.1 mmol) in 3:1 $CHCl_3$/MeOH and refluxing for 1h. MeOH was then added and the reaction mixture was placed in an ice bath to recrystallize to give the products (90-94% yield).

Zn2VTP

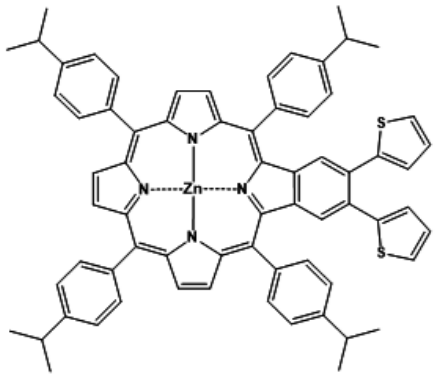

$C_{68}H_{56}N_4S_2Zn$; purple, crystalline solid; 90% yield; ^{1}H NMR (500 MHz, $CDCl_3$) δ 8.95 (d, J = 4.7 Hz, 2H), 8.88 (s, 2H), 8.83 (d, J = 4.6 Hz, 2H), 8.11 (dd, J = 21.7, 7.9 Hz, 8H), 7.62 (dd, J = 22.1, 7.9 Hz, 8H), 7.53 (s, 2H), 7.27 (d, J = 1.1 Hz, 2H), 6.96 (dd, J = 5.1, 3.5 Hz, 2H), 6.84 (dd, J = 3.5, 1.1 Hz, 2H), 3.3—3.22 (m, 4H), 1.54 (s, 6H), 1.52 (s, 6H), 1.51 (s, 6H), 1.49 (s, 6H). ^{13}C NMR (126 MHz, $CDCl_3$) δ 149.22, 148.23, 139.82, 139.38, 134.66, 133.62, 127.29, 127.11, 126.68, 125.94, 125.83, 124.80, 34.29, 34.11, 24.29. UV/VIS (DCB): λ_{max} (log ε) = 446 (5.46), 564 (4.34), 604 (3.75) nm. HRMS (ESI): m/z: calculated for $C_{68}H_{56}N_4S_2Zn$: 1058.339; found 1058.485.

Zn3VTP

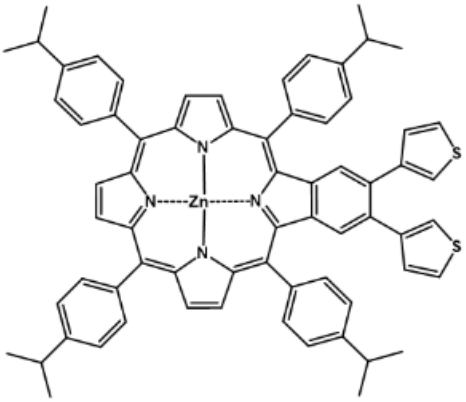

$C_{68}H_{56}N_4S_2Zn$; purple, crystalline solid; 92% yield; ^{1}H NMR (500 MHz, $CDCl_3$) δ 8.96 (d, J = 4.7 Hz, 2H), 8.89 (s, 2H), 8.83 (d, J = 4.7 Hz, 2H), 8.13 (dd, J = 13.9, 7.9 Hz, 9H), 7.67 (d, J = 7.9 Hz, 4H), 7.61 (d, J = 7.9 Hz, 5H), 7.52 (s, 2H), 7.18 (dd, J = 4.9, 3.0 Hz, 2H), 6.99 (dd, J = 2.9, 1.2 Hz, 2H), 6.76 (dd, J = 4.9, 1.2 Hz, 2H), 3.31 – 3.26 (m, 4H), 1.57 (s, 12H), 1.55 (s, 12H). ^{13}C NMR (126 MHz, $CDCl_3$) δ 152.07, 150.44, 149.84, 149.07, 148.85, 148.13, 146.13, 142.94, 140.92, 140.20, 139.50, 134.66, 134.49, 133.44, 133.15, 132.19, 132.08, 131.36, 130.96, 129.37, 126.89, 125.89, 124.76, 124.49, 123.18, 122.93, 117.83, 34.43, 34.26, 24.58, 24.47. UV/VIS (DCB): λ_{max} (log ε) = 444 (5.48), 563 (4.27), 605 (3.44) nm. HRMS (ESI): calculated for $C_{68}H_{56}N_4S_2Zn$: 1058.339 and obtained 1058.499.

Zn2VTBr

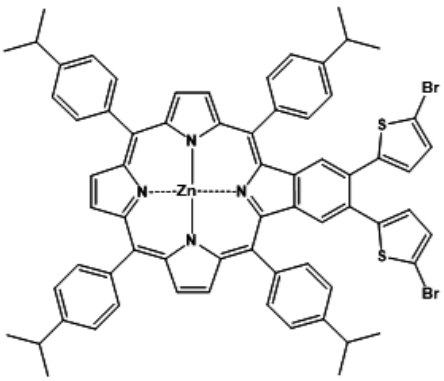

$C_{68}H_{56}N_4S_2Zn$; purple, crystalline solid; 94% yield; ^{1}H NMR (500 MHz, $CDCl_3$) δ 8.95 (d, J = 4.6 Hz, 2H), 8.88 (s, 2H), 8.83 (d, J = 4.6 Hz, 2H), 8.13 (d, J = 7.9 Hz, 5H), 8.09 (d, J = 7.9 Hz, 5H), 7.64 (d, J = 7.9 Hz, 4H), 7.60 (d, J = 7.9 Hz, 4H), 7.53 (s, 2H), 7.27 (s, 1H), 6.96 (dd, J = 5.1, 3.5 Hz, 2H), 6.84 (d, J = 2.4 Hz, 2H), 3.28—3.23 (m, 4H), 1.54 (s, 5H), 1.52 (s, 8H), 1.51 (s, 6H), 1.49 (s, 5H).. ^{13}C NMR (126 MHz, $CDCl_3$) δ 151.88, 149.78, 148.96, 148.81, 148.00, 145.69, 143.74, 140.51, 140.02, 139.42, 134.34, 133.18, 132.06, 131.37, 131.29, 130.93, 127.50, 127.22, 126.73, 125.96,

125.83, 124.62, 122.80, 117.88, 53.42, 34.28, 34.11, 29.74, 24.31, 1.03. UV/VIS (DCB): λ_{max} (log ε) = 443 (5.54), 566 (4.33), 601 (3.19) nm. HRMS (ESI): m/z: calculated for $C_{68}H_{56}N_4S_2Zn$: 1214.142; found 1214.158.

ZnF2VTBr

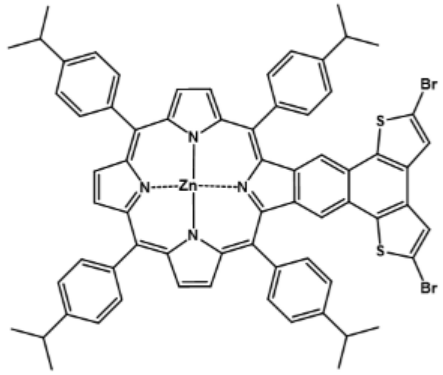

$C_{68}H_{56}N_4S_2Zn$; purple, crystalline solid; 91% yield; ^{1}H NMR (500 MHz, $CDCl_3$) δ 8.94 (d, *J* = 4.6 Hz, 2H), 8.86 (s, 2H), 8.78 (d, *J* = 4.6 Hz, 2H), 8.31 (s, 2H), 8.16 (dd, *J* = 12.2, 7.8 Hz, 8H), 7.82 (d, *J* = 7.9 Hz, 4H), 7.61 (d, *J* = 7.8 Hz, 4H), 7.50 (d, *J* = 5.1 Hz, 2H), 3.53 – 3.47 (m, 2H), 3.31 – 3.25 (m, 2H), 1.74 (s, 5H), 1.73 (s, 6H), 1.57 (s, 6H), 1.53 (s, 7H). ^{13}C NMR (500 MHz, $CDCl_3$) δ 152.46, 149.47, 148.86, 148.40, 147.98, 146.46, 140.55, 140.05, 138.37, 136.66, 134.28, 133.23, 126.27, 124.62, 77.26, 77.00, 76.75, 34.32, 34.11, 29.40, 24.40, 24.32. UV/VIS (DCB): λ_{max} (log ε) = 446 (5.51), 575 (4.27), 617 (3.73) nm. HRMS (ESI): m/z: calculated for $C_{68}H_{56}N_4S_2Zn$: 1212.145; found 1212.144.

ZnF3VTP

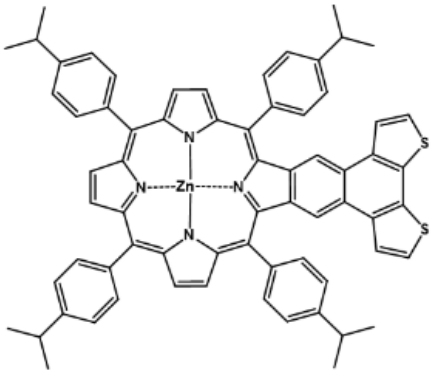

$C_{68}H_{56}N_4S_2Zn$; purple, crystalline solid; 90% yield; ^{1}H NMR (500 MHz, $CDCl_3$) δ 8.94 (d, J = 4.3 Hz, 2H), 8.84 (s, 2H), 8.79 (d, J = 4.3 Hz, 2H), 8.52 (s, 2H), 8.21 (d, J = 7.4 Hz, 4H), 8.13 (d, J = 7.3 Hz, 4H), 7.83 (d, J = 7.3 Hz, 4H), 7.66 (d, J = 4.8 Hz, 2H), 7.60 (d, J = 7.2 Hz, 4H), 7.48 (d, J = 5.0 Hz, 2H), 3.52 – 3.46 (m, 2H), 3.30 – 3.24 (m, 2H), 1.75 (d, J = 6.9 Hz, 12H), 1.25 (s, 12H). ^{13}C NMR (500 MHz, $CDCl_3$) δ 152.58, 149.61, 148.85, 148.51, 148.14, 146.91, 141.32, 140.19, 138.04, 135.49, 134.43, 133.66, 132.32, 132.18, 131.11, 130.56, 126.43, 124.78, 123.86, 123.40, 121.21, 116.89, 34.62, 34.27, 29.88, 24.67, 24.47. UV/VIS (DCB): λ_{max} (log ε) = 453 (5.19), 572 (4.06), 616 (3.68) nm. HRMS (ESI): m/z: calculated for $C_{68}H_{56}N_4S_2Zn$: 1056.324; found 1056.482.

2.8.3 NMR Spectra

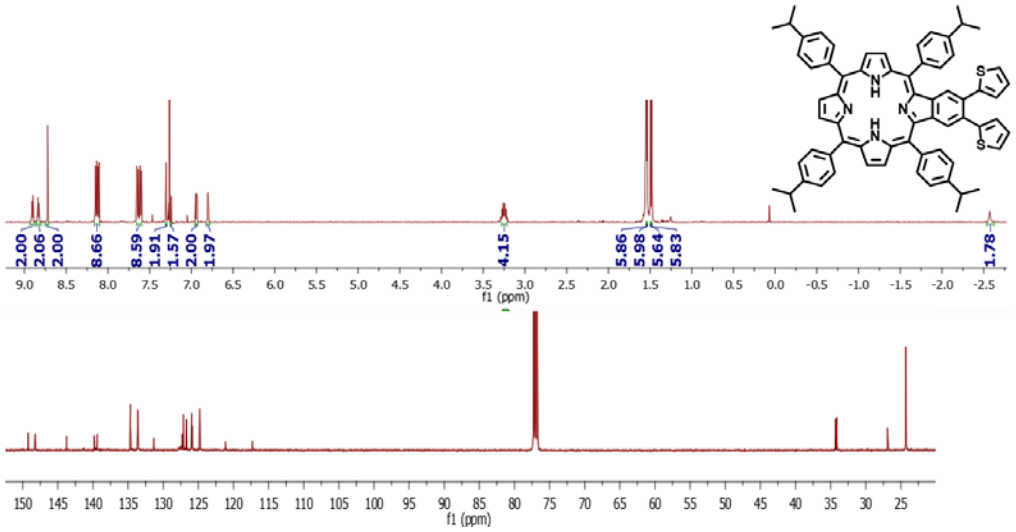

Figure 2.14: 2VTP NMR Spectra

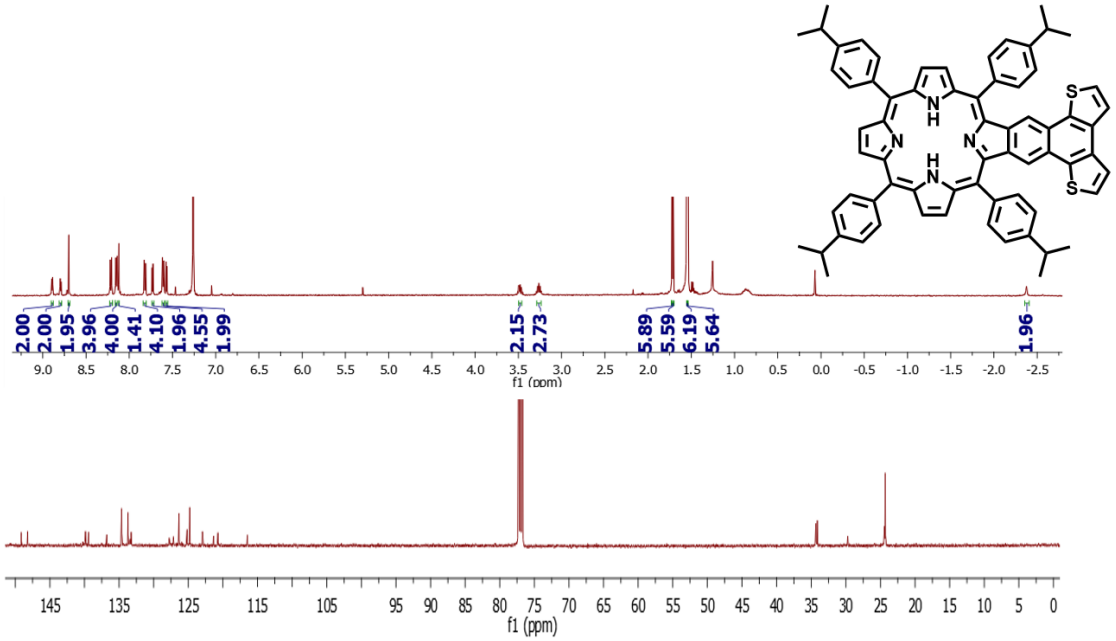

Figure 2.15: F2VTP NMR Spectra

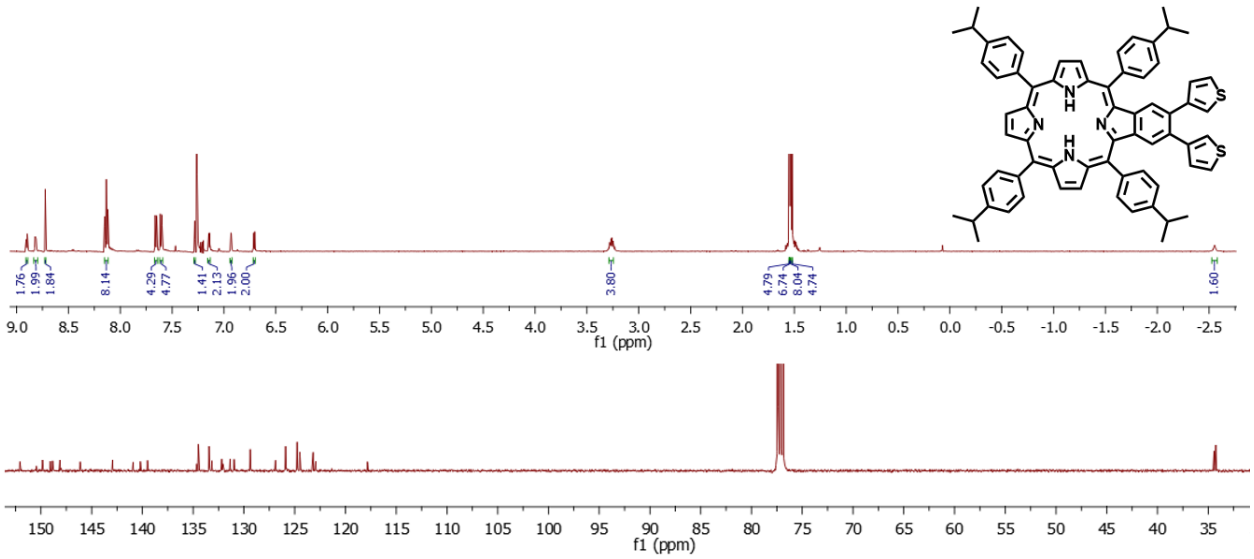

Figure 2.16: 3VTP NMR Spectra

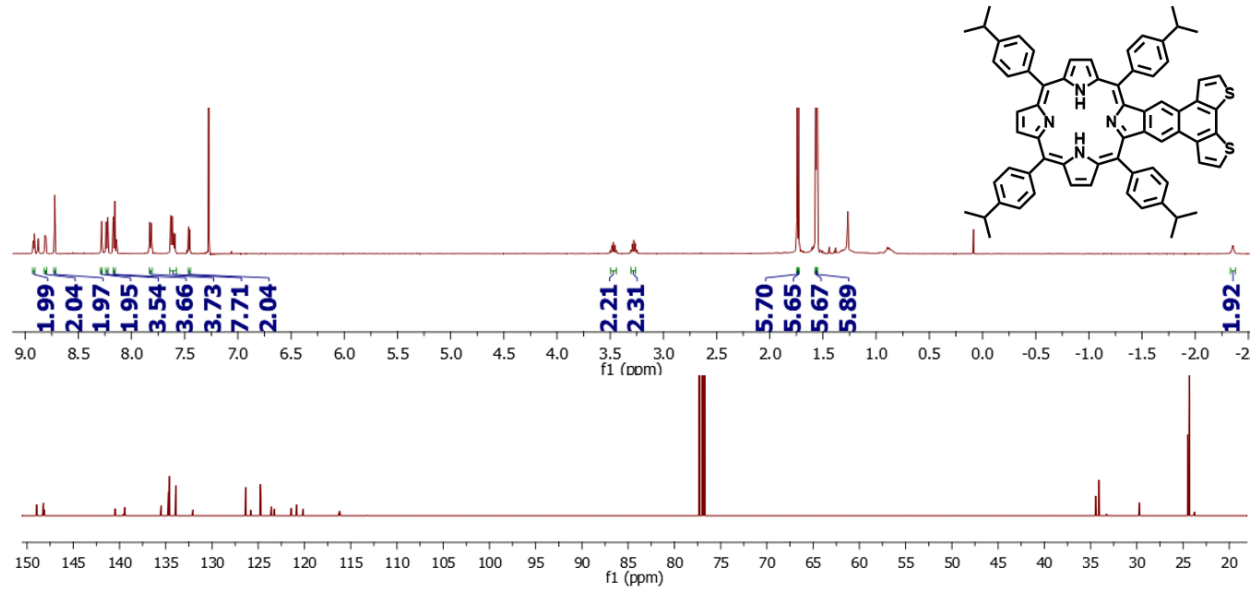

Figure 2.17: F3VTP NMR Spectra

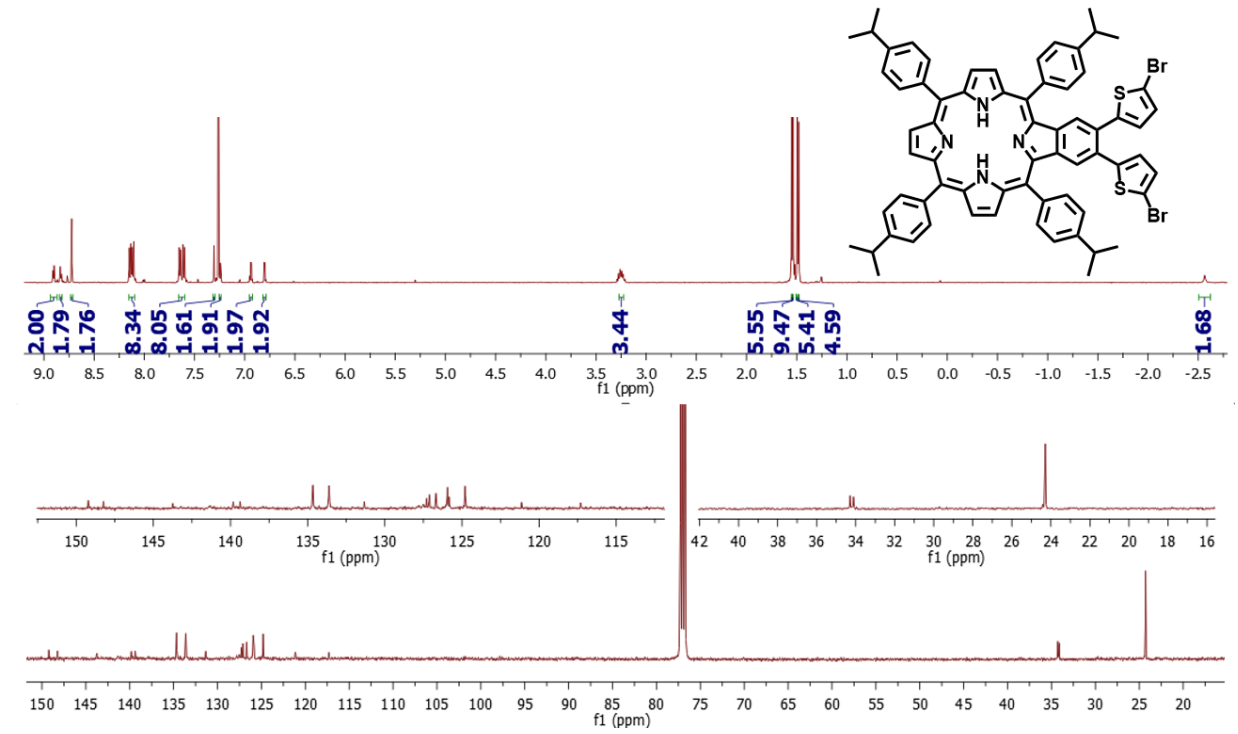

Figure 2.18: 2vtBr NMR Spectra

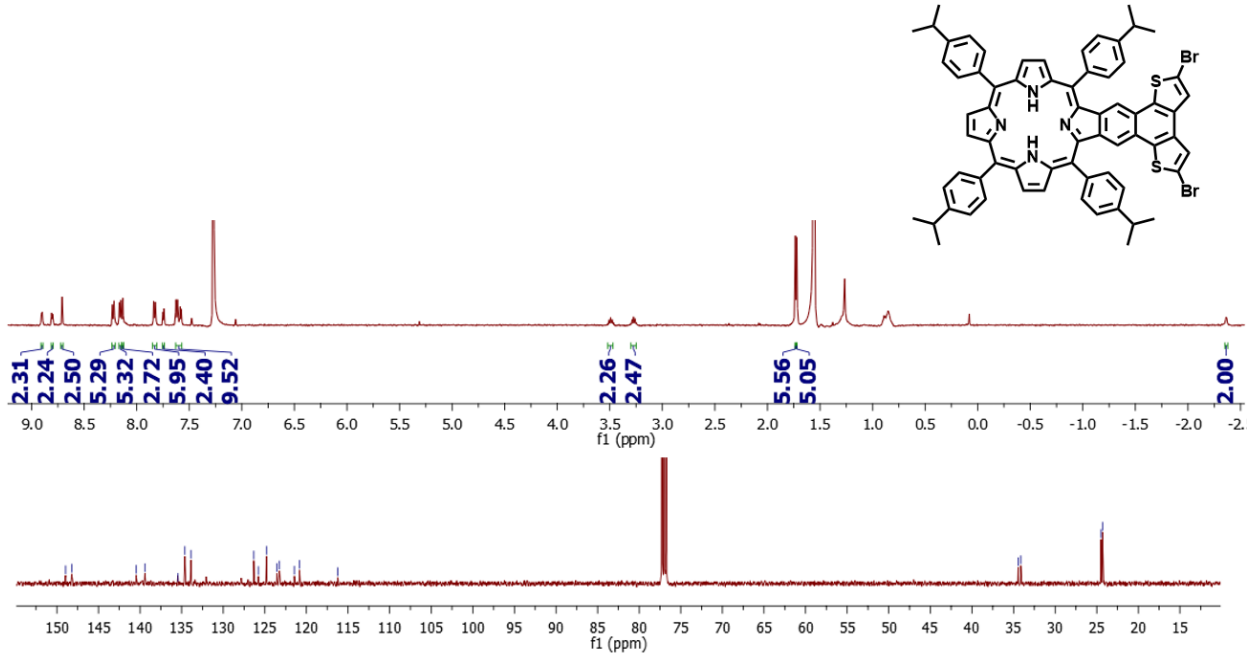

Figure 2.19: F2vtBr NMR Spectra

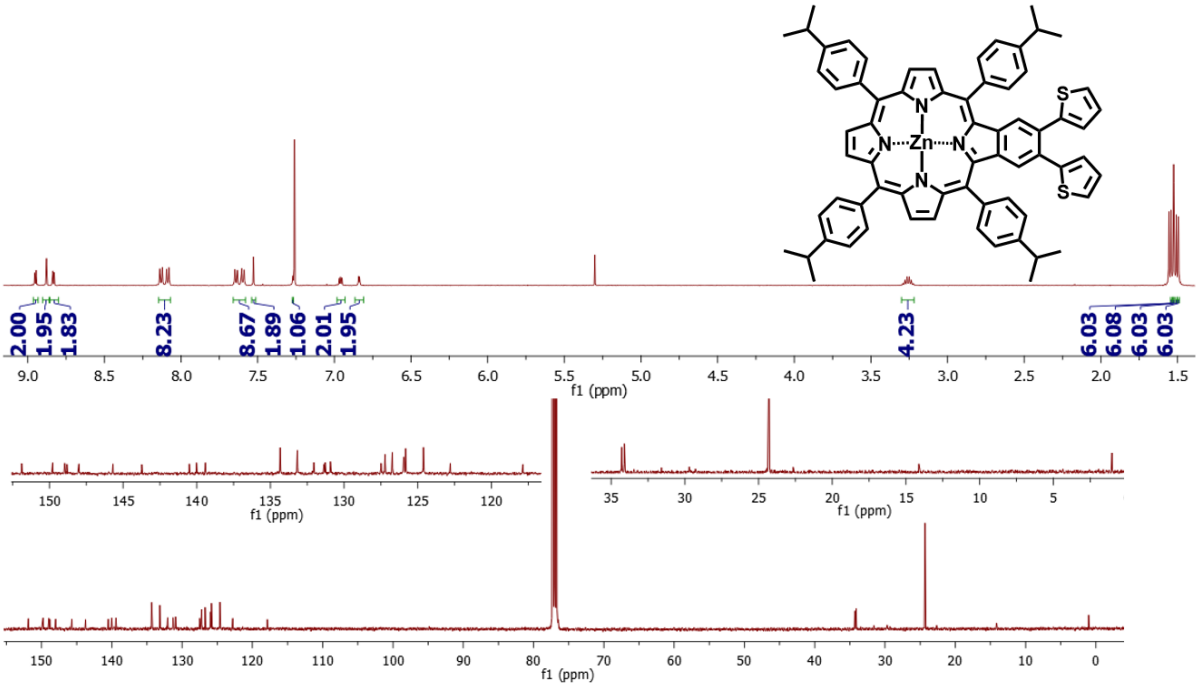

Figure 2.20: Zn2VP NMR Spectra

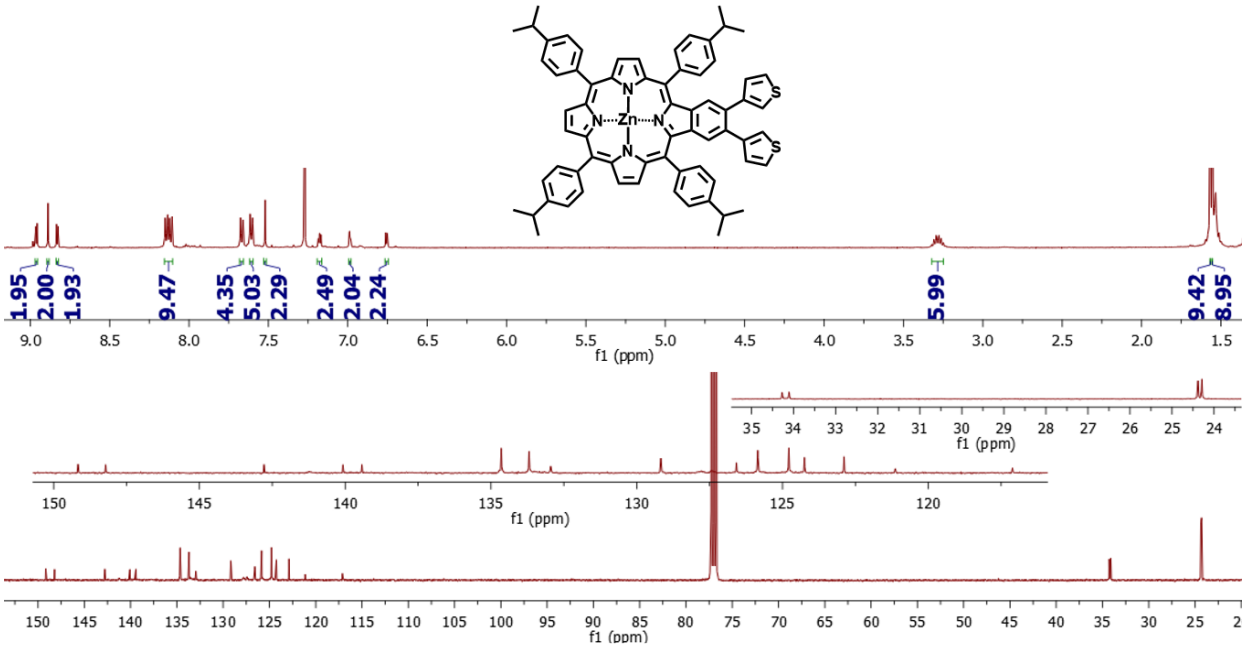

Figure 2.21: Zn3VTP NMR Spectra

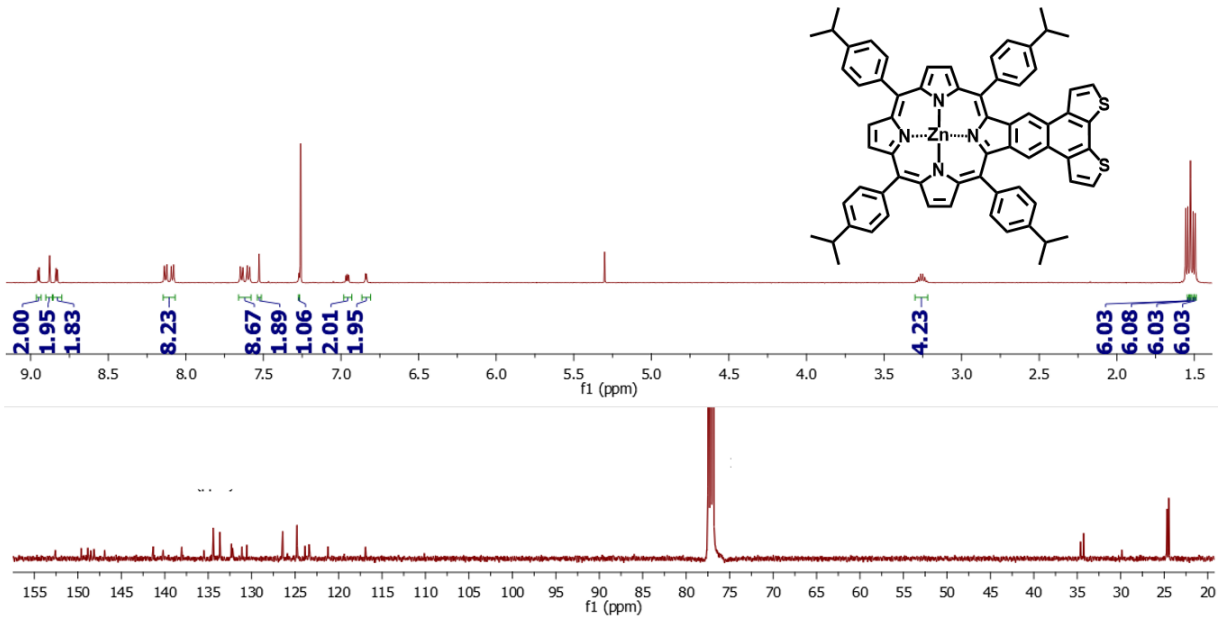

Figure 2.22: ZnF3VTP NMR Spectra

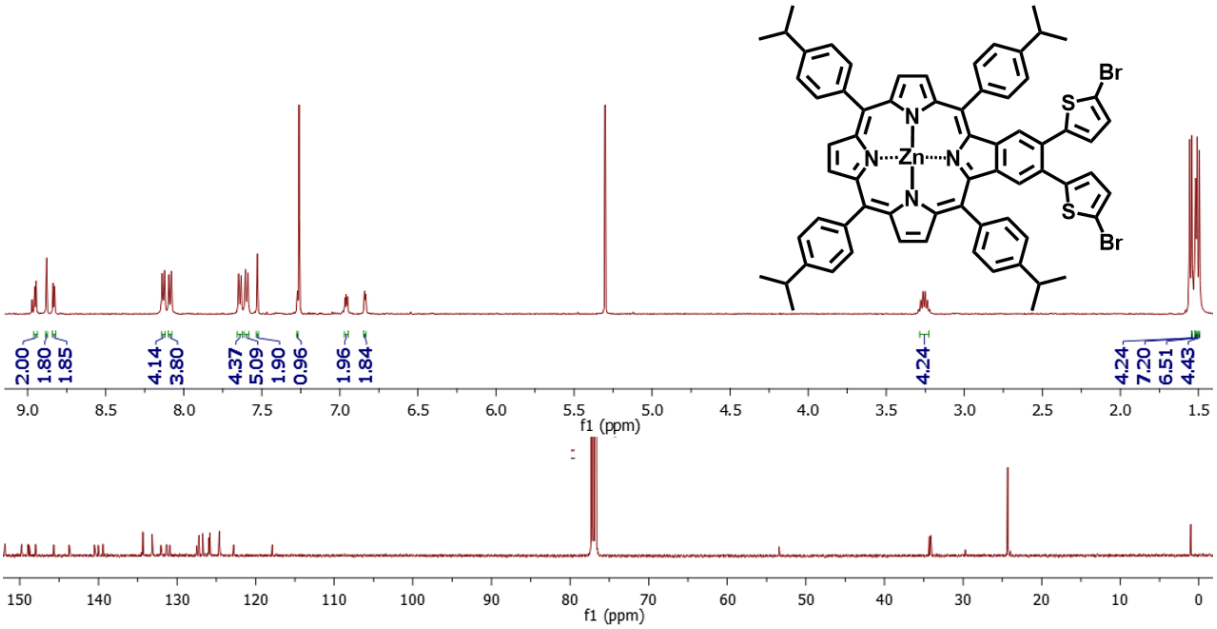

Figure 2.23: Zn2vtBr NMR Spectra

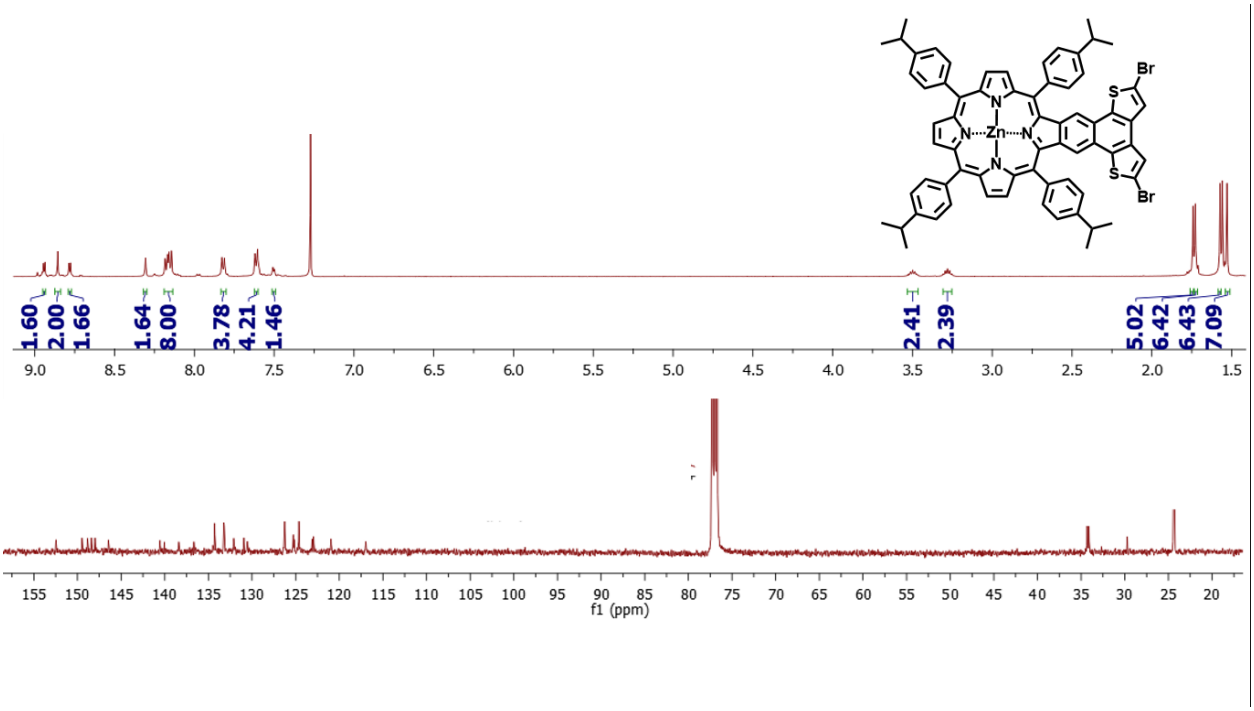

Figure 2.26: ZnF2vtBr NMR Spectra

2.8.4 Oscillator Tables

Table 2.2: 2VTP Oscillator Table

2VTP	Transition Energy (eV)	Wavelength (nm)	Oscillator Strength (f)	Orbital Transition		% Probability
Singlet-A	2.0996	591	0.0111	HOMO -1	LUMO	41.2%
				HOMO	LUMO +1	58.0%
Singlet-A	2.2335	555	0.0123	HOMO -1	LUMO +1	40.3%
				HOMO	LUMO	59.0%
Singlet-A	2.8542	435	0.6552	HOMO -2	LUMO +1	34.4%
				HOMO -1	LUMO	36.7%
				HOMO	LUMO +1	23.6%

Table 2.3: F2VTP Oscillator Table

F2VTP	Transition Energy (eV)	Wavelength (nm)	Oscillator Strength (f)	Orbital Transition		% Probability
Singlet-A	2.0996	601	0.0006	HOMO -1	LUMO	50.6%
				HOMO	LUMO +1	48.1%
Singlet-A	2.1961	564	0.0038	HOMO -1	LUMO +1	44.3%
				HOMO	LUMO	54.3%
Singlet-A	2.7051	458	0.7062	HOMO -3	LUMO	14.8%
				HOMO -2	LUMO +1	3.1%
				HOMO-1	LUMO	42.3%
				HOMO	LUMO+1	37.7%

Table 2.4: 3VTP Oscillator Table

3VTP	Transition Energy (eV)	Wavelength (nm)	Oscillator Strength (f)	Orbital Transition		% Probability
Singlet-A	2.0484	605	0.0005	HOMO -1	LUMO	44.2%
				HOMO	LUMO +1	54.1%
Singlet-A	2.2051	562	0.003	HOMO -1	LUMO +1	44.7%
				HOMO	LUMO	53.5%
Singlet-A	2.6693	464	0.5521	HOMO -2	LUMO	25.2%
				HOMO -1	LUMO	38.4%
				HOMO	LUMO +1	33.7%

Table 2.5: F3VTP Oscillator Table

F3VTP	Transition Energy (eV)	Wavelength (nm)	Oscillator Strength (f)	Orbital Transition		% Probability
Singlet-A	2.0718	598	0.0005	HOMO -1	LUMO +1	44.6%
				HOMO	LUMO	53.7%
Singlet-A	2.2141	560	0.0029	HOMO -1	LUMO	51.9%
				HOMO	LUMO+1	46.2%
Singlet-A	2.6736	464	0.5161	HOMO -2	LUMO	26.8%
				HOMO -2	LUMO +1	33.3%
				HOMO	LUMO	37.1%

Table 2.6: 2vtBr Oscillator Table

2vtBr	Transition Energy (eV)	Wavelength (nm)	Oscillator Strength (f)	Orbital Transition		% Probability
Singlet-A	2.0994	591	0.0071	HOMO -1	LUMO	41.8%
				HOMO	LUMO +1	53.5%
Singlet-A	2.2298	556	0.0031	HOMO -1	LUMO +1	42.4%
				HOMO	LUMO	56.7%
Singlet-A	2.8204	440	0.2667	HOMO -2	LUMO	3.6%
				HOMO -2	LUMO +1	28.4%
				HOMO-1	LUMO	20.4%
				HOMO-1	LUMO+1	18.0%
				HOMO	LUMO	12.5%
				HOMO-	LUMO+ +1	13.5%

Table 2.7: F2vtBr Oscillator Table

F2vtBr	Transition Energy (eV)	Wavelength (nm)	Oscillator Strength (f)	Orbital Transition		% Probability
Singlet-A	2.0678	600	0.0071	HOMO -1	LUMO	48.8%
				HOMO	LUMO +1	53.5%
Singlet-A	2.1987	564	0.0031	HOMO -1	LUMO +1	44.0%
				HOMO	LUMO	54.7%
Singlet-A	2.725	456	0.2667	HOMO -3	LUMO	11.3%
				HOMO -2	LUMO +1	2.7%
				HOMO-1	LUMO	44.7%
				HOMO-1	LUMO+2	2.0%
				HOMO	LUMO +1	37.9%

Table 2.8: Zn2VTP Oscillator Table

Zn2VTP	Transition Energy (eV)	Wavelength (nm)	Oscillator Strength (f)	Orbital Transition		% Probability
Singlet-A	2.1992	564	0.0002	HOMO -1	LUMO	54.0%
				HOMO	LUMO +1	45.3%
Singlet-A	2.2187	559	0.0033	HOMO -1	LUMO +1	42.1%
				HOMO	LUMO	57.0%
Singlet-A	2.8194	440	2.4815	HOMO -1	LUMO +1	55.4%
				HOMO	LUMO	39.2%

Table 2.9: Zn3VTP Oscillator Table

Zn3VTP	Transition Energy (eV)	Wavelength (nm)	Oscillator Strength (f)	Orbital Transition		% Probability
Singlet-A	2.1439	578.3	0.0275	HOMO-1	LUMO +1	30.2%
				HOMO	LUMO	69.0%
Singlet-A	2.2034	562.71	0.0006	HOMO-1	LUMO +1	54.1%
				HOMO	LUMO	44.1%
Singlet-A	2.1062	589	0.1721	HOMO -1	LUMO	19.8%
				HOMO	LUMO +2	79.8%

Table 2.10: ZnF3VTP Oscillator Table

ZnF3VTP	Transition Energy (eV)	Wavelength (nm)	Oscillator Strength (f)	Orbital Transition		% Probability
Singlet-A	2.1505	577	0.0219	HOMO -1	LUMO +1	31.4%
				HOMO	LUMO	67.8%
Singlet-A	2.207	562	0.0005	HOMO -1	LUMO	55.0%
				HOMO	LUMO+1	43.1%
Singlet-A	2.7474	451	0.4586	HOMO -2	LUMO	35.0%
				HOMO -1	LUMO +1	39.7%
				HOMO	LUMO	22.5%

Table 2.11: Zn2vtBr Oscillator Table

Zn2vtBr	Transition Energy (eV)	Wavelength (nm)	Oscillator Strength (f)	Orbital Transition		% Probability
Singlet-A	2.1945	565	0.0002	HOMO -1	LUMO	52.0%
				HOMO	LUMO +1	53.5%
Singlet-A	2.2121	561	0.0006	HOMO -1	LUMO +1	43.7%
				HOMO	LUMO	55.2%
Singlet-A	2.784	445	2.5474	HOMO -2	LUMO	3.3%
				HOMO -1	LUMO +1	52.4%
				HOMO	LUMO	39.4%

Table 2.12: ZnF2vtBr Oscillator Table

ZnF2vtBr	Transition Energy (eV)	Wavelength (nm)	Oscillator Strength (f)	Orbital Transition		% Probability
Singlet-A	2.1453	578	0.0081	HOMO -1	LUMO+1	34.7%
				HOMO	LUMO	53.5%
Singlet-A	2.1838	568	0.0015	HOMO -1	LUMO	57.0%
				HOMO	LUMO+1	41.6%
Singlet-A	2.7291	454	2.3078	HOMO -3	LUMO +1	4.5%
				HOMO -1	LUMO	36.2%
				HOMO-1	LUMO +2	2.6%
				HOMO	LUMO+1	54.3%

2.8.5 Tauc Plot Tables

Table 2.13: 2VTP Tauc Tables

Wavelength (nm)	Absorbance	Photon Energy (eV)	Relationship - Indirect ($\alpha h\nu^{1/2}$)
800	0.00123	1.55	0.04363
799	9.16E-04	1.55194	0.0377
798	7.19E-04	1.55388	0.03343
797	6.67E-04	1.55583	0.03221
796	4.28E-04	1.55779	0.02583
795	3.09E-04	1.55975	0.02194
794	5.45E-04	1.56171	0.02916
793	4.41E-04	1.56368	0.02625

Wavelength (nm)	Absorbance	Photon Energy (eV)	Relationship - Indirect ($\alpha h\nu^{1/2}$)
792	5.13E-04	1.56566	0.02835
791	5.86E-04	1.56764	0.03031
790	5.55E-04	1.56962	0.02951
789	5.96E-04	1.57161	0.03061
788	7.23E-04	1.5736	0.03374
787	5.40E-04	1.5756	0.02918
786	6.15E-04	1.57761	0.03116
785	8.74E-04	1.57962	0.03717
784	7.84E-04	1.58163	0.03521
783	7.42E-04	1.58365	0.03427
782	7.88E-04	1.58568	0.03536
781	8.37E-04	1.58771	0.03646
780	6.41E-04	1.58974	0.03193
779	6.43E-04	1.59178	0.03199
778	6.10E-04	1.59383	0.03117
777	8.02E-04	1.59588	0.03578
776	8.33E-04	1.59794	0.03649
775	7.88E-04	1.6	0.0355
774	7.50E-04	1.60207	0.03467
773	7.55E-04	1.60414	0.03481
772	5.31E-04	1.60622	0.02919
771	5.06E-04	1.6083	0.02852
770	7.98E-04	1.61039	0.03585
769	6.80E-04	1.61248	0.03311
768	6.28E-04	1.61458	0.03184
767	3.44E-04	1.61669	0.02357
766	3.87E-04	1.6188	0.02504
765	1.20E-04	1.62092	0.01397
764	4.66E-04	1.62304	0.02749
763	6.89E-04	1.62516	0.03346
762	6.30E-04	1.6273	0.03202
761	5.90E-04	1.62943	0.03101
760	6.31E-04	1.63158	0.0321
759	6.11E-04	1.63373	0.0316
758	6.56E-04	1.63588	0.03276
757	6.43E-04	1.63804	0.03245
756	4.45E-04	1.64021	0.02701
755	2.68E-04	1.64238	0.02098
754	4.20E-04	1.64456	0.02628

Wavelength (nm)	Absorbance	Photon Energy (eV)	Relationship - Indirect ($\alpha h\nu^{1/2}$)
753	1.60E-04	1.64675	0.01621
752	6.51E-04	1.64894	0.03277
751	9.02E-04	1.65113	0.03858
750	9.73E-04	1.65333	0.04012
749	0.001	1.65554	0.04071
748	9.69E-04	1.65775	0.04007
747	9.45E-04	1.65997	0.03961
746	8.98E-04	1.6622	0.03864
745	8.16E-04	1.66443	0.03685
744	9.17E-04	1.66667	0.0391
743	5.23E-04	1.66891	0.02955
742	9.94E-04	1.67116	0.04075
741	7.82E-04	1.67341	0.03618
740	0.00113	1.67568	0.04357
739	8.73E-04	1.67794	0.03827
738	0.00106	1.68022	0.04221
737	0.00114	1.6825	0.04387
736	0.00118	1.68478	0.0445
735	0.00116	1.68707	0.04415
734	0.00115	1.68937	0.04403
733	8.59E-04	1.69168	0.03812
732	0.00106	1.69399	0.04247
731	0.00119	1.69631	0.04488
730	0.00153	1.69863	0.05091
729	0.00147	1.70096	0.05006
728	0.00148	1.7033	0.05015
727	0.00142	1.70564	0.04913
726	0.00115	1.70799	0.04433
725	0.00134	1.71034	0.04793
724	0.00132	1.71271	0.04761
723	0.00141	1.71508	0.04911
722	0.00165	1.71745	0.05322
721	0.00149	1.71983	0.05069
720	0.00176	1.72222	0.05503
719	0.00188	1.72462	0.05691
718	0.00182	1.72702	0.05612
717	0.00177	1.72943	0.05539
716	0.00211	1.73184	0.06047
715	0.00188	1.73427	0.05717

Wavelength (nm)	Absorbance	Photon Energy (eV)	Relationship - Indirect ($\alpha h\nu^{1/2}$)
714	0.00193	1.73669	0.05794
713	0.00195	1.73913	0.05824
712	0.00203	1.74157	0.0595
711	0.00195	1.74402	0.05837
710	0.00184	1.74648	0.05668
709	0.00201	1.74894	0.05927
708	0.0019	1.75141	0.05775
707	0.00203	1.75389	0.05964
706	0.00221	1.75637	0.06226
705	0.00219	1.75887	0.06202
704	0.00249	1.76136	0.06616
703	0.00209	1.76387	0.06065
702	0.00225	1.76638	0.06305
701	0.00225	1.7689	0.06309
700	0.00248	1.77143	0.0663
699	0.00236	1.77396	0.0647
698	0.00243	1.7765	0.06573
697	0.0026	1.77905	0.06795
696	0.00243	1.78161	0.06582
695	0.00256	1.78417	0.0676
694	0.00273	1.78674	0.06988
693	0.00267	1.78932	0.06915
692	0.00285	1.79191	0.07149
691	0.00284	1.7945	0.07135
690	0.00293	1.7971	0.07258
689	0.00325	1.79971	0.07646
688	0.00347	1.80233	0.07912
687	0.00369	1.80495	0.08159
686	0.00356	1.80758	0.08026
685	0.00363	1.81022	0.08106
684	0.00376	1.81287	0.08251
683	0.0042	1.81552	0.08729
682	0.0042	1.81818	0.08734
681	0.00424	1.82085	0.08791
680	0.00431	1.82353	0.08866
679	0.00463	1.82622	0.09193
678	0.00464	1.82891	0.09216
677	0.00477	1.83161	0.09343
676	0.00524	1.83432	0.098

Wavelength (nm)	Absorbance	Photon Energy (eV)	Relationship - Indirect ($\alpha h\nu^{1/2}$)
675	0.00549	1.83704	0.10043
674	0.00511	1.83976	0.09696
673	0.00552	1.8425	0.10089
672	0.00561	1.84524	0.10178
671	0.00591	1.84799	0.10451
670	0.00607	1.85075	0.10598
669	0.00615	1.85351	0.10678
668	0.00646	1.85629	0.10954
667	0.00662	1.85907	0.11095
666	0.00685	1.86186	0.11291
665	0.00683	1.86466	0.11285
664	0.00726	1.86747	0.11644
663	0.00742	1.87029	0.11781
662	0.00731	1.87311	0.11701
661	0.00757	1.87595	0.11919
660	0.00762	1.87879	0.11968
659	0.00772	1.88164	0.12052
658	0.00776	1.8845	0.12091
657	0.00779	1.88737	0.12122
656	0.00762	1.89024	0.12004
655	0.00801	1.89313	0.12314
654	0.00777	1.89602	0.12139
653	0.00774	1.89893	0.12122
652	0.00771	1.90184	0.12107
651	0.00754	1.90476	0.11986
650	0.00746	1.90769	0.11933
649	0.00713	1.91063	0.11675
648	0.00713	1.91358	0.11679
647	0.00677	1.91654	0.11392
646	0.00661	1.9195	0.11268
645	0.00662	1.92248	0.11282
644	0.00637	1.92547	0.11074
643	0.00605	1.92846	0.10799
642	0.00617	1.93146	0.10912
641	0.00566	1.93448	0.10459
640	0.00565	1.9375	0.10459
639	0.00575	1.94053	0.10561
638	0.00564	1.94357	0.10474
637	0.00581	1.94662	0.10637

Wavelength (nm)	Absorbance	Photon Energy (eV)	Relationship - Indirect ($\alpha h\nu^{1/2}$)
636	0.00594	1.94969	0.10761
635	0.00597	1.95276	0.10802
634	0.00615	1.95584	0.10969
633	0.00623	1.95893	0.1105
632	0.00618	1.96203	0.11012
631	0.00652	1.96513	0.11317
630	0.00706	1.96825	0.11784
629	0.00714	1.97138	0.11865
628	0.0075	1.97452	0.12166
627	0.00779	1.97767	0.12415
626	0.00819	1.98083	0.12735
625	0.00834	1.984	0.12861
624	0.00903	1.98718	0.13397
623	0.00954	1.99037	0.13782
622	0.01031	1.99357	0.14338
621	0.01067	1.99678	0.14595
620	0.01156	2	0.15203
619	0.01245	2.00323	0.15791
618	0.01313	2.00647	0.16232
617	0.01407	2.00972	0.16813
616	0.01525	2.01299	0.17521
615	0.01612	2.01626	0.18029
614	0.01729	2.01954	0.18686
613	0.0185	2.02284	0.19343
612	0.01976	2.02614	0.20009
611	0.0212	2.02946	0.20743
610	0.02239	2.03279	0.21334
609	0.02416	2.03612	0.22179
608	0.02548	2.03947	0.22796
607	0.02702	2.04283	0.23493
606	0.02832	2.0462	0.24073
605	0.02975	2.04959	0.24692
604	0.03076	2.05298	0.25131
603	0.03176	2.05638	0.25555
602	0.03238	2.0598	0.25825
601	0.03265	2.06323	0.25955
600	0.03274	2.06667	0.26012
599	0.0327	2.07012	0.26017
598	0.03187	2.07358	0.25708

Wavelength (nm)	Absorbance	Photon Energy (eV)	Relationship - Indirect ($\alpha h\nu^{1/2}$)
597	0.03128	2.07705	0.25489
596	0.03038	2.08054	0.2514
595	0.02895	2.08403	0.24561
594	0.02766	2.08754	0.24029
593	0.02636	2.09106	0.23479
592	0.02483	2.09459	0.22805
591	0.02306	2.09814	0.21998
590	0.02159	2.10169	0.21303
589	0.02043	2.10526	0.20741
588	0.01928	2.10884	0.20164
587	0.01818	2.11244	0.19597
586	0.0174	2.11604	0.19188
585	0.01709	2.11966	0.19035
584	0.01669	2.12329	0.18827
583	0.01635	2.12693	0.18649
582	0.01603	2.13058	0.18482
581	0.01609	2.13425	0.1853
580	0.01624	2.13793	0.18633
579	0.01671	2.14162	0.18918
578	0.01686	2.14533	0.19019
577	0.017	2.14905	0.19114
576	0.01718	2.15278	0.19231
575	0.01748	2.15652	0.19418
574	0.01795	2.16028	0.19691
573	0.01826	2.16405	0.19878
572	0.01856	2.16783	0.20059
571	0.01911	2.17163	0.20369
570	0.01936	2.17544	0.20525
569	0.01965	2.17926	0.20696
568	0.02015	2.1831	0.20976
567	0.02059	2.18695	0.21222
566	0.02099	2.19081	0.21445
565	0.02152	2.19469	0.21733
564	0.02197	2.19858	0.21979
563	0.02231	2.20249	0.22168
562	0.02309	2.20641	0.22571
561	0.0235	2.21034	0.22789
560	0.02398	2.21429	0.23045
559	0.02447	2.21825	0.23299

Wavelength (nm)	Absorbance	Photon Energy (eV)	Relationship - Indirect ($\alpha h\nu^{1/2}$)
558	0.02471	2.22222	0.23435
557	0.02521	2.22621	0.2369
556	0.02572	2.23022	0.2395
555	0.02602	2.23423	0.2411
554	0.02641	2.23827	0.24313
553	0.02689	2.24231	0.24553
552	0.02732	2.24638	0.24773
551	0.02809	2.25045	0.25142
550	0.02863	2.25455	0.25407
549	0.02948	2.25865	0.25803
548	0.03027	2.26277	0.26169
547	0.03152	2.26691	0.2673
546	0.03236	2.27106	0.2711
545	0.03408	2.27523	0.27847
544	0.03592	2.27941	0.28615
543	0.03807	2.28361	0.29485
542	0.04042	2.28782	0.30411
541	0.04325	2.29205	0.31485
540	0.04633	2.2963	0.32617
539	0.04958	2.30056	0.33775
538	0.05333	2.30483	0.3506
537	0.05719	2.30912	0.36341
536	0.06122	2.31343	0.37633
535	0.06551	2.31776	0.38967
534	0.07021	2.3221	0.40377
533	0.07504	2.32645	0.41784
532	0.08006	2.33083	0.43199
531	0.08453	2.33522	0.44429
530	0.08863	2.33962	0.45537
529	0.09226	2.34405	0.46503
528	0.09525	2.34848	0.47297
527	0.09793	2.35294	0.48001
526	0.09955	2.35741	0.48443
525	0.10065	2.3619	0.48758
524	0.10083	2.36641	0.48846
523	0.10038	2.37094	0.48785
522	0.09933	2.37548	0.48575
521	0.09723	2.38004	0.48105
520	0.094	2.38462	0.47346

Wavelength (nm)	Absorbance	Photon Energy (eV)	Relationship - Indirect ($\alpha h\nu^{1/2}$)
519	0.09056	2.38921	0.46515
518	0.08683	2.39382	0.45591
517	0.0824	2.39845	0.44455
516	0.07816	2.4031	0.4334
515	0.07436	2.40777	0.42313
514	0.0706	2.41245	0.4127
513	0.06706	2.41715	0.40261
512	0.06414	2.42188	0.39413
511	0.06114	2.42661	0.38518
510	0.05844	2.43137	0.37695
509	0.05588	2.43615	0.36896
508	0.05329	2.44094	0.36067
507	0.05094	2.44576	0.35296
506	0.04867	2.45059	0.34534
505	0.04682	2.45545	0.33906
504	0.04501	2.46032	0.33278
503	0.04351	2.46521	0.3275
502	0.04232	2.47012	0.32332
501	0.04129	2.47505	0.31968
500	0.04077	2.48	0.31799
499	0.04056	2.48497	0.31747
498	0.04061	2.48996	0.31799
497	0.04081	2.49497	0.31908
496	0.04094	2.5	0.31992
495	0.04146	2.50505	0.32226
494	0.04235	2.51012	0.32605
493	0.04338	2.51521	0.33031
492	0.04426	2.52033	0.33401
491	0.04516	2.52546	0.33772
490	0.04635	2.53061	0.34248
489	0.04741	2.53579	0.34673
488	0.04886	2.54098	0.35234
487	0.04995	2.5462	0.35663
486	0.05111	2.55144	0.36112
485	0.05234	2.5567	0.36581
484	0.05336	2.56198	0.36973
483	0.05428	2.56729	0.37331
482	0.05574	2.57261	0.37868
481	0.05694	2.57796	0.38314

Wavelength (nm)	Absorbance	Photon Energy (eV)	Relationship - Indirect ($\alpha h\nu^{1/2}$)
480	0.05824	2.58333	0.38788
479	0.05953	2.58873	0.39257
478	0.06084	2.59414	0.39726
477	0.06279	2.59958	0.40403
476	0.06482	2.60504	0.41091
475	0.06696	2.61053	0.4181
474	0.06967	2.61603	0.42693
473	0.07263	2.62156	0.43635
472	0.07557	2.62712	0.44558
471	0.07901	2.6327	0.45608
470	0.08259	2.6383	0.4668
469	0.08651	2.64392	0.47826
468	0.09128	2.64957	0.49178
467	0.09611	2.65525	0.50516
466	0.1013	2.66094	0.51918
465	0.10705	2.66667	0.53428
464	0.11339	2.67241	0.55048
463	0.12028	2.67819	0.56756
462	0.12785	2.68398	0.58578
461	0.13597	2.6898	0.60476
460	0.14519	2.69565	0.6256
459	0.15541	2.70153	0.64795
458	0.16745	2.70742	0.67332
457	0.18077	2.71335	0.70035
456	0.19625	2.7193	0.73052
455	0.21441	2.72527	0.76442
454	0.23534	2.73128	0.80173
453	0.25958	2.73731	0.84295
452	0.28799	2.74336	0.88886
451	0.32114	2.74945	0.93966
450	0.35949	2.75556	0.99528
449	0.40427	2.76169	1.05663
448	0.45534	2.76786	1.12264
447	0.51413	2.77405	1.19424
446	0.58098	2.78027	1.27093
445	0.65557	2.78652	1.35158
444	0.7378	2.79279	1.43545
443	0.82746	2.7991	1.52189
442	0.92226	2.80543	1.60852

Wavelength (nm)	Absorbance	Photon Energy (eV)	Relationship - Indirect ($\alpha h\nu^{1/2}$)
441	1.01817	2.81179	1.692
440	1.11083	2.81818	1.76933
439	1.1957	2.8246	1.83776
438	1.26596	2.83105	1.89314
437	1.31569	2.83753	1.93217
436	1.34031	2.84404	1.95241
435	1.33537	2.85057	1.95105
434	1.29991	2.85714	1.92718
433	1.23821	2.86374	1.88306
432	1.15762	2.87037	1.82285
431	1.06689	2.87703	1.75199
430	0.97426	2.88372	1.67616
429	0.88677	2.89044	1.60099
428	0.80911	2.8972	1.53106
427	0.7435	2.90398	1.4694
426	0.6898	2.9108	1.417
425	0.64732	2.91765	1.37428
424	0.6145	2.92453	1.34057
423	0.58828	2.93144	1.31321
422	0.56717	2.93839	1.29096
421	0.54828	2.94537	1.27078
420	0.52987	2.95238	1.25075
419	0.51102	2.95943	1.22977
418	0.49133	2.96651	1.20728
417	0.47078	2.97362	1.18318
416	0.44924	2.98077	1.15718
415	0.42776	2.98795	1.13055
414	0.40615	2.99517	1.10295
413	0.38452	3.00242	1.07448
412	0.36259	3.00971	1.04465
411	0.34056	3.01703	1.01364
410	0.3177	3.02439	0.98023
409	0.29533	3.03178	0.94624
408	0.27383	3.03922	0.91226
407	0.25351	3.04668	0.87884
406	0.23526	3.05419	0.84767
405	0.21884	3.06173	0.81855
404	0.20462	3.06931	0.79249
403	0.19267	3.07692	0.76995

Wavelength (nm)	Absorbance	Photon Energy (eV)	Relationship - Indirect ($\alpha h\nu^{1/2}$)
402	0.18274	3.08458	0.75079
401	0.1742	3.09227	0.73395
400	0.16691	3.1	0.71933
399	0.16059	3.10777	0.70646
398	0.15503	3.11558	0.69499
397	0.15	3.12343	0.68447
396	0.14483	3.13131	0.67344
395	0.14091	3.13924	0.66509
394	0.13713	3.14721	0.65694
393	0.13357	3.15522	0.64918
392	0.13051	3.16327	0.64252
391	0.12811	3.17136	0.6374
390	0.12571	3.17949	0.63222
389	0.12358	3.18766	0.62765
388	0.12138	3.19588	0.62283
387	0.11964	3.20413	0.61913
386	0.11822	3.21244	0.61627
385	0.11642	3.22078	0.61234
384	0.1151	3.22917	0.60964
383	0.11378	3.2376	0.60693
382	0.11235	3.24607	0.6039
381	0.1115	3.25459	0.60239
380	0.11014	3.26316	0.59951
379	0.10916	3.27177	0.59761
378	0.10821	3.28042	0.59579
377	0.10678	3.28912	0.59264
376	0.10539	3.29787	0.58955
375	0.10391	3.30667	0.58616
374	0.1023	3.31551	0.58238
373	0.10051	3.3244	0.57803
372	0.09886	3.33333	0.57405
371	0.09683	3.34232	0.5689
370	0.09483	3.35135	0.56375
369	0.09294	3.36043	0.55885
368	0.0916	3.36957	0.55556
367	0.09009	3.37875	0.55171
366	0.08888	3.38798	0.54874
365	0.08772	3.39726	0.54592
364	0.08643	3.40659	0.54261

Wavelength (nm)	Absorbance	Photon Energy (eV)	Relationship - Indirect ($\alpha h\nu^{1/2}$)
363	0.08586	3.41598	0.54156
362	0.08483	3.42541	0.53905
361	0.08411	3.4349	0.53749
360	0.083	3.44444	0.53467
359	0.08204	3.45404	0.53234
358	0.08156	3.46369	0.5315
357	0.08066	3.47339	0.52931
356	0.08015	3.48315	0.52838
355	0.07919	3.49296	0.52595
354	0.07861	3.50282	0.52475
353	0.07793	3.51275	0.52321
352	0.07728	3.52273	0.52177
351	0.07664	3.53276	0.52034
350	0.07612	3.54286	0.51929

Table 2.14: F2VTP Tauc Tables

Wavelength (nm)	Absorbance	Photon Energy (eV)	Relationship - Indirect ($\alpha h\nu^{1/2}$)
800	2.75E-04	1.55	0.04363
799	1.35E-04	1.55194	0.0377
798	1.66E-04	1.55388	0.03343
797	1.43E-04	1.55583	0.03221
796	1.46E-04	1.55779	0.02583
795	2.72E-04	1.55975	0.02194
794	2.60E-04	1.56171	0.02916
793	2.76E-04	1.56368	0.02625
792	2.57E-04	1.56566	0.02835
791	2.55E-04	1.56764	0.03031
790	2.66E-04	1.56962	0.02951
789	2.99E-04	1.57161	0.03061
788	3.20E-04	1.5736	0.03374
787	2.98E-04	1.5756	0.02918
786	3.99E-04	1.57761	0.03116
785	4.35E-04	1.57962	0.03717
784	4.03E-04	1.58163	0.03521
783	3.98E-04	1.58365	0.03427
782	2.97E-04	1.58568	0.03536
781	2.40E-04	1.58771	0.03646

Wavelength (nm)	Absorbance	Photon Energy (eV)	Relationship - Indirect ($\alpha h\nu^{1/2}$)
780	2.45E-04	1.58974	0.03193
779	2.74E-04	1.59178	0.03199
778	2.97E-04	1.59383	0.03117
777	3.68E-04	1.59588	0.03578
776	4.64E-04	1.59794	0.03649
775	4.32E-04	1.6	0.0355
774	3.95E-04	1.60207	0.03467
773	3.76E-04	1.60414	0.03481
772	3.07E-04	1.60622	0.02919
771	3.55E-04	1.6083	0.02852
770	3.32E-04	1.61039	0.03585
769	2.42E-04	1.61248	0.03311
768	2.38E-04	1.61458	0.03184
767	2.24E-04	1.61669	0.02357
766	3.35E-04	1.6188	0.02504
765	4.41E-04	1.62092	0.01397
764	4.34E-04	1.62304	0.02749
763	3.68E-04	1.62516	0.03346
762	2.44E-04	1.6273	0.03202
761	2.19E-04	1.62943	0.03101
760	2.45E-04	1.63158	0.0321
759	2.84E-04	1.63373	0.0316
758	3.86E-04	1.63588	0.03276
757	3.30E-04	1.63804	0.03245
756	3.15E-04	1.64021	0.02701
755	3.23E-04	1.64238	0.02098
754	2.57E-04	1.64456	0.02628
753	2.65E-04	1.64675	0.01621
752	2.42E-04	1.64894	0.03277
751	2.37E-04	1.65113	0.03858
750	2.62E-04	1.65333	0.04012
749	2.59E-04	1.65554	0.04071
748	2.26E-04	1.65775	0.04007
747	2.88E-04	1.65997	0.03961
746	2.85E-04	1.6622	0.03864
745	3.37E-04	1.66443	0.03685
744	4.33E-04	1.66667	0.0391
743	3.15E-04	1.66891	0.02955
742	3.23E-04	1.67116	0.04075

Wavelength (nm)	Absorbance	Photon Energy (eV)	Relationship - Indirect ($\alpha h\nu^{1/2}$)
741	3.08E-04	1.67341	0.03618
740	3.39E-04	1.67568	0.04357
739	3.66E-04	1.67794	0.03827
738	2.94E-04	1.68022	0.04221
737	2.05E-04	1.6825	0.04387
736	2.20E-04	1.68478	0.0445
735	3.20E-04	1.68707	0.04415
734	3.70E-04	1.68937	0.04403
733	5.17E-04	1.69168	0.03812
732	3.79E-04	1.69399	0.04247
731	2.97E-04	1.69631	0.04488
730	3.40E-04	1.69863	0.05091
729	2.74E-04	1.70096	0.05006
728	4.00E-04	1.7033	0.05015
727	5.28E-04	1.70564	0.04913
726	5.78E-04	1.70799	0.04433
725	5.44E-04	1.71034	0.04793
724	5.70E-04	1.71271	0.04761
723	5.33E-04	1.71508	0.04911
722	4.57E-04	1.71745	0.05322
721	5.11E-04	1.71983	0.05069
720	5.68E-04	1.72222	0.05503
719	6.85E-04	1.72462	0.05691
718	7.58E-04	1.72702	0.05612
717	7.46E-04	1.72943	0.05539
716	7.20E-04	1.73184	0.06047
715	6.29E-04	1.73427	0.05717
714	7.30E-04	1.73669	0.05794
713	8.28E-04	1.73913	0.05824
712	9.07E-04	1.74157	0.0595
711	0.00104	1.74402	0.05837
710	9.27E-04	1.74648	0.05668
709	9.56E-04	1.74894	0.05927
708	9.63E-04	1.75141	0.05775
707	0.00102	1.75389	0.05964
706	0.0012	1.75637	0.06226
705	0.00126	1.75887	0.06202
704	0.00129	1.76136	0.06616
703	0.00125	1.76387	0.06065

Wavelength (nm)	Absorbance	Photon Energy (eV)	Relationship - Indirect ($\alpha h\nu^{1/2}$)
702	0.0012	1.76638	0.06305
701	0.00128	1.7689	0.06309
700	0.00139	1.77143	0.0663
699	0.00143	1.77396	0.0647
698	0.00154	1.7765	0.06573
697	0.00157	1.77905	0.06795
696	0.00159	1.78161	0.06582
695	0.00166	1.78417	0.0676
694	0.0017	1.78674	0.06988
693	0.00179	1.78932	0.06915
692	0.00184	1.79191	0.07149
691	0.00188	1.7945	0.07135
690	0.00196	1.7971	0.07258
689	0.0019	1.79971	0.07646
688	0.00199	1.80233	0.07912
687	0.00203	1.80495	0.08159
686	0.00204	1.80758	0.08026
685	0.00203	1.81022	0.08106
684	0.00209	1.81287	0.08251
683	0.00225	1.81552	0.08729
682	0.0023	1.81818	0.08734
681	0.00253	1.82085	0.08791
680	0.0027	1.82353	0.08866
679	0.00275	1.82622	0.09193
678	0.00294	1.82891	0.09216
677	0.00304	1.83161	0.09343
676	0.0031	1.83432	0.098
675	0.00335	1.83704	0.10043
674	0.00357	1.83976	0.09696
673	0.00383	1.8425	0.10089
672	0.00418	1.84524	0.10178
671	0.00444	1.84799	0.10451
670	0.00476	1.85075	0.10598
669	0.00518	1.85351	0.10678
668	0.00568	1.85629	0.10954
667	0.00622	1.85907	0.11095
666	0.00684	1.86186	0.11291
665	0.00741	1.86466	0.11285
664	0.00789	1.86747	0.11644

Wavelength (nm)	Absorbance	Photon Energy (eV)	Relationship - Indirect ($\alpha h\nu^{1/2}$)
663	0.00842	1.87029	0.11781
662	0.00887	1.87311	0.11701
661	0.00932	1.87595	0.11919
660	0.00964	1.87879	0.11968
659	0.00989	1.88164	0.12052
658	0.01003	1.8845	0.12091
657	0.01003	1.88737	0.12122
656	0.00998	1.89024	0.12004
655	0.00982	1.89313	0.12314
654	0.00966	1.89602	0.12139
653	0.0095	1.89893	0.12122
652	0.0092	1.90184	0.12107
651	0.00893	1.90476	0.11986
650	0.00863	1.90769	0.11933
649	0.0083	1.91063	0.11675
648	0.00805	1.91358	0.11679
647	0.00778	1.91654	0.11392
646	0.0075	1.9195	0.11268
645	0.00715	1.92248	0.11282
644	0.00678	1.92547	0.11074
643	0.00641	1.92846	0.10799
642	0.006	1.93146	0.10912
641	0.0056	1.93448	0.10459
640	0.00539	1.9375	0.10459
639	0.00519	1.94053	0.10561
638	0.00504	1.94357	0.10474
637	0.00503	1.94662	0.10637
636	0.00495	1.94969	0.10761
635	0.0049	1.95276	0.10802
634	0.00489	1.95584	0.10969
633	0.00493	1.95893	0.1105
632	0.00499	1.96203	0.11012
631	0.0052	1.96513	0.11317
630	0.00546	1.96825	0.11784
629	0.00577	1.97138	0.11865
628	0.00617	1.97452	0.12166
627	0.00654	1.97767	0.12415
626	0.00694	1.98083	0.12735
625	0.00735	1.984	0.12861

Wavelength (nm)	Absorbance	Photon Energy (eV)	Relationship - Indirect ($\alpha h\nu^{1/2}$)
624	0.00784	1.98718	0.13397
623	0.00841	1.99037	0.13782
622	0.00914	1.99357	0.14338
621	0.01005	1.99678	0.14595
620	0.01097	2	0.15203
619	0.01195	2.00323	0.15791
618	0.01314	2.00647	0.16232
617	0.01431	2.00972	0.16813
616	0.01561	2.01299	0.17521
615	0.01715	2.01626	0.18029
614	0.01863	2.01954	0.18686
613	0.02027	2.02284	0.19343
612	0.022	2.02614	0.20009
611	0.02362	2.02946	0.20743
610	0.02523	2.03279	0.21334
609	0.02665	2.03612	0.22179
608	0.02787	2.03947	0.22796
607	0.02888	2.04283	0.23493
606	0.02957	2.0462	0.24073
605	0.03	2.04959	0.24692
604	0.03011	2.05298	0.25131
603	0.02995	2.05638	0.25555
602	0.02948	2.0598	0.25825
601	0.0288	2.06323	0.25955
600	0.02777	2.06667	0.26012
599	0.02665	2.07012	0.26017
598	0.02528	2.07358	0.25708
597	0.0239	2.07705	0.25489
596	0.02227	2.08054	0.2514
595	0.02076	2.08403	0.24561
594	0.01931	2.08754	0.24029
593	0.01797	2.09106	0.23479
592	0.01682	2.09459	0.22805
591	0.01574	2.09814	0.21998
590	0.01482	2.10169	0.21303
589	0.0139	2.10526	0.20741
588	0.01315	2.10884	0.20164
587	0.01239	2.11244	0.19597
586	0.0118	2.11604	0.19188

Wavelength (nm)	Absorbance	Photon Energy (eV)	Relationship - Indirect ($\alpha h\nu^{1/2}$)
585	0.01138	2.11966	0.19035
584	0.01096	2.12329	0.18827
583	0.01067	2.12693	0.18649
582	0.01049	2.13058	0.18482
581	0.01043	2.13425	0.1853
580	0.01042	2.13793	0.18633
579	0.01057	2.14162	0.18918
578	0.01084	2.14533	0.19019
577	0.0112	2.14905	0.19114
576	0.01174	2.15278	0.19231
575	0.01238	2.15652	0.19418
574	0.01311	2.16028	0.19691
573	0.01404	2.16405	0.19878
572	0.01502	2.16783	0.20059
571	0.01614	2.17163	0.20369
570	0.01731	2.17544	0.20525
569	0.01842	2.17926	0.20696
568	0.01957	2.1831	0.20976
567	0.02067	2.18695	0.21222
566	0.02179	2.19081	0.21445
565	0.02288	2.19469	0.21733
564	0.02395	2.19858	0.21979
563	0.02495	2.20249	0.22168
562	0.02592	2.20641	0.22571
561	0.02667	2.21034	0.22789
560	0.02738	2.21429	0.23045
559	0.02809	2.21825	0.23299
558	0.02864	2.22222	0.23435
557	0.02923	2.22621	0.2369
556	0.02984	2.23022	0.2395
555	0.0303	2.23423	0.2411
554	0.03067	2.23827	0.24313
553	0.03106	2.24231	0.24553
552	0.03134	2.24638	0.24773
551	0.03177	2.25045	0.25142
550	0.03235	2.25455	0.25407
549	0.03299	2.25865	0.25803
548	0.03397	2.26277	0.26169
547	0.03506	2.26691	0.2673

Wavelength (nm)	Absorbance	Photon Energy (eV)	Relationship - Indirect ($\alpha h\nu^{1/2}$)
546	0.03658	2.27106	0.2711
545	0.03863	2.27523	0.27847
544	0.041	2.27941	0.28615
543	0.04392	2.28361	0.29485
542	0.04724	2.28782	0.30411
541	0.05087	2.29205	0.31485
540	0.05492	2.2963	0.32617
539	0.0594	2.30056	0.33775
538	0.06409	2.30483	0.3506
537	0.06898	2.30912	0.36341
536	0.07393	2.31343	0.37633
535	0.07871	2.31776	0.38967
534	0.08344	2.3221	0.40377
533	0.08779	2.32645	0.41784
532	0.09173	2.33083	0.43199
531	0.09514	2.33522	0.44429
530	0.09785	2.33962	0.45537
529	0.09973	2.34405	0.46503
528	0.10093	2.34848	0.47297
527	0.10134	2.35294	0.48001
526	0.10074	2.35741	0.48443
525	0.09942	2.3619	0.48758
524	0.09715	2.36641	0.48846
523	0.09407	2.37094	0.48785
522	0.09053	2.37548	0.48575
521	0.0866	2.38004	0.48105
520	0.08268	2.38462	0.47346
519	0.07851	2.38921	0.46515
518	0.07449	2.39382	0.45591
517	0.07063	2.39845	0.44455
516	0.06697	2.4031	0.4334
515	0.06349	2.40777	0.42313
514	0.06001	2.41245	0.4127
513	0.05664	2.41715	0.40261
512	0.05341	2.42188	0.39413
511	0.05028	2.42661	0.38518
510	0.04727	2.43137	0.37695
509	0.04448	2.43615	0.36896
508	0.04175	2.44094	0.36067

Wavelength (nm)	Absorbance	Photon Energy (eV)	Relationship - Indirect ($\alpha h\nu^{1/2}$)
507	0.03921	2.44576	0.35296
506	0.03686	2.45059	0.34534
505	0.03476	2.45545	0.33906
504	0.03304	2.46032	0.33278
503	0.03159	2.46521	0.3275
502	0.03045	2.47012	0.32332
501	0.02954	2.47505	0.31968
500	0.02884	2.48	0.31799
499	0.02831	2.48497	0.31747
498	0.02795	2.48996	0.31799
497	0.02767	2.49497	0.31908
496	0.02745	2.5	0.31992
495	0.02729	2.50505	0.32226
494	0.02721	2.51012	0.32605
493	0.02711	2.51521	0.33031
492	0.02715	2.52033	0.33401
491	0.02721	2.52546	0.33772
490	0.02742	2.53061	0.34248
489	0.02759	2.53579	0.34673
488	0.02775	2.54098	0.35234
487	0.02821	2.5462	0.35663
486	0.02868	2.55144	0.36112
485	0.02932	2.5567	0.36581
484	0.03025	2.56198	0.36973
483	0.03119	2.56729	0.37331
482	0.03241	2.57261	0.37868
481	0.03396	2.57796	0.38314
480	0.03577	2.58333	0.38788
479	0.03792	2.58873	0.39257
478	0.04056	2.59414	0.39726
477	0.04356	2.59958	0.40403
476	0.04704	2.60504	0.41091
475	0.05124	2.61053	0.4181
474	0.05601	2.61603	0.42693
473	0.06163	2.62156	0.43635
472	0.06832	2.62712	0.44558
471	0.07605	2.6327	0.45608
470	0.08509	2.6383	0.4668
469	0.09568	2.64392	0.47826

Wavelength (nm)	Absorbance	Photon Energy (eV)	Relationship - Indirect ($\alpha h\nu^{1/2}$)
468	0.10819	2.64957	0.49178
467	0.12275	2.65525	0.50516
466	0.13977	2.66094	0.51918
465	0.15982	2.66667	0.53428
464	0.1831	2.67241	0.55048
463	0.21028	2.67819	0.56756
462	0.24156	2.68398	0.58578
461	0.27747	2.6898	0.60476
460	0.31864	2.69565	0.6256
459	0.36516	2.70153	0.64795
458	0.41742	2.70742	0.67332
457	0.47554	2.71335	0.70035
456	0.53908	2.7193	0.73052
455	0.6073	2.72527	0.76442
454	0.67879	2.73128	0.80173
453	0.75157	2.73731	0.84295
452	0.82303	2.74336	0.88886
451	0.89002	2.74945	0.93966
450	0.94896	2.75556	0.99528
449	0.99567	2.76169	1.05663
448	1.02628	2.76786	1.12264
447	1.03723	2.77405	1.19424
446	1.02687	2.78027	1.27093
445	0.99531	2.78652	1.35158
444	0.94519	2.79279	1.43545
443	0.88124	2.7991	1.52189
442	0.80899	2.80543	1.60852
441	0.73375	2.81179	1.692
440	0.66003	2.81818	1.76933
439	0.59187	2.8246	1.83776
438	0.53161	2.83105	1.89314
437	0.48073	2.83753	1.93217
436	0.4396	2.84404	1.95241
435	0.40798	2.85057	1.95105
434	0.38558	2.85714	1.92718
433	0.37171	2.86374	1.88306
432	0.36555	2.87037	1.82285
431	0.36633	2.87703	1.75199
430	0.3731	2.88372	1.67616

Wavelength (nm)	Absorbance	Photon Energy (eV)	Relationship - Indirect ($\alpha h\nu^{1/2}$)
429	0.38483	2.89044	1.60099
428	0.40069	2.8972	1.53106
427	0.4199	2.90398	1.4694
426	0.44149	2.9108	1.417
425	0.4643	2.91765	1.37428
424	0.4867	2.92453	1.34057
423	0.50638	2.93144	1.31321
422	0.52052	2.93839	1.29096
421	0.52687	2.94537	1.27078
420	0.52279	2.95238	1.25075
419	0.50695	2.95943	1.22977
418	0.48157	2.96651	1.20728
417	0.44928	2.97362	1.18318
416	0.41288	2.98077	1.15718
415	0.37578	2.98795	1.13055
414	0.34075	2.99517	1.10295
413	0.30952	3.00242	1.07448
412	0.28303	3.00971	1.04465
411	0.26165	3.01703	1.01364
410	0.24555	3.02439	0.98023
409	0.23451	3.03178	0.94624
408	0.2278	3.03922	0.91226
407	0.22478	3.04668	0.87884
406	0.22448	3.05419	0.84767
405	0.22594	3.06173	0.81855
404	0.22858	3.06931	0.79249
403	0.23158	3.07692	0.76995
402	0.2344	3.08458	0.75079
401	0.23654	3.09227	0.73395
400	0.23759	3.1	0.71933
399	0.23728	3.10777	0.70646
398	0.23561	3.11558	0.69499
397	0.2325	3.12343	0.68447
396	0.22817	3.13131	0.67344
395	0.22284	3.13924	0.66509
394	0.21678	3.14721	0.65694
393	0.21029	3.15522	0.64918
392	0.20368	3.16327	0.64252
391	0.19711	3.17136	0.6374

Wavelength (nm)	Absorbance	Photon Energy (eV)	Relationship - Indirect ($\alpha h\nu^{1/2}$)
390	0.19085	3.17949	0.63222
389	0.18488	3.18766	0.62765
388	0.17919	3.19588	0.62283
387	0.17386	3.20413	0.61913
386	0.16883	3.21244	0.61627
385	0.16414	3.22078	0.61234
384	0.15968	3.22917	0.60964
383	0.1554	3.2376	0.60693
382	0.15127	3.24607	0.6039
381	0.14739	3.25459	0.60239
380	0.14383	3.26316	0.59951
379	0.14049	3.27177	0.59761
378	0.13736	3.28042	0.59579
377	0.1344	3.28912	0.59264
376	0.13166	3.29787	0.58955
375	0.12908	3.30667	0.58616
374	0.12682	3.31551	0.58238
373	0.12489	3.3244	0.57803
372	0.12299	3.33333	0.57405
371	0.12131	3.34232	0.5689
370	0.11967	3.35135	0.56375
369	0.118	3.36043	0.55885
368	0.11648	3.36957	0.55556
367	0.11486	3.37875	0.55171
366	0.11325	3.38798	0.54874
365	0.11161	3.39726	0.54592
364	0.10973	3.40659	0.54261
363	0.10775	3.41598	0.54156
362	0.10555	3.42541	0.53905
361	0.10314	3.4349	0.53749
360	0.10069	3.44444	0.53467
359	0.09813	3.45404	0.53234
358	0.0956	3.46369	0.5315
357	0.09308	3.47339	0.52931
356	0.09062	3.48315	0.52838
355	0.08825	3.49296	0.52595
354	0.08603	3.50282	0.52475
353	0.08406	3.51275	0.52321
352	0.08215	3.52273	0.52177

Wavelength (nm)	Absorbance	Photon Energy (eV)	Relationship - Indirect ($\alpha h\nu^{1/2}$)
351	0.08054	3.53276	0.52034
350	0.07901	3.54286	0.51929

Table 2.15: 3VTP Tauc Tabless

Wavelength (nm)	Absorbance	Photon Energy (eV)	Relationship - Indirect ($\alpha h\nu^{1/2}$)
800	0.00141	1.55	0.04363
799	0.00125	1.55194	0.0377
798	0.00103	1.55388	0.03343
797	9.97E-04	1.55583	0.03221
796	7.91E-04	1.55779	0.02583
795	6.47E-04	1.55975	0.02194
794	7.48E-04	1.56171	0.02916
793	5.81E-04	1.56368	0.02625
792	6.51E-04	1.56566	0.02835
791	7.51E-04	1.56764	0.03031
790	6.73E-04	1.56962	0.02951
789	7.69E-04	1.57161	0.03061
788	8.70E-04	1.5736	0.03374
787	8.03E-04	1.5756	0.02918
786	7.59E-04	1.57761	0.03116
785	0.0011	1.57962	0.03717
784	0.00101	1.58163	0.03521
783	8.79E-04	1.58365	0.03427
782	0.00109	1.58568	0.03536
781	9.56E-04	1.58771	0.03646
780	9.32E-04	1.58974	0.03193
779	9.23E-04	1.59178	0.03199
778	9.15E-04	1.59383	0.03117
777	9.96E-04	1.59588	0.03578
776	9.65E-04	1.59794	0.03649
775	7.98E-04	1.6	0.0355
774	8.81E-04	1.60207	0.03467
773	8.23E-04	1.60414	0.03481
772	7.85E-04	1.60622	0.02919
771	7.43E-04	1.6083	0.02852
770	8.70E-04	1.61039	0.03585
769	6.33E-04	1.61248	0.03311

Wavelength (nm)	Absorbance	Photon Energy (eV)	Relationship - Indirect ($\alpha h\nu^{1/2}$)
768	6.10E-04	1.61458	0.03184
767	6.12E-04	1.61669	0.02357
766	5.77E-04	1.6188	0.02504
765	3.43E-04	1.62092	0.01397
764	6.24E-04	1.62304	0.02749
763	7.84E-04	1.62516	0.03346
762	7.47E-04	1.6273	0.03202
761	7.85E-04	1.62943	0.03101
760	7.27E-04	1.63158	0.0321
759	6.96E-04	1.63373	0.0316
758	7.46E-04	1.63588	0.03276
757	7.54E-04	1.63804	0.03245
756	5.78E-04	1.64021	0.02701
755	3.02E-04	1.64238	0.02098
754	4.46E-04	1.64456	0.02628
753	3.69E-04	1.64675	0.01621
752	9.08E-04	1.64894	0.03277
751	0.00112	1.65113	0.03858
750	0.00112	1.65333	0.04012
749	0.00111	1.65554	0.04071
748	0.00126	1.65775	0.04007
747	0.00103	1.65997	0.03961
746	8.51E-04	1.6622	0.03864
745	7.43E-04	1.66443	0.03685
744	8.38E-04	1.66667	0.0391
743	3.81E-04	1.66891	0.02955
742	8.83E-04	1.67116	0.04075
741	7.31E-04	1.67341	0.03618
740	0.00113	1.67568	0.04357
739	0.00102	1.67794	0.03827
738	0.00111	1.68022	0.04221
737	0.00113	1.6825	0.04387
736	0.00111	1.68478	0.0445
735	0.00117	1.68707	0.04415
734	9.03E-04	1.68937	0.04403
733	8.18E-04	1.69168	0.03812
732	0.00108	1.69399	0.04247
731	0.00122	1.69631	0.04488
730	0.00138	1.69863	0.05091

Wavelength (nm)	Absorbance	Photon Energy (eV)	Relationship - Indirect ($\alpha h\nu^{1/2}$)
729	0.00143	1.70096	0.05006
728	0.00123	1.7033	0.05015
727	0.00128	1.70564	0.04913
726	0.0012	1.70799	0.04433
725	0.00129	1.71034	0.04793
724	0.0013	1.71271	0.04761
723	0.00132	1.71508	0.04911
722	0.00164	1.71745	0.05322
721	0.00153	1.71983	0.05069
720	0.00154	1.72222	0.05503
719	0.00167	1.72462	0.05691
718	0.00156	1.72702	0.05612
717	0.00158	1.72943	0.05539
716	0.00177	1.73184	0.06047
715	0.00166	1.73427	0.05717
714	0.00158	1.73669	0.05794
713	0.00159	1.73913	0.05824
712	0.0017	1.74157	0.0595
711	0.00163	1.74402	0.05837
710	0.00158	1.74648	0.05668
709	0.00153	1.74894	0.05927
708	0.00168	1.75141	0.05775
707	0.00162	1.75389	0.05964
706	0.00182	1.75637	0.06226
705	0.00191	1.75887	0.06202
704	0.00204	1.76136	0.06616
703	0.0018	1.76387	0.06065
702	0.00181	1.76638	0.06305
701	0.0018	1.7689	0.06309
700	0.002	1.77143	0.0663
699	0.00198	1.77396	0.0647
698	0.00202	1.7765	0.06573
697	0.00212	1.77905	0.06795
696	0.002	1.78161	0.06582
695	0.0021	1.78417	0.0676
694	0.00238	1.78674	0.06988
693	0.00249	1.78932	0.06915
692	0.00249	1.79191	0.07149
691	0.00244	1.7945	0.07135

Wavelength (nm)	Absorbance	Photon Energy (eV)	Relationship - Indirect ($\alpha h\nu^{1/2}$)
690	0.00259	1.7971	0.07258
689	0.00285	1.79971	0.07646
688	0.00302	1.80233	0.07912
687	0.00326	1.80495	0.08159
686	0.0032	1.80758	0.08026
685	0.00317	1.81022	0.08106
684	0.00327	1.81287	0.08251
683	0.00349	1.81552	0.08729
682	0.0034	1.81818	0.08734
681	0.00354	1.82085	0.08791
680	0.00347	1.82353	0.08866
679	0.00368	1.82622	0.09193
678	0.00367	1.82891	0.09216
677	0.00359	1.83161	0.09343
676	0.0038	1.83432	0.098
675	0.00392	1.83704	0.10043
674	0.00369	1.83976	0.09696
673	0.00387	1.8425	0.10089
672	0.00394	1.84524	0.10178
671	0.00417	1.84799	0.10451
670	0.00436	1.85075	0.10598
669	0.00445	1.85351	0.10678
668	0.00471	1.85629	0.10954
667	0.00499	1.85907	0.11095
666	0.00551	1.86186	0.11291
665	0.00542	1.86466	0.11285
664	0.00606	1.86747	0.11644
663	0.00644	1.87029	0.11781
662	0.00658	1.87311	0.11701
661	0.0072	1.87595	0.11919
660	0.00762	1.87879	0.11968
659	0.00843	1.88164	0.12052
658	0.0089	1.8845	0.12091
657	0.00953	1.88737	0.12122
656	0.00995	1.89024	0.12004
655	0.01095	1.89313	0.12314
654	0.0113	1.89602	0.12139
653	0.01153	1.89893	0.12122
652	0.01179	1.90184	0.12107

Wavelength (nm)	Absorbance	Photon Energy (eV)	Relationship - Indirect ($\alpha h\nu^{1/2}$)
651	0.01185	1.90476	0.11986
650	0.0117	1.90769	0.11933
649	0.01128	1.91063	0.11675
648	0.01103	1.91358	0.11679
647	0.01033	1.91654	0.11392
646	0.00984	1.9195	0.11268
645	0.00937	1.92248	0.11282
644	0.00886	1.92547	0.11074
643	0.00818	1.92846	0.10799
642	0.00789	1.93146	0.10912
641	0.00702	1.93448	0.10459
640	0.00678	1.9375	0.10459
639	0.00653	1.94053	0.10561
638	0.00627	1.94357	0.10474
637	0.00641	1.94662	0.10637
636	0.00608	1.94969	0.10761
635	0.00599	1.95276	0.10802
634	0.00588	1.95584	0.10969
633	0.00575	1.95893	0.1105
632	0.00573	1.96203	0.11012
631	0.00604	1.96513	0.11317
630	0.0063	1.96825	0.11784
629	0.00617	1.97138	0.11865
628	0.00646	1.97452	0.12166
627	0.00677	1.97767	0.12415
626	0.007	1.98083	0.12735
625	0.00709	1.984	0.12861
624	0.00759	1.98718	0.13397
623	0.00812	1.99037	0.13782
622	0.00896	1.99357	0.14338
621	0.00927	1.99678	0.14595
620	0.01019	2	0.15203
619	0.01097	2.00323	0.15791
618	0.01161	2.00647	0.16232
617	0.01258	2.00972	0.16813
616	0.0137	2.01299	0.17521
615	0.01472	2.01626	0.18029
614	0.01597	2.01954	0.18686
613	0.01739	2.02284	0.19343

Wavelength (nm)	Absorbance	Photon Energy (eV)	Relationship - Indirect ($\alpha h\nu^{1/2}$)
612	0.01905	2.02614	0.20009
611	0.02069	2.02946	0.20743
610	0.02258	2.03279	0.21334
609	0.0249	2.03612	0.22179
608	0.02704	2.03947	0.22796
607	0.02926	2.04283	0.23493
606	0.03151	2.0462	0.24073
605	0.03343	2.04959	0.24692
604	0.03522	2.05298	0.25131
603	0.03678	2.05638	0.25555
602	0.03787	2.0598	0.25825
601	0.0386	2.06323	0.25955
600	0.03967	2.06667	0.26012
599	0.04004	2.07012	0.26017
598	0.03952	2.07358	0.25708
597	0.03895	2.07705	0.25489
596	0.03806	2.08054	0.2514
595	0.03642	2.08403	0.24561
594	0.03458	2.08754	0.24029
593	0.03269	2.09106	0.23479
592	0.03054	2.09459	0.22805
591	0.02792	2.09814	0.21998
590	0.02542	2.10169	0.21303
589	0.02322	2.10526	0.20741
588	0.02114	2.10884	0.20164
587	0.01917	2.11244	0.19597
586	0.01749	2.11604	0.19188
585	0.01622	2.11966	0.19035
584	0.01489	2.12329	0.18827
583	0.01387	2.12693	0.18649
582	0.01292	2.13058	0.18482
581	0.01239	2.13425	0.1853
580	0.01179	2.13793	0.18633
579	0.01187	2.14162	0.18918
578	0.01164	2.14533	0.19019
577	0.01118	2.14905	0.19114
576	0.01133	2.15278	0.19231
575	0.01138	2.15652	0.19418
574	0.01174	2.16028	0.19691

Wavelength (nm)	Absorbance	Photon Energy (eV)	Relationship - Indirect ($\alpha h\nu^{1/2}$)
573	0.01217	2.16405	0.19878
572	0.01264	2.16783	0.20059
571	0.01342	2.17163	0.20369
570	0.01395	2.17544	0.20525
569	0.01457	2.17926	0.20696
568	0.01532	2.1831	0.20976
567	0.01598	2.18695	0.21222
566	0.01705	2.19081	0.21445
565	0.01795	2.19469	0.21733
564	0.01895	2.19858	0.21979
563	0.01965	2.20249	0.22168
562	0.02096	2.20641	0.22571
561	0.02204	2.21034	0.22789
560	0.02297	2.21429	0.23045
559	0.02384	2.21825	0.23299
558	0.02462	2.22222	0.23435
557	0.02549	2.22621	0.2369
556	0.02605	2.23022	0.2395
555	0.0266	2.23423	0.2411
554	0.027	2.23827	0.24313
553	0.02737	2.24231	0.24553
552	0.02771	2.24638	0.24773
551	0.02791	2.25045	0.25142
550	0.02814	2.25455	0.25407
549	0.02849	2.25865	0.25803
548	0.0285	2.26277	0.26169
547	0.0294	2.26691	0.2673
546	0.02959	2.27106	0.2711
545	0.0306	2.27523	0.27847
544	0.03203	2.27941	0.28615
543	0.0336	2.28361	0.29485
542	0.03547	2.28782	0.30411
541	0.03809	2.29205	0.31485
540	0.04122	2.2963	0.32617
539	0.04476	2.30056	0.33775
538	0.04916	2.30483	0.3506
537	0.05377	2.30912	0.36341
536	0.05916	2.31343	0.37633
535	0.06491	2.31776	0.38967

Wavelength (nm)	Absorbance	Photon Energy (eV)	Relationship - Indirect ($\alpha h\nu^{1/2}$)
534	0.07123	2.3221	0.40377
533	0.07812	2.32645	0.41784
532	0.0853	2.33083	0.43199
531	0.09225	2.33522	0.44429
530	0.0988	2.33962	0.45537
529	0.10511	2.34405	0.46503
528	0.11074	2.34848	0.47297
527	0.11572	2.35294	0.48001
526	0.11968	2.35741	0.48443
525	0.12274	2.3619	0.48758
524	0.12465	2.36641	0.48846
523	0.12574	2.37094	0.48785
522	0.12585	2.37548	0.48575
521	0.12465	2.38004	0.48105
520	0.12212	2.38462	0.47346
519	0.11843	2.38921	0.46515
518	0.11407	2.39382	0.45591
517	0.10887	2.39845	0.44455
516	0.10313	2.4031	0.4334
515	0.09754	2.40777	0.42313
514	0.09201	2.41245	0.4127
513	0.08667	2.41715	0.40261
512	0.08186	2.42188	0.39413
511	0.07712	2.42661	0.38518
510	0.0726	2.43137	0.37695
509	0.06806	2.43615	0.36896
508	0.06357	2.44094	0.36067
507	0.05931	2.44576	0.35296
506	0.05513	2.45059	0.34534
505	0.05145	2.45545	0.33906
504	0.04804	2.46032	0.33278
503	0.04497	2.46521	0.3275
502	0.04243	2.47012	0.32332
501	0.04017	2.47505	0.31968
500	0.03855	2.48	0.31799
499	0.03743	2.48497	0.31747
498	0.03662	2.48996	0.31799
497	0.03602	2.49497	0.31908
496	0.036	2.5	0.31992

Wavelength (nm)	Absorbance	Photon Energy (eV)	Relationship - Indirect ($\alpha h\nu^{1/2}$)
495	0.03607	2.50505	0.32226
494	0.03665	2.51012	0.32605
493	0.0372	2.51521	0.33031
492	0.03763	2.52033	0.33401
491	0.03813	2.52546	0.33772
490	0.03882	2.53061	0.34248
489	0.03934	2.53579	0.34673
488	0.04029	2.54098	0.35234
487	0.04091	2.5462	0.35663
486	0.0415	2.55144	0.36112
485	0.04191	2.5567	0.36581
484	0.04187	2.56198	0.36973
483	0.04182	2.56729	0.37331
482	0.04192	2.57261	0.37868
481	0.04149	2.57796	0.38314
480	0.04104	2.58333	0.38788
479	0.04055	2.58873	0.39257
478	0.03995	2.59414	0.39726
477	0.03967	2.59958	0.40403
476	0.03937	2.60504	0.41091
475	0.03916	2.61053	0.4181
474	0.03943	2.61603	0.42693
473	0.0398	2.62156	0.43635
472	0.04027	2.62712	0.44558
471	0.04109	2.6327	0.45608
470	0.04184	2.6383	0.4668
469	0.04265	2.64392	0.47826
468	0.04416	2.64957	0.49178
467	0.04543	2.65525	0.50516
466	0.04685	2.66094	0.51918
465	0.0486	2.66667	0.53428
464	0.05052	2.67241	0.55048
463	0.05273	2.67819	0.56756
462	0.05543	2.68398	0.58578
461	0.0584	2.6898	0.60476
460	0.06194	2.69565	0.6256
459	0.06635	2.70153	0.64795
458	0.07178	2.70742	0.67332
457	0.07794	2.71335	0.70035

Wavelength (nm)	Absorbance	Photon Energy (eV)	Relationship - Indirect ($\alpha h\nu^{1/2}$)
456	0.086	2.7193	0.73052
455	0.09605	2.72527	0.76442
454	0.1089	2.73128	0.80173
453	0.12486	2.73731	0.84295
452	0.14548	2.74336	0.88886
451	0.17147	2.74945	0.93966
450	0.20374	2.75556	0.99528
449	0.24452	2.76169	1.05663
448	0.29432	2.76786	1.12264
447	0.3558	2.77405	1.19424
446	0.43101	2.78027	1.27093
445	0.5214	2.78652	1.35158
444	0.62831	2.79279	1.43545
443	0.75423	2.7991	1.52189
442	0.89812	2.80543	1.60852
441	1.05765	2.81179	1.692
440	1.22776	2.81818	1.76933
439	1.40267	2.8246	1.83776
438	1.57253	2.83105	1.89314
437	1.72494	2.83753	1.93217
436	1.84632	2.84404	1.95241
435	1.92045	2.85057	1.95105
434	1.93481	2.85714	1.92718
433	1.88551	2.86374	1.88306
432	1.77953	2.87037	1.82285
431	1.63312	2.87703	1.75199
430	1.46655	2.88372	1.67616
429	1.29936	2.89044	1.60099
428	1.14751	2.8972	1.53106
427	1.0199	2.90398	1.4694
426	0.92056	2.9108	1.417
425	0.84885	2.91765	1.37428
424	0.80119	2.92453	1.34057
423	0.77169	2.93144	1.31321
422	0.75482	2.93839	1.29096
421	0.7434	2.94537	1.27078
420	0.73195	2.95238	1.25075
419	0.71632	2.95943	1.22977
418	0.69505	2.96651	1.20728

Wavelength (nm)	Absorbance	Photon Energy (eV)	Relationship - Indirect ($\alpha h\nu^{1/2}$)
417	0.66863	2.97362	1.18318
416	0.63919	2.98077	1.15718
415	0.60848	2.98795	1.13055
414	0.57816	2.99517	1.10295
413	0.54784	3.00242	1.07448
412	0.51782	3.00971	1.04465
411	0.48684	3.01703	1.01364
410	0.4546	3.02439	0.98023
409	0.42128	3.03178	0.94624
408	0.38793	3.03922	0.91226
407	0.35553	3.04668	0.87884
406	0.32517	3.05419	0.84767
405	0.29802	3.06173	0.81855
404	0.27421	3.06931	0.79249
403	0.25442	3.07692	0.76995
402	0.23792	3.08458	0.75079
401	0.22447	3.09227	0.73395
400	0.21327	3.1	0.71933
399	0.20392	3.10777	0.70646
398	0.19563	3.11558	0.69499
397	0.18851	3.12343	0.68447
396	0.1814	3.13131	0.67344
395	0.17559	3.13924	0.66509
394	0.17031	3.14721	0.65694
393	0.16545	3.15522	0.64918
392	0.16135	3.16327	0.64252
391	0.15796	3.17136	0.6374
390	0.15501	3.17949	0.63222
389	0.15227	3.18766	0.62765
388	0.14964	3.19588	0.62283
387	0.14768	3.20413	0.61913
386	0.14608	3.21244	0.61627
385	0.1444	3.22078	0.61234
384	0.14291	3.22917	0.60964
383	0.14177	3.2376	0.60693
382	0.14056	3.24607	0.6039
381	0.13988	3.25459	0.60239
380	0.1385	3.26316	0.59951
379	0.13788	3.27177	0.59761

Wavelength (nm)	Absorbance	Photon Energy (eV)	Relationship - Indirect ($\alpha h\nu^{1/2}$)
378	0.137	3.28042	0.59579
377	0.13561	3.28912	0.59264
376	0.13417	3.29787	0.58955
375	0.13259	3.30667	0.58616
374	0.13066	3.31551	0.58238
373	0.12834	3.3244	0.57803
372	0.126	3.33333	0.57405
371	0.12323	3.34232	0.5689
370	0.12004	3.35135	0.56375
369	0.1175	3.36043	0.55885
368	0.11511	3.36957	0.55556
367	0.11272	3.37875	0.55171
366	0.11067	3.38798	0.54874
365	0.10887	3.39726	0.54592
364	0.10688	3.40659	0.54261
363	0.1055	3.41598	0.54156
362	0.10378	3.42541	0.53905
361	0.10248	3.4349	0.53749
360	0.10092	3.44444	0.53467
359	0.09949	3.45404	0.53234
358	0.09812	3.46369	0.5315
357	0.0967	3.47339	0.52931
356	0.09554	3.48315	0.52838
355	0.09417	3.49296	0.52595
354	0.09309	3.50282	0.52475
353	0.09185	3.51275	0.52321
352	0.09096	3.52273	0.52177
351	0.08968	3.53276	0.52034
350	0.08875	3.54286	0.51929

Table 2.16: F3VTP Tauc Tables

Wavelength (nm)	Absorbance	Photon Energy (eV)	Relationship - Indirect ($\alpha h\nu^{1/2}$)
800	0.00111	1.55	0.04363
799	0.00102	1.55194	0.0377
798	9.79E-04	1.55388	0.03343
797	0.00101	1.55583	0.03221
796	0.00106	1.55779	0.02583
795	0.00112	1.55975	0.02194

Wavelength (nm)	Absorbance	Photon Energy (eV)	Relationship - Indirect ($\alpha h\nu^{1/2}$)
794	0.00111	1.56171	0.02916
793	0.00117	1.56368	0.02625
792	0.00113	1.56566	0.02835
791	0.00118	1.56764	0.03031
790	0.00126	1.56962	0.02951
789	0.00122	1.57161	0.03061
788	0.00124	1.5736	0.03374
787	0.0012	1.5756	0.02918
786	0.00122	1.57761	0.03116
785	0.00129	1.57962	0.03717
784	0.00125	1.58163	0.03521
783	0.00131	1.58365	0.03427
782	0.0013	1.58568	0.03536
781	0.00124	1.58771	0.03646
780	0.00122	1.58974	0.03193
779	0.00119	1.59178	0.03199
778	0.00117	1.59383	0.03117
777	0.0013	1.59588	0.03578
776	0.00131	1.59794	0.03649
775	0.00126	1.6	0.0355
774	0.00127	1.60207	0.03467
773	0.00118	1.60414	0.03481
772	0.00119	1.60622	0.02919
771	0.00118	1.6083	0.02852
770	0.00119	1.61039	0.03585
769	0.00111	1.61248	0.03311
768	0.00115	1.61458	0.03184
767	0.00121	1.61669	0.02357
766	0.00123	1.6188	0.02504
765	0.00128	1.62092	0.01397
764	0.0013	1.62304	0.02749
763	0.00118	1.62516	0.03346
762	0.00111	1.6273	0.03202
761	0.00118	1.62943	0.03101
760	0.00113	1.63158	0.0321
759	0.00122	1.63373	0.0316
758	0.00127	1.63588	0.03276
757	0.00121	1.63804	0.03245
756	0.00122	1.64021	0.02701
755	0.00122	1.64238	0.02098

Wavelength (nm)	Absorbance	Photon Energy (eV)	Relationship - Indirect ($\alpha h\nu^{1/2}$)
754	0.00127	1.64456	0.02628
753	0.00125	1.64675	0.01621
752	0.00127	1.64894	0.03277
751	0.00128	1.65113	0.03858
750	0.0012	1.65333	0.04012
749	0.0012	1.65554	0.04071
748	0.00117	1.65775	0.04007
747	0.00125	1.65997	0.03961
746	0.00126	1.6622	0.03864
745	0.00137	1.66443	0.03685
744	0.00136	1.66667	0.0391
743	0.00133	1.66891	0.02955
742	0.00128	1.67116	0.04075
741	0.00126	1.67341	0.03618
740	0.00143	1.67568	0.04357
739	0.00137	1.67794	0.03827
738	0.00134	1.68022	0.04221
737	0.00136	1.6825	0.04387
736	0.0014	1.68478	0.0445
735	0.00141	1.68707	0.04415
734	0.00146	1.68937	0.04403
733	0.00148	1.69168	0.03812
732	0.00149	1.69399	0.04247
731	0.00153	1.69631	0.04488
730	0.00161	1.69863	0.05091
729	0.00162	1.70096	0.05006
728	0.0017	1.7033	0.05015
727	0.00178	1.70564	0.04913
726	0.00184	1.70799	0.04433
725	0.00191	1.71034	0.04793
724	0.00188	1.71271	0.04761
723	0.00187	1.71508	0.04911
722	0.00183	1.71745	0.05322
721	0.00188	1.71983	0.05069
720	0.00205	1.72222	0.05503
719	0.00217	1.72462	0.05691
718	0.00225	1.72702	0.05612
717	0.00227	1.72943	0.05539
716	0.00227	1.73184	0.06047
715	0.00229	1.73427	0.05717

Wavelength (nm)	Absorbance	Photon Energy (eV)	Relationship - Indirect ($\alpha h\nu^{1/2}$)
714	0.00244	1.73669	0.05794
713	0.00254	1.73913	0.05824
712	0.00267	1.74157	0.0595
711	0.00282	1.74402	0.05837
710	0.00283	1.74648	0.05668
709	0.00293	1.74894	0.05927
708	0.00298	1.75141	0.05775
707	0.00303	1.75389	0.05964
706	0.00315	1.75637	0.06226
705	0.00325	1.75887	0.06202
704	0.00335	1.76136	0.06616
703	0.00347	1.76387	0.06065
702	0.00359	1.76638	0.06305
701	0.00368	1.7689	0.06309
700	0.0038	1.77143	0.0663
699	0.00387	1.77396	0.0647
698	0.004	1.7765	0.06573
697	0.00409	1.77905	0.06795
696	0.00419	1.78161	0.06582
695	0.00429	1.78417	0.0676
694	0.00435	1.78674	0.06988
693	0.00443	1.78932	0.06915
692	0.00458	1.79191	0.07149
691	0.00469	1.7945	0.07135
690	0.00483	1.7971	0.07258
689	0.00497	1.79971	0.07646
688	0.00506	1.80233	0.07912
687	0.00508	1.80495	0.08159
686	0.00519	1.80758	0.08026
685	0.00528	1.81022	0.08106
684	0.00538	1.81287	0.08251
683	0.00568	1.81552	0.08729
682	0.00575	1.81818	0.08734
681	0.0059	1.82085	0.08791
680	0.00612	1.82353	0.08866
679	0.00619	1.82622	0.09193
678	0.00639	1.82891	0.09216
677	0.00655	1.83161	0.09343
676	0.00663	1.83432	0.098
675	0.00682	1.83704	0.10043

Wavelength (nm)	Absorbance	Photon Energy (eV)	Relationship - Indirect ($\alpha h\nu^{1/2}$)
674	0.00701	1.83976	0.09696
673	0.00725	1.8425	0.10089
672	0.00754	1.84524	0.10178
671	0.00774	1.84799	0.10451
670	0.00802	1.85075	0.10598
669	0.00837	1.85351	0.10678
668	0.00864	1.85629	0.10954
667	0.0091	1.85907	0.11095
666	0.00947	1.86186	0.11291
665	0.00978	1.86466	0.11285
664	0.01012	1.86747	0.11644
663	0.01037	1.87029	0.11781
662	0.0106	1.87311	0.11701
661	0.01073	1.87595	0.11919
660	0.01083	1.87879	0.11968
659	0.01075	1.88164	0.12052
658	0.0106	1.8845	0.12091
657	0.01039	1.88737	0.12122
656	0.01006	1.89024	0.12004
655	0.00983	1.89313	0.12314
654	0.00953	1.89602	0.12139
653	0.00926	1.89893	0.12122
652	0.00895	1.90184	0.12107
651	0.0085	1.90476	0.11986
650	0.00823	1.90769	0.11933
649	0.00795	1.91063	0.11675
648	0.00769	1.91358	0.11679
647	0.00753	1.91654	0.11392
646	0.00732	1.9195	0.11268
645	0.00703	1.92248	0.11282
644	0.00684	1.92547	0.11074
643	0.00669	1.92846	0.10799
642	0.00645	1.93146	0.10912
641	0.00627	1.93448	0.10459
640	0.00622	1.9375	0.10459
639	0.00613	1.94053	0.10561
638	0.00618	1.94357	0.10474
637	0.00623	1.94662	0.10637
636	0.0062	1.94969	0.10761
635	0.00618	1.95276	0.10802

Wavelength (nm)	Absorbance	Photon Energy (eV)	Relationship - Indirect ($\alpha h\nu^{1/2}$)
634	0.00625	1.95584	0.10969
633	0.00639	1.95893	0.1105
632	0.00661	1.96203	0.11012
631	0.00681	1.96513	0.11317
630	0.00708	1.96825	0.11784
629	0.00746	1.97138	0.11865
628	0.00782	1.97452	0.12166
627	0.00821	1.97767	0.12415
626	0.0086	1.98083	0.12735
625	0.00893	1.984	0.12861
624	0.00938	1.98718	0.13397
623	0.00997	1.99037	0.13782
622	0.01066	1.99357	0.14338
621	0.01146	1.99678	0.14595
620	0.01222	2	0.15203
619	0.01306	2.00323	0.15791
618	0.0139	2.00647	0.16232
617	0.0148	2.00972	0.16813
616	0.01593	2.01299	0.17521
615	0.01709	2.01626	0.18029
614	0.0183	2.01954	0.18686
613	0.01952	2.02284	0.19343
612	0.02069	2.02614	0.20009
611	0.02184	2.02946	0.20743
610	0.02295	2.03279	0.21334
609	0.02393	2.03612	0.22179
608	0.02479	2.03947	0.22796
607	0.02546	2.04283	0.23493
606	0.02586	2.0462	0.24073
605	0.02613	2.04959	0.24692
604	0.0261	2.05298	0.25131
603	0.02592	2.05638	0.25555
602	0.02557	2.0598	0.25825
601	0.02495	2.06323	0.25955
600	0.02408	2.06667	0.26012
599	0.02308	2.07012	0.26017
598	0.02205	2.07358	0.25708
597	0.02087	2.07705	0.25489
596	0.01957	2.08054	0.2514
595	0.01841	2.08403	0.24561

Wavelength (nm)	Absorbance	Photon Energy (eV)	Relationship - Indirect ($\alpha h\nu^{1/2}$)
594	0.0172	2.08754	0.24029
593	0.01621	2.09106	0.23479
592	0.01525	2.09459	0.22805
591	0.01443	2.09814	0.21998
590	0.01365	2.10169	0.21303
589	0.01299	2.10526	0.20741
588	0.01252	2.10884	0.20164
587	0.01203	2.11244	0.19597
586	0.01186	2.11604	0.19188
585	0.01171	2.11966	0.19035
584	0.01169	2.12329	0.18827
583	0.01174	2.12693	0.18649
582	0.01188	2.13058	0.18482
581	0.01215	2.13425	0.1853
580	0.01245	2.13793	0.18633
579	0.01298	2.14162	0.18918
578	0.01349	2.14533	0.19019
577	0.0141	2.14905	0.19114
576	0.01484	2.15278	0.19231
575	0.01556	2.15652	0.19418
574	0.01649	2.16028	0.19691
573	0.01747	2.16405	0.19878
572	0.01846	2.16783	0.20059
571	0.01952	2.17163	0.20369
570	0.02048	2.17544	0.20525
569	0.02138	2.17926	0.20696
568	0.02219	2.1831	0.20976
567	0.02299	2.18695	0.21222
566	0.0237	2.19081	0.21445
565	0.0244	2.19469	0.21733
564	0.02493	2.19858	0.21979
563	0.02539	2.20249	0.22168
562	0.02574	2.20641	0.22571
561	0.02588	2.21034	0.22789
560	0.02602	2.21429	0.23045
559	0.02614	2.21825	0.23299
558	0.02625	2.22222	0.23435
557	0.02636	2.22621	0.2369
556	0.02657	2.23022	0.2395
555	0.02664	2.23423	0.2411

Wavelength (nm)	Absorbance	Photon Energy (eV)	Relationship - Indirect ($\alpha h\nu^{1/2}$)
554	0.02676	2.23827	0.24313
553	0.02693	2.24231	0.24553
552	0.02708	2.24638	0.24773
551	0.02749	2.25045	0.25142
550	0.02804	2.25455	0.25407
549	0.02892	2.25865	0.25803
548	0.03004	2.26277	0.26169
547	0.03126	2.26691	0.2673
546	0.03286	2.27106	0.2711
545	0.03485	2.27523	0.27847
544	0.03711	2.27941	0.28615
543	0.0398	2.28361	0.29485
542	0.04278	2.28782	0.30411
541	0.04591	2.29205	0.31485
540	0.04936	2.2963	0.32617
539	0.05308	2.30056	0.33775
538	0.05681	2.30483	0.3506
537	0.06066	2.30912	0.36341
536	0.06449	2.31343	0.37633
535	0.06818	2.31776	0.38967
534	0.07181	2.3221	0.40377
533	0.07502	2.32645	0.41784
532	0.0778	2.33083	0.43199
531	0.08012	2.33522	0.44429
530	0.08195	2.33962	0.45537
529	0.08328	2.34405	0.46503
528	0.08415	2.34848	0.47297
527	0.08431	2.35294	0.48001
526	0.08375	2.35741	0.48443
525	0.08258	2.3619	0.48758
524	0.08082	2.36641	0.48846
523	0.07867	2.37094	0.48785
522	0.07624	2.37548	0.48575
521	0.07356	2.38004	0.48105
520	0.07088	2.38462	0.47346
519	0.0681	2.38921	0.46515
518	0.06522	2.39382	0.45591
517	0.06269	2.39845	0.44455
516	0.06021	2.4031	0.4334
515	0.05778	2.40777	0.42313

Wavelength (nm)	Absorbance	Photon Energy (eV)	Relationship - Indirect ($\alpha h\nu^{1/2}$)
514	0.05562	2.41245	0.4127
513	0.05347	2.41715	0.40261
512	0.05148	2.42188	0.39413
511	0.04964	2.42661	0.38518
510	0.04804	2.43137	0.37695
509	0.04647	2.43615	0.36896
508	0.04507	2.44094	0.36067
507	0.04386	2.44576	0.35296
506	0.0427	2.45059	0.34534
505	0.04194	2.45545	0.33906
504	0.04133	2.46032	0.33278
503	0.04089	2.46521	0.3275
502	0.0407	2.47012	0.32332
501	0.04076	2.47505	0.31968
500	0.04087	2.48	0.31799
499	0.0411	2.48497	0.31747
498	0.04141	2.48996	0.31799
497	0.04159	2.49497	0.31908
496	0.04198	2.5	0.31992
495	0.04234	2.50505	0.32226
494	0.04278	2.51012	0.32605
493	0.04329	2.51521	0.33031
492	0.04378	2.52033	0.33401
491	0.04439	2.52546	0.33772
490	0.04489	2.53061	0.34248
489	0.04545	2.53579	0.34673
488	0.04618	2.54098	0.35234
487	0.04703	2.5462	0.35663
486	0.04808	2.55144	0.36112
485	0.04925	2.5567	0.36581
484	0.05056	2.56198	0.36973
483	0.052	2.56729	0.37331
482	0.05376	2.57261	0.37868
481	0.05581	2.57796	0.38314
480	0.05808	2.58333	0.38788
479	0.06084	2.58873	0.39257
478	0.06393	2.59414	0.39726
477	0.06738	2.59958	0.40403
476	0.07147	2.60504	0.41091
475	0.07599	2.61053	0.4181

Wavelength (nm)	Absorbance	Photon Energy (eV)	Relationship - Indirect ($\alpha h\nu^{1/2}$)
474	0.08109	2.61603	0.42693
473	0.08726	2.62156	0.43635
472	0.09414	2.62712	0.44558
471	0.10207	2.6327	0.45608
470	0.11119	2.6383	0.4668
469	0.12136	2.64392	0.47826
468	0.13309	2.64957	0.49178
467	0.14642	2.65525	0.50516
466	0.16164	2.66094	0.51918
465	0.17893	2.66667	0.53428
464	0.19847	2.67241	0.55048
463	0.22041	2.67819	0.56756
462	0.24501	2.68398	0.58578
461	0.27271	2.6898	0.60476
460	0.30344	2.69565	0.6256
459	0.33736	2.70153	0.64795
458	0.37433	2.70742	0.67332
457	0.41432	2.71335	0.70035
456	0.45683	2.7193	0.73052
455	0.50096	2.72527	0.76442
454	0.5453	2.73128	0.80173
453	0.58839	2.73731	0.84295
452	0.6287	2.74336	0.88886
451	0.66418	2.74945	0.93966
450	0.69292	2.75556	0.99528
449	0.71314	2.76169	1.05663
448	0.72358	2.76786	1.12264
447	0.72339	2.77405	1.19424
446	0.71286	2.78027	1.27093
445	0.69305	2.78652	1.35158
444	0.66587	2.79279	1.43545
443	0.63393	2.7991	1.52189
442	0.59987	2.80543	1.60852
441	0.56636	2.81179	1.692
440	0.53537	2.81818	1.76933
439	0.50842	2.8246	1.83776
438	0.48625	2.83105	1.89314
437	0.46904	2.83753	1.93217
436	0.45617	2.84404	1.95241
435	0.44699	2.85057	1.95105

Wavelength (nm)	Absorbance	Photon Energy (eV)	Relationship - Indirect ($\alpha h\nu^{1/2}$)
434	0.44085	2.85714	1.92718
433	0.43688	2.86374	1.88306
432	0.4348	2.87037	1.82285
431	0.43418	2.87703	1.75199
430	0.4346	2.88372	1.67616
429	0.4361	2.89044	1.60099
428	0.43819	2.8972	1.53106
427	0.44061	2.90398	1.4694
426	0.44285	2.9108	1.417
425	0.44392	2.91765	1.37428
424	0.44279	2.92453	1.34057
423	0.43857	2.93144	1.31321
422	0.43027	2.93839	1.29096
421	0.41745	2.94537	1.27078
420	0.3992	2.95238	1.25075
419	0.37833	2.95943	1.22977
418	0.3552	2.96651	1.20728
417	0.33111	2.97362	1.18318
416	0.30743	2.98077	1.15718
415	0.28553	2.98795	1.13055
414	0.26581	2.99517	1.10295
413	0.24869	3.00242	1.07448
412	0.23436	3.00971	1.04465
411	0.22268	3.01703	1.01364
410	0.21367	3.02439	0.98023
409	0.20694	3.03178	0.94624
408	0.20219	3.03922	0.91226
407	0.19897	3.04668	0.87884
406	0.19689	3.05419	0.84767
405	0.19552	3.06173	0.81855
404	0.1945	3.06931	0.79249
403	0.19366	3.07692	0.76995
402	0.19262	3.08458	0.75079
401	0.19127	3.09227	0.73395
400	0.18938	3.1	0.71933
399	0.18697	3.10777	0.70646
398	0.18398	3.11558	0.69499
397	0.18042	3.12343	0.68447
396	0.17649	3.13131	0.67344
395	0.17213	3.13924	0.66509

Wavelength (nm)	Absorbance	Photon Energy (eV)	Relationship - Indirect ($\alpha h\nu^{1/2}$)
394	0.16755	3.14721	0.65694
393	0.163	3.15522	0.64918
392	0.1585	3.16327	0.64252
391	0.15425	3.17136	0.6374
390	0.15012	3.17949	0.63222
389	0.14623	3.18766	0.62765
388	0.1425	3.19588	0.62283
387	0.13889	3.20413	0.61913
386	0.13557	3.21244	0.61627
385	0.13236	3.22078	0.61234
384	0.12936	3.22917	0.60964
383	0.12643	3.2376	0.60693
382	0.12364	3.24607	0.6039
381	0.12104	3.25459	0.60239
380	0.11859	3.26316	0.59951
379	0.1164	3.27177	0.59761
378	0.11419	3.28042	0.59579
377	0.11211	3.28912	0.59264
376	0.1101	3.29787	0.58955
375	0.10816	3.30667	0.58616
374	0.10649	3.31551	0.58238
373	0.10492	3.3244	0.57803
372	0.1034	3.33333	0.57405
371	0.10193	3.34232	0.5689
370	0.09986	3.35135	0.56375
369	0.09852	3.36043	0.55885
368	0.09715	3.36957	0.55556
367	0.09582	3.37875	0.55171
366	0.09448	3.38798	0.54874
365	0.09309	3.39726	0.54592
364	0.09151	3.40659	0.54261
363	0.08989	3.41598	0.54156
362	0.08822	3.42541	0.53905
361	0.08636	3.4349	0.53749
360	0.08463	3.44444	0.53467
359	0.08284	3.45404	0.53234
358	0.08096	3.46369	0.5315
357	0.0794	3.47339	0.52931
356	0.07763	3.48315	0.52838
355	0.07615	3.49296	0.52595

Wavelength (nm)	Absorbance	Photon Energy (eV)	Relationship - Indirect ($\alpha h\nu^{1/2}$)
354	0.0747	3.50282	0.52475
353	0.07318	3.51275	0.52321
352	0.07198	3.52273	0.52177
351	0.07077	3.53276	0.52034
350	0.06973	3.54286	0.51929

Table 2.17: 2vtBr Tauc Tables

Wavelength (nm)	Absorbance	Photon Energy (eV)	Relationship - Indirect ($\alpha h\nu^{1/2}$)
800	8.28E-04	1.55	0.04363
799	6.24E-04	1.55194	0.0377
798	4.91E-04	1.55388	0.03343
797	3.55E-04	1.55583	0.03221
796	2.11E-04	1.55779	0.02583
795	1.35E-05	1.55975	0.02194
794	2.19E-04	1.56171	0.02916
793	-1.76E-06	1.56368	0.02625
792	9.07E-05	1.56566	0.02835
791	1.70E-04	1.56764	0.03031
790	1.42E-04	1.56962	0.02951
789	2.33E-04	1.57161	0.03061
788	2.38E-04	1.5736	0.03374
787	6.36E-05	1.5756	0.02918
786	2.20E-04	1.57761	0.03116
785	5.40E-04	1.57962	0.03717
784	3.56E-04	1.58163	0.03521
783	1.37E-04	1.58365	0.03427
782	3.47E-04	1.58568	0.03536
781	2.65E-04	1.58771	0.03646
780	2.51E-04	1.58974	0.03193
779	1.21E-04	1.59178	0.03199
778	3.66E-05	1.59383	0.03117
777	2.93E-04	1.59588	0.03578
776	2.48E-04	1.59794	0.03649
775	9.19E-05	1.6	0.0355
774	1.66E-04	1.60207	0.03467
773	1.51E-04	1.60414	0.03481
772	-5.96E-05	1.60622	0.02919
771	8.33E-05	1.6083	0.02852

Wavelength (nm)	Absorbance	Photon Energy (eV)	Relationship - Indirect ($\alpha h\nu^{1/2}$)
770	2.52E-04	1.61039	0.03585
769	-3.35E-05	1.61248	0.03311
768	4.44E-05	1.61458	0.03184
767	-1.94E-04	1.61669	0.02357
766	-2.25E-04	1.6188	0.02504
765	-4.31E-04	1.62092	0.01397
764	-1.92E-04	1.62304	0.02749
763	1.00E-05	1.62516	0.03346
762	-6.20E-05	1.6273	0.03202
761	1.78E-05	1.62943	0.03101
760	4.37E-05	1.63158	0.0321
759	-2.10E-05	1.63373	0.0316
758	-2.11E-05	1.63588	0.03276
757	1.07E-05	1.63804	0.03245
756	-2.20E-04	1.64021	0.02701
755	-3.39E-04	1.64238	0.02098
754	-3.29E-04	1.64456	0.02628
753	-2.86E-04	1.64675	0.01621
752	2.09E-04	1.64894	0.03277
751	3.78E-04	1.65113	0.03858
750	4.54E-04	1.65333	0.04012
749	2.92E-04	1.65554	0.04071
748	4.04E-04	1.65775	0.04007
747	3.87E-04	1.65997	0.03961
746	1.74E-04	1.6622	0.03864
745	2.55E-05	1.66443	0.03685
744	3.41E-04	1.66667	0.0391
743	-4.52E-05	1.66891	0.02955
742	1.33E-04	1.67116	0.04075
741	5.70E-05	1.67341	0.03618
740	1.90E-04	1.67568	0.04357
739	-2.18E-05	1.67794	0.03827
738	1.70E-04	1.68022	0.04221
737	1.33E-04	1.6825	0.04387
736	2.17E-04	1.68478	0.0445
735	1.65E-04	1.68707	0.04415
734	4.60E-05	1.68937	0.04403
733	-1.28E-04	1.69168	0.03812
732	1.44E-04	1.69399	0.04247

Wavelength (nm)	Absorbance	Photon Energy (eV)	Relationship - Indirect ($\alpha h\nu^{1/2}$)
731	3.83E-04	1.69631	0.04488
730	2.70E-04	1.69863	0.05091
729	4.71E-04	1.70096	0.05006
728	2.67E-04	1.7033	0.05015
727	3.42E-04	1.70564	0.04913
726	9.75E-05	1.70799	0.04433
725	1.67E-04	1.71034	0.04793
724	9.63E-05	1.71271	0.04761
723	1.86E-04	1.71508	0.04911
722	3.69E-04	1.71745	0.05322
721	2.27E-04	1.71983	0.05069
720	3.26E-04	1.72222	0.05503
719	3.73E-04	1.72462	0.05691
718	4.59E-04	1.72702	0.05612
717	4.33E-04	1.72943	0.05539
716	5.90E-04	1.73184	0.06047
715	4.18E-04	1.73427	0.05717
714	4.39E-04	1.73669	0.05794
713	4.01E-04	1.73913	0.05824
712	4.25E-04	1.74157	0.0595
711	4.19E-04	1.74402	0.05837
710	2.58E-04	1.74648	0.05668
709	3.31E-04	1.74894	0.05927
708	3.36E-04	1.75141	0.05775
707	3.39E-04	1.75389	0.05964
706	4.94E-04	1.75637	0.06226
705	5.66E-04	1.75887	0.06202
704	5.96E-04	1.76136	0.06616
703	4.33E-04	1.76387	0.06065
702	4.57E-04	1.76638	0.06305
701	4.15E-04	1.7689	0.06309
700	6.14E-04	1.77143	0.0663
699	5.56E-04	1.77396	0.0647
698	4.71E-04	1.7765	0.06573
697	5.08E-04	1.77905	0.06795
696	3.16E-04	1.78161	0.06582
695	5.02E-04	1.78417	0.0676
694	6.07E-04	1.78674	0.06988
693	5.88E-04	1.78932	0.06915

Wavelength (nm)	Absorbance	Photon Energy (eV)	Relationship - Indirect ($\alpha h\nu^{1/2}$)
692	6.34E-04	1.79191	0.07149
691	5.18E-04	1.7945	0.07135
690	6.18E-04	1.7971	0.07258
689	7.29E-04	1.79971	0.07646
688	0.00101	1.80233	0.07912
687	0.00112	1.80495	0.08159
686	0.00102	1.80758	0.08026
685	0.00107	1.81022	0.08106
684	0.00117	1.81287	0.08251
683	0.00141	1.81552	0.08729
682	0.00142	1.81818	0.08734
681	0.00136	1.82085	0.08791
680	0.00134	1.82353	0.08866
679	0.00149	1.82622	0.09193
678	0.00156	1.82891	0.09216
677	0.00165	1.83161	0.09343
676	0.00187	1.83432	0.098
675	0.00193	1.83704	0.10043
674	0.00167	1.83976	0.09696
673	0.00189	1.8425	0.10089
672	0.00183	1.84524	0.10178
671	0.00201	1.84799	0.10451
670	0.00216	1.85075	0.10598
669	0.00221	1.85351	0.10678
668	0.00229	1.85629	0.10954
667	0.00224	1.85907	0.11095
666	0.00248	1.86186	0.11291
665	0.00245	1.86466	0.11285
664	0.00279	1.86747	0.11644
663	0.00287	1.87029	0.11781
662	0.00261	1.87311	0.11701
661	0.00286	1.87595	0.11919
660	0.00284	1.87879	0.11968
659	0.00296	1.88164	0.12052
658	0.00295	1.8845	0.12091
657	0.00292	1.88737	0.12122
656	0.00282	1.89024	0.12004
655	0.00311	1.89313	0.12314
654	0.00286	1.89602	0.12139

Wavelength (nm)	Absorbance	Photon Energy (eV)	Relationship - Indirect ($\alpha h\nu^{1/2}$)
653	0.00281	1.89893	0.12122
652	0.00277	1.90184	0.12107
651	0.00275	1.90476	0.11986
650	0.00256	1.90769	0.11933
649	0.00243	1.91063	0.11675
648	0.00242	1.91358	0.11679
647	0.00222	1.91654	0.11392
646	0.00226	1.9195	0.11268
645	0.00231	1.92248	0.11282
644	0.00227	1.92547	0.11074
643	0.00216	1.92846	0.10799
642	0.00231	1.93146	0.10912
641	0.00196	1.93448	0.10459
640	0.00215	1.9375	0.10459
639	0.00224	1.94053	0.10561
638	0.00214	1.94357	0.10474
637	0.00257	1.94662	0.10637
636	0.00257	1.94969	0.10761
635	0.00272	1.95276	0.10802
634	0.00292	1.95584	0.10969
633	0.00295	1.95893	0.1105
632	0.00304	1.96203	0.11012
631	0.00324	1.96513	0.11317
630	0.0037	1.96825	0.11784
629	0.00365	1.97138	0.11865
628	0.00392	1.97452	0.12166
627	0.00417	1.97767	0.12415
626	0.00436	1.98083	0.12735
625	0.00442	1.984	0.12861
624	0.00488	1.98718	0.13397
623	0.00519	1.99037	0.13782
622	0.00602	1.99357	0.14338
621	0.00618	1.99678	0.14595
620	0.00683	2	0.15203
619	0.0075	2.00323	0.15791
618	0.00789	2.00647	0.16232
617	0.00865	2.00972	0.16813
616	0.00952	2.01299	0.17521
615	0.01013	2.01626	0.18029

Wavelength (nm)	Absorbance	Photon Energy (eV)	Relationship - Indirect ($\alpha h\nu^{1/2}$)
614	0.01086	2.01954	0.18686
613	0.01201	2.02284	0.19343
612	0.01313	2.02614	0.20009
611	0.01389	2.02946	0.20743
610	0.01498	2.03279	0.21334
609	0.01632	2.03612	0.22179
608	0.01749	2.03947	0.22796
607	0.01863	2.04283	0.23493
606	0.01967	2.0462	0.24073
605	0.02067	2.04959	0.24692
604	0.02147	2.05298	0.25131
603	0.022	2.05638	0.25555
602	0.02227	2.0598	0.25825
601	0.02237	2.06323	0.25955
600	0.02309	2.06667	0.26012
599	0.02314	2.07012	0.26017
598	0.02229	2.07358	0.25708
597	0.02162	2.07705	0.25489
596	0.021	2.08054	0.2514
595	0.01966	2.08403	0.24561
594	0.0184	2.08754	0.24029
593	0.01734	2.09106	0.23479
592	0.01592	2.09459	0.22805
591	0.01437	2.09814	0.21998
590	0.01293	2.10169	0.21303
589	0.0118	2.10526	0.20741
588	0.0108	2.10884	0.20164
587	0.00977	2.11244	0.19597
586	0.00901	2.11604	0.19188
585	0.00871	2.11966	0.19035
584	0.00817	2.12329	0.18827
583	0.00777	2.12693	0.18649
582	0.00732	2.13058	0.18482
581	0.0072	2.13425	0.1853
580	0.00713	2.13793	0.18633
579	0.00742	2.14162	0.18918
578	0.0074	2.14533	0.19019
577	0.00729	2.14905	0.19114
576	0.00748	2.15278	0.19231

Wavelength (nm)	Absorbance	Photon Energy (eV)	Relationship - Indirect ($\alpha h\nu^{1/2}$)
575	0.00752	2.15652	0.19418
574	0.00778	2.16028	0.19691
573	0.00794	2.16405	0.19878
572	0.00825	2.16783	0.20059
571	0.00864	2.17163	0.20369
570	0.00883	2.17544	0.20525
569	0.00899	2.17926	0.20696
568	0.00936	2.1831	0.20976
567	0.00975	2.18695	0.21222
566	0.01034	2.19081	0.21445
565	0.01063	2.19469	0.21733
564	0.01115	2.19858	0.21979
563	0.01138	2.20249	0.22168
562	0.01217	2.20641	0.22571
561	0.01255	2.21034	0.22789
560	0.01292	2.21429	0.23045
559	0.01329	2.21825	0.23299
558	0.01366	2.22222	0.23435
557	0.01387	2.22621	0.2369
556	0.01408	2.23022	0.2395
555	0.01425	2.23423	0.2411
554	0.01454	2.23827	0.24313
553	0.01476	2.24231	0.24553
552	0.01504	2.24638	0.24773
551	0.01555	2.25045	0.25142
550	0.01588	2.25455	0.25407
549	0.01653	2.25865	0.25803
548	0.01694	2.26277	0.26169
547	0.01789	2.26691	0.2673
546	0.01846	2.27106	0.2711
545	0.01968	2.27523	0.27847
544	0.02114	2.27941	0.28615
543	0.02263	2.28361	0.29485
542	0.02436	2.28782	0.30411
541	0.02654	2.29205	0.31485
540	0.02892	2.2963	0.32617
539	0.03146	2.30056	0.33775
538	0.03462	2.30483	0.3506
537	0.03792	2.30912	0.36341

Wavelength (nm)	Absorbance	Photon Energy (eV)	Relationship - Indirect ($\alpha h\nu^{1/2}$)
536	0.04119	2.31343	0.37633
535	0.04478	2.31776	0.38967
534	0.04848	2.3221	0.40377
533	0.0525	2.32645	0.41784
532	0.05662	2.33083	0.43199
531	0.06032	2.33522	0.44429
530	0.06345	2.33962	0.45537
529	0.06635	2.34405	0.46503
528	0.06885	2.34848	0.47297
527	0.07105	2.35294	0.48001
526	0.07221	2.35741	0.48443
525	0.07305	2.3619	0.48758
524	0.07308	2.36641	0.48846
523	0.07246	2.37094	0.48785
522	0.07137	2.37548	0.48575
521	0.06944	2.38004	0.48105
520	0.06664	2.38462	0.47346
519	0.06352	2.38921	0.46515
518	0.06023	2.39382	0.45591
517	0.05651	2.39845	0.44455
516	0.05301	2.4031	0.4334
515	0.04973	2.40777	0.42313
514	0.04643	2.41245	0.4127
513	0.04347	2.41715	0.40261
512	0.04102	2.42188	0.39413
511	0.03863	2.42661	0.38518
510	0.03634	2.43137	0.37695
509	0.03411	2.43615	0.36896
508	0.03178	2.44094	0.36067
507	0.02953	2.44576	0.35296
506	0.0273	2.45059	0.34534
505	0.02545	2.45545	0.33906
504	0.02372	2.46032	0.33278
503	0.02202	2.46521	0.3275
502	0.0209	2.47012	0.32332
501	0.0197	2.47505	0.31968
500	0.0189	2.48	0.31799
499	0.0182	2.48497	0.31747
498	0.01784	2.48996	0.31799

Wavelength (nm)	Absorbance	Photon Energy (eV)	Relationship - Indirect ($\alpha h\nu^{1/2}$)
497	0.01763	2.49497	0.31908
496	0.0174	2.5	0.31992
495	0.01734	2.50505	0.32226
494	0.0177	2.51012	0.32605
493	0.01813	2.51521	0.33031
492	0.01825	2.52033	0.33401
491	0.01831	2.52546	0.33772
490	0.01887	2.53061	0.34248
489	0.019	2.53579	0.34673
488	0.01945	2.54098	0.35234
487	0.01979	2.5462	0.35663
486	0.02007	2.55144	0.36112
485	0.02038	2.5567	0.36581
484	0.02058	2.56198	0.36973
483	0.02087	2.56729	0.37331
482	0.02163	2.57261	0.37868
481	0.02216	2.57796	0.38314
480	0.02284	2.58333	0.38788
479	0.02359	2.58873	0.39257
478	0.02428	2.59414	0.39726
477	0.02546	2.59958	0.40403
476	0.02695	2.60504	0.41091
475	0.02804	2.61053	0.4181
474	0.02979	2.61603	0.42693
473	0.03176	2.62156	0.43635
472	0.03367	2.62712	0.44558
471	0.03584	2.6327	0.45608
470	0.03811	2.6383	0.4668
469	0.04049	2.64392	0.47826
468	0.04349	2.64957	0.49178
467	0.04666	2.65525	0.50516
466	0.04999	2.66094	0.51918
465	0.05362	2.66667	0.53428
464	0.05765	2.67241	0.55048
463	0.06216	2.67819	0.56756
462	0.06732	2.68398	0.58578
461	0.07309	2.6898	0.60476
460	0.07933	2.69565	0.6256
459	0.08692	2.70153	0.64795

Wavelength (nm)	Absorbance	Photon Energy (eV)	Relationship - Indirect ($\alpha h\nu^{1/2}$)
458	0.09585	2.70742	0.67332
457	0.10593	2.71335	0.70035
456	0.11816	2.7193	0.73052
455	0.13266	2.72527	0.76442
454	0.14985	2.73128	0.80173
453	0.17016	2.73731	0.84295
452	0.1943	2.74336	0.88886
451	0.22271	2.74945	0.93966
450	0.25583	2.75556	0.99528
449	0.29478	2.76169	1.05663
448	0.339	2.76786	1.12264
447	0.38988	2.77405	1.19424
446	0.44765	2.78027	1.27093
445	0.51221	2.78652	1.35158
444	0.58275	2.79279	1.43545
443	0.65894	2.7991	1.52189
442	0.73907	2.80543	1.60852
441	0.81891	2.81179	1.692
440	0.89495	2.81818	1.76933
439	0.96259	2.8246	1.83776
438	1.01706	2.83105	1.89314
437	1.05268	2.83753	1.93217
436	1.06561	2.84404	1.95241
435	1.05261	2.85057	1.95105
434	1.01329	2.85714	1.92718
433	0.95131	2.86374	1.88306
432	0.87313	2.87037	1.82285
431	0.78629	2.87703	1.75199
430	0.6981	2.88372	1.67616
429	0.61527	2.89044	1.60099
428	0.54101	2.8972	1.53106
427	0.47769	2.90398	1.4694
426	0.42561	2.9108	1.417
425	0.3843	2.91765	1.37428
424	0.35238	2.92453	1.34057
423	0.32787	2.93144	1.31321
422	0.30987	2.93839	1.29096
421	0.29665	2.94537	1.27078
420	0.28645	2.95238	1.25075

Wavelength (nm)	Absorbance	Photon Energy (eV)	Relationship - Indirect ($\alpha h\nu^{1/2}$)
419	0.27892	2.95943	1.22977
418	0.27264	2.96651	1.20728
417	0.26688	2.97362	1.18318
416	0.26097	2.98077	1.15718
415	0.25446	2.98795	1.13055
414	0.24687	2.99517	1.10295
413	0.23778	3.00242	1.07448
412	0.22729	3.00971	1.04465
411	0.21492	3.01703	1.01364
410	0.20099	3.02439	0.98023
409	0.18636	3.03178	0.94624
408	0.17162	3.03922	0.91226
407	0.15735	3.04668	0.87884
406	0.14437	3.05419	0.84767
405	0.13267	3.06173	0.81855
404	0.12251	3.06931	0.79249
403	0.11436	3.07692	0.76995
402	0.10772	3.08458	0.75079
401	0.10249	3.09227	0.73395
400	0.09813	3.1	0.71933
399	0.0949	3.10777	0.70646
398	0.09209	3.11558	0.69499
397	0.08993	3.12343	0.68447
396	0.08742	3.13131	0.67344
395	0.08609	3.13924	0.66509
394	0.08466	3.14721	0.65694
393	0.08307	3.15522	0.64918
392	0.08174	3.16327	0.64252
391	0.08072	3.17136	0.6374
390	0.07974	3.17949	0.63222
389	0.07857	3.18766	0.62765
388	0.07727	3.19588	0.62283
387	0.07651	3.20413	0.61913
386	0.07566	3.21244	0.61627
385	0.07459	3.22078	0.61234
384	0.07411	3.22917	0.60964
383	0.07329	3.2376	0.60693
382	0.07252	3.24607	0.6039
381	0.07204	3.25459	0.60239

Wavelength (nm)	Absorbance	Photon Energy (eV)	Relationship - Indirect ($\alpha h\nu^{1/2}$)
380	0.07107	3.26316	0.59951
379	0.07067	3.27177	0.59761
378	0.07024	3.28042	0.59579
377	0.06927	3.28912	0.59264
376	0.06845	3.29787	0.58955
375	0.06738	3.30667	0.58616
374	0.06633	3.31551	0.58238
373	0.06504	3.3244	0.57803
372	0.06401	3.33333	0.57405
371	0.06258	3.34232	0.5689
370	0.06104	3.35135	0.56375
369	0.05983	3.36043	0.55885
368	0.05895	3.36957	0.55556
367	0.05789	3.37875	0.55171
366	0.05706	3.38798	0.54874
365	0.05629	3.39726	0.54592
364	0.05552	3.40659	0.54261
363	0.05516	3.41598	0.54156
362	0.05451	3.42541	0.53905
361	0.05417	3.4349	0.53749
360	0.05351	3.44444	0.53467
359	0.05283	3.45404	0.53234
358	0.05241	3.46369	0.5315
357	0.05176	3.47339	0.52931
356	0.05168	3.48315	0.52838
355	0.05114	3.49296	0.52595
354	0.05067	3.50282	0.52475
353	0.05026	3.51275	0.52321
352	0.0501	3.52273	0.52177
351	0.04952	3.53276	0.52034
350	0.04934	3.54286	0.51929

Table 2.18: F2vtBr Tauc Tables

Wavelength (nm)	Absorbance	Photon Energy (eV)	Relationship - Indirect ($\alpha h\nu^{1/2}$)
800	0.00133	1.55	0.04363
799	0.0012	1.55194	0.0377
798	0.00122	1.55388	0.03343

Wavelength (nm)	Absorbance	Photon Energy (eV)	Relationship - Indirect ($\alpha h\nu^{1/2}$)
797	0.00124	1.55583	0.03221
796	0.00127	1.55779	0.02583
795	0.00133	1.55975	0.02194
794	0.00138	1.56171	0.02916
793	0.00131	1.56368	0.02625
792	0.00139	1.56566	0.02835
791	0.0015	1.56764	0.03031
790	0.00147	1.56962	0.02951
789	0.00151	1.57161	0.03061
788	0.00151	1.5736	0.03374
787	0.00145	1.5756	0.02918
786	0.00155	1.57761	0.03116
785	0.00162	1.57962	0.03717
784	0.00162	1.58163	0.03521
783	0.00169	1.58365	0.03427
782	0.00166	1.58568	0.03536
781	0.00157	1.58771	0.03646
780	0.00162	1.58974	0.03193
779	0.00161	1.59178	0.03199
778	0.00167	1.59383	0.03117
777	0.00182	1.59588	0.03578
776	0.00187	1.59794	0.03649
775	0.00182	1.6	0.0355
774	0.00181	1.60207	0.03467
773	0.00182	1.60414	0.03481
772	0.00178	1.60622	0.02919
771	0.00182	1.6083	0.02852
770	0.00181	1.61039	0.03585
769	0.00172	1.61248	0.03311
768	0.00171	1.61458	0.03184
767	0.00175	1.61669	0.02357
766	0.00187	1.6188	0.02504
765	0.00186	1.62092	0.01397
764	0.00189	1.62304	0.02749
763	0.00181	1.62516	0.03346
762	0.0017	1.6273	0.03202
761	0.00183	1.62943	0.03101
760	0.00184	1.63158	0.0321
759	0.00199	1.63373	0.0316

Wavelength (nm)	Absorbance	Photon Energy (eV)	Relationship - Indirect ($\alpha h\nu^{1/2}$)
758	0.00203	1.63588	0.03276
757	0.00199	1.63804	0.03245
756	0.00201	1.64021	0.02701
755	0.00201	1.64238	0.02098
754	0.00204	1.64456	0.02628
753	0.00206	1.64675	0.01621
752	0.00202	1.64894	0.03277
751	0.00207	1.65113	0.03858
750	0.00209	1.65333	0.04012
749	0.00213	1.65554	0.04071
748	0.00222	1.65775	0.04007
747	0.00227	1.65997	0.03961
746	0.00232	1.6622	0.03864
745	0.00244	1.66443	0.03685
744	0.00255	1.66667	0.0391
743	0.00254	1.66891	0.02955
742	0.00258	1.67116	0.04075
741	0.00265	1.67341	0.03618
740	0.00279	1.67568	0.04357
739	0.00284	1.67794	0.03827
738	0.00298	1.68022	0.04221
737	0.00319	1.6825	0.04387
736	0.00343	1.68478	0.0445
735	0.0036	1.68707	0.04415
734	0.00371	1.68937	0.04403
733	0.00394	1.69168	0.03812
732	0.00402	1.69399	0.04247
731	0.0043	1.69631	0.04488
730	0.00461	1.69863	0.05091
729	0.00481	1.70096	0.05006
728	0.00505	1.7033	0.05015
727	0.00526	1.70564	0.04913
726	0.00539	1.70799	0.04433
725	0.00555	1.71034	0.04793
724	0.00568	1.71271	0.04761
723	0.00574	1.71508	0.04911
722	0.0057	1.71745	0.05322
721	0.00574	1.71983	0.05069
720	0.00585	1.72222	0.05503

Wavelength (nm)	Absorbance	Photon Energy (eV)	Relationship - Indirect ($\alpha h\nu^{1/2}$)
719	0.00586	1.72462	0.05691
718	0.00585	1.72702	0.05612
717	0.00575	1.72943	0.05539
716	0.00556	1.73184	0.06047
715	0.00543	1.73427	0.05717
714	0.00546	1.73669	0.05794
713	0.00538	1.73913	0.05824
712	0.00534	1.74157	0.0595
711	0.00521	1.74402	0.05837
710	0.005	1.74648	0.05668
709	0.00488	1.74894	0.05927
708	0.00472	1.75141	0.05775
707	0.00472	1.75389	0.05964
706	0.00464	1.75637	0.06226
705	0.00465	1.75887	0.06202
704	0.00464	1.76136	0.06616
703	0.00457	1.76387	0.06065
702	0.00464	1.76638	0.06305
701	0.00448	1.7689	0.06309
700	0.00449	1.77143	0.0663
699	0.00454	1.77396	0.0647
698	0.0046	1.7765	0.06573
697	0.00468	1.77905	0.06795
696	0.00469	1.78161	0.06582
695	0.00467	1.78417	0.0676
694	0.00469	1.78674	0.06988
693	0.00479	1.78932	0.06915
692	0.00494	1.79191	0.07149
691	0.00504	1.7945	0.07135
690	0.00509	1.7971	0.07258
689	0.00507	1.79971	0.07646
688	0.00507	1.80233	0.07912
687	0.00503	1.80495	0.08159
686	0.00504	1.80758	0.08026
685	0.00515	1.81022	0.08106
684	0.00525	1.81287	0.08251
683	0.0054	1.81552	0.08729
682	0.00537	1.81818	0.08734
681	0.00551	1.82085	0.08791

Wavelength (nm)	Absorbance	Photon Energy (eV)	Relationship - Indirect ($\alpha h\nu^{1/2}$)
680	0.00564	1.82353	0.08866
679	0.00584	1.82622	0.09193
678	0.00615	1.82891	0.09216
677	0.00631	1.83161	0.09343
676	0.00641	1.83432	0.098
675	0.00651	1.83704	0.10043
674	0.00672	1.83976	0.09696
673	0.00686	1.8425	0.10089
672	0.00704	1.84524	0.10178
671	0.00721	1.84799	0.10451
670	0.00723	1.85075	0.10598
669	0.00742	1.85351	0.10678
668	0.00757	1.85629	0.10954
667	0.00775	1.85907	0.11095
666	0.00806	1.86186	0.11291
665	0.00817	1.86466	0.11285
664	0.00831	1.86747	0.11644
663	0.00845	1.87029	0.11781
662	0.00846	1.87311	0.11701
661	0.00855	1.87595	0.11919
660	0.00858	1.87879	0.11968
659	0.00846	1.88164	0.12052
658	0.00844	1.8845	0.12091
657	0.00827	1.88737	0.12122
656	0.00811	1.89024	0.12004
655	0.00808	1.89313	0.12314
654	0.00789	1.89602	0.12139
653	0.00786	1.89893	0.12122
652	0.0078	1.90184	0.12107
651	0.00763	1.90476	0.11986
650	0.00761	1.90769	0.11933
649	0.00759	1.91063	0.11675
648	0.00761	1.91358	0.11679
647	0.00771	1.91654	0.11392
646	0.00778	1.9195	0.11268
645	0.00782	1.92248	0.11282
644	0.00794	1.92547	0.11074
643	0.00807	1.92846	0.10799
642	0.00804	1.93146	0.10912

Wavelength (nm)	Absorbance	Photon Energy (eV)	Relationship - Indirect ($\alpha h\nu^{1/2}$)
641	0.00808	1.93448	0.10459
640	0.00819	1.9375	0.10459
639	0.00841	1.94053	0.10561
638	0.00862	1.94357	0.10474
637	0.00881	1.94662	0.10637
636	0.00886	1.94969	0.10761
635	0.00889	1.95276	0.10802
634	0.00908	1.95584	0.10969
633	0.00918	1.95893	0.1105
632	0.00943	1.96203	0.11012
631	0.00962	1.96513	0.11317
630	0.00993	1.96825	0.11784
629	0.01028	1.97138	0.11865
628	0.01066	1.97452	0.12166
627	0.01109	1.97767	0.12415
626	0.01146	1.98083	0.12735
625	0.01194	1.984	0.12861
624	0.01242	1.98718	0.13397
623	0.01298	1.99037	0.13782
622	0.01372	1.99357	0.14338
621	0.01443	1.99678	0.14595
620	0.01524	2	0.15203
619	0.01604	2.00323	0.15791
618	0.01686	2.00647	0.16232
617	0.01776	2.00972	0.16813
616	0.0187	2.01299	0.17521
615	0.01978	2.01626	0.18029
614	0.02072	2.01954	0.18686
613	0.02174	2.02284	0.19343
612	0.02265	2.02614	0.20009
611	0.0234	2.02946	0.20743
610	0.02412	2.03279	0.21334
609	0.02469	2.03612	0.22179
608	0.02506	2.03947	0.22796
607	0.02521	2.04283	0.23493
606	0.02513	2.0462	0.24073
605	0.02475	2.04959	0.24692
604	0.02431	2.05298	0.25131
603	0.0237	2.05638	0.25555

Wavelength (nm)	Absorbance	Photon Energy (eV)	Relationship - Indirect ($\alpha h\nu^{1/2}$)
602	0.02299	2.0598	0.25825
601	0.0222	2.06323	0.25955
600	0.02102	2.06667	0.26012
599	0.01989	2.07012	0.26017
598	0.01891	2.07358	0.25708
597	0.0179	2.07705	0.25489
596	0.01676	2.08054	0.2514
595	0.01586	2.08403	0.24561
594	0.01499	2.08754	0.24029
593	0.01427	2.09106	0.23479
592	0.01374	2.09459	0.22805
591	0.01338	2.09814	0.21998
590	0.013	2.10169	0.21303
589	0.0128	2.10526	0.20741
588	0.01266	2.10884	0.20164
587	0.01261	2.11244	0.19597
586	0.01277	2.11604	0.19188
585	0.01295	2.11966	0.19035
584	0.01335	2.12329	0.18827
583	0.01374	2.12693	0.18649
582	0.0143	2.13058	0.18482
581	0.01492	2.13425	0.1853
580	0.01553	2.13793	0.18633
579	0.01627	2.14162	0.18918
578	0.01688	2.14533	0.19019
577	0.01766	2.14905	0.19114
576	0.01858	2.15278	0.19231
575	0.01932	2.15652	0.19418
574	0.02028	2.16028	0.19691
573	0.02109	2.16405	0.19878
572	0.0217	2.16783	0.20059
571	0.02243	2.17163	0.20369
570	0.0229	2.17544	0.20525
569	0.02327	2.17926	0.20696
568	0.02361	2.1831	0.20976
567	0.02376	2.18695	0.21222
566	0.02383	2.19081	0.21445
565	0.02392	2.19469	0.21733
564	0.02388	2.19858	0.21979

Wavelength (nm)	Absorbance	Photon Energy (eV)	Relationship - Indirect ($\alpha h\nu^{1/2}$)
563	0.02384	2.20249	0.22168
562	0.02382	2.20641	0.22571
561	0.02371	2.21034	0.22789
560	0.02363	2.21429	0.23045
559	0.02362	2.21825	0.23299
558	0.02374	2.22222	0.23435
557	0.02394	2.22621	0.2369
556	0.02435	2.23022	0.2395
555	0.02482	2.23423	0.2411
554	0.02535	2.23827	0.24313
553	0.02603	2.24231	0.24553
552	0.02693	2.24638	0.24773
551	0.02804	2.25045	0.25142
550	0.02938	2.25455	0.25407
549	0.03099	2.25865	0.25803
548	0.03276	2.26277	0.26169
547	0.03462	2.26691	0.2673
546	0.03672	2.27106	0.2711
545	0.03917	2.27523	0.27847
544	0.04166	2.27941	0.28615
543	0.04442	2.28361	0.29485
542	0.04722	2.28782	0.30411
541	0.04981	2.29205	0.31485
540	0.05247	2.2963	0.32617
539	0.055	2.30056	0.33775
538	0.05733	2.30483	0.3506
537	0.05952	2.30912	0.36341
536	0.06137	2.31343	0.37633
535	0.06297	2.31776	0.38967
534	0.06424	2.3221	0.40377
533	0.06501	2.32645	0.41784
532	0.06544	2.33083	0.43199
531	0.06545	2.33522	0.44429
530	0.06508	2.33962	0.45537
529	0.06443	2.34405	0.46503
528	0.0635	2.34848	0.47297
527	0.06217	2.35294	0.48001
526	0.06054	2.35741	0.48443
525	0.05873	2.3619	0.48758

Wavelength (nm)	Absorbance	Photon Energy (eV)	Relationship - Indirect ($\alpha h\nu^{1/2}$)
524	0.05679	2.36641	0.48846
523	0.05488	2.37094	0.48785
522	0.05311	2.37548	0.48575
521	0.05156	2.38004	0.48105
520	0.05016	2.38462	0.47346
519	0.04882	2.38921	0.46515
518	0.04769	2.39382	0.45591
517	0.04688	2.39845	0.44455
516	0.04605	2.4031	0.4334
515	0.04532	2.40777	0.42313
514	0.04473	2.41245	0.4127
513	0.04399	2.41715	0.40261
512	0.04343	2.42188	0.39413
511	0.04299	2.42661	0.38518
510	0.04256	2.43137	0.37695
509	0.04226	2.43615	0.36896
508	0.04198	2.44094	0.36067
507	0.04177	2.44576	0.35296
506	0.04159	2.45059	0.34534
505	0.04156	2.45545	0.33906
504	0.04156	2.46032	0.33278
503	0.04173	2.46521	0.3275
502	0.04193	2.47012	0.32332
501	0.04229	2.47505	0.31968
500	0.04266	2.48	0.31799
499	0.04304	2.48497	0.31747
498	0.04351	2.48996	0.31799
497	0.0438	2.49497	0.31908
496	0.0442	2.5	0.31992
495	0.04458	2.50505	0.32226
494	0.04503	2.51012	0.32605
493	0.0457	2.51521	0.33031
492	0.04645	2.52033	0.33401
491	0.04738	2.52546	0.33772
490	0.04838	2.53061	0.34248
489	0.04939	2.53579	0.34673
488	0.05074	2.54098	0.35234
487	0.05236	2.5462	0.35663
486	0.05411	2.55144	0.36112

Wavelength (nm)	Absorbance	Photon Energy (eV)	Relationship - Indirect ($\alpha h\nu^{1/2}$)
485	0.05629	2.5567	0.36581
484	0.05863	2.56198	0.36973
483	0.06121	2.56729	0.37331
482	0.06433	2.57261	0.37868
481	0.0678	2.57796	0.38314
480	0.07164	2.58333	0.38788
479	0.07614	2.58873	0.39257
478	0.08119	2.59414	0.39726
477	0.08689	2.59958	0.40403
476	0.09348	2.60504	0.41091
475	0.10088	2.61053	0.4181
474	0.10936	2.61603	0.42693
473	0.11924	2.62156	0.43635
472	0.13044	2.62712	0.44558
471	0.14311	2.6327	0.45608
470	0.15737	2.6383	0.4668
469	0.17325	2.64392	0.47826
468	0.19105	2.64957	0.49178
467	0.21094	2.65525	0.50516
466	0.23291	2.66094	0.51918
465	0.25695	2.66667	0.53428
464	0.28317	2.67241	0.55048
463	0.31129	2.67819	0.56756
462	0.34132	2.68398	0.58578
461	0.3732	2.6898	0.60476
460	0.40611	2.69565	0.6256
459	0.43967	2.70153	0.64795
458	0.47313	2.70742	0.67332
457	0.50517	2.71335	0.70035
456	0.53462	2.7193	0.73052
455	0.55971	2.72527	0.76442
454	0.57904	2.73128	0.80173
453	0.591	2.73731	0.84295
452	0.59449	2.74336	0.88886
451	0.58926	2.74945	0.93966
450	0.57548	2.75556	0.99528
449	0.55428	2.76169	1.05663
448	0.52708	2.76786	1.12264
447	0.49574	2.77405	1.19424

Wavelength (nm)	Absorbance	Photon Energy (eV)	Relationship - Indirect ($\alpha h\nu^{1/2}$)
446	0.46236	2.78027	1.27093
445	0.42874	2.78652	1.35158
444	0.3965	2.79279	1.43545
443	0.36694	2.7991	1.52189
442	0.34089	2.80543	1.60852
441	0.31872	2.81179	1.692
440	0.30064	2.81818	1.76933
439	0.28615	2.8246	1.83776
438	0.27481	2.83105	1.89314
437	0.26618	2.83753	1.93217
436	0.25934	2.84404	1.95241
435	0.25389	2.85057	1.95105
434	0.24942	2.85714	1.92718
433	0.2455	2.86374	1.88306
432	0.242	2.87037	1.82285
431	0.23873	2.87703	1.75199
430	0.23527	2.88372	1.67616
429	0.23149	2.89044	1.60099
428	0.22713	2.8972	1.53106
427	0.22222	2.90398	1.4694
426	0.21649	2.9108	1.417
425	0.20995	2.91765	1.37428
424	0.20252	2.92453	1.34057
423	0.19429	2.93144	1.31321
422	0.18545	2.93839	1.29096
421	0.17636	2.94537	1.27078
420	0.16699	2.95238	1.25075
419	0.15857	2.95943	1.22977
418	0.15104	2.96651	1.20728
417	0.14447	2.97362	1.18318
416	0.1391	2.98077	1.15718
415	0.13502	2.98795	1.13055
414	0.13187	2.99517	1.10295
413	0.12983	3.00242	1.07448
412	0.12851	3.00971	1.04465
411	0.12781	3.01703	1.01364
410	0.12777	3.02439	0.98023
409	0.12804	3.03178	0.94624
408	0.12863	3.03922	0.91226

Wavelength (nm)	Absorbance	Photon Energy (eV)	Relationship - Indirect ($\alpha h\nu^{1/2}$)
407	0.12937	3.04668	0.87884
406	0.12998	3.05419	0.84767
405	0.13051	3.06173	0.81855
404	0.13091	3.06931	0.79249
403	0.13116	3.07692	0.76995
402	0.13129	3.08458	0.75079
401	0.13118	3.09227	0.73395
400	0.13083	3.1	0.71933
399	0.13033	3.10777	0.70646
398	0.12965	3.11558	0.69499
397	0.12882	3.12343	0.68447
396	0.12781	3.13131	0.67344
395	0.12665	3.13924	0.66509
394	0.12535	3.14721	0.65694
393	0.12406	3.15522	0.64918
392	0.12277	3.16327	0.64252
391	0.12152	3.17136	0.6374
390	0.12015	3.17949	0.63222
389	0.1187	3.18766	0.62765
388	0.11719	3.19588	0.62283
387	0.11552	3.20413	0.61913
386	0.11382	3.21244	0.61627
385	0.11198	3.22078	0.61234
384	0.11017	3.22917	0.60964
383	0.10825	3.2376	0.60693
382	0.10632	3.24607	0.6039
381	0.10449	3.25459	0.60239
380	0.1026	3.26316	0.59951
379	0.10077	3.27177	0.59761
378	0.09891	3.28042	0.59579
377	0.09703	3.28912	0.59264
376	0.0951	3.29787	0.58955
375	0.09313	3.30667	0.58616
374	0.09124	3.31551	0.58238
373	0.08915	3.3244	0.57803
372	0.08716	3.33333	0.57405
371	0.08518	3.34232	0.5689
370	0.0827	3.35135	0.56375
369	0.08049	3.36043	0.55885

Wavelength (nm)	Absorbance	Photon Energy (eV)	Relationship - Indirect ($\alpha h\nu^{1/2}$)
368	0.07838	3.36957	0.55556
367	0.07635	3.37875	0.55171
366	0.07446	3.38798	0.54874
365	0.07267	3.39726	0.54592
364	0.07074	3.40659	0.54261
363	0.06886	3.41598	0.54156
362	0.0671	3.42541	0.53905
361	0.06543	3.4349	0.53749
360	0.0639	3.44444	0.53467
359	0.06242	3.45404	0.53234
358	0.06107	3.46369	0.5315
357	0.0598	3.47339	0.52931
356	0.05853	3.48315	0.52838
355	0.05747	3.49296	0.52595
354	0.0564	3.50282	0.52475
353	0.0554	3.51275	0.52321
352	0.05454	3.52273	0.52177
351	0.0537	3.53276	0.52034
350	0.05293	3.54286	0.51929

Table 2.19: Zn2VTP Tauc Tables

Wavelength (nm)	Absorbance	Photon Energy (eV)	Relationship - Indirect ($\alpha h\nu^{1/2}$)
800	-1.74E-04	1.55	--
799	-9.82E-05	1.55194	--
798	2.64E-04	1.55388	0.02024
797	-3.83E-05	1.55583	--
796	-2.56E-05	1.55779	--
795	-2.45E-04	1.55975	--
794	-8.82E-04	1.56171	--
793	-2.60E-04	1.56368	--
792	4.76E-04	1.56566	0.0273
791	-2.16E-04	1.56764	--
790	-5.52E-04	1.56962	--
789	1.62E-04	1.57161	0.01595
788	-6.67E-04	1.5736	--
787	-4.80E-04	1.5756	--
786	-2.14E-04	1.57761	--

Wavelength (nm)	Absorbance	Photon Energy (eV)	Relationship - Indirect ($\alpha h\nu^{1/2}$)
785	1.18E-04	1.57962	0.01368
784	-4.77E-04	1.58163	--
783	5.21E-04	1.58365	0.02871
782	9.31E-04	1.58568	0.03843
781	4.70E-04	1.58771	0.02731
780	1.78E-04	1.58974	0.01683
779	2.94E-05	1.59178	0.00684
778	7.57E-04	1.59383	0.03473
777	9.69E-04	1.59588	0.03933
776	8.44E-04	1.59794	0.03673
775	9.82E-04	1.6	0.03964
774	0.00121	1.60207	0.04409
773	0.00115	1.60414	0.04295
772	7.64E-04	1.60622	0.03503
771	5.55E-04	1.6083	0.02987
770	0.00154	1.61039	0.04974
769	0.00159	1.61248	0.05057
768	0.00192	1.61458	0.05569
767	0.0012	1.61669	0.04407
766	0.00181	1.6188	0.0542
765	0.00156	1.62092	0.05025
764	9.27E-04	1.62304	0.03878
763	0.00145	1.62516	0.04856
762	0.00109	1.6273	0.04211
761	0.00132	1.62943	0.04646
760	0.00116	1.63158	0.04346
759	0.00162	1.63373	0.05152
758	0.00196	1.63588	0.05665
757	0.00216	1.63804	0.05947
756	0.00186	1.64021	0.05529
755	0.0018	1.64238	0.05431
754	0.00145	1.64456	0.04887
753	0.0016	1.64675	0.05128
752	0.00207	1.64894	0.05836
751	0.0019	1.65113	0.05605
750	0.00179	1.65333	0.05444
749	0.00239	1.65554	0.06284
748	0.00243	1.65775	0.06344
747	0.00179	1.65997	0.05456

Wavelength (nm)	Absorbance	Photon Energy (eV)	Relationship - Indirect ($\alpha h\nu^{1/2}$)
746	0.00194	1.6622	0.05682
745	0.00228	1.66443	0.06157
744	0.00207	1.66667	0.05874
743	0.00177	1.66891	0.05438
742	0.00183	1.67116	0.05526
741	0.00196	1.67341	0.05728
740	0.00237	1.67568	0.06297
739	0.00228	1.67794	0.06185
738	0.0022	1.68022	0.06083
737	0.00252	1.6825	0.06517
736	0.00241	1.68478	0.0637
735	0.00209	1.68707	0.05932
734	0.00241	1.68937	0.06385
733	0.00203	1.69168	0.05863
732	0.00265	1.69399	0.067
731	0.00254	1.69631	0.0657
730	0.00213	1.69863	0.06012
729	0.00254	1.70096	0.0657
728	0.00256	1.7033	0.0661
727	0.00234	1.70564	0.06312
726	0.00261	1.70799	0.06681
725	0.00219	1.71034	0.06116
724	0.00226	1.71271	0.06226
723	0.00287	1.71508	0.07017
722	0.00214	1.71745	0.06059
721	0.00223	1.71983	0.06199
720	0.00222	1.72222	0.0618
719	0.00213	1.72462	0.06057
718	0.00214	1.72702	0.06086
717	0.00284	1.72943	0.07008
716	0.00233	1.73184	0.06357
715	0.0023	1.73427	0.06317
714	0.00179	1.73669	0.05571
713	0.00254	1.73913	0.06643
712	0.00231	1.74157	0.06346
711	0.00231	1.74402	0.06343
710	0.00249	1.74648	0.06594
709	0.00279	1.74894	0.06986
708	0.0028	1.75141	0.07

Wavelength (nm)	Absorbance	Photon Energy (eV)	Relationship - Indirect ($\alpha h\nu^{1/2}$)
707	0.00282	1.75389	0.07034
706	0.00289	1.75637	0.07122
705	0.00262	1.75887	0.06787
704	0.00269	1.76136	0.06885
703	0.00272	1.76387	0.06931
702	0.00245	1.76638	0.06575
701	0.00297	1.7689	0.07248
700	0.00285	1.77143	0.07102
699	0.00257	1.77396	0.06752
698	0.00245	1.7765	0.066
697	0.00285	1.77905	0.07116
696	0.00272	1.78161	0.06964
695	0.00276	1.78417	0.07017
694	0.00284	1.78674	0.0713
693	0.00258	1.78932	0.06792
692	0.00231	1.79191	0.06433
691	0.00298	1.7945	0.07316
690	0.00281	1.7971	0.07103
689	0.00253	1.79971	0.06746
688	0.0028	1.80233	0.07107
687	0.00238	1.80495	0.06549
686	0.00241	1.80758	0.06598
685	0.00237	1.81022	0.06544
684	0.00265	1.81287	0.06929
683	0.00277	1.81552	0.07097
682	0.00276	1.81818	0.07081
681	0.00246	1.82085	0.06688
680	0.00262	1.82353	0.06913
679	0.00262	1.82622	0.06918
678	0.00293	1.82891	0.07325
677	0.00257	1.83161	0.06862
676	0.00245	1.83432	0.06698
675	0.00306	1.83704	0.07493
674	0.00285	1.83976	0.07242
673	0.00266	1.8425	0.06999
672	0.00292	1.84524	0.07337
671	0.00253	1.84799	0.06841
670	0.00286	1.85075	0.0728
669	0.00258	1.85351	0.06909

Wavelength (nm)	Absorbance	Photon Energy (eV)	Relationship - Indirect ($\alpha h\nu^{1/2}$)
668	0.00262	1.85629	0.0698
667	0.00276	1.85907	0.07158
666	0.00247	1.86186	0.06783
665	0.0025	1.86466	0.06821
664	0.00252	1.86747	0.06857
663	0.00227	1.87029	0.06515
662	0.00278	1.87311	0.0721
661	0.00262	1.87595	0.07014
660	0.00256	1.87879	0.06939
659	0.00255	1.88164	0.06931
658	0.00248	1.8845	0.06842
657	0.00227	1.88737	0.06542
656	0.00253	1.89024	0.0692
655	0.00231	1.89313	0.06613
654	0.00233	1.89602	0.06645
653	0.00243	1.89893	0.0679
652	0.00237	1.90184	0.06708
651	0.00242	1.90476	0.06792
650	0.00235	1.90769	0.06689
649	0.00238	1.91063	0.0675
648	0.00198	1.91358	0.06161
647	0.00229	1.91654	0.06623
646	0.00235	1.9195	0.06722
645	0.00248	1.92248	0.0691
644	0.0024	1.92547	0.06797
643	0.00255	1.92846	0.07008
642	0.00254	1.93146	0.07007
641	0.00214	1.93448	0.0643
640	0.0023	1.9375	0.06672
639	0.00245	1.94053	0.06893
638	0.00259	1.94357	0.07089
637	0.0027	1.94662	0.07254
636	0.00278	1.94969	0.07369
635	0.00267	1.95276	0.07225
634	0.00304	1.95584	0.07706
633	0.00261	1.95893	0.07154
632	0.0028	1.96203	0.07417
631	0.00276	1.96513	0.07371
630	0.00326	1.96825	0.08012

Wavelength (nm)	Absorbance	Photon Energy (eV)	Relationship - Indirect ($\alpha h\nu^{1/2}$)
629	0.00301	1.97138	0.077
628	0.00317	1.97452	0.07916
627	0.00356	1.97767	0.08396
626	0.00345	1.98083	0.08269
625	0.00312	1.984	0.07871
624	0.00336	1.98718	0.08166
623	0.00391	1.99037	0.08827
622	0.00368	1.99357	0.08571
621	0.00366	1.99678	0.0855
620	0.00398	2	0.08922
619	0.00438	2.00323	0.09362
618	0.00427	2.00647	0.09259
617	0.00441	2.00972	0.09409
616	0.00487	2.01299	0.09897
615	0.00531	2.01626	0.10351
614	0.00568	2.01954	0.10711
613	0.00596	2.02284	0.10981
612	0.00668	2.02614	0.11635
611	0.00732	2.02946	0.1219
610	0.00772	2.03279	0.12526
609	0.00816	2.03612	0.1289
608	0.00913	2.03947	0.13647
607	0.00955	2.04283	0.13965
606	0.00998	2.0462	0.14289
605	0.01034	2.04959	0.14554
604	0.01057	2.05298	0.14733
603	0.01039	2.05638	0.14619
602	0.01032	2.0598	0.14582
601	0.01011	2.06323	0.14443
600	0.00962	2.06667	0.141
599	0.00929	2.07012	0.13866
598	0.00955	2.07358	0.14071
597	0.00904	2.07705	0.137
596	0.00886	2.08054	0.13575
595	0.00874	2.08403	0.13497
594	0.00842	2.08754	0.13259
593	0.00887	2.09106	0.1362
592	0.00857	2.09459	0.13399
591	0.00889	2.09814	0.1366

Wavelength (nm)	Absorbance	Photon Energy (eV)	Relationship - Indirect ($\alpha h\nu^{1/2}$)
590	0.00929	2.10169	0.13973
589	0.00931	2.10526	0.13999
588	0.0099	2.10884	0.14446
587	0.01012	2.11244	0.14619
586	0.01056	2.11604	0.14949
585	0.01104	2.11966	0.15297
584	0.0113	2.12329	0.1549
583	0.0124	2.12693	0.16238
582	0.01335	2.13058	0.16867
581	0.01423	2.13425	0.17428
580	0.01602	2.13793	0.18508
579	0.01691	2.14162	0.19028
578	0.01839	2.14533	0.19864
577	0.01942	2.14905	0.20429
576	0.02141	2.15278	0.21468
575	0.02373	2.15652	0.22621
574	0.02598	2.16028	0.23692
573	0.02878	2.16405	0.24956
572	0.03082	2.16783	0.25848
571	0.03311	2.17163	0.26815
570	0.03529	2.17544	0.27708
569	0.03719	2.17926	0.28468
568	0.03948	2.1831	0.2936
567	0.0407	2.18695	0.29834
566	0.04129	2.19081	0.30075
565	0.04174	2.19469	0.30266
564	0.04168	2.19858	0.30271
563	0.04104	2.20249	0.30065
562	0.03983	2.20641	0.29645
561	0.03888	2.21034	0.29314
560	0.03652	2.21429	0.28435
559	0.0346	2.21825	0.27703
558	0.03288	2.22222	0.27031
557	0.03083	2.22621	0.26197
556	0.02903	2.23022	0.25445
555	0.02704	2.23423	0.24577
554	0.02539	2.23827	0.23839
553	0.02349	2.24231	0.22949
552	0.0226	2.24638	0.22534

Wavelength (nm)	Absorbance	Photon Energy (eV)	Relationship - Indirect ($\alpha h\nu^{1/2}$)
551	0.02091	2.25045	0.21691
550	0.0201	2.25455	0.21289
549	0.01915	2.25865	0.20797
548	0.0188	2.26277	0.20623
547	0.01777	2.26691	0.20071
546	0.01741	2.27106	0.19883
545	0.01626	2.27523	0.19234
544	0.01522	2.27941	0.18627
543	0.01455	2.28361	0.18227
542	0.0141	2.28782	0.17957
541	0.01287	2.29205	0.17175
540	0.01179	2.2963	0.16451
539	0.01158	2.30056	0.16322
538	0.01053	2.30483	0.15576
537	0.01019	2.30912	0.15339
536	0.00991	2.31343	0.15138
535	0.00942	2.31776	0.1478
534	0.00898	2.3221	0.14437
533	0.00948	2.32645	0.14848
532	0.009	2.33083	0.14486
531	0.00917	2.33522	0.1463
530	0.0089	2.33962	0.14427
529	0.00886	2.34405	0.14411
528	0.00952	2.34848	0.14952
527	0.00908	2.35294	0.14619
526	0.00906	2.35741	0.14617
525	0.00957	2.3619	0.15032
524	0.00993	2.36641	0.15332
523	0.00958	2.37094	0.15069
522	0.0099	2.37548	0.15333
521	0.00976	2.38004	0.15241
520	0.01008	2.38462	0.15503
519	0.00951	2.38921	0.1507
518	0.01004	2.39382	0.15503
517	0.0102	2.39845	0.1564
516	0.01049	2.4031	0.15874
515	0.01005	2.40777	0.15558
514	0.01065	2.41245	0.16029
513	0.01052	2.41715	0.15943

Wavelength (nm)	Absorbance	Photon Energy (eV)	Relationship - Indirect ($\alpha h\nu^{1/2}$)
512	0.01025	2.42188	0.15754
511	0.01042	2.42661	0.15904
510	0.01092	2.43137	0.16294
509	0.01082	2.43615	0.16233
508	0.01095	2.44094	0.16347
507	0.01171	2.44576	0.16921
506	0.01155	2.45059	0.16821
505	0.01149	2.45545	0.16795
504	0.01192	2.46032	0.17123
503	0.01216	2.46521	0.17314
502	0.01284	2.47012	0.17807
501	0.01297	2.47505	0.17918
500	0.01332	2.48	0.18177
499	0.01379	2.48497	0.18511
498	0.01398	2.48996	0.1866
497	0.01474	2.49497	0.19177
496	0.01555	2.5	0.19715
495	0.01527	2.50505	0.19558
494	0.01581	2.51012	0.19919
493	0.01653	2.51521	0.20392
492	0.01644	2.52033	0.20354
491	0.01642	2.52546	0.20364
490	0.017	2.53061	0.2074
489	0.01722	2.53579	0.20898
488	0.01745	2.54098	0.21056
487	0.01749	2.5462	0.21103
486	0.01743	2.55144	0.21089
485	0.01808	2.5567	0.21502
484	0.01804	2.56198	0.21497
483	0.01829	2.56729	0.21672
482	0.01822	2.57261	0.21652
481	0.0188	2.57796	0.22012
480	0.01929	2.58333	0.22324
479	0.01936	2.58873	0.22389
478	0.01956	2.59414	0.22528
477	0.01977	2.59958	0.22669
476	0.02039	2.60504	0.23046
475	0.02096	2.61053	0.23392
474	0.02112	2.61603	0.23504

Wavelength (nm)	Absorbance	Photon Energy (eV)	Relationship - Indirect ($\alpha h\nu^{1/2}$)
473	0.02145	2.62156	0.23712
472	0.0228	2.62712	0.24473
471	0.02341	2.6327	0.24826
470	0.0246	2.6383	0.25475
469	0.0262	2.64392	0.26319
468	0.02798	2.64957	0.27228
467	0.03066	2.65525	0.28532
466	0.03307	2.66094	0.29665
465	0.03629	2.66667	0.3111
464	0.04024	2.67241	0.32792
463	0.04502	2.67819	0.34724
462	0.05201	2.68398	0.37362
461	0.06036	2.6898	0.40292
460	0.07049	2.69565	0.43589
459	0.0837	2.70153	0.47553
458	0.10007	2.70742	0.52051
457	0.12036	2.71335	0.57146
456	0.14492	2.7193	0.62775
455	0.17452	2.72527	0.68965
454	0.20916	2.73128	0.75583
453	0.2489	2.73731	0.82542
452	0.2925	2.74336	0.89579
451	0.33948	2.74945	0.96612
450	0.38714	2.75556	1.03285
449	0.43435	2.76169	1.09523
448	0.47566	2.76786	1.14741
447	0.51133	2.77405	1.19099
446	0.53773	2.78027	1.22271
445	0.55372	2.78652	1.24215
444	0.55953	2.79279	1.25006
443	0.55421	2.7991	1.24551
442	0.54088	2.80543	1.23183
441	0.52071	2.81179	1.21001
440	0.4939	2.81818	1.17978
439	0.46289	2.8246	1.14345
438	0.42879	2.83105	1.10178
437	0.39328	2.83753	1.05638
436	0.35567	2.84404	1.00575
435	0.31797	2.85057	0.95205

Wavelength (nm)	Absorbance	Photon Energy (eV)	Relationship - Indirect ($\alpha h\nu^{1/2}$)
434	0.28252	2.85714	0.89844
433	0.24902	2.86374	0.84446
432	0.21964	2.87037	0.79401
431	0.1934	2.87703	0.74593
430	0.17156	2.88372	0.70338
429	0.15451	2.89044	0.66828
428	0.14077	2.8972	0.63862
427	0.12982	2.90398	0.61399
426	0.1214	2.9108	0.59445
425	0.11451	2.91765	0.57802
424	0.10827	2.92453	0.56272
423	0.10209	2.93144	0.54707
422	0.09824	2.93839	0.53729
421	0.09245	2.94537	0.52181
420	0.08837	2.95238	0.51078
419	0.08281	2.95943	0.49503
418	0.0784	2.96651	0.48225
417	0.07299	2.97362	0.46587
416	0.06787	2.98077	0.44977
415	0.06252	2.98795	0.43222
414	0.05782	2.99517	0.41615
413	0.05338	3.00242	0.40034
412	0.04858	3.00971	0.38238
411	0.04402	3.01703	0.36442
410	0.03986	3.02439	0.34721
409	0.03611	3.03178	0.33089
408	0.03348	3.03922	0.31898
407	0.03053	3.04668	0.30496
406	0.02778	3.05419	0.29128
405	0.02583	3.06173	0.28121
404	0.02459	3.06931	0.27473
403	0.02203	3.07692	0.26037
402	0.02131	3.08458	0.25637
401	0.02123	3.09227	0.25621
400	0.01977	3.1	0.24758
399	0.0189	3.10777	0.24237
398	0.01806	3.11558	0.23723
397	0.01762	3.12343	0.23456
396	0.0183	3.13131	0.23941

Wavelength (nm)	Absorbance	Photon Energy (eV)	Relationship - Indirect ($\alpha h\nu^{1/2}$)
395	0.01715	3.13924	0.23201
394	0.01571	3.14721	0.22236
393	0.01614	3.15522	0.22567
392	0.01582	3.16327	0.22371
391	0.01598	3.17136	0.22514
390	0.01443	3.17949	0.21421
389	0.01449	3.18766	0.21492
388	0.0144	3.19588	0.21449
387	0.01443	3.20413	0.21504
386	0.01382	3.21244	0.21067
385	0.01371	3.22078	0.21016
384	0.01358	3.22917	0.20938
383	0.01308	3.2376	0.20577
382	0.01293	3.24607	0.20487
381	0.01342	3.25459	0.20895
380	0.01337	3.26316	0.20887
379	0.01378	3.27177	0.21232
378	0.01362	3.28042	0.21137
377	0.01161	3.28912	0.19545
376	0.01372	3.29787	0.2127
375	0.01254	3.30667	0.20361
374	0.01275	3.31551	0.20564
373	0.01263	3.3244	0.20487
372	0.01341	3.33333	0.21142
371	0.01417	3.34232	0.21765
370	0.01285	3.35135	0.20753
369	0.01394	3.36043	0.21645
368	0.01443	3.36957	0.22047
367	0.01317	3.37875	0.21092
366	0.01478	3.38798	0.22379
365	0.01397	3.39726	0.21782
364	0.01318	3.40659	0.21187
363	0.01458	3.41598	0.22316
362	0.01488	3.42541	0.22577
361	0.01498	3.4349	0.22687
360	0.01465	3.44444	0.22466
359	0.01505	3.45404	0.22801
358	0.01519	3.46369	0.22936
357	0.01439	3.47339	0.22354

Wavelength (nm)	Absorbance	Photon Energy (eV)	Relationship - Indirect ($\alpha h\nu^{1/2}$)
356	0.01602	3.48315	0.2362
355	0.01645	3.49296	0.23969
354	0.01535	3.50282	0.23191
353	0.01586	3.51275	0.23606
352	0.0153	3.52273	0.23218
351	0.01656	3.53276	0.24191
350	0.01545	3.54286	0.23396

Table 2.20: Zn3VTP Tauc Tables

Wavelength (nm)	Absorbance	Photon Energy (eV)	Relationship - Indirect ($\alpha h\nu^{1/2}$)
800	-1.74E-04	1.55	--
799	-9.82E-05	1.55194	--
798	2.64E-04	1.55388	0.02024
797	-3.83E-05	1.55583	--
796	-2.56E-05	1.55779	--
795	-2.45E-04	1.55975	--
794	-8.82E-04	1.56171	--
793	-2.60E-04	1.56368	--
792	4.76E-04	1.56566	0.0273
791	-2.16E-04	1.56764	--
790	-5.52E-04	1.56962	--
789	1.62E-04	1.57161	0.01595
788	-6.67E-04	1.5736	--
787	-4.80E-04	1.5756	--
786	-2.14E-04	1.57761	--
785	1.18E-04	1.57962	0.01368
784	-4.77E-04	1.58163	--
783	5.21E-04	1.58365	0.02871
782	9.31E-04	1.58568	0.03843
781	4.70E-04	1.58771	0.02731
780	1.78E-04	1.58974	0.01683
779	2.94E-05	1.59178	0.00684
778	7.57E-04	1.59383	0.03473
777	9.69E-04	1.59588	0.03933
776	8.44E-04	1.59794	0.03673
775	9.82E-04	1.6	0.03964
774	0.00121	1.60207	0.04409

Wavelength (nm)	Absorbance	Photon Energy (eV)	Relationship - Indirect ($\alpha h\nu^{1/2}$)
773	0.00115	1.60414	0.04295
772	7.64E-04	1.60622	0.03503
771	5.55E-04	1.6083	0.02987
770	0.00154	1.61039	0.04974
769	0.00159	1.61248	0.05057
768	0.00192	1.61458	0.05569
767	0.0012	1.61669	0.04407
766	0.00181	1.6188	0.0542
765	0.00156	1.62092	0.05025
764	9.27E-04	1.62304	0.03878
763	0.00145	1.62516	0.04856
762	0.00109	1.6273	0.04211
761	0.00132	1.62943	0.04646
760	0.00116	1.63158	0.04346
759	0.00162	1.63373	0.05152
758	0.00196	1.63588	0.05665
757	0.00216	1.63804	0.05947
756	0.00186	1.64021	0.05529
755	0.0018	1.64238	0.05431
754	0.00145	1.64456	0.04887
753	0.0016	1.64675	0.05128
752	0.00207	1.64894	0.05836
751	0.0019	1.65113	0.05605
750	0.00179	1.65333	0.05444
749	0.00239	1.65554	0.06284
748	0.00243	1.65775	0.06344
747	0.00179	1.65997	0.05456
746	0.00194	1.6622	0.05682
745	0.00228	1.66443	0.06157
744	0.00207	1.66667	0.05874
743	0.00177	1.66891	0.05438
742	0.00183	1.67116	0.05526
741	0.00196	1.67341	0.05728
740	0.00237	1.67568	0.06297
739	0.00228	1.67794	0.06185
738	0.0022	1.68022	0.06083
737	0.00252	1.6825	0.06517
736	0.00241	1.68478	0.0637
735	0.00209	1.68707	0.05932

Wavelength (nm)	Absorbance	Photon Energy (eV)	Relationship - Indirect ($\alpha h\nu^{1/2}$)
734	0.00241	1.68937	0.06385
733	0.00203	1.69168	0.05863
732	0.00265	1.69399	0.067
731	0.00254	1.69631	0.0657
730	0.00213	1.69863	0.06012
729	0.00254	1.70096	0.0657
728	0.00256	1.7033	0.0661
727	0.00234	1.70564	0.06312
726	0.00261	1.70799	0.06681
725	0.00219	1.71034	0.06116
724	0.00226	1.71271	0.06226
723	0.00287	1.71508	0.07017
722	0.00214	1.71745	0.06059
721	0.00223	1.71983	0.06199
720	0.00222	1.72222	0.0618
719	0.00213	1.72462	0.06057
718	0.00214	1.72702	0.06086
717	0.00284	1.72943	0.07008
716	0.00233	1.73184	0.06357
715	0.0023	1.73427	0.06317
714	0.00179	1.73669	0.05571
713	0.00254	1.73913	0.06643
712	0.00231	1.74157	0.06346
711	0.00231	1.74402	0.06343
710	0.00249	1.74648	0.06594
709	0.00279	1.74894	0.06986
708	0.0028	1.75141	0.07
707	0.00282	1.75389	0.07034
706	0.00289	1.75637	0.07122
705	0.00262	1.75887	0.06787
704	0.00269	1.76136	0.06885
703	0.00272	1.76387	0.06931
702	0.00245	1.76638	0.06575
701	0.00297	1.7689	0.07248
700	0.00285	1.77143	0.07102
699	0.00257	1.77396	0.06752
698	0.00245	1.7765	0.066
697	0.00285	1.77905	0.07116
696	0.00272	1.78161	0.06964

Wavelength (nm)	Absorbance	Photon Energy (eV)	Relationship - Indirect ($\alpha h\nu^{1/2}$)
695	0.00276	1.78417	0.07017
694	0.00284	1.78674	0.0713
693	0.00258	1.78932	0.06792
692	0.00231	1.79191	0.06433
691	0.00298	1.7945	0.07316
690	0.00281	1.7971	0.07103
689	0.00253	1.79971	0.06746
688	0.0028	1.80233	0.07107
687	0.00238	1.80495	0.06549
686	0.00241	1.80758	0.06598
685	0.00237	1.81022	0.06544
684	0.00265	1.81287	0.06929
683	0.00277	1.81552	0.07097
682	0.00276	1.81818	0.07081
681	0.00246	1.82085	0.06688
680	0.00262	1.82353	0.06913
679	0.00262	1.82622	0.06918
678	0.00293	1.82891	0.07325
677	0.00257	1.83161	0.06862
676	0.00245	1.83432	0.06698
675	0.00306	1.83704	0.07493
674	0.00285	1.83976	0.07242
673	0.00266	1.8425	0.06999
672	0.00292	1.84524	0.07337
671	0.00253	1.84799	0.06841
670	0.00286	1.85075	0.0728
669	0.00258	1.85351	0.06909
668	0.00262	1.85629	0.0698
667	0.00276	1.85907	0.07158
666	0.00247	1.86186	0.06783
665	0.0025	1.86466	0.06821
664	0.00252	1.86747	0.06857
663	0.00227	1.87029	0.06515
662	0.00278	1.87311	0.0721
661	0.00262	1.87595	0.07014
660	0.00256	1.87879	0.06939
659	0.00255	1.88164	0.06931
658	0.00248	1.8845	0.06842
657	0.00227	1.88737	0.06542

Wavelength (nm)	Absorbance	Photon Energy (eV)	Relationship - Indirect ($\alpha h\nu^{1/2}$)
656	0.00253	1.89024	0.0692
655	0.00231	1.89313	0.06613
654	0.00233	1.89602	0.06645
653	0.00243	1.89893	0.0679
652	0.00237	1.90184	0.06708
651	0.00242	1.90476	0.06792
650	0.00235	1.90769	0.06689
649	0.00238	1.91063	0.0675
648	0.00198	1.91358	0.06161
647	0.00229	1.91654	0.06623
646	0.00235	1.9195	0.06722
645	0.00248	1.92248	0.0691
644	0.0024	1.92547	0.06797
643	0.00255	1.92846	0.07008
642	0.00254	1.93146	0.07007
641	0.00214	1.93448	0.0643
640	0.0023	1.9375	0.06672
639	0.00245	1.94053	0.06893
638	0.00259	1.94357	0.07089
637	0.0027	1.94662	0.07254
636	0.00278	1.94969	0.07369
635	0.00267	1.95276	0.07225
634	0.00304	1.95584	0.07706
633	0.00261	1.95893	0.07154
632	0.0028	1.96203	0.07417
631	0.00276	1.96513	0.07371
630	0.00326	1.96825	0.08012
629	0.00301	1.97138	0.077
628	0.00317	1.97452	0.07916
627	0.00356	1.97767	0.08396
626	0.00345	1.98083	0.08269
625	0.00312	1.984	0.07871
624	0.00336	1.98718	0.08166
623	0.00391	1.99037	0.08827
622	0.00368	1.99357	0.08571
621	0.00366	1.99678	0.0855
620	0.00398	2	0.08922
619	0.00438	2.00323	0.09362
618	0.00427	2.00647	0.09259

Wavelength (nm)	Absorbance	Photon Energy (eV)	Relationship - Indirect ($\alpha h\nu^{1/2}$)
617	0.00441	2.00972	0.09409
616	0.00487	2.01299	0.09897
615	0.00531	2.01626	0.10351
614	0.00568	2.01954	0.10711
613	0.00596	2.02284	0.10981
612	0.00668	2.02614	0.11635
611	0.00732	2.02946	0.1219
610	0.00772	2.03279	0.12526
609	0.00816	2.03612	0.1289
608	0.00913	2.03947	0.13647
607	0.00955	2.04283	0.13965
606	0.00998	2.0462	0.14289
605	0.01034	2.04959	0.14554
604	0.01057	2.05298	0.14733
603	0.01039	2.05638	0.14619
602	0.01032	2.0598	0.14582
601	0.01011	2.06323	0.14443
600	0.00962	2.06667	0.141
599	0.00929	2.07012	0.13866
598	0.00955	2.07358	0.14071
597	0.00904	2.07705	0.137
596	0.00886	2.08054	0.13575
595	0.00874	2.08403	0.13497
594	0.00842	2.08754	0.13259
593	0.00887	2.09106	0.1362
592	0.00857	2.09459	0.13399
591	0.00889	2.09814	0.1366
590	0.00929	2.10169	0.13973
589	0.00931	2.10526	0.13999
588	0.0099	2.10884	0.14446
587	0.01012	2.11244	0.14619
586	0.01056	2.11604	0.14949
585	0.01104	2.11966	0.15297
584	0.0113	2.12329	0.1549
583	0.0124	2.12693	0.16238
582	0.01335	2.13058	0.16867
581	0.01423	2.13425	0.17428
580	0.01602	2.13793	0.18508
579	0.01691	2.14162	0.19028

Wavelength (nm)	Absorbance	Photon Energy (eV)	Relationship - Indirect ($\alpha h\nu^{1/2}$)
578	0.01839	2.14533	0.19864
577	0.01942	2.14905	0.20429
576	0.02141	2.15278	0.21468
575	0.02373	2.15652	0.22621
574	0.02598	2.16028	0.23692
573	0.02878	2.16405	0.24956
572	0.03082	2.16783	0.25848
571	0.03311	2.17163	0.26815
570	0.03529	2.17544	0.27708
569	0.03719	2.17926	0.28468
568	0.03948	2.1831	0.2936
567	0.0407	2.18695	0.29834
566	0.04129	2.19081	0.30075
565	0.04174	2.19469	0.30266
564	0.04168	2.19858	0.30271
563	0.04104	2.20249	0.30065
562	0.03983	2.20641	0.29645
561	0.03888	2.21034	0.29314
560	0.03652	2.21429	0.28435
559	0.0346	2.21825	0.27703
558	0.03288	2.22222	0.27031
557	0.03083	2.22621	0.26197
556	0.02903	2.23022	0.25445
555	0.02704	2.23423	0.24577
554	0.02539	2.23827	0.23839
553	0.02349	2.24231	0.22949
552	0.0226	2.24638	0.22534
551	0.02091	2.25045	0.21691
550	0.0201	2.25455	0.21289
549	0.01915	2.25865	0.20797
548	0.0188	2.26277	0.20623
547	0.01777	2.26691	0.20071
546	0.01741	2.27106	0.19883
545	0.01626	2.27523	0.19234
544	0.01522	2.27941	0.18627
543	0.01455	2.28361	0.18227
542	0.0141	2.28782	0.17957
541	0.01287	2.29205	0.17175
540	0.01179	2.2963	0.16451

Wavelength (nm)	Absorbance	Photon Energy (eV)	Relationship - Indirect ($\alpha h\nu^{1/2}$)
539	0.01158	2.30056	0.16322
538	0.01053	2.30483	0.15576
537	0.01019	2.30912	0.15339
536	0.00991	2.31343	0.15138
535	0.00942	2.31776	0.1478
534	0.00898	2.3221	0.14437
533	0.00948	2.32645	0.14848
532	0.009	2.33083	0.14486
531	0.00917	2.33522	0.1463
530	0.0089	2.33962	0.14427
529	0.00886	2.34405	0.14411
528	0.00952	2.34848	0.14952
527	0.00908	2.35294	0.14619
526	0.00906	2.35741	0.14617
525	0.00957	2.3619	0.15032
524	0.00993	2.36641	0.15332
523	0.00958	2.37094	0.15069
522	0.0099	2.37548	0.15333
521	0.00976	2.38004	0.15241
520	0.01008	2.38462	0.15503
519	0.00951	2.38921	0.1507
518	0.01004	2.39382	0.15503
517	0.0102	2.39845	0.1564
516	0.01049	2.4031	0.15874
515	0.01005	2.40777	0.15558
514	0.01065	2.41245	0.16029
513	0.01052	2.41715	0.15943
512	0.01025	2.42188	0.15754
511	0.01042	2.42661	0.15904
510	0.01092	2.43137	0.16294
509	0.01082	2.43615	0.16233
508	0.01095	2.44094	0.16347
507	0.01171	2.44576	0.16921
506	0.01155	2.45059	0.16821
505	0.01149	2.45545	0.16795
504	0.01192	2.46032	0.17123
503	0.01216	2.46521	0.17314
502	0.01284	2.47012	0.17807
501	0.01297	2.47505	0.17918

Wavelength (nm)	Absorbance	Photon Energy (eV)	Relationship - Indirect ($\alpha h\nu^{1/2}$)
500	0.01332	2.48	0.18177
499	0.01379	2.48497	0.18511
498	0.01398	2.48996	0.1866
497	0.01474	2.49497	0.19177
496	0.01555	2.5	0.19715
495	0.01527	2.50505	0.19558
494	0.01581	2.51012	0.19919
493	0.01653	2.51521	0.20392
492	0.01644	2.52033	0.20354
491	0.01642	2.52546	0.20364
490	0.017	2.53061	0.2074
489	0.01722	2.53579	0.20898
488	0.01745	2.54098	0.21056
487	0.01749	2.5462	0.21103
486	0.01743	2.55144	0.21089
485	0.01808	2.5567	0.21502
484	0.01804	2.56198	0.21497
483	0.01829	2.56729	0.21672
482	0.01822	2.57261	0.21652
481	0.0188	2.57796	0.22012
480	0.01929	2.58333	0.22324
479	0.01936	2.58873	0.22389
478	0.01956	2.59414	0.22528
477	0.01977	2.59958	0.22669
476	0.02039	2.60504	0.23046
475	0.02096	2.61053	0.23392
474	0.02112	2.61603	0.23504
473	0.02145	2.62156	0.23712
472	0.0228	2.62712	0.24473
471	0.02341	2.6327	0.24826
470	0.0246	2.6383	0.25475
469	0.0262	2.64392	0.26319
468	0.02798	2.64957	0.27228
467	0.03066	2.65525	0.28532
466	0.03307	2.66094	0.29665
465	0.03629	2.66667	0.3111
464	0.04024	2.67241	0.32792
463	0.04502	2.67819	0.34724
462	0.05201	2.68398	0.37362

Wavelength (nm)	Absorbance	Photon Energy (eV)	Relationship - Indirect ($\alpha h\nu^{1/2}$)
461	0.06036	2.6898	0.40292
460	0.07049	2.69565	0.43589
459	0.0837	2.70153	0.47553
458	0.10007	2.70742	0.52051
457	0.12036	2.71335	0.57146
456	0.14492	2.7193	0.62775
455	0.17452	2.72527	0.68965
454	0.20916	2.73128	0.75583
453	0.2489	2.73731	0.82542
452	0.2925	2.74336	0.89579
451	0.33948	2.74945	0.96612
450	0.38714	2.75556	1.03285
449	0.43435	2.76169	1.09523
448	0.47566	2.76786	1.14741
447	0.51133	2.77405	1.19099
446	0.53773	2.78027	1.22271
445	0.55372	2.78652	1.24215
444	0.55953	2.79279	1.25006
443	0.55421	2.7991	1.24551
442	0.54088	2.80543	1.23183
441	0.52071	2.81179	1.21001
440	0.4939	2.81818	1.17978
439	0.46289	2.8246	1.14345
438	0.42879	2.83105	1.10178
437	0.39328	2.83753	1.05638
436	0.35567	2.84404	1.00575
435	0.31797	2.85057	0.95205
434	0.28252	2.85714	0.89844
433	0.24902	2.86374	0.84446
432	0.21964	2.87037	0.79401
431	0.1934	2.87703	0.74593
430	0.17156	2.88372	0.70338
429	0.15451	2.89044	0.66828
428	0.14077	2.8972	0.63862
427	0.12982	2.90398	0.61399
426	0.1214	2.9108	0.59445
425	0.11451	2.91765	0.57802
424	0.10827	2.92453	0.56272
423	0.10209	2.93144	0.54707

Wavelength (nm)	Absorbance	Photon Energy (eV)	Relationship - Indirect ($\alpha h\nu^{1/2}$)
422	0.09824	2.93839	0.53729
421	0.09245	2.94537	0.52181
420	0.08837	2.95238	0.51078
419	0.08281	2.95943	0.49503
418	0.0784	2.96651	0.48225
417	0.07299	2.97362	0.46587
416	0.06787	2.98077	0.44977
415	0.06252	2.98795	0.43222
414	0.05782	2.99517	0.41615
413	0.05338	3.00242	0.40034
412	0.04858	3.00971	0.38238
411	0.04402	3.01703	0.36442
410	0.03986	3.02439	0.34721
409	0.03611	3.03178	0.33089
408	0.03348	3.03922	0.31898
407	0.03053	3.04668	0.30496
406	0.02778	3.05419	0.29128
405	0.02583	3.06173	0.28121
404	0.02459	3.06931	0.27473
403	0.02203	3.07692	0.26037
402	0.02131	3.08458	0.25637
401	0.02123	3.09227	0.25621
400	0.01977	3.1	0.24758
399	0.0189	3.10777	0.24237
398	0.01806	3.11558	0.23723
397	0.01762	3.12343	0.23456
396	0.0183	3.13131	0.23941
395	0.01715	3.13924	0.23201
394	0.01571	3.14721	0.22236
393	0.01614	3.15522	0.22567
392	0.01582	3.16327	0.22371
391	0.01598	3.17136	0.22514
390	0.01443	3.17949	0.21421
389	0.01449	3.18766	0.21492
388	0.0144	3.19588	0.21449
387	0.01443	3.20413	0.21504
386	0.01382	3.21244	0.21067
385	0.01371	3.22078	0.21016
383	0.01308	3.2376	0.20577

Wavelength (nm)	Absorbance	Photon Energy (eV)	Relationship - Indirect ($\alpha h\nu^{1/2}$)
382	0.01293	3.24607	0.20487
381	0.01342	3.25459	0.20895
380	0.01337	3.26316	0.20887
379	0.01378	3.27177	0.21232
378	0.01362	3.28042	0.21137
377	0.01161	3.28912	0.19545
376	0.01372	3.29787	0.2127
375	0.01254	3.30667	0.20361
374	0.01275	3.31551	0.20564
373	0.01263	3.3244	0.20487
372	0.01341	3.33333	0.21142
371	0.01417	3.34232	0.21765
370	0.01285	3.35135	0.20753
369	0.01394	3.36043	0.21645
368	0.01443	3.36957	0.22047
367	0.01317	3.37875	0.21092
366	0.01478	3.38798	0.22379
365	0.01397	3.39726	0.21782
364	0.01318	3.40659	0.21187
363	0.01458	3.41598	0.22316
362	0.01488	3.42541	0.22577
361	0.01498	3.4349	0.22687
360	0.01465	3.44444	0.22466
359	0.01505	3.45404	0.22801
358	0.01519	3.46369	0.22936
357	0.01439	3.47339	0.22354
356	0.01602	3.48315	0.2362
355	0.01645	3.49296	0.23969
354	0.01535	3.50282	0.23191
353	0.01586	3.51275	0.23606
352	0.0153	3.52273	0.23218
351	0.01656	3.53276	0.24191
350	0.01545	3.54286	0.23396

Table 2.21: ZnF3VTP Tauc Tables

Wavelength (nm)	Absorbance	Photon Energy (eV)	Relationship - Indirect ($\alpha h\nu^{1/2}$)
800	-7.51E-04	1.55	--

Wavelength (nm)	Absorbance	Photon Energy (eV)	Relationship - Indirect ($\alpha h\nu^{1/2}$)
799	-1.28E-04	1.55194	--
798	-3.24E-04	1.55388	--
797	-7.73E-04	1.55583	--
796	-5.30E-04	1.55779	--
795	-7.30E-04	1.55975	--
794	-0.00107	1.56171	--
793	-4.47E-04	1.56368	--
792	1.37E-04	1.56566	0.01466
791	-3.84E-04	1.56764	--
790	-9.01E-04	1.56962	--
789	-2.00E-04	1.57161	--
788	-5.72E-04	1.5736	--
787	-6.84E-04	1.5756	--
786	-8.67E-04	1.57761	--
785	-6.07E-04	1.57962	--
784	-8.20E-04	1.58163	--
783	-3.69E-05	1.58365	--
782	-1.17E-04	1.58568	--
781	-6.12E-04	1.58771	--
780	-0.00116	1.58974	--
779	-0.00124	1.59178	--
778	-2.27E-04	1.59383	--
777	-5.76E-04	1.59588	--
776	-6.97E-04	1.59794	--
775	-7.81E-04	1.6	--
774	-2.66E-04	1.60207	--
773	-8.14E-04	1.60414	--
772	-0.00123	1.60622	--
771	-0.00121	1.6083	--
770	-5.58E-04	1.61039	--
769	-4.97E-04	1.61248	--
768	-6.49E-04	1.61458	--
767	-7.24E-04	1.61669	--
766	-3.64E-04	1.6188	--
765	-1.00E-03	1.62092	--
764	-7.92E-04	1.62304	--
763	-5.12E-04	1.62516	--
762	-0.00111	1.6273	--
761	-9.23E-04	1.62943	--

Wavelength (nm)	Absorbance	Photon Energy (eV)	Relationship - Indirect ($\alpha h\nu^{1/2}$)
760	-0.00155	1.63158	--
759	-9.03E-04	1.63373	--
758	-8.08E-04	1.63588	--
757	-6.80E-04	1.63804	--
756	-4.79E-04	1.64021	--
755	-7.33E-04	1.64238	--
754	-7.33E-04	1.64456	--
753	-9.11E-04	1.64675	--
752	-9.71E-04	1.64894	--
751	-0.00107	1.65113	--
750	-0.00135	1.65333	--
749	-6.63E-04	1.65554	--
748	-7.16E-04	1.65775	--
747	-0.00127	1.65997	--
746	-6.91E-04	1.6622	--
745	-8.91E-04	1.66443	--
744	-7.37E-04	1.66667	--
743	-0.00122	1.66891	--
742	-0.00134	1.67116	--
741	-0.00162	1.67341	--
740	-7.66E-04	1.67568	--
739	-9.01E-04	1.67794	--
738	-0.00126	1.68022	--
737	-6.17E-04	1.6825	--
736	-9.06E-04	1.68478	--
735	-0.00142	1.68707	--
734	-0.00105	1.68937	--
733	-0.00112	1.69168	--
732	-8.83E-04	1.69399	--
731	-9.87E-04	1.69631	--
730	-0.00141	1.69863	--
729	-0.0011	1.70096	--
728	-0.00134	1.7033	--
727	-0.00121	1.70564	--
726	-9.83E-04	1.70799	--
725	-0.00159	1.71034	--
724	-0.00145	1.71271	--
723	-0.00115	1.71508	--
722	-0.00127	1.71745	--

Wavelength (nm)	Absorbance	Photon Energy (eV)	Relationship - Indirect ($\alpha h\nu^{1/2}$)
721	-0.00148	1.71983	--
720	-0.00116	1.72222	--
719	-0.00169	1.72462	--
718	-0.00161	1.72702	--
717	-0.00112	1.72943	--
716	-0.00133	1.73184	--
715	-0.00131	1.73427	--
714	-0.00176	1.73669	--
713	-0.00116	1.73913	--
712	-0.00162	1.74157	--
711	-0.00186	1.74402	--
710	-0.0015	1.74648	--
709	-0.00117	1.74894	--
708	-0.00137	1.75141	--
707	-0.00159	1.75389	--
706	-0.00147	1.75637	--
705	-0.00124	1.75887	--
704	-0.00126	1.76136	--
703	-0.00136	1.76387	--
702	-0.00178	1.76638	--
701	-0.00114	1.7689	--
700	-0.00162	1.77143	--
699	-0.00162	1.77396	--
698	-0.00149	1.7765	--
697	-0.00122	1.77905	--
696	-0.00159	1.78161	--
695	-0.00126	1.78417	--
694	-0.00144	1.78674	--
693	-0.00143	1.78932	--
692	-0.0018	1.79191	--
691	-0.00149	1.7945	--
690	-0.00139	1.7971	--
689	-0.0016	1.79971	--
688	-0.00149	1.80233	--
687	-0.00178	1.80495	--
686	-0.00179	1.80758	--
685	-0.00199	1.81022	--
684	-0.00157	1.81287	--
683	-0.00149	1.81552	--

Wavelength (nm)	Absorbance	Photon Energy (eV)	Relationship - Indirect ($\alpha h\nu^{1/2}$)
682	-0.0016	1.81818	--
681	-0.00178	1.82085	--
680	-0.00139	1.82353	--
679	-0.00185	1.82622	--
678	-0.00137	1.82891	--
677	-0.00196	1.83161	--
676	-0.00184	1.83432	--
675	-0.00129	1.83704	--
674	-0.00136	1.83976	--
673	-0.0017	1.8425	--
672	-0.00145	1.84524	--
671	-0.00161	1.84799	--
670	-0.00141	1.85075	--
669	-0.00171	1.85351	--
668	-0.00155	1.85629	--
667	-0.0014	1.85907	--
666	-0.0014	1.86186	--
665	-0.00173	1.86466	--
664	-0.0015	1.86747	--
663	-0.00175	1.87029	--
662	-0.00126	1.87311	--
661	-0.0013	1.87595	--
660	-0.00143	1.87879	--
659	-0.00146	1.88164	--
658	-0.00177	1.8845	--
657	-0.00177	1.88737	--
656	-0.00164	1.89024	--
655	-0.00193	1.89313	--
654	-0.00182	1.89602	--
653	-0.00191	1.89893	--
652	-0.00183	1.90184	--
651	-0.00189	1.90476	--
650	-0.00189	1.90769	--
649	-0.00189	1.91063	--
648	-0.00227	1.91358	--
647	-0.00196	1.91654	--
646	-0.0019	1.9195	--
645	-0.00178	1.92248	--
644	-0.00189	1.92547	--

Wavelength (nm)	Absorbance	Photon Energy (eV)	Relationship - Indirect ($\alpha h\nu^{1/2}$)
643	-0.00168	1.92846	--
642	-0.00171	1.93146	--
641	-0.00199	1.93448	--
640	-0.00174	1.9375	--
639	-0.00165	1.94053	--
638	-0.00159	1.94357	--
637	-0.00159	1.94662	--
636	-0.00145	1.94969	--
635	-0.00143	1.95276	--
634	-9.37E-04	1.95584	--
633	-0.00128	1.95893	--
632	-0.00105	1.96203	--
631	-8.00E-04	1.96513	--
630	-8.91E-05	1.96825	--
629	-1.98E-04	1.97138	--
628	4.43E-04	1.97452	0.02959
627	0.00112	1.97767	0.04707
626	0.00165	1.98083	0.05711
625	0.00189	1.984	0.06119
624	0.00324	1.98718	0.08028
623	0.00448	1.99037	0.09439
622	0.00519	1.99357	0.10177
621	0.00647	1.99678	0.11364
620	0.00783	2	0.12515
619	0.00908	2.00323	0.13488
618	0.00958	2.00647	0.13864
617	0.01014	2.00972	0.14276
616	0.01068	2.01299	0.14659
615	0.01073	2.01626	0.14707
614	0.01037	2.01954	0.14474
613	0.00966	2.02284	0.13977
612	0.00888	2.02614	0.13412
611	0.00782	2.02946	0.12598
610	0.00681	2.03279	0.11769
609	0.00573	2.03612	0.10805
608	0.00512	2.03947	0.10215
607	0.00417	2.04283	0.09235
606	0.00374	2.0462	0.08744
605	0.00327	2.04959	0.0819

Wavelength (nm)	Absorbance	Photon Energy (eV)	Relationship - Indirect ($\alpha h\nu^{1/2}$)
604	0.00308	2.05298	0.07951
603	0.00256	2.05638	0.07258
602	0.00237	2.0598	0.0699
601	0.00235	2.06323	0.06965
600	0.00183	2.06667	0.06145
599	0.00185	2.07012	0.06195
598	0.00206	2.07358	0.06539
597	0.00174	2.07705	0.06005
596	0.00183	2.08054	0.06178
595	0.00172	2.08403	0.0598
594	0.00158	2.08754	0.05751
593	0.00194	2.09106	0.06371
592	0.00195	2.09459	0.06385
591	0.0021	2.09814	0.06634
590	0.00265	2.10169	0.07466
589	0.00267	2.10526	0.07499
588	0.00362	2.10884	0.08739
587	0.00376	2.11244	0.08909
586	0.00433	2.11604	0.0957
585	0.00514	2.11966	0.10436
584	0.00572	2.12329	0.11017
583	0.00706	2.12693	0.12256
582	0.00835	2.13058	0.1334
581	0.00962	2.13425	0.14329
580	0.01156	2.13793	0.15718
579	0.01284	2.14162	0.16585
578	0.01494	2.14533	0.17906
577	0.01635	2.14905	0.18744
576	0.01822	2.15278	0.19803
575	0.01978	2.15652	0.20656
574	0.02059	2.16028	0.2109
573	0.02174	2.16405	0.21689
572	0.02153	2.16783	0.21604
571	0.02097	2.17163	0.21341
570	0.02056	2.17544	0.21149
569	0.01972	2.17926	0.20731
568	0.01954	2.1831	0.20656
567	0.01858	2.18695	0.20159
566	0.01718	2.19081	0.19402

Wavelength (nm)	Absorbance	Photon Energy (eV)	Relationship - Indirect ($\alpha h\nu^{1/2}$)
565	0.01633	2.19469	0.18932
564	0.01572	2.19858	0.18589
563	0.01453	2.20249	0.17887
562	0.01351	2.20641	0.17264
561	0.01279	2.21034	0.16813
560	0.01143	2.21429	0.15907
559	0.01088	2.21825	0.15535
558	0.01084	2.22222	0.15518
557	0.01069	2.22621	0.15423
556	0.01085	2.23022	0.15557
555	0.01094	2.23423	0.15637
554	0.01089	2.23827	0.15616
553	0.01097	2.24231	0.15684
552	0.01136	2.24638	0.15973
551	0.01094	2.25045	0.1569
550	0.0112	2.25455	0.15891
549	0.01113	2.25865	0.15852
548	0.01112	2.26277	0.15866
547	0.0107	2.26691	0.15573
546	0.01064	2.27106	0.15548
545	0.01004	2.27523	0.15115
544	0.00948	2.27941	0.14699
543	0.00942	2.28361	0.14667
542	0.00953	2.28782	0.14763
541	0.00922	2.29205	0.14538
540	0.00875	2.2963	0.14173
539	0.00953	2.30056	0.14809
538	0.00917	2.30483	0.14538
537	0.00947	2.30912	0.1479
536	0.00993	2.31343	0.15155
535	0.00995	2.31776	0.15186
534	0.01012	2.3221	0.15333
533	0.01065	2.32645	0.15739
532	0.01014	2.33083	0.1537
531	0.01037	2.33522	0.15565
530	0.01028	2.33962	0.15506
529	0.00983	2.34405	0.15183
528	0.01016	2.34848	0.15443
527	0.00926	2.35294	0.14759

Wavelength (nm)	Absorbance	Photon Energy (eV)	Relationship - Indirect ($\alpha h\nu^{1/2}$)
526	0.00907	2.35741	0.14622
525	0.00869	2.3619	0.14327
524	0.00875	2.36641	0.14387
523	0.00808	2.37094	0.13839
522	0.00767	2.37548	0.13494
521	0.00746	2.38004	0.13323
520	0.00692	2.38462	0.12845
519	0.00578	2.38921	0.11748
518	0.00612	2.39382	0.12107
517	0.006	2.39845	0.11997
516	0.00597	2.4031	0.11977
515	0.00549	2.40777	0.11496
514	0.00553	2.41245	0.11555
513	0.00525	2.41715	0.11264
512	0.00485	2.42188	0.10833
511	0.00451	2.42661	0.10466
510	0.00473	2.43137	0.1072
509	0.0046	2.43615	0.1059
508	0.00427	2.44094	0.10212
507	0.00442	2.44576	0.10397
506	0.00409	2.45059	0.10007
505	0.00396	2.45545	0.09856
504	0.004	2.46032	0.09923
503	0.00389	2.46521	0.09799
502	0.00398	2.47012	0.09917
501	0.00348	2.47505	0.09287
500	0.00364	2.48	0.09504
499	0.0039	2.48497	0.0984
498	0.00337	2.48996	0.09166
497	0.00379	2.49497	0.09727
496	0.00395	2.5	0.09934
495	0.00372	2.50505	0.0965
494	0.00381	2.51012	0.09779
493	0.00412	2.51521	0.10177
492	0.00367	2.52033	0.09621
491	0.00345	2.52546	0.09337
490	0.00358	2.53061	0.0952
489	0.00376	2.53579	0.09763
488	0.00373	2.54098	0.09737

Wavelength (nm)	Absorbance	Photon Energy (eV)	Relationship - Indirect ($\alpha h\nu^{1/2}$)
487	0.0038	2.5462	0.0984
486	0.00363	2.55144	0.09627
485	0.00404	2.5567	0.10164
484	0.00402	2.56198	0.10153
483	0.00432	2.56729	0.10536
482	0.00403	2.57261	0.10179
481	0.00479	2.57796	0.11112
480	0.00549	2.58333	0.11908
479	0.00604	2.58873	0.12503
478	0.00657	2.59414	0.13053
477	0.00768	2.59958	0.14127
476	0.00886	2.60504	0.15195
475	0.01033	2.61053	0.16421
474	0.01192	2.61603	0.17662
473	0.0138	2.62156	0.19019
472	0.01733	2.62712	0.21336
471	0.02019	2.6327	0.23055
470	0.0246	2.6383	0.25474
469	0.03011	2.64392	0.28215
468	0.03728	2.64957	0.31428
467	0.04654	2.65525	0.35154
466	0.0572	2.66094	0.39014
465	0.07012	2.66667	0.43241
464	0.08623	2.67241	0.48004
463	0.1059	2.67819	0.53256
462	0.12971	2.68398	0.59003
461	0.15677	2.6898	0.64938
460	0.18778	2.69565	0.71147
459	0.22238	2.70153	0.77509
458	0.2584	2.70742	0.83642
457	0.29553	2.71335	0.89547
456	0.33039	2.7193	0.94786
455	0.3602	2.72527	0.99079
454	0.3828	2.73128	1.02252
453	0.39558	2.73731	1.04059
452	0.39736	2.74336	1.04408
451	0.38799	2.74945	1.03284
450	0.37095	2.75556	1.01103
449	0.34718	2.76169	0.97919

Wavelength (nm)	Absorbance	Photon Energy (eV)	Relationship - Indirect ($\alpha h\nu^{1/2}$)
448	0.31963	2.76786	0.94059
447	0.29102	2.77405	0.8985
446	0.26286	2.78027	0.85488
445	0.23594	2.78652	0.81084
444	0.21009	2.79279	0.76599
443	0.18586	2.7991	0.72128
442	0.16394	2.80543	0.67818
441	0.14394	2.81179	0.63617
440	0.12529	2.81818	0.59421
439	0.10955	2.8246	0.55626
438	0.09691	2.83105	0.52378
437	0.08771	2.83753	0.49888
436	0.08081	2.84404	0.4794
435	0.07583	2.85057	0.46492
434	0.07322	2.85714	0.45737
433	0.0722	2.86374	0.4547
432	0.07299	2.87037	0.45772
431	0.07325	2.87703	0.45908
430	0.07425	2.88372	0.46273
429	0.07519	2.89044	0.4662
428	0.07615	2.8972	0.4697
427	0.07491	2.90398	0.4664
426	0.07379	2.9108	0.46346
425	0.07065	2.91765	0.45401
424	0.06694	2.92453	0.44245
423	0.06173	2.93144	0.42538
422	0.05762	2.93839	0.41148
421	0.05165	2.94537	0.39002
420	0.04759	2.95238	0.37483
419	0.04271	2.95943	0.35552
418	0.03852	2.96651	0.33806
417	0.03519	2.97362	0.3235
416	0.03197	2.98077	0.30869
415	0.02954	2.98795	0.29707
414	0.02851	2.99517	0.29224
413	0.02808	3.00242	0.29037
412	0.02774	3.00971	0.28897
411	0.02842	3.01703	0.29282
410	0.02896	3.02439	0.29595

Wavelength (nm)	Absorbance	Photon Energy (eV)	Relationship - Indirect ($\alpha h\nu^{1/2}$)
409	0.03034	3.03178	0.3033
408	0.03197	3.03922	0.31171
407	0.03273	3.04668	0.3158
406	0.03397	3.05419	0.32211
405	0.03517	3.06173	0.32816
404	0.03604	3.06931	0.33261
403	0.03582	3.07692	0.33201
402	0.03599	3.08458	0.33318
401	0.03727	3.09227	0.3395
400	0.0366	3.1	0.33683
399	0.03566	3.10777	0.3329
398	0.03427	3.11558	0.32678
397	0.03317	3.12343	0.32185
396	0.03367	3.13131	0.32472
395	0.03124	3.13924	0.31315
394	0.0293	3.14721	0.30369
393	0.02904	3.15522	0.30271
392	0.02794	3.16327	0.29729
391	0.02734	3.17136	0.29448
390	0.02511	3.17949	0.28254
389	0.02495	3.18766	0.28202
388	0.02406	3.19588	0.27731
387	0.02365	3.20413	0.2753
386	0.02242	3.21244	0.26834
385	0.02137	3.22078	0.26233
384	0.02061	3.22917	0.25798
383	0.01956	3.2376	0.25163
382	0.01871	3.24607	0.24646
381	0.01833	3.25459	0.24426
380	0.01769	3.26316	0.24028
379	0.01782	3.27177	0.24143
378	0.01738	3.28042	0.23876
377	0.01511	3.28912	0.22295
376	0.01686	3.29787	0.23582
375	0.01475	3.30667	0.22088
374	0.01432	3.31551	0.2179
373	0.01392	3.3244	0.2151
372	0.0145	3.33333	0.21986
371	0.01487	3.34232	0.22294

Wavelength (nm)	Absorbance	Photon Energy (eV)	Relationship - Indirect ($\alpha h\nu^{1/2}$)
370	0.01299	3.35135	0.20861
369	0.01384	3.36043	0.21562
368	0.01387	3.36957	0.21617
367	0.01276	3.37875	0.2076
366	0.01407	3.38798	0.21836
365	0.01285	3.39726	0.20894
364	0.01151	3.40659	0.19804
363	0.01347	3.41598	0.21449
362	0.01299	3.42541	0.21095
361	0.01321	3.4349	0.21301
360	0.01243	3.44444	0.20695
359	0.01212	3.45404	0.20457
358	0.0126	3.46369	0.20891
357	0.01141	3.47339	0.19912
356	0.01198	3.48315	0.20431
355	0.01306	3.49296	0.2136
354	0.01141	3.50282	0.19988
353	0.01231	3.51275	0.20794
352	0.01169	3.52273	0.20291
351	0.01257	3.53276	0.21072
350	0.01129	3.54286	0.19997

Table 2.22: Zn2vtBr Tauc Tables

Wavelength (nm)	Absorbance	Photon Energy (eV)	Relationship - Indirect ($\alpha h\nu^{1/2}$)
800	-1.58E-04	1.55	--
799	2.52E-04	1.55194	0.01978
798	-2.29E-04	1.55388	--
797	-3.70E-04	1.55583	--
796	-1.75E-04	1.55779	--
795	5.14E-04	1.55975	0.0283
794	-9.14E-04	1.56171	--
793	-4.33E-04	1.56368	--
792	2.73E-04	1.56566	0.02068
791	-2.53E-04	1.56764	--
790	-9.48E-04	1.56962	--
789	-1.22E-04	1.57161	--
788	-1.40E-04	1.5736	--

Wavelength (nm)	Absorbance	Photon Energy (eV)	Relationship - Indirect ($\alpha h\nu^{1/2}$)
787	-4.58E-04	1.5756	--
786	-4.26E-04	1.57761	--
785	-3.37E-04	1.57962	--
784	-7.98E-04	1.58163	--
783	-2.19E-04	1.58365	--
782	2.21E-05	1.58568	0.00593
781	-7.98E-04	1.58771	--
780	-0.00158	1.58974	--
779	-0.00101	1.59178	--
778	-8.93E-04	1.59383	--
777	-5.43E-04	1.59588	--
776	-6.18E-04	1.59794	--
775	-8.71E-04	1.6	--
774	-4.83E-04	1.60207	--
773	-8.17E-04	1.60414	--
772	-0.0017	1.60622	--
771	-0.00148	1.6083	--
770	-6.54E-04	1.61039	--
769	-7.73E-04	1.61248	--
768	-5.27E-04	1.61458	--
767	-0.00123	1.61669	--
766	-7.24E-04	1.6188	--
765	-0.00109	1.62092	--
764	-0.0014	1.62304	--
763	-0.00101	1.62516	--
762	-0.00171	1.6273	--
761	-0.00145	1.62943	--
760	-0.00188	1.63158	--
759	-0.00142	1.63373	--
758	-0.00143	1.63588	--
757	-9.32E-04	1.63804	--
756	-0.00124	1.64021	--
755	-0.00149	1.64238	--
754	-0.00154	1.64456	--
753	-0.00171	1.64675	--
752	-0.00165	1.64894	--
751	-0.00201	1.65113	--
750	-0.00233	1.65333	--
749	-0.00121	1.65554	--

Wavelength (nm)	Absorbance	Photon Energy (eV)	Relationship - Indirect ($\alpha h\nu^{1/2}$)
748	-0.00149	1.65775	--
747	-0.00208	1.65997	--
746	-0.00192	1.6622	--
745	-0.00166	1.66443	--
744	-0.00167	1.66667	--
743	-0.00197	1.66891	--
742	-0.00225	1.67116	--
741	-0.00232	1.67341	--
740	-0.00165	1.67568	--
739	-0.0018	1.67794	--
738	-0.00208	1.68022	--
737	-0.00169	1.6825	--
736	-0.00184	1.68478	--
735	-0.00224	1.68707	--
734	-0.00224	1.68937	--
733	-0.00267	1.69168	--
732	-0.00196	1.69399	--
731	-0.00191	1.69631	--
730	-0.00266	1.69863	--
729	-0.00221	1.70096	--
728	-0.00254	1.7033	--
727	-0.00251	1.70564	--
726	-0.00225	1.70799	--
725	-0.00292	1.71034	--
724	-0.00244	1.71271	--
723	-0.00226	1.71508	--
722	-0.00277	1.71745	--
721	-0.00283	1.71983	--
720	-0.00232	1.72222	--
719	-0.00299	1.72462	--
718	-0.00291	1.72702	--
717	-0.00229	1.72943	--
716	-0.00283	1.73184	--
715	-0.00297	1.73427	--
714	-0.00318	1.73669	--
713	-0.00279	1.73913	--
712	-0.00318	1.74157	--
711	-0.00334	1.74402	--
710	-0.00311	1.74648	--

Wavelength (nm)	Absorbance	Photon Energy (eV)	Relationship - Indirect ($\alpha h\nu^{1/2}$)
709	-0.00295	1.74894	--
708	-0.00296	1.75141	--
707	-0.0032	1.75389	--
706	-0.00286	1.75637	--
705	-0.00309	1.75887	--
704	-0.00306	1.76136	--
703	-0.00339	1.76387	--
702	-0.00358	1.76638	--
701	-0.00294	1.7689	--
700	-0.00307	1.77143	--
699	-0.00348	1.77396	--
698	-0.00348	1.7765	--
697	-0.00309	1.77905	--
696	-0.00325	1.78161	--
695	-0.00321	1.78417	--
694	-0.00317	1.78674	--
693	-0.00342	1.78932	--
692	-0.00374	1.79191	--
691	-0.00322	1.7945	--
690	-0.00332	1.7971	--
689	-0.00352	1.79971	--
688	-0.00356	1.80233	--
687	-0.00401	1.80495	--
686	-0.00389	1.80758	--
685	-0.00383	1.81022	--
684	-0.00376	1.81287	--
683	-0.00359	1.81552	--
682	-0.00356	1.81818	--
681	-0.00372	1.82085	--
680	-0.00368	1.82353	--
679	-0.00391	1.82622	--
678	-0.00343	1.82891	--
677	-0.00375	1.83161	--
676	-0.0038	1.83432	--
675	-0.00341	1.83704	--
674	-0.00367	1.83976	--
673	-0.00378	1.8425	--
672	-0.00381	1.84524	--
671	-0.00379	1.84799	--

Wavelength (nm)	Absorbance	Photon Energy (eV)	Relationship - Indirect ($\alpha h\nu^{1/2}$)
670	-0.00364	1.85075	--
669	-0.00405	1.85351	--
668	-0.00368	1.85629	--
667	-0.00379	1.85907	--
666	-0.00393	1.86186	--
665	-0.00391	1.86466	--
664	-0.00405	1.86747	--
663	-0.00453	1.87029	--
662	-0.00398	1.87311	--
661	-0.00411	1.87595	--
660	-0.00407	1.87879	--
659	-0.00414	1.88164	--
658	-0.0044	1.8845	--
657	-0.00437	1.88737	--
656	-0.00428	1.89024	--
655	-0.00421	1.89313	--
654	-0.00436	1.89602	--
653	-0.00456	1.89893	--
652	-0.00429	1.90184	--
651	-0.00457	1.90476	--
650	-0.00465	1.90769	--
649	-0.00435	1.91063	--
648	-0.00478	1.91358	--
647	-0.00452	1.91654	--
646	-0.0048	1.9195	--
645	-0.00447	1.92248	--
644	-0.00457	1.92547	--
643	-0.0045	1.92846	--
642	-0.00468	1.93146	--
641	-0.00511	1.93448	--
640	-0.00484	1.9375	--
639	-0.00481	1.94053	--
638	-0.00474	1.94357	--
637	-0.00467	1.94662	--
636	-0.00479	1.94969	--
635	-0.00512	1.95276	--
634	-0.00475	1.95584	--
633	-0.00505	1.95893	--
632	-0.00505	1.96203	--

Wavelength (nm)	Absorbance	Photon Energy (eV)	Relationship - Indirect ($\alpha h\nu^{1/2}$)
631	-0.00488	1.96513	--
630	-0.00466	1.96825	--
629	-0.00505	1.97138	--
628	-0.00483	1.97452	--
627	-0.0045	1.97767	--
626	-0.00462	1.98083	--
625	-0.00512	1.984	--
624	-0.00484	1.98718	--
623	-0.00435	1.99037	--
622	-0.0047	1.99357	--
621	-0.00456	1.99678	--
620	-0.00427	2	--
619	-0.00405	2.00323	--
618	-0.00421	2.00647	--
617	-0.00379	2.00972	--
616	-0.00333	2.01299	--
615	-0.00287	2.01626	--
614	-0.00269	2.01954	--
613	-0.00208	2.02284	--
612	-0.00161	2.02614	--
611	-9.10E-04	2.02946	--
610	-9.92E-05	2.03279	--
609	4.58E-04	2.03612	0.03054
608	0.00121	2.03947	0.04965
607	0.00167	2.04283	0.05834
606	0.00219	2.0462	0.06695
605	0.00269	2.04959	0.07425
604	0.00327	2.05298	0.08189
603	0.00287	2.05638	0.07677
602	0.00282	2.0598	0.07625
601	0.00256	2.06323	0.07266
600	0.00182	2.06667	0.0613
599	0.00155	2.07012	0.05672
598	0.00174	2.07358	0.06001
597	0.00137	2.07705	0.05337
596	0.00115	2.08054	0.0489
595	0.00105	2.08403	0.04681
594	6.78E-04	2.08754	0.03762
593	9.46E-04	2.09106	0.04448

Wavelength (nm)	Absorbance	Photon Energy (eV)	Relationship - Indirect ($\alpha h\nu^{1/2}$)
592	8.36E-04	2.09459	0.04186
591	0.00112	2.09814	0.04838
590	0.00126	2.10169	0.05155
589	0.00118	2.10526	0.04987
588	0.00197	2.10884	0.06445
587	0.00175	2.11244	0.06073
586	0.00202	2.11604	0.06535
585	0.00256	2.11966	0.07364
584	0.0024	2.12329	0.0714
583	0.00361	2.12693	0.08765
582	0.00444	2.13058	0.09727
581	0.00525	2.13425	0.10586
580	0.0065	2.13793	0.11787
579	0.00745	2.14162	0.12629
578	0.00899	2.14533	0.13884
577	0.00983	2.14905	0.14534
576	0.01186	2.15278	0.15979
575	0.0142	2.15652	0.175
574	0.01648	2.16028	0.18869
573	0.01948	2.16405	0.20533
572	0.02178	2.16783	0.2173
571	0.0245	2.17163	0.23066
570	0.02701	2.17544	0.24241
569	0.02954	2.17926	0.2537
568	0.03233	2.1831	0.26567
567	0.03391	2.18695	0.2723
566	0.0349	2.19081	0.2765
565	0.03551	2.19469	0.27918
564	0.03592	2.19858	0.281
563	0.03536	2.20249	0.27906
562	0.03472	2.20641	0.27679
561	0.03369	2.21034	0.27286
560	0.03155	2.21429	0.26431
559	0.02964	2.21825	0.2564
558	0.02789	2.22222	0.24897
557	0.0258	2.22621	0.23967
556	0.02423	2.23022	0.23246
555	0.0224	2.23423	0.22371
554	0.0205	2.23827	0.2142

Wavelength (nm)	Absorbance	Photon Energy (eV)	Relationship - Indirect ($\alpha h\nu^{1/2}$)
553	0.01891	2.24231	0.20591
552	0.01764	2.24638	0.19907
551	0.01608	2.25045	0.19026
550	0.01547	2.25455	0.18674
549	0.0142	2.25865	0.1791
548	0.01381	2.26277	0.17675
547	0.01296	2.26691	0.17141
546	0.01215	2.27106	0.16613
545	0.01095	2.27523	0.15787
544	0.00964	2.27941	0.14824
543	0.00866	2.28361	0.14065
542	0.00847	2.28782	0.13921
541	0.00672	2.29205	0.1241
540	0.00534	2.2963	0.11079
539	0.00491	2.30056	0.10625
538	0.00392	2.30483	0.0951
537	0.00327	2.30912	0.08687
536	0.00302	2.31343	0.08354
535	0.00239	2.31776	0.0745
534	0.00165	2.3221	0.06181
533	0.00196	2.32645	0.06755
532	0.00119	2.33083	0.05273
531	0.00166	2.33522	0.06233
530	0.0012	2.33962	0.05306
529	9.60E-04	2.34405	0.04744
528	0.00138	2.34848	0.05702
527	8.85E-04	2.35294	0.04564
526	0.00109	2.35741	0.05071
525	0.00112	2.3619	0.05145
524	0.0015	2.36641	0.05948
523	0.00156	2.37094	0.06088
522	0.00138	2.37548	0.0573
521	0.00155	2.38004	0.06065
520	0.00177	2.38462	0.065
519	8.70E-04	2.38921	0.04558
518	0.00173	2.39382	0.06438
517	0.00171	2.39845	0.06402
516	0.00187	2.4031	0.06709
515	0.00176	2.40777	0.06516

Wavelength (nm)	Absorbance	Photon Energy (eV)	Relationship - Indirect ($\alpha h\nu^{1/2}$)
514	0.00217	2.41245	0.07244
513	0.00214	2.41715	0.07194
512	0.00193	2.42188	0.06834
511	0.002	2.42661	0.06961
510	0.00228	2.43137	0.07442
509	0.00233	2.43615	0.07534
508	0.00227	2.44094	0.07451
507	0.00275	2.44576	0.08195
506	0.00252	2.45059	0.07862
505	0.00259	2.45545	0.07982
504	0.0029	2.46032	0.08446
503	0.003	2.46521	0.08598
502	0.00332	2.47012	0.0906
501	0.00311	2.47505	0.08776
500	0.00323	2.48	0.08948
499	0.00385	2.48497	0.09784
498	0.00367	2.48996	0.09556
497	0.004	2.49497	0.09993
496	0.00446	2.5	0.10554
495	0.0041	2.50505	0.10135
494	0.00435	2.51012	0.10451
493	0.00469	2.51521	0.10863
492	0.00438	2.52033	0.10501
491	0.0043	2.52546	0.10421
490	0.00461	2.53061	0.10796
489	0.00462	2.53579	0.10829
488	0.00467	2.54098	0.10893
487	0.00467	2.5462	0.10906
486	0.00426	2.55144	0.10426
485	0.00444	2.5567	0.1065
484	0.00421	2.56198	0.10389
483	0.00402	2.56729	0.10156
482	0.00353	2.57261	0.09535
481	0.00374	2.57796	0.09817
480	0.00351	2.58333	0.09522
479	0.00315	2.58873	0.09036
478	0.00326	2.59414	0.092
477	0.00308	2.59958	0.08942
476	0.0035	2.60504	0.09547

Wavelength (nm)	Absorbance	Photon Energy (eV)	Relationship - Indirect ($\alpha h\nu^{1/2}$)
475	0.00338	2.61053	0.09397
474	0.00312	2.61603	0.09041
473	0.00299	2.62156	0.08855
472	0.00379	2.62712	0.09972
471	0.00356	2.6327	0.0968
470	0.0041	2.6383	0.104
469	0.00482	2.64392	0.11286
468	0.00586	2.64957	0.12465
467	0.00785	2.65525	0.14438
466	0.00912	2.66094	0.15574
465	0.0112	2.66667	0.17282
464	0.01403	2.67241	0.19367
463	0.01817	2.67819	0.22058
462	0.02453	2.68398	0.25656
461	0.03212	2.6898	0.29395
460	0.04112	2.69565	0.33293
459	0.05405	2.70153	0.38211
458	0.07042	2.70742	0.43666
457	0.09065	2.71335	0.49595
456	0.11552	2.7193	0.56047
455	0.1456	2.72527	0.62993
454	0.18172	2.73128	0.70451
453	0.22355	2.73731	0.78225
452	0.2702	2.74336	0.86096
451	0.32022	2.74945	0.93831
450	0.37169	2.75556	1.01203
449	0.42425	2.76169	1.08242
448	0.47063	2.76786	1.14133
447	0.51073	2.77405	1.19029
446	0.54161	2.78027	1.22712
445	0.56112	2.78652	1.25043
444	0.56903	2.79279	1.26063
443	0.56482	2.7991	1.25737
442	0.55261	2.80543	1.24512
441	0.53188	2.81179	1.22292
440	0.50494	2.81818	1.1929
439	0.47303	2.8246	1.15591
438	0.43822	2.83105	1.11383
437	0.40171	2.83753	1.06764

Wavelength (nm)	Absorbance	Photon Energy (eV)	Relationship - Indirect ($\alpha h\nu^{1/2}$)
436	0.36388	2.84404	1.0173
435	0.32629	2.85057	0.96442
434	0.29198	2.85714	0.91337
433	0.26105	2.86374	0.86462
432	0.23501	2.87037	0.82132
431	0.21399	2.87703	0.78463
430	0.19838	2.88372	0.75636
429	0.18752	2.89044	0.73622
428	0.18005	2.8972	0.72226
427	0.17307	2.90398	0.70894
426	0.167	2.9108	0.69721
425	0.15974	2.91765	0.68269
424	0.15093	2.92453	0.66439
423	0.14017	2.93144	0.64101
422	0.13031	2.93839	0.6188
421	0.11805	2.94537	0.58965
420	0.10756	2.95238	0.56352
419	0.09715	2.95943	0.5362
418	0.08761	2.96651	0.50981
417	0.07926	2.97362	0.48548
416	0.07038	2.98077	0.45804
415	0.06249	2.98795	0.43212
414	0.05604	2.99517	0.40971
413	0.05005	3.00242	0.38765
412	0.04441	3.00971	0.3656
411	0.0397	3.01703	0.3461
410	0.03449	3.02439	0.32299
409	0.03091	3.03178	0.3061
408	0.02806	3.03922	0.29205
407	0.02477	3.04668	0.27469
406	0.02213	3.05419	0.25995
405	0.02036	3.06173	0.24968
404	0.01914	3.06931	0.24239
403	0.01605	3.07692	0.22222
402	0.01533	3.08458	0.21743
401	0.01494	3.09227	0.21495
400	0.01383	3.1	0.20707
399	0.0121	3.10777	0.19392
398	0.01093	3.11558	0.18457

Wavelength (nm)	Absorbance	Photon Energy (eV)	Relationship - Indirect ($\alpha h\nu^{1/2}$)
397	0.0108	3.12343	0.18366
396	0.01054	3.13131	0.1817
395	0.00905	3.13924	0.16852
394	0.00761	3.14721	0.15479
393	0.00772	3.15522	0.15606
392	0.00734	3.16327	0.15239
391	0.00746	3.17136	0.15379
390	0.00598	3.17949	0.13783
389	0.00638	3.18766	0.14256
388	0.0059	3.19588	0.13728
387	0.00611	3.20413	0.13996
386	0.00557	3.21244	0.13377
385	0.00512	3.22078	0.12837
384	0.00505	3.22917	0.12772
383	0.00459	3.2376	0.12192
382	0.0049	3.24607	0.12618
381	0.00539	3.25459	0.1324
380	0.00606	3.26316	0.14067
379	0.00522	3.27177	0.13074
378	0.00502	3.28042	0.12833
377	0.00356	3.28912	0.10826
376	0.00552	3.29787	0.1349
375	0.00418	3.30667	0.11756
374	0.00396	3.31551	0.11458
373	0.00441	3.3244	0.12103
372	0.00457	3.33333	0.12341
371	0.00572	3.34232	0.13831
370	0.0043	3.35135	0.12001
369	0.00495	3.36043	0.12895
368	0.00514	3.36957	0.13158
367	0.00429	3.37875	0.12036
366	0.00657	3.38798	0.14924
365	0.00521	3.39726	0.13301
364	0.00403	3.40659	0.11722
363	0.00598	3.41598	0.14296
362	0.00674	3.42541	0.152
361	0.00703	3.4349	0.15534
360	0.00678	3.44444	0.15279
359	0.00684	3.45404	0.15371

Wavelength (nm)	Absorbance	Photon Energy (eV)	Relationship - Indirect ($\alpha h\nu^{1/2}$)
358	0.00727	3.46369	0.15866
357	0.00624	3.47339	0.14717
356	0.00804	3.48315	0.16737
355	0.00888	3.49296	0.17615
354	0.00855	3.50282	0.17305
353	0.00795	3.51275	0.16716
352	0.0088	3.52273	0.17611
351	0.00895	3.53276	0.17779
350	0.00908	3.54286	0.17936

Table 2.23: ZnF2vtBr Tauc Tables

Wavelength (nm)	Absorbance	Photon Energy (eV)	Relationship - Indirect ($\alpha h\nu^{1/2}$)
800	-5.33E-04	1.55	--
799	-4.61E-04	1.55194	--
798	1.14E-04	1.55388	0.01333
797	-0.00108	1.55583	--
796	-5.16E-04	1.55779	--
795	-7.84E-04	1.55975	--
794	-0.00153	1.56171	--
793	-8.15E-04	1.56368	--
792	-3.23E-04	1.56566	--
791	-8.24E-04	1.56764	--
790	-9.41E-04	1.56962	--
789	-7.33E-04	1.57161	--
788	-9.59E-04	1.5736	--
787	-9.78E-04	1.5756	--
786	-0.00136	1.57761	--
785	-8.99E-04	1.57962	--
784	-0.00143	1.58163	--
783	-0.00135	1.58365	--
782	-5.29E-04	1.58568	--
781	-0.00141	1.58771	--
780	-0.00225	1.58974	--
779	-0.0017	1.59178	--
778	-0.0016	1.59383	--
777	-0.00145	1.59588	--
776	-0.0015	1.59794	--

Wavelength (nm)	Absorbance	Photon Energy (eV)	Relationship - Indirect ($\alpha h\nu^{1/2}$)
775	-0.00181	1.6	--
774	-0.00132	1.60207	--
773	-0.0019	1.60414	--
772	-0.00212	1.60622	--
771	-0.00245	1.6083	--
770	-0.00145	1.61039	--
769	-0.00169	1.61248	--
768	-0.0014	1.61458	--
767	-0.00176	1.61669	--
766	-0.00144	1.6188	--
765	-0.00161	1.62092	--
764	-0.00234	1.62304	--
763	-0.00197	1.62516	--
762	-0.00264	1.6273	--
761	-0.00278	1.62943	--
760	-0.00286	1.63158	--
759	-0.00231	1.63373	--
758	-0.00226	1.63588	--
757	-0.00204	1.63804	--
756	-0.00218	1.64021	--
755	-0.00255	1.64238	--
754	-0.00254	1.64456	--
753	-0.0025	1.64675	--
752	-0.00248	1.64894	--
751	-0.00258	1.65113	--
750	-0.00311	1.65333	--
749	-0.00249	1.65554	--
748	-0.00255	1.65775	--
747	-0.00318	1.65997	--
746	-0.00274	1.6622	--
745	-0.00266	1.66443	--
744	-0.00266	1.66667	--
743	-0.00315	1.66891	--
742	-0.00312	1.67116	--
741	-0.00334	1.67341	--
740	-0.00309	1.67568	--
739	-0.00327	1.67794	--
738	-0.00338	1.68022	--
737	-0.0033	1.6825	--

Wavelength (nm)	Absorbance	Photon Energy (eV)	Relationship - Indirect ($\alpha h\nu^{1/2}$)
736	-0.00304	1.68478	--
735	-0.00358	1.68707	--
734	-0.00328	1.68937	--
733	-0.00357	1.69168	--
732	-0.00353	1.69399	--
731	-0.00346	1.69631	--
730	-0.00396	1.69863	--
729	-0.00365	1.70096	--
728	-0.00379	1.7033	--
727	-0.00389	1.70564	--
726	-0.0036	1.70799	--
725	-0.00408	1.71034	--
724	-0.00407	1.71271	--
723	-0.0037	1.71508	--
722	-0.00407	1.71745	--
721	-0.00411	1.71983	--
720	-0.00411	1.72222	--
719	-0.00453	1.72462	--
718	-0.00435	1.72702	--
717	-0.00377	1.72943	--
716	-0.00455	1.73184	--
715	-0.00419	1.73427	--
714	-0.00454	1.73669	--
713	-0.00437	1.73913	--
712	-0.00455	1.74157	--
711	-0.00476	1.74402	--
710	-0.0048	1.74648	--
709	-0.00429	1.74894	--
708	-0.00454	1.75141	--
707	-0.00469	1.75389	--
706	-0.00457	1.75637	--
705	-0.00455	1.75887	--
704	-0.00457	1.76136	--
703	-0.00469	1.76387	--
702	-0.00503	1.76638	--
701	-0.00452	1.7689	--
700	-0.00458	1.77143	--
699	-0.00487	1.77396	--
698	-0.00474	1.7765	--

Wavelength (nm)	Absorbance	Photon Energy (eV)	Relationship - Indirect ($\alpha h\nu^{1/2}$)
697	-0.00477	1.77905	--
696	-0.00486	1.78161	--
695	-0.00482	1.78417	--
694	-0.0048	1.78674	--
693	-0.00521	1.78932	--
692	-0.00521	1.79191	--
691	-0.00507	1.7945	--
690	-0.00498	1.7971	--
689	-0.00528	1.79971	--
688	-0.0052	1.80233	--
687	-0.00561	1.80495	--
686	-0.0056	1.80758	--
685	-0.00571	1.81022	--
684	-0.00533	1.81287	--
683	-0.00516	1.81552	--
682	-0.00541	1.81818	--
681	-0.00567	1.82085	--
680	-0.00551	1.82353	--
679	-0.00566	1.82622	--
678	-0.00535	1.82891	--
677	-0.00564	1.83161	--
676	-0.00583	1.83432	--
675	-0.00527	1.83704	--
674	-0.00548	1.83976	--
673	-0.00581	1.8425	--
672	-0.00561	1.84524	--
671	-0.00589	1.84799	--
670	-0.0058	1.85075	--
669	-0.00607	1.85351	--
668	-0.00591	1.85629	--
667	-0.00573	1.85907	--
666	-0.00602	1.86186	--
665	-0.00602	1.86466	--
664	-0.00621	1.86747	--
663	-0.00652	1.87029	--
662	-0.00602	1.87311	--
661	-0.00623	1.87595	--
660	-0.0063	1.87879	--
659	-0.00624	1.88164	--

Wavelength (nm)	Absorbance	Photon Energy (eV)	Relationship - Indirect ($\alpha h\nu^{1/2}$)
658	-0.0065	1.8845	--
657	-0.00669	1.88737	--
656	-0.00673	1.89024	--
655	-0.0067	1.89313	--
654	-0.00665	1.89602	--
653	-0.0068	1.89893	--
652	-0.00689	1.90184	--
651	-0.00678	1.90476	--
650	-0.00702	1.90769	--
649	-0.00681	1.91063	--
648	-0.00728	1.91358	--
647	-0.00692	1.91654	--
646	-0.00699	1.9195	--
645	-0.00697	1.92248	--
644	-0.00708	1.92547	--
643	-0.00703	1.92846	--
642	-0.00706	1.93146	--
641	-0.00737	1.93448	--
640	-0.00717	1.9375	--
639	-0.00706	1.94053	--
638	-0.00697	1.94357	--
637	-0.00674	1.94662	--
636	-0.00667	1.94969	--
635	-0.00686	1.95276	--
634	-0.00631	1.95584	--
633	-0.00653	1.95893	--
632	-0.00625	1.96203	--
631	-0.00593	1.96513	--
630	-0.00499	1.96825	--
629	-0.00496	1.97138	--
628	-0.00402	1.97452	--
627	-0.00283	1.97767	--
626	-0.00203	1.98083	--
625	-0.00123	1.984	--
624	2.94E-04	1.98718	0.02419
623	0.00212	1.99037	0.06496
622	0.00328	1.99357	0.08082
621	0.00487	1.99678	0.09864
620	0.00646	2	0.11371

Wavelength (nm)	Absorbance	Photon Energy (eV)	Relationship - Indirect ($\alpha h\nu^{1/2}$)
619	0.00779	2.00323	0.12495
618	0.00823	2.00647	0.12854
617	0.00882	2.00972	0.13313
616	0.00875	2.01299	0.13273
615	0.00831	2.01626	0.12945
614	0.0072	2.01954	0.12056
613	0.00584	2.02284	0.10872
612	0.00461	2.02614	0.0966
611	0.00301	2.02946	0.07821
610	0.00176	2.03279	0.0598
609	5.71E-04	2.03612	0.03411
608	-2.26E-04	2.03947	--
607	-0.0011	2.04283	--
606	-0.00163	2.0462	--
605	-0.00204	2.04959	--
604	-0.00202	2.05298	--
603	-0.00247	2.05638	--
602	-0.00239	2.0598	--
601	-0.00212	2.06323	--
600	-0.00249	2.06667	--
599	-0.00237	2.07012	--
598	-0.00212	2.07358	--
597	-0.00209	2.07705	--
596	-0.0016	2.08054	--
595	-0.00165	2.08403	--
594	-0.0014	2.08754	--
593	-8.67E-04	2.09106	--
592	-6.63E-04	2.09459	--
591	1.70E-04	2.09814	0.01889
590	0.00112	2.10169	0.04851
589	0.00169	2.10526	0.05959
588	0.00339	2.10884	0.08458
587	0.00418	2.11244	0.09393
586	0.0059	2.11604	0.11174
585	0.00737	2.11966	0.12495
584	0.00919	2.12329	0.13966
583	0.01164	2.12693	0.15734
582	0.01421	2.13058	0.17401
581	0.01692	2.13425	0.19

Wavelength (nm)	Absorbance	Photon Energy (eV)	Relationship - Indirect ($\alpha h\nu^{1/2}$)
580	0.02015	2.13793	0.20757
579	0.02287	2.14162	0.22132
578	0.02572	2.14533	0.23488
577	0.0275	2.14905	0.24312
576	0.0295	2.15278	0.252
575	0.03102	2.15652	0.25866
574	0.03137	2.16028	0.26032
573	0.03163	2.16405	0.26163
572	0.03039	2.16783	0.25665
571	0.02887	2.17163	0.25039
570	0.02712	2.17544	0.24289
569	0.02562	2.17926	0.23629
568	0.02455	2.1831	0.23152
567	0.02247	2.18695	0.2217
566	0.02051	2.19081	0.21199
565	0.01854	2.19469	0.20173
564	0.01691	2.19858	0.19284
563	0.015	2.20249	0.18178
562	0.01363	2.20641	0.17343
561	0.01273	2.21034	0.16776
560	0.01101	2.21429	0.15615
559	0.01026	2.21825	0.15087
558	0.01016	2.22222	0.15024
557	0.00982	2.22621	0.14786
556	0.00988	2.23022	0.14844
555	0.00984	2.23423	0.14824
554	0.00969	2.23827	0.14729
553	0.00995	2.24231	0.14939
552	0.00948	2.24638	0.14596
551	0.00873	2.25045	0.1402
550	0.00852	2.25455	0.13864
549	0.00771	2.25865	0.13196
548	0.00725	2.26277	0.12804
547	0.00622	2.26691	0.11872
546	0.00575	2.27106	0.11429
545	0.00435	2.27523	0.09948
544	0.00364	2.27941	0.09106
543	0.00283	2.28361	0.08039
542	0.00265	2.28782	0.07787

Wavelength (nm)	Absorbance	Photon Energy (eV)	Relationship - Indirect ($\alpha h\nu^{1/2}$)
541	0.00186	2.29205	0.06537
540	0.00133	2.2963	0.05527
539	0.0013	2.30056	0.05464
538	8.97E-04	2.30483	0.04546
537	7.70E-04	2.30912	0.04216
536	8.06E-04	2.31343	0.04317
535	7.52E-04	2.31776	0.04175
534	3.72E-04	2.3221	0.02941
533	5.19E-04	2.32645	0.03474
532	2.62E-04	2.33083	0.02472
531	3.43E-04	2.33522	0.0283
530	-2.98E-04	2.33962	--
529	-6.22E-04	2.34405	--
528	-2.61E-04	2.34848	--
527	-6.72E-04	2.35294	--
526	-9.56E-04	2.35741	--
525	-8.40E-04	2.3619	--
524	-5.03E-04	2.36641	--
523	-6.62E-04	2.37094	--
522	-4.79E-04	2.37548	--
521	-5.75E-04	2.38004	--
520	-5.35E-04	2.38462	--
519	-0.00115	2.38921	--
518	-3.28E-04	2.39382	--
517	-9.65E-05	2.39845	--
516	4.38E-04	2.4031	0.03243
515	8.07E-05	2.40777	0.01394
514	6.87E-04	2.41245	0.04071
513	9.23E-04	2.41715	0.04723
512	3.83E-04	2.42188	0.03044
511	7.33E-04	2.42661	0.04217
510	0.00121	2.43137	0.05417
509	0.00102	2.43615	0.04989
508	0.0011	2.44094	0.05189
507	0.00163	2.44576	0.06323
506	0.00123	2.45059	0.05484
505	0.00128	2.45545	0.05613
504	0.00149	2.46032	0.06052
503	0.00161	2.46521	0.06292

Wavelength (nm)	Absorbance	Photon Energy (eV)	Relationship - Indirect ($\alpha h\nu^{1/2}$)
502	0.00186	2.47012	0.06783
501	0.00174	2.47505	0.06554
500	0.0018	2.48	0.06675
499	0.00219	2.48497	0.07381
498	0.0019	2.48996	0.06873
497	0.00234	2.49497	0.07634
496	0.00262	2.5	0.08091
495	0.00227	2.50505	0.07538
494	0.00241	2.51012	0.07781
493	0.00262	2.51521	0.08125
492	0.00233	2.52033	0.0767
491	0.00249	2.52546	0.07937
490	0.00248	2.53061	0.07929
489	0.00269	2.53579	0.08257
488	0.00268	2.54098	0.08255
487	0.00278	2.5462	0.08407
486	0.00272	2.55144	0.08334
485	0.00316	2.5567	0.08993
484	0.00327	2.56198	0.09158
483	0.00378	2.56729	0.09855
482	0.00379	2.57261	0.09879
481	0.0048	2.57796	0.1112
480	0.00579	2.58333	0.1223
479	0.00672	2.58873	0.1319
478	0.00791	2.59414	0.14327
477	0.00988	2.59958	0.16028
476	0.01194	2.60504	0.17633
475	0.01528	2.61053	0.19972
474	0.01894	2.61603	0.22261
473	0.02355	2.62156	0.24846
472	0.03093	2.62712	0.28507
471	0.03872	2.6327	0.31928
470	0.04985	2.6383	0.36264
469	0.06345	2.64392	0.40959
468	0.08087	2.64957	0.46289
467	0.10286	2.65525	0.52262
466	0.12864	2.66094	0.58507
465	0.1599	2.66667	0.65299
464	0.19681	2.67241	0.72523

Wavelength (nm)	Absorbance	Photon Energy (eV)	Relationship - Indirect ($\alpha h\nu^{1/2}$)
463	0.23856	2.67819	0.79931
462	0.28639	2.68398	0.87674
461	0.33695	2.6898	0.95202
460	0.38927	2.69565	1.02437
459	0.43944	2.70153	1.08957
458	0.48379	2.70742	1.14447
457	0.51813	2.71335	1.18569
456	0.53824	2.7193	1.20981
455	0.54197	2.72527	1.21533
454	0.52921	2.73128	1.20226
453	0.50359	2.73731	1.17409
452	0.46833	2.74336	1.13349
451	0.428	2.74945	1.08478
450	0.3887	2.75556	1.03493
449	0.3499	2.76169	0.98301
448	0.31394	2.76786	0.93217
447	0.27975	2.77405	0.88094
446	0.24724	2.78027	0.82909
445	0.21684	2.78652	0.77731
444	0.18767	2.79279	0.72397
443	0.16129	2.7991	0.67192
442	0.13918	2.80543	0.62487
441	0.12086	2.81179	0.58295
440	0.10627	2.81818	0.54725
439	0.09576	2.8246	0.52008
438	0.08894	2.83105	0.5018
437	0.08558	2.83753	0.49279
436	0.08492	2.84404	0.49145
435	0.08548	2.85057	0.49362
434	0.0881	2.85714	0.50173
433	0.09165	2.86374	0.51231
432	0.09641	2.87037	0.52605
431	0.09938	2.87703	0.53471
430	0.1016	2.88372	0.54128
429	0.10284	2.89044	0.5452
428	0.10224	2.8972	0.54425
427	0.09853	2.90398	0.53492
426	0.09383	2.9108	0.52262
425	0.08713	2.91765	0.50419

Wavelength (nm)	Absorbance	Photon Energy (eV)	Relationship - Indirect ($\alpha h\nu^{1/2}$)
424	0.07923	2.92453	0.48137
423	0.06988	2.93144	0.45259
422	0.06281	2.93839	0.42959
421	0.05386	2.94537	0.39828
420	0.04759	2.95238	0.37486
419	0.04082	2.95943	0.34755
418	0.03536	2.96651	0.32389
417	0.03166	2.97362	0.30682
416	0.02792	2.98077	0.2885
415	0.02626	2.98795	0.28013
414	0.02531	2.99517	0.27535
413	0.02557	3.00242	0.27709
412	0.02599	3.00971	0.27968
411	0.02642	3.01703	0.2823
410	0.02672	3.02439	0.28428
409	0.02809	3.03178	0.29183
408	0.02832	3.03922	0.29337
407	0.02881	3.04668	0.29627
406	0.02829	3.05419	0.29396
405	0.02843	3.06173	0.29504
404	0.02827	3.06931	0.29458
403	0.02652	3.07692	0.28563
402	0.02675	3.08458	0.28725
401	0.02717	3.09227	0.28985
400	0.02672	3.1	0.2878
399	0.02562	3.10777	0.28219
398	0.0246	3.11558	0.27687
397	0.02451	3.12343	0.2767
396	0.02562	3.13131	0.28325
395	0.02459	3.13924	0.27782
394	0.0236	3.14721	0.27251
393	0.02374	3.15522	0.27371
392	0.023	3.16327	0.26974
391	0.02273	3.17136	0.26848
390	0.02121	3.17949	0.25968
389	0.02135	3.18766	0.26089
388	0.0202	3.19588	0.25407
387	0.01994	3.20413	0.25279
386	0.01914	3.21244	0.24797

Wavelength (nm)	Absorbance	Photon Energy (eV)	Relationship - Indirect ($\alpha h\nu^{1/2}$)
385	0.01762	3.22078	0.23825
384	0.01708	3.22917	0.23488
383	0.01587	3.2376	0.22665
382	0.01409	3.24607	0.2139
381	0.01329	3.25459	0.20795
380	0.01355	3.26316	0.21024
379	0.01321	3.27177	0.20787
378	0.01253	3.28042	0.20277
377	0.00985	3.28912	0.17999
376	0.01134	3.29787	0.19337
375	0.00895	3.30667	0.17199
374	0.00873	3.31551	0.1701
373	0.00707	3.3244	0.15331
372	0.00752	3.33333	0.15834
371	0.00792	3.34232	0.16274
370	0.00573	3.35135	0.13858
369	0.00584	3.36043	0.14004
368	0.00604	3.36957	0.14272
367	0.004	3.37875	0.1163
366	0.00544	3.38798	0.13578
365	0.00401	3.39726	0.11678
364	0.00215	3.40659	0.08566
363	0.00369	3.41598	0.11227
362	0.00326	3.42541	0.10574
361	0.0028	3.4349	0.09808
360	0.00193	3.44444	0.08162
359	0.002	3.45404	0.08303
358	0.00179	3.46369	0.07883
357	7.93E-04	3.47339	0.05248
356	0.00158	3.48315	0.07427
355	0.00245	3.49296	0.09258
354	0.0012	3.50282	0.06495
353	0.00158	3.51275	0.07444
352	0.00127	3.52273	0.06693
351	0.00203	3.53276	0.08477
350	8.60E-04	3.54286	0.05519

2.8.6 NICS-scan Distance Tables

Table 2.24: 2VT and F2VT NICS Table

Distance (Å)	2VT			F2VT		
	PiZZ	NCS	SOM	PiZZ	NCS	SOM
-1.4	-5.9719	-6.0017	-5.8219	-5.3024	-5.2644	-5.1524
0	-7.7539	-7.754	-7.4656	-7.1434	-7.0926	-6.8551
1.4	-6.5058	-6.5552	-5.6541	-6.4858	-6.4392	-5.6341
2.6	-0.1843	-0.4068	-0.2518	-5.5351	-5.4918	-5.6026
3.8	10.7281	10.3149	10.9171	-3.632	-3.585	-3.443
5	6.5101	6.2417	6.3344	-0.9617	-0.9214	-1.1374

Table 2.25: 3VT and F3VT NICS Table

Distance (Å)	3VT			F3VT		
	PiZZ	NCS	SOM	PiZZ	NCS	SOM
-1.4	-5.5615	-5.483	-4.607	-5.062	-5.0229	-4.9439
0	-7.0752	-6.9433	-5.5549	-6.6493	-6.4144	-6.3348
1.4	-5.097	-4.9445	-2.7262	-5.2401	-5.1906	-4.3327
2.6	3.274	3.0458	0.1963	-3.7837	-3.7411	-3.39
3.8	18.0796	17.1049	0.6834	-2.5004	-2.4668	-1.5997
5	11.255	10.7187	20.9094	-0.6748	-0.653	-0.2075

Table 2.26: 2VTP and F2VTP NICS Tables

Distance (Å)	2VTP			F2VTP		
	PiZZ	NCS	SOM	PiZZ	NCS	SOM
-4.4	-5.68	-5.6801	-5.7596	-7.1969	-7.1969	-6.5609
-3.8	-12.848	-12.848	-12.863	-11.916	-11.916	-10.691
-2.8	-22.563	-22.566	-22.579	-23.385	-23.385	-21.646
0	-28.083	-28.085	-28.556	-31.514	-31.514	-32.179
2.8	-14.367	-14.372	-14.186	-14.064	-14.064	-11.367
3.8	-8.286	-8.2903	-8.0431	-0.4751	-0.4751	0.3005
4.4	-6.2005	-6.2023	-5.9833	-13.66	-10.461	-11.564
5.8	-4.2231	-4.2224	-4.1421	-15.917	-15.917	-15.439
7	-2.2708	-2.2689	-2.2916	-15.16	-15.16	-14.702
8.2	-1.5158	-1.5141	-1.5978	-11.902	-11.902	-11.781
9.2	-1.2482	-1.2473	-1.3181	-9.4029	-9.4029	-9.3645
10	-0.5768	-0.5765	-0.6122	-5.4845	-5.4845	-5.5201

Table 2.27: 3VTP and F3VTP NICS Tables

Distance (Å)	3VTP			F3VTP		
	PiZZ	NCS	SOM	PiZZ	NCS	SOM
-4.4	-3.475	-3.4745	-3.2452	-7.5459	-5.9407	-7.2562
-3.8	-9.0515	-9.0476	-8.5307	-13.23	-11.56	-12.64
-2.8	-17.83	-17.83	-17.191	-23.763	-20.681	-23.044
0	-27.23	-27.233	-26.933	-29.36	-29.41	-28.919
2.8	-17.996	-18.002	-15.972	-18.576	-18.561	-16.297
3.8	-4.4244	-4.4302	-2.8225	-9.7091	-9.6938	-7.8185
4.4	-2.6395	-2.6409	-2.0126	-7.6563	-7.6381	-6.6764
5.8	-1.9334	-1.9375	-1.9252	-9.1846	-9.1612	-8.7318
7	-3.1603	-3.16	-3.9376	-8.2754	-8.2473	-8.3549
8.2	-3.4337	-3.4307	-5.4972	-7.0815	-7.0512	-7.8199
9.2	-4.7227	-4.722	-7.6408	-5.8732	-5.8437	-6.7778
10	-4.1447	-4.1459	-8.1843	-4.4003	-4.3725	-5.2029

Table 2.28: 2vtBr and F2VTP NICS Tables

Distance (Å)	2vtBr			F2vtBr		
	PiZZ	NCS	SOM	PiZZ	NCS	SOM
-4.4	-1.5882	-1.5889	-1.6634	-3.0917	-3.0502	-1.9043
-3.8	-3.7346	-3.7342	-3.7148	-4.9296	-4.8819	-2.8278
-2.8	-6.5799	-6.5796	-6.5889	-8.9729	-8.9287	-6.3158
0	-9.1656	-9.1662	-9.6267	-11.199	-11.241	-13.482
2.8	-4.2646	-4.2677	-4.0705	-7.5776	-7.5519	-6.2528
3.8	-2.0587	-2.0618	-1.8063	-1.4357	-1.4095	-1.0629
4.4	-1.308	-1.3104	-1.0877	-5.5315	-5.4981	-2.9339
5.8	-1.2373	-1.238	-1.1713	-6.3337	-6.2976	-5.5133
7	-0.6986	-0.6987	-0.7581	-5.3977	-5.3652	-5.2391
8.2	-0.2109	-0.2109	-0.3576	-4.1915	-4.1624	-4.6058
9.2	-0.0623	-0.0624	-0.2076	-3.251	-3.2261	-3.867
10	-0.0547	-0.0042	-0.1559	-2.0412	-2.0209	-2.7301

Table 2.29: Zn2VTP NICS Table

Distance (Å)	Zn2VTP		
	PiZZ	NCS	SOM
-4.4	-2.7019	-2.671	-1.0202
-3.8	-4.9265	-4.8959	-5.7402
-2.8	-7.2379	-7.2015	-12.8655
0	-9.4487	-9.4081	-14.8383
2.8	-3.7428	-3.7162	-11.0281
3.8	-2.145	-2.4092	-6.5767
4.4	-1.542	-1.5161	-3.4579
5.8	-1.2802	-1.2523	-0.896
7	-0.5885	-0.5653	0.0128
8.2	-0.1244	-0.114	0.3175
9.2	-0.0011	-0.0015	0.3447
10	0.046	0.0446	0.3377

Table 2.30: Zn3VTP and ZnF3VTP NICS Tables

Distance (Å)	Zn3VTP			ZnF3VTP		
	PiZZ	NCS	SOM	PiZZ	NCS	SOM
-4.4	-2.0751	-2.0503	-1.7602	-2.8053	-2.7691	-2.5133
-3.8	-4.3754	-4.3439	-3.2226	-5.1764	-5.1403	-3.9866
-2.8	-6.6025	-6.5642	-3.7609	-7.398	-7.3619	-4.3643
0	-9.7355	-9.6895	-4.6576	-10.4846	-10.4448	-4.8649
2.8	-4.2661	-4.2257	-1.0173	-5.0754	-5.0463	-2.0204
3.8	-0.8708	-0.8291	2.0037	-2.8817	-2.854	-0.2249
4.4	-0.6275	-0.5803	1.3579	-2.3042	-2.2757	-0.6621
5.8	-0.707	-0.6551	0.152	-3.1176	-3.0852	-2.5228
7	-0.9687	-0.9223	-1.0243	-2.8929	-2.8607	-2.9156
8.2	-0.7689	-0.7372	-1.6447	-2.4095	-2.379	-3.0967
9.2	-0.5237	-0.5178	-0.3625	-1.9549	-1.9272	-2.8073
10	-0.2666	-0.2816	-0.2495	-1.444	-1.4194	-2.1989

Table 2.31: Zn2vtBr and ZnF2vtBr NICS Tables

Distance (Å)	Zn2vtBr			ZnF2vtBr		
	PiZZ	NCS	SOM	PiZZ	NCS	SOM
-4.4	-2.1659	-2.1447	-0.7305	-3.9852	-3.9454	-3.7574
-3.8	-4.3522	-4.3243	-4.9137	-6.5112	-6.4679	-5.9174
-2.8	-6.6895	-6.6558	-11.1453	-9.456	-9.4188	-7.6074
0	-9.4638	-9.4249	-13.2707	-13.508	-13.4622	-8.9892
2.8	-4.4299	-4.4059	-11.0622	-7.1643	-7.1287	-4.4334
3.8	-2.5343	-2.5136	-6.6798	-3.023	-2.9888	-3.7431
4.4	-1.7173	-1.6963	-3.614	-6.7638	-6.7253	-5.862
5.8	-1.435	-1.4117	-1.2115	-6.904	-6.8658	-6.832
7	-0.7835	-0.7641	-0.3449	-5.712	-5.6785	-5.8123
8.2	-0.228	-0.22	0.0606	-4.2518	-4.2219	-4.7803
9.2	-0.0551	-0.0576	0.149	-3.2712	-3.2456	-3.9601
10	0.019	0.014	0.1945	-2.0371	-2.0161	-2.7825

2.8.7 X-ray Crystallography

Table 2.32: 2VTP Crystal Data and Structure Refinement

Identification code	str0182lt100kcu
Empirical formula	C68 H60 N4 S2
Formula weight	997.32
Temperature	100.00(10) K
Wavelength	1.54184 Å
Crystal system	Monoclinic
Space group	C 1 2/c 1
Unit cell dimensions	a = 29.5314(3) Å a= 90°.
	b = 18.04690(10) Å b= 118.9270(10)°.
	c = 12.62760(10) Å g = 90°.
Volume	5890.24(10) $Å^3$
Z	4
Density (calculated)	1.125 Mg/m^3
Absorption coefficient	1.140 mm^{-1}
F(000)	2112
Crystal size	0.078 x 0.061 x 0.036 mm^3
Theta range for data collection	2.986 to 74.494°.
Index ranges	-36<=h<=35, -17<=k<=22, -15<=l<=15
Reflections collected	31680
Independent reflections	6006 [R(int) = 0.0224]
Completeness to theta = 67.684°	100.0 %
Absorption correction	Gaussian

Max. and min. transmission 1.000 and 0.944

Refinement method Full-matrix least-squares on F^2

Data / restraints / parameters 6006 / 10 / 362

Goodness-of-fit on F^2 1.020

Final R indices [I>2sigma(I)] R1 = 0.0524, wR2 = 0.1428

R indices (all data) R1 = 0.0544, wR2 = 0.1448

Extinction coefficient n/a

Largest diff. peak and hole 1.043 and -0.626 e.$Å^{-3}$

Table 2.33 3VTP Crystal Data and Structure Refinement

Identification code str0349lt200kcu65mm

Empirical formula C68 H60 N4 S2

Formula weight 997.32

Temperature 199.99(10) K

Wavelength 1.54184 Å

Crystal system Monoclinic

Space group I 1 2/a 1

Unit cell dimensions a = 12.54270(10) Å □ 90°.

b = 18.1602(2) Å □ 93.3200(10)°.

c = 26.3580(3) Å □ 90°.

Volume 5993.69(11) $Å^3$

Z 4

Density (calculated) 1.105 Mg/m^3

Absorption coefficient 1.120 mm^{-1}

F(000) 2112

Crystal size 0.09 x 0.03 x 0.02 mm^3

Theta range for data collection 2.957 to 78.989°.

Index ranges -7<=h<=15, -21<=k<=22, -33<=l<=33

Reflections collected 19279

Independent reflections 6326 [R(int) = 0.0178]

Completeness to theta = 67.684° 99.4 %

Absorption correction Semi-empirical from equivalents

Max. and min. transmission 1.00000 and 0.60196

Refinement method Full-matrix least-squares on F^2

Data / restraints / parameters 6326 / 77 / 355

Goodness-of-fit on F^2 1.059

Final R indices [I>2sigma(I)] R1 = 0.0595, wR2 = 0.1785

R indices (all data) R1 = 0.0641, wR2 = 0.1848

Extinction coefficient n/a

Largest diff. peak and hole 0.896 and -0.267 e.$Å^{-3}$

2.9 References

[1] a) A. V. Cheprakov, in Handbooks of Porphyrin Science, Vol. 13 (Eds: K. M. Kadish, K. M. Smith, R. Guilard), World Scientific Publ., Singapore, **2011**, *The Synthesis of pi-Extended Porphyrins,* pages 1-149; b) Szliszka, E.; Czuba, Z. P.; Domino, M.; Mazur, B.; Zydowicz, G.; Krol, W. *Molecules* **2009**, *14* (2), 738–754.; c) Solonenko, D.; Gasiorowski, J.; Apaydin, D.; Oppelt, K.; Nuss, M.; Keawsongsaeng, W.; Salvan, G.; Hingerl, K.; Serdar Sariciftci, N.; Zahn, D. R. T.; Thamyongkit, P. *Journal of Physical Chemistry C* **2017**, *121*

(39); d) Borisov, S. M.; Nuss, G.; Klimant, I. *Anal Chem* **2008**, *80* (24), 9435–9442; e) Yang, X. Q.; Duan, J. J.; Su, J.; Peng, X.; Yi, Z. Y.; Li, R. N.; Lu, J.; Wang, S. F.; Chen, T.; Wang, D. *ACS Nano* **2022**, *16* (8), 13092–13100; f) Elghamry, I.; Tietze, L. F. Journal of heterocyclic chemistry, **2005**, *42* (4) 503—508; g) Carvalho, C. M. B.; Brocksom, T. J.; Thiago de Oliveira, K. *Chem Soc Rev* **2013**, *42* (8), 3302–3317.

[2] a) Thompson, M. E.; Diev, V.; Hanson, K.; Forrest, S. R. Fusing Porphyrins with PAH and Heterocycles for Optoelectronic Applications, 2017; b) Yamada, H.; Kuzuhara, D.; Takahashi, T.; Shimizu, Y.; Uota, K.; Okujima, T.; Uno, H.; Ono, N. *Org Lett* **2008**, *10* (14), 2947–2950; c) Pijeat, J.; Chaussy, L.; Simoës, R.; Isopi, J.; Lauret, J. S.; Paolucci, F.; Marcaccio, M.; Campidelli, S. *ChemistryOpen* **2021**, *10* (10), 997–1003; d) Diev, V. v.; Schlenker, C. W.; Hanson, K.; Zhong, Q.; Zimmerman, J. D.; Forrest, S. R.; Thompson, M. E. *Journal of Organic Chemistry* **2012**, *77* (1), 143–159; e) Birin, K. P.; Abdulaeva, I. A.; Polivanovskaia, D. A.; Martynov, A. G.; Shokurov, A. v.; Gorbunova, Y. G.; Tsivadze, A. Y. *Dyes and Pigments* **2021**, *186;* f) Gao, R. Gao, R. *Synthesis And Characterization Of Polycyclic Aromatic Synthesis And Characterization Of Polycyclic Aromatic Hydrocarbon (Pah)-Porphyrin Hybrids Hydrocarbon (Pah)-Porphyrin Hybrids*; 2016.

[3] a) Omori, H.; Hiroto, S.; Takeda, Y.; Fliegl, H.; Minakata, S.; Shinokubo, H. *J Am Chem Soc* **2019**, *141* (12), 4800–4805; b) Chatterjee, T.; Shetti, V. S.; Sharma, R.; Ravikanth, M. *Chem. Rev.* 2017, 117, 4, 3254–3328; c) Abdulaeva, I. A.; Birin, K. P.; Bessmertnykh-Lemeune, A.; Tsivadze, A. Y.; Gorbunova, Y. G. *Coordination Chemistry Reviews,* **2020***, 407*; d) Fukui, N.; Fujimoto, K.; Yorimitsu, H.; Osuka, A. ***Dalton Trans.***, **2017**,***46***, 13322-1334; e) Sessler, J. L.; Seidel, D. *Angewandte Chemie - International Edition* **2003**, *42* (42), 5134–5175.

[4] a) Crossley, M. J.; Burn, P. L. ***J. Chem. Soc., Chem. Commun.***, **1991**, 1569-1571; b) Fukuzumi, S.; Ohkubo, K.; Zhu, W.; Sintic, M.; Khoury, T.; Sintic, P. J.; Wenbo, E.; Ou, Z.; Crossley, M. J.; Kadish, K. M. *J Am Chem Soc* **2008**, *130* (29), 9451–9458; c) Birin, K. P.; Poddubnaya, A. I.; Abdulaeva, I. A.; Gorbunova, Y. G.; Tsivadze, A. Y. *Dyes and Pigments* **2018**, *156*, 243–249; d) Moss, A.; Jang, Y.; Arvidson, J.; Nesterov, V. N.; D'Souza, F.; Wang, H. *Chem Sci* **2022**, *13* (34), 9880–9890; e) Abdulaeva, I. A.; Polivanovskaia, D. A.; Birin, K. P.; Gorbunova, Y. G.; Tsivadze, A. Y. *Mendeleev Communications* **2020**, *30* (2), 162–164; f) Shremzer, E. S.; Polivanovskaia, D. A.; Birin, K. P.; Gorbunova, Y. G.; Tsivadze, A. Y. *Dyes and Pigments* **2023**, *210*.

[5] a) Polivanovskaia, D. A.; Konstantinova, A. N.; Birin, K. P.; Sokolov, V. S.; Batishchev, O. v.; Gorbunova, Y. G. *Membranes (Basel)* **2022**, *12* (9); b) Li, Y.; Zhou, M.; Xu, L.; Zhou, B.; Rao, Y.; Nie, H.; Gu, T.; Zhou, J.; Liang, X.; Yin, B.; Zhu, W.; Osuka, A.; Song, J. *Org Lett* **2020**, *22* (15), 6001–6005; c) Boerner, L. J. K.; Mazumder, S.; Pink, M.; Baik, M. H.; Zaleski, J. M. *European Journal* **2011**, *17* (51), 14539–14551; d) Kumar, S.; Choudhuri, I.; Pathak, B. *J Mater Chem C Mater* **2016**, *4* (38), 9069–9077.

[6] a) Liang, T.; Xiao, L.; Gao, K.; Xu, W.; Peng, X.; Cao, Y. *ACS Appl Mater Interfaces* **2017**, *9* (8), 7131–7138; b) Hama, A. K.; Algso, M. A. S.; Kavak, E.; Kivrak, A. *Russian Journal of*

Organic Chemistry **2020**, *56* (7), 1272–1278; c) Mitsushige, Y.; Yamaguchi, S.; Lee, B. S.; Sung, Y. M.; Kuhri, S.; Schierl, C. A.; Guldi, D. M.; Kim, D.; Matsuo, Y. *J. Am. Chem. Soc.* 2012, 134, 40, 16540–16543; d) Arteaga, D.; Cotta, R.; Ortiz, A.; Insuasty, B.; Martin, N.; Echegoyen, L. *Dyes and Pigments* **2015**, *112*, 127–137; e) Shen, P.; Liu, X.; Jiang, S.; Wang, L.; Yi, L.; Ye, D.; Zhao, B.; Tan, S. *Dyes and Pigments* **2012**, *92* (3), 1042–1051; f) Xiang, N.; Huang, X.; Feng, X.; Liu, Y.; Zhao, B.; Deng, L.; Shen, P.; Fei, J.; Tan, S. *Dyes and Pigments* **2011**, *88* (1), 75–83; g) Yang, L. L.; Hu, X. L.; Tang, Z. Q.; Li, X. F. *Chem Lett* **2015**, *44* (11), 1515–1517.

[7] a) Gu, Z.; Tang, P.; Zhao, B.; Luo, H.; Guo, X.; Chen, H.; Yu, G.; Liu, X.; Shen, P.; Tan, S. *Macromolecules* **2012**, *45* (5), 2359–2366; b) Gupta, N.; Nagar, M. R.; Anamika; Gautam, P.; Maiti, B.; Jou, J. H.; Kuila, B. K. *ACS Appl Polym Mater* **2022**; c) Chai, H.; Xu, Z.; Li, H.; Zhong, F.; Bai, S.; Chen, L. *ACS Appl Electron Mater* **2022**, *4* (10), 4947–4954; d) Hou, C. C.; Ma, C.; Zhang, S. N.; Wang, L. Y.; Wang, K. X.; Chen, J. S. *ACS Appl. Energy Mater.* **2022**, 5, 11, 13802–13807

[8] a) Jinadasa, R. G. W.; Fang, Y.; Kumar, S.; Osinski, A. J.; Jiang, X.; Ziegler, C. J.; Kadish, K. M.; Wang, H. *Journal of Organic Chemistry* **2015**, *80* (24), 12076–12087; b) Deshpande, R.; Jiang, L.; Schmidt, G.; Rakovan, J.; Wang, X.; Wheeler, K.; Wang, H. *Org Lett* **2009**, *11* (19), 4251–4253; c) Hu, Y.; Thomas, M. B.; Webre, W. A.; Moss, A.; Jinadasa, R. G. W.; Nesterov, V. N.; D'Souza, F.; Wang, H. *Angewandte Chemie - International Edition* **2020**, *59* (45), 20075–20082.

[9] Arsenyan, P.; Paegle, E.; Belyakov, S. *Tetrahedron Lett* **2010**, *51* (1), 205–208

[10] a) Kim, J. B.; Leonard, J. J.; Longo, F. R. *National Institutes of Health Fellow*; 1970; Vol. 57; b) Albers, V. M.; Knorr, H. *J Chem Phys* **1936**, *4* (7), 422–425.

[11] Marchetti, B.; Karsili, T. N. V.; Kelly, O.; Kapetanopoulos, P.; Ashfold, M. N. R. *Journal of Chemical Physics* **2015**, *142* (22); c) *2-bromothiophene*. Spectrabase.com. https://spectrabase.com/spectrum/9n4b4b2jGXv (accessed 2023-01-20).

[12] Bufaroosha, M.; al Neyadi, S. S.; Alzamly, A.; Toutounji, M.; il Saleh, N. '; Abuhattab, Y.; Al-Hemyari, A.; Alyammahi, A.; Alzahmi, S.; Altubji, M.; Al-Ajeil, R. *World Journal of Chemical Education* **2020**, *8* (2), 87–91.

[13] Taniguchi, M.; Lindsey, J. S.; David; Bocian, F.; Holten, D. *Journ. of Photochemistry and Photobiology C: Photochemistry Reviews*, **2021**, 46.

[14] Stanger, A. *Journal of Organic Chemistry* **2006**, *71* (3), 883–893.

[15] Kleinpeter, E.; Klod, S.; Koch, A. *Journal of Molecular Structure: THEOCHEM* **2007**, *811* (1–3), 45–60.

[16] Gaussian 16, Revision C.01, Frisch, M. J.; Trucks, G. W.; Schlegel, H. B.; Scuseria, G. E.; Robb, M. A.; Cheeseman, J. R.; Scalmani, G.; Barone, V.; Petersson, G. A.; Nakatsuji, H.;

Li, X.; Caricato, M.; Marenich, A. V.; Bloino, J.; Janesko, B. G.; Gomperts, R.; Mennucci, B.; Hratchian, H. P.; Ortiz, J. V.; Izmaylov, A. F.; Sonnenberg, J. L.; Williams-Young, D.; Ding, F.; Lipparini, F.; Egidi, F.; Goings, J.; Peng, B.; Petrone, A.; Henderson, T.; Ranasinghe, D.; Zakrzewski, V. G.; Gao, J.; Rega, N.; Zheng, G.; Liang, W.; Hada, M.; Ehara, M.; Toyota, K.; Fukuda, R.; Hasegawa, J.; Ishida, M.; Nakajima, T.; Honda, Y.; Kitao, O.; Nakai, H.; Vreven, T.; Throssell, K.; Montgomery, J. A., Jr.; Peralta, J. E.; Ogliaro, F.; Bearpark, M. J.; Heyd, J. J.; Brothers, E. N.; Kudin, K. N.; Staroverov, V. N.; Keith, T. A.; Kobayashi, R.; Normand, J.; Raghavachari, K.; Rendell, A. P.; Burant, J. C.; Iyengar, S. S.; Tomasi, J.; Cossi, M.; Millam, J. M.; Klene, M.; Adamo, C.; Cammi, R.; Ochterski, J. W.; Martin, R. L.; Morokuma, K.; Farkas, O.; Foresman, J. B.; Fox, D. J. Gaussian, Inc., Wallingford CT, 2016.

[17] Gershoni-Poranne, R.; Stanger, A. *Chemistry - A European Journal* **2014**, *20* (19), 5673–5688.

[18] Song, C. X.; Chen, P.; Tang, Y. Carboxylation of Styrenes with CBr4 and DMSO via Cooperative Photoredox and Cobalt Catalysis. *RSC Adv* **2017**, *7* (19), 11233–11243.

CHAPTER 3

PORPHYRIN OLIGOMERS DERIVED FROM NAPHTHODITHIOPHENE-FUSED PORPHYRINS

3.1 Introduction

Sonogashira coupling has been a popular *sp*^{2}-*sp* cross-coupling reaction since the late 1970s due to its mild conditions and versatility. Figure 3.1 shows the two independent catalytic cycles, involving palladium and copper respectively, undergone during the Sonogashira reaction. First the palladium complex undergoes σ-complexation-dehydropalladation-reductive elimination with the base, usually an amine, to generate a Pd^0 complex which can then undergo oxidative addition. From there, the two catalytic cycles merge in a trans-metalation. To induce deprotonation of the acetylide in the presence of an amine, a π-alkyne-Cu complex must be formed which then allows for the formation of palladium-acetylide.

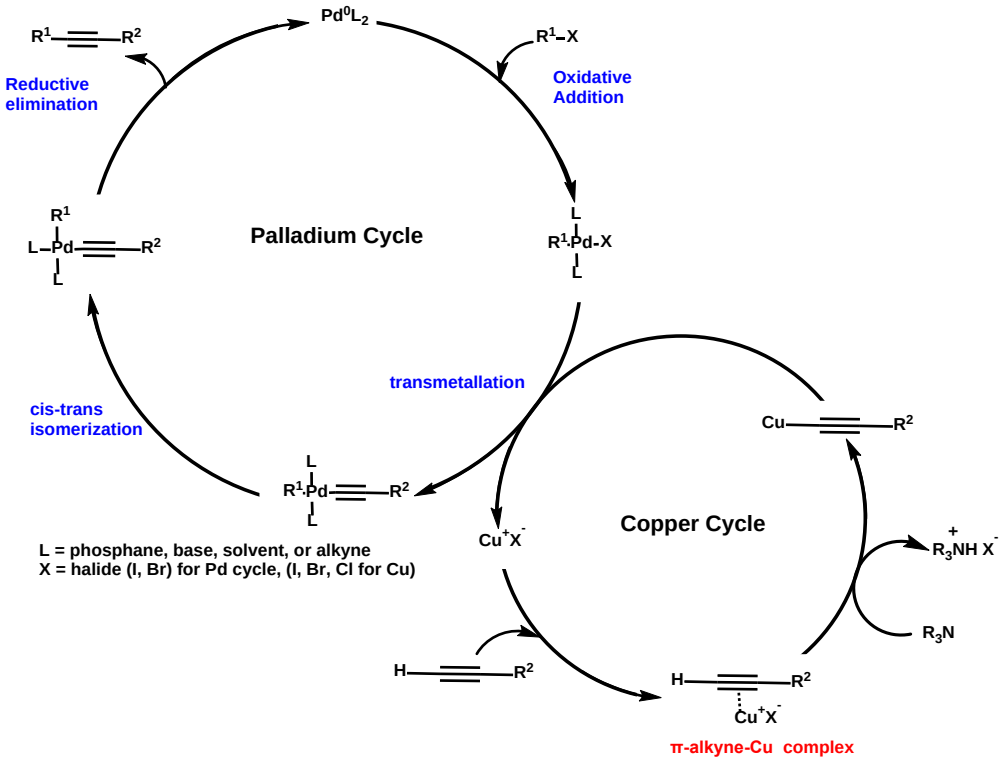

Figure 3.1: General Sonogashira coupling mechanism.

Although it has not been studied to our knowledge, it is likely that the π-alkyne-Cu complex facilitates the formation of the palladium-acetylide because Cu^{+} and Pd^{2+} are both soft acids, which could allow for an easier transmetallation step. Once the alkyne is coordinated to the palladium, it can undergo trans/cis isomerization and then reductive elimination. In the last twenty years, significant efforts have been devoted to developing reaction conditions, such as using various copper salts, replacing inorganic bases with amines, or even ligand-free conditions, [1] to extend the utility of this reaction to work beyond the scope of aryl iodides and terminal alkynes. Among the numerous conditions developed for Sonogashira coupling reaction, the most employed procedure utilizes the catalytic system of $CuI/PdCl_2(PPh_3)_2$ in DMF in the presence of an amine due to its broader scope and high yields. This procedure has commonly been used to further functionalize porphyrins through their *meso*-positions. [2] Functionalization of porphyrin at the β-positions of porphyrins through carbon-carbon coupling reactions has not been widely studied or reported. Those that have been, by groups such as Van Lier [3] and Osuka [4], have used metal-inserted β-haloporphyrins to generate their hetero-coupling sonogashira products.

Sonogashira coupling reactions have been used to synthesize porphyrin oligomers. Generally, the two common synthetic routes, shown in Figure 3.2, to construct porphyrin dimers and oligomers through this type of coupling include: 1) using an aryl-dihalide and a *meso*-ethynylporphyrin or 2) combination of bisacetylenes and *meso*-haloporphyrins. The second route remains the primary methodology used for synthesizing arylene-ethynylene linked porphyrins. However, this synthetic route has limitations in terms of molecular design; a problem specific with Sonogashira coupling reactions in this synthetic route is the potential of

glaser coupling. The first route offers comparable yields but reduces the chance of Glaser coupling. Furthermore, the accessibility of biacetylene precursors makes this reaction easy to perform. In this chapter we will explore the synthesis of porphyrin arrays utilizing route 2 through porphyrin β-positions.

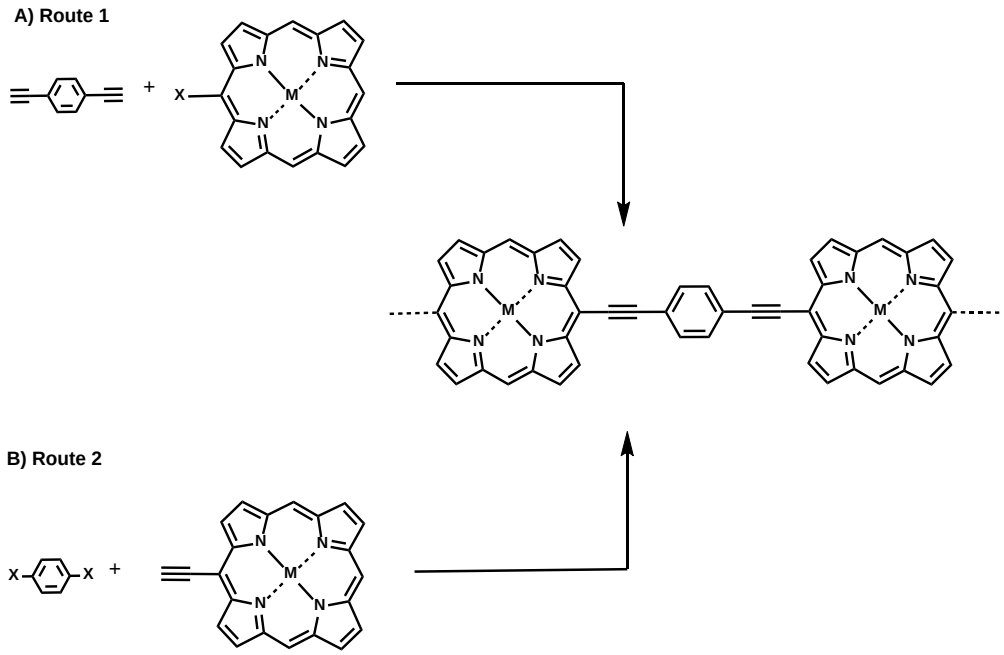

Figure 3.2: Two general synthetic routes for creating porphyrin oligomers through porphyrin *meso*-positions. It should be noted that this methodology has been used for various cross-coupling reactions and is not limited to Sonogashira coupling.

3.2 Molecular Design and Synthesis: Synthetic Route

Most of the porphyrin dimers and oligomers constructed through carbon-carbon cross-coupling reactions reported in the literature are linked directly between the porphyrin cores or through linkers at the meso-position. [5] Porphyrin dimers or oligomers connected through porphyrin b-position have been rarely reported due to synthetic difficulty. In designing the porphyrin oligomers in this chapter, we considered utilizing the bromination chemistry of naphthodithiophenyl component if the naphthodithiophenyl-fused porphyrins studied in

Chapter 2. If the 5-position of the thiophene moieties can be brominated selectively, further extension of the naphthodithiophenyl -fused porphyrins by means of carbon-carbon cross coupling reactions would be possible. By using standard Sonogashira coupling reaction conditions, reported in Scheme 1, the previously synthesized F2vtBr porphyrin was reacted with excess phenylacetylene and the Sonogashira product **dPAp** was obtained in 96% yield. Encouraged by the success synthesis of **dPAp**, similar conditions were repeated with 1,4-diethynylbenzene (PEB) and compound **bPEBp** was obtained at 90% yield.

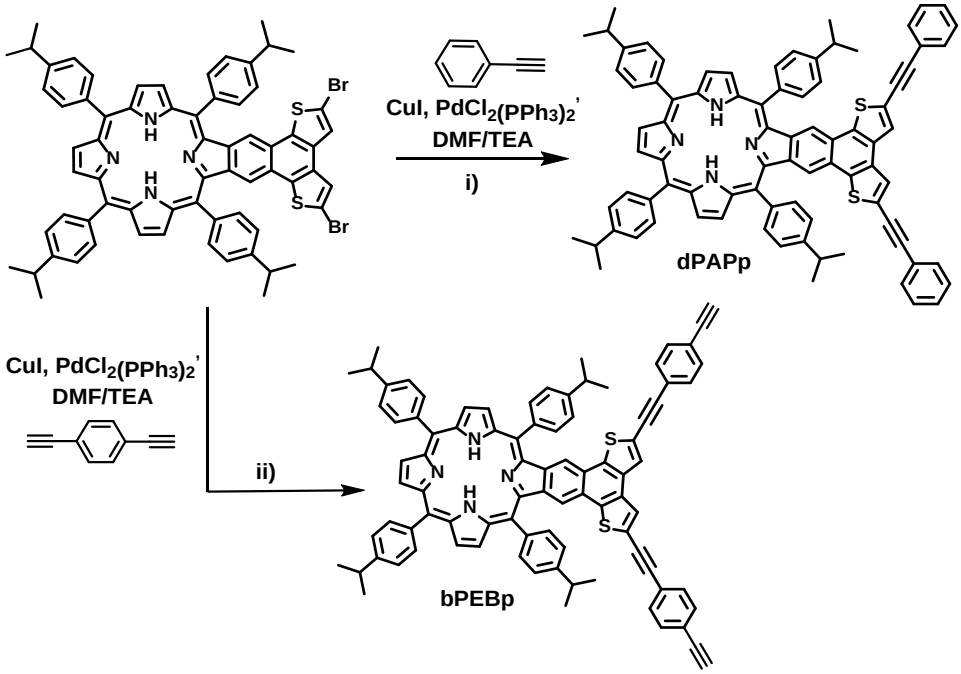

Scheme 3.1: Sonogashira cross-coupling reactions performed on F2VTBr. Conditions: i) 1 eq of the porphyrin F2vtBr, 20 eq of phenylacyetylene, 2 mol% $PdCl_2(PPh_3)_2$, 4 mol% CuI, DMF/TEA, 40°C, stirred overnight, 96% yield; ii) 1 eq of the porphyrin F2vtBr, 2 eq of 1,4-diethynylbenzene, 2 mol% $PdCl_2(PPh_3)_2$, 4 mol% CuI, DMF/TEA, 40°C, stirred overnight.

The successful development of the reactions shown above stimulated us to design a project trajectory for synthesizing β-π-extended porphyrin trimers and dimers. The prepared **bPEBp** could serve as a good starting reagent for the synthesis of a trimer through Sonogashira coupling reaction. However, a foreseeable problem is to control the reaction at the trimer

formation step without further extension to form a polymer. One way to do that would be to synthesize a new mono-bromo porphyrin which could then be coupled to the terminal acetylene positions and essentially act as a cap. Another benefit of synthesizing this molecule is that it would also serve as a good dimer starting reagent since the fused mono-bromo porphyrin could react with PEB to generate a mono-PEB derivative of bPEBp.

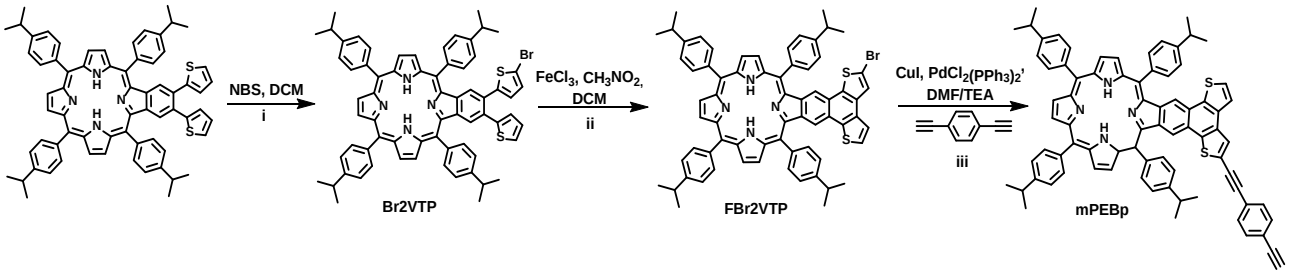

Scheme 3.2: Synthesis of the porphyrin precursor for the porphyrin oligomers. Conditions: i) 1 eq of recrystallized NBS and 1 eq of 2VTP was dissolved in dichloromethane and sonicated for 30s; ii) Br2VTP was dissolved in dichloromethane was combined with 20 eq $FeCl_3$ dissolved in 1 mL nitromethane, and stirred at room temperature for 15 min. iii) 20 eq of p-diethynylbenzene, 2 mol% $PdCl_2(PPh_3)_2$, 4 mol% CuI, dimethylformamide/triethylamine, 40°C, and stirred overnight.

Scheme 3.2 shows a single addition of bromine on the thiophene component of our previously reported **2VTP**. Monobromination of **2VTP** was achieved through sonication for a very short time, i.e, 30 seconds. Longer sonication time resulted in multiple bromination of the **2VTP**. Next, a Scholl reaction was performed generating **FBr2VTP** in 86% yield. A Sonogashira coupling reaction was performed with the same conditions as those done in Scheme 3.1 with excess PEB and **mPEBp** was formed in 80% yield. With the prepared **mPEBp** and **FBr2VTP,** the first freebase dimer was obtained in 89% yield. The next step was to generate a zinc-inserted derivative – **2ZnD**, synthesized in 95% yield— which was obtained by reacting to the free base dimer with a $Zn(OAc)_2$. Metalation of both porphyrin cores could be easily achieved. We were interested in metalating only one of the porphyrin cores with zinc, leaving the other as a freebase porphyrin. There are only three [6] instances reported in the literature where Zn

porphyrin and freebase porphyrins were linked together; however, all of them were linked at a meso-position either directly or via linker. To our knowledge, the dimer prepared in this work would be the first porphyrin freebase/Zn dimers linked at β-positions.

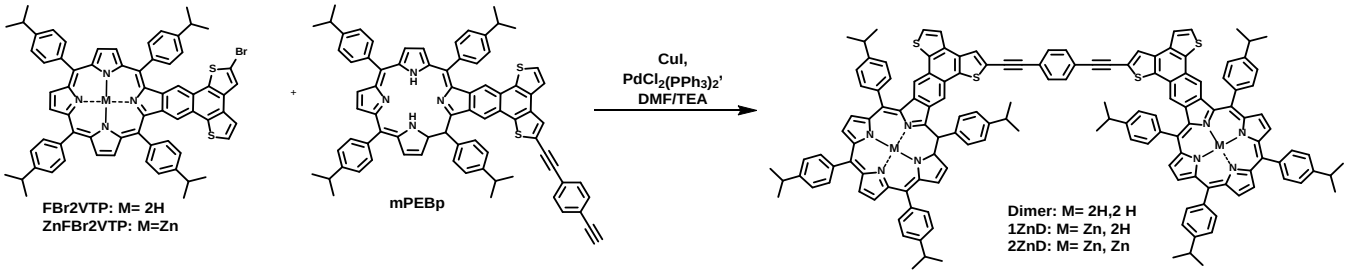

Scheme 3.3: Synthesis of β-linked porphyrin dimers.

To generate a freebase/Zn heterodimer, we chose to insert Zinc into **FBr2VTP** instead of **mPEBp**. The reason for this is because we could capitalize on already having a **ZnFBr2VTP** derivative to also create a Zn-Freebase-Zn trimer later. **ZnFBr2VTP** and one equivalent of freebase **mPEBp** were reacted under Sonogashira conditions and the heterodimer **1ZnD** was successfully generated in 92% yield.

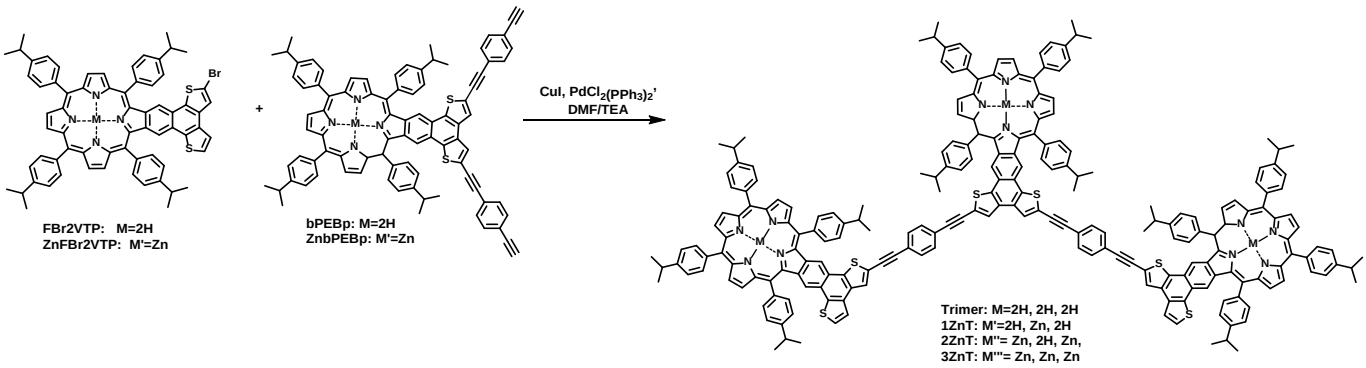

Scheme 3.4: Synthesis of porphyrin trimers.

Scheme 3.4 shows the synthesis of the freebase trimer and its zinc derivatives. To generate the freebase trimer, **FBr2VTP** and **bPEBp** were mixed in a 2:1 ratio and reacted under Sonogashira coupling condition and the desired freebase trimer was produced in 96% yield. As

with its dimer counterpart, we were especially curious about how we could control the placement of the zinc-insertions. To obtain Zn-insertion in all of the porphyrins was facile as it required reacting the freebase trimer with ten equivalents of $Zn(OAc)_2$ and the **3ZnT** was obtained in 90% yield. Insertion of only one Zn was completed by preparing a **ZnbPEBp** derivative and reacting it with two equivalents of freebase **FBr2VTP** with the previously reported conditions and **1ZnT** was generated in 85% yield. To obtain a Zn-Freebase-Zn porphyrin trimer, we flipped the porphyrin that was metalated. Two equivalents of **ZnFBr2VTP** were reacted with one equivalent of the freebase **bPEBP** and we were able to obtain **2ZnT** with an 87% yield.

3.3 Optical Properties

3.3.1 UV-VIS Spectroscopy

Figure 3.3 shows the molar absorptivity of the freebase monomers in dichloromethane (DCM). The Soret bands for **Br2VTP** (436 nm) and **FBr2VTP** (450 nm) are comparable to that of **2vtBr** and **F2vtBr** shown in chapter 2. The addition of one (**mPEBp**, 451 nm) or two (**bPEBP**, 451 nm) PEB linkers does not seem to drastically affect the position of Soret band of the porphyrin; however, does appear to increase with increased addition of PEB. Furthermore, the spectra show an increase in peak intensity around 300-400 nm. The Q bands for each of the porphyrins seem to experience only minor shifts (2-5 nm) between them. The normalized absorption spectra of **ZnbPEBp** and **ZnFBr2VTP** can be found in the experimental section. Both **ZnFBr2VTP** and **ZnbPEBp** have a Soret at 453 nm with two Q bands present. **ZnFBr2VTP** displays Q bands at 573 nm and 616 nm whereas **ZnbPEBp** displays bands at 575 nm and 617 nm.

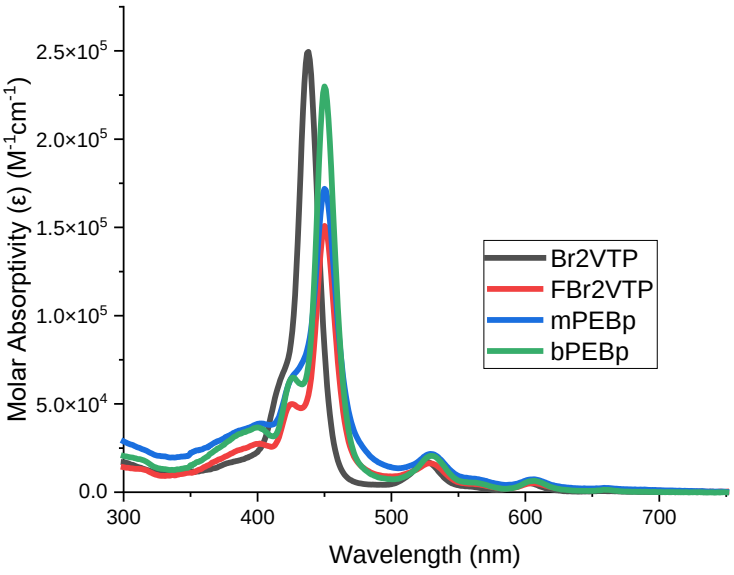

Figure 3.3: Molar absorptivity of freebase monomers in 1,2-dichlorobenzene.

The molar absorptivity of the freebase dimer can be found in Figure 3.4. The freebase dimer shows a Soret at 450 nm and Q bands at 528, 568, 607 and 636 nm. The normalized UV-VIS of the zinc inserted dimers can be found in the experimental section 3.7.6. The insertion of zinc does not drastically alter the position of the Soret for either **1ZnD** (451 nm) or **2ZnD** (452 nm). However, the number of Q bands does change depending on whether one or both porphyrins are metalated. **1ZnD** presents as a true mixture of freebase and zinc porphyrins and therefore displays three Q bands at 528 nm, 571 nm, and 612 nm. The UV-VIS absorption spectrum of **2ZnD** presents as a typical zinc inserted porphyrin with only two Q bands at 575 nm and 616 nm.

The molar absorptivity of the freebase trimer can be seen in Figure 3.5 with a Soret at 451 nm and four Q bands showing at 530, 568, 608, and 658 nm. The normalized UV-VIS of the zinc-inserted trimers in the experimental section. The addition of zinc into the trimer results in similar Soret bands of 450 nm (**2ZnT**), 451 nm (**1ZnT**), and 452 nm (**3ZnT**). Like the zinc inserted

dimers, **1ZnT** and **2ZnT** experience three Q bands at 528, 571, and 605 nm and 529, 573, and 609 nm respectively. When all the porphyrins are metalated, as with **3ZnT**, an expected two Q bands were observed.

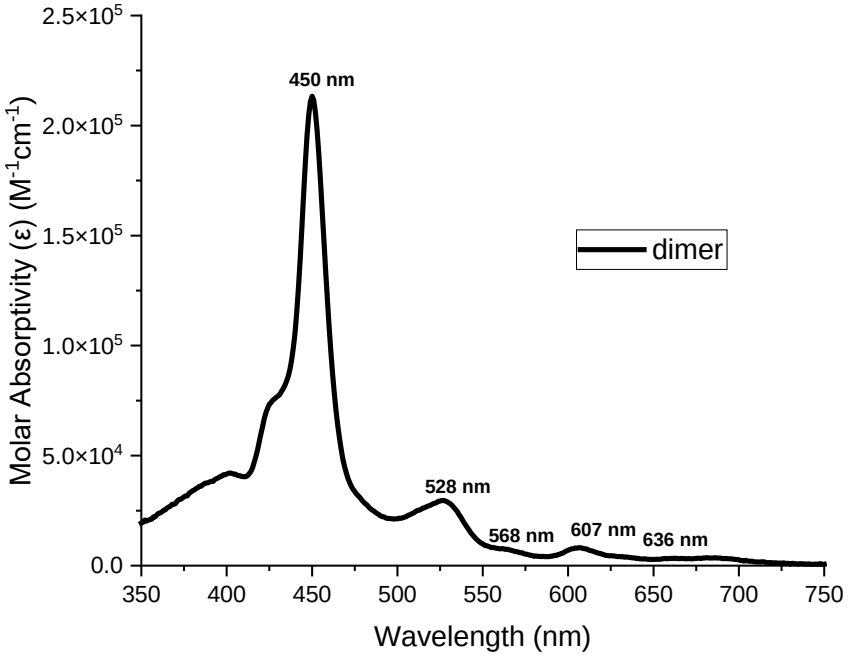

Figure 3.4: Molar absorptivity of freebase dimer in 1,2-dichlorobenzene.

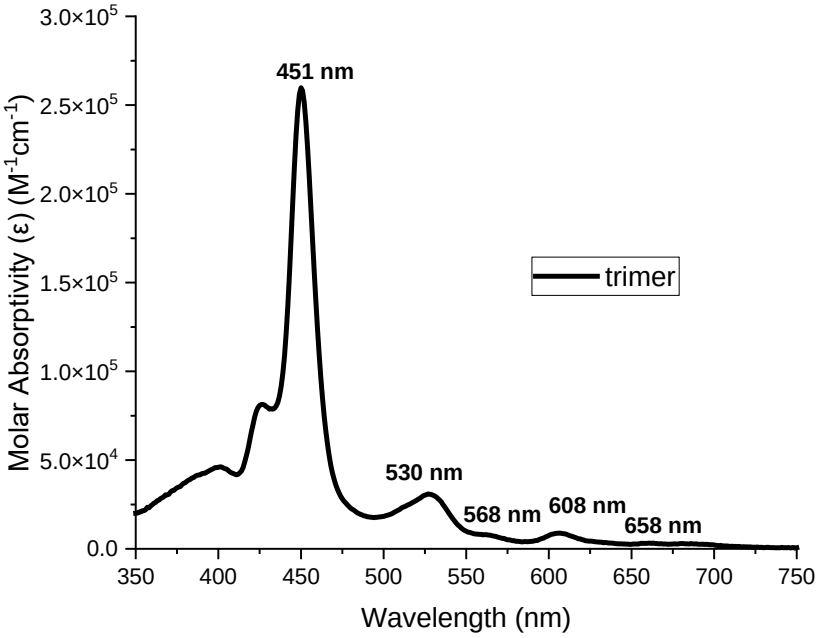

Figure 3.5: Molar Absorptivity of freebase Trimer in 1,2-dichlorobenzene.

3.3.2 Fluorescence Spectroscopy

Fluorescence emission spectra were obtained in dry chloroform. All the π-extended porphyrin monomers display a similar two peak pattern. The zinc inserted porphyrins, **ZnFBr2VTP** (620 nm and 680 nm)**,** and **ZnbPEBp** (621 nm and 682 nm) show a more intense peak around 620 nm and a less intense peak around 680 nm. For the freebase fused monomers **FBr2VTP** (665 nm and 737nm)**, mPEBp** (664 nm and 737nm)**,** and **bPEBp** (664 nm and 738nm) two almost equally intense peaks were observed. The unfused **Br2VTP** monomer has a smaller intensity peak around 672 nm and the higher intensity peak around 730 nm. These peaks appear broader with a less minima between the two compared to the other monomers.

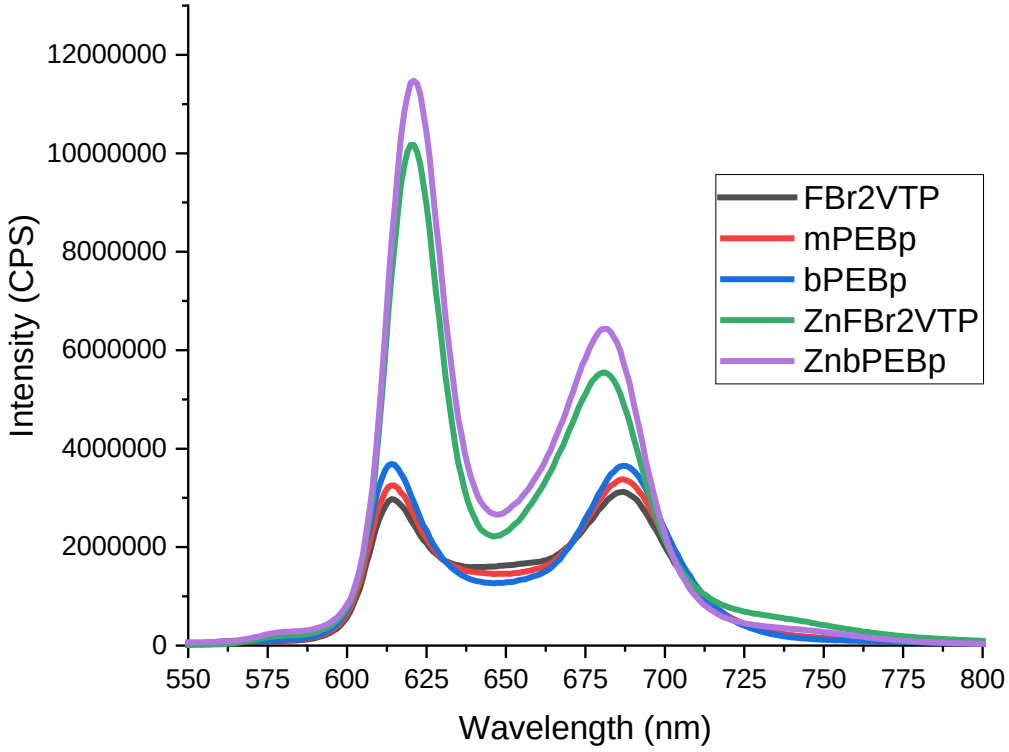

Figure 3.6: Fluorescence spectra of both freebase and zinc monomers

The fluorescence intensity of the freebase **dimer** and its zinc inserted analogues were obtained in dry chloroform. The freebase and zinc analogues show different peak patterns. The

free base dimer only shows two peaks with almost the same intensity with the narrower peak around 664 nm and a broader peak around 738 nm. The zinc derivatives **1ZnD** and **2ZnD,** however, show three peaks around similar wavelengths varying in intensity. **1ZnD** has the lowest intensity peak occurring around 620 nm, with the remaining two peaks being closer in intensity; the slightly more intense peak is found in the middle around 664 nm and the last peak occurs around 738 nm. The middle peak experiences a larger broadening as the peak further redshifts, unlike the freebase dimer. **2ZnD** shows a spectrum of three different peaks with similar intensities. The blue shifted peak has a sharp and intense peak around 620 nm before it decreases and then broadens out to the second most intense peak which shows at 681 nm. The weakest intensity peak occurs around 737 nm. It is important to consider that both porphyrins in the dimer are the same – therefore the differences in the intensity and placement of the peaks indicates that there must be some communication between the two porphyrins.

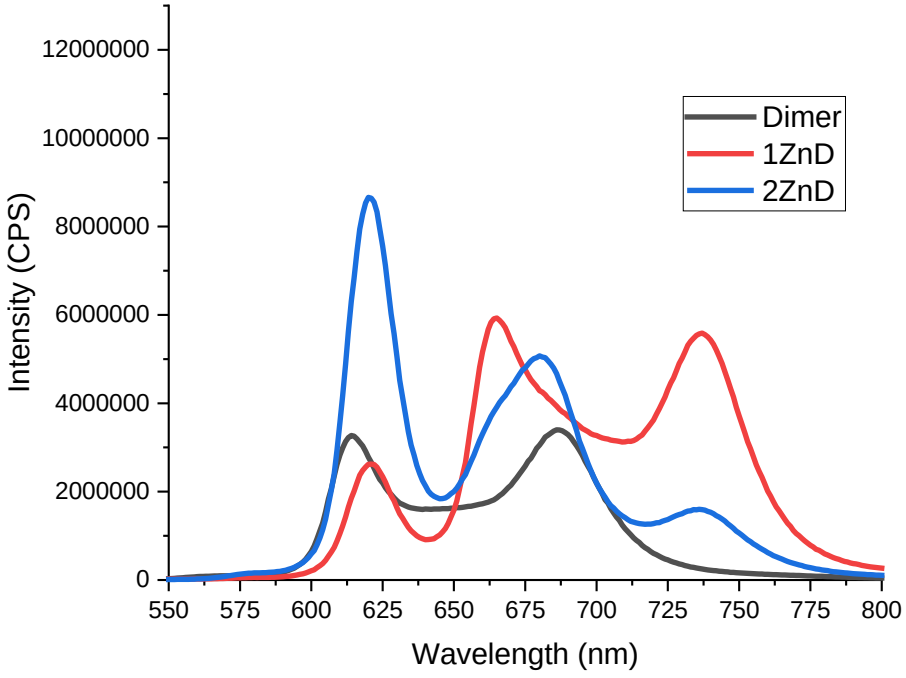

Figure 3.7: Fluorescence spectra of dimers

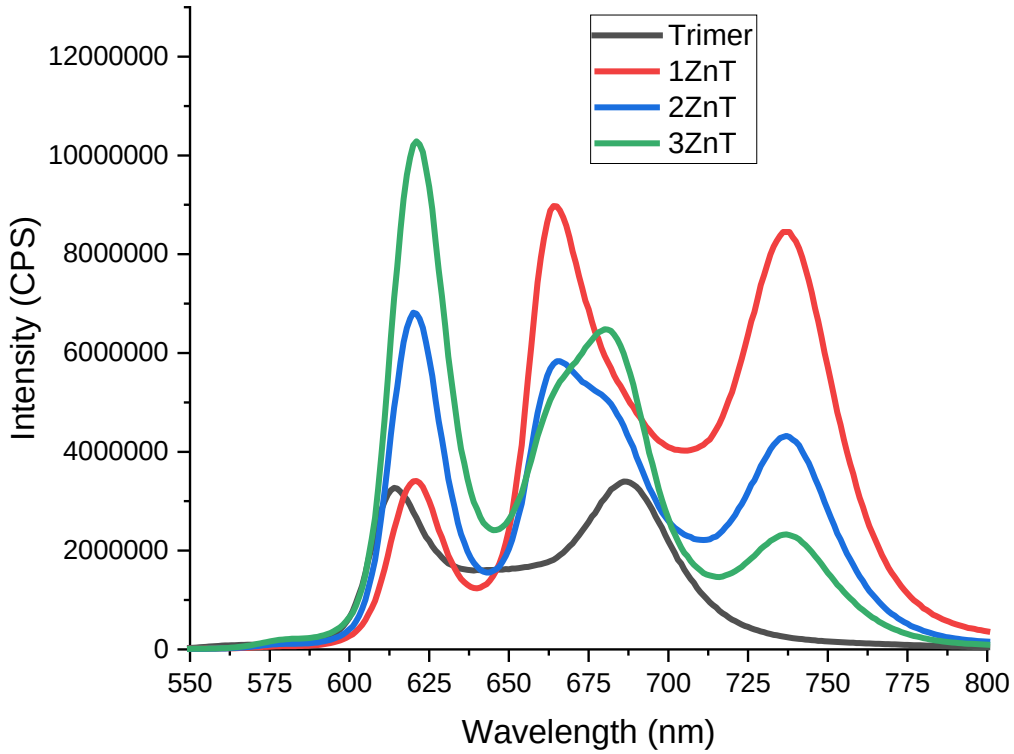

Figure 3.8: Fluorescence spectra of trimers

The fluorescence emission spectra of the porphyrin trimers were also obtained in dry chloroform. Similarly, as the dimers, a difference in peak patterns was observed based on whether the porphyrin is freebase or inserted with at least one zinc. The freebase **trimer** exhibits two peaks of almost equal intensity with the red-shifted peak (665 nm) exhibiting a nominally higher intensity and broadening than that of the blue-shifted peak (736 nm). The addition of only one zinc into a porphyrin core provides **1ZnT** with three peaks. The blue shifted peak has the lowest intensity and is seen around (620 nm). The other two peaks have a closer intensity level with the center peak (664 nm) being marginally higher than the more redshifted peak (737 nm). The presence of two zinc inserted porphyrins, **2ZnT**, in the motif results in peaks of closer intensity occurring around similar wavelengths as its **1ZnT** analogue. However, for **2ZnT** the more intense peak is the one furthest blue shifted (620 nm) and the peak with the

least intensity peak at 736 nm. The central peak (665 nm), the second most intense peak, experiences a slight shoulder on the right side of the peak around 675 nm. For the **3ZnT** porphyrin we see a similar pattern to that of its **2ZnT** counterpart. The most intense peak appears around 621 nm and the peak with the least intensity peak (739 nm) is the furthest red shifted. Unlike the two-zinc inserted derivative, the central peak (680 nm) of **3ZnT** experiences a shoulder to the left of it around 660 nm. This trimer exhibits vastly different intensities between the three peaks than compared to either of the other zinc-inserted trimers. It is interesting to note that both the **1ZnT** and **3ZnT** experience a similar peak pattern as those of **1ZnD** and **2ZnD**.

3.4 DFT Studies

The basis set B3LYP-6-31(d,p) level of theory was used for the DFT calculations of all monomers and dimers. Problems with the trimer data will be discussed later in this section. The TDDFT level of theory used was B3LYP-6-31(d,p) scrf iefpcm in dichlorobenzene.

3.4.1 HOMO-LUMO Orbitals and Energy

Figure 3.9 shows the calculated isodensity surfaces for **FBr2VTP, mPEBp, bPEBp, ZnFBr2VTP,** and **ZnbPEBp.** The HOMO-1 for all but **FBr2VTP** shows isodensity on the porphyrin ring only. The isodensity of the HOMO of each monomer is present along the naphthodithiophenyl-motif for all but **FBr2VTP** in which the isodensity remains only on the porphyrin core. Minor isodensity appears once again on the benzene ring fused to the porphyrin core for **FBr2VTP** in the LUMO before it fully extends to the thiophene rings in LUMO+1. The LUMO of the remaining four compounds show isodensity predominantly on the

porphyrin core. In the case of **bPEBp** and **ZnbPEBp** the isodensity extends onto one of the PEB moieties. Whereas isodensity of **mPEBp** and **ZnFBr2VTP** is largely on the porphyrin core with minor density on the benzene ring fused to it. The LUMO+1 isodensity plots show the isodensity of **mPEBp** extending from the porphyrin core up through the PEB linker; **bPEBp** has isodensity largely on the porphyrin ring with some extending up to the thiophene ring and into the triple bond. **ZnbPEBp** experience similar isodensity as in the LUMO, however the intensity is less on the PEB moiety and more on the porphyrin core. **ZnFBr2VTP** displays similar isodensity to that if its freebase analogue in LUMO+1.

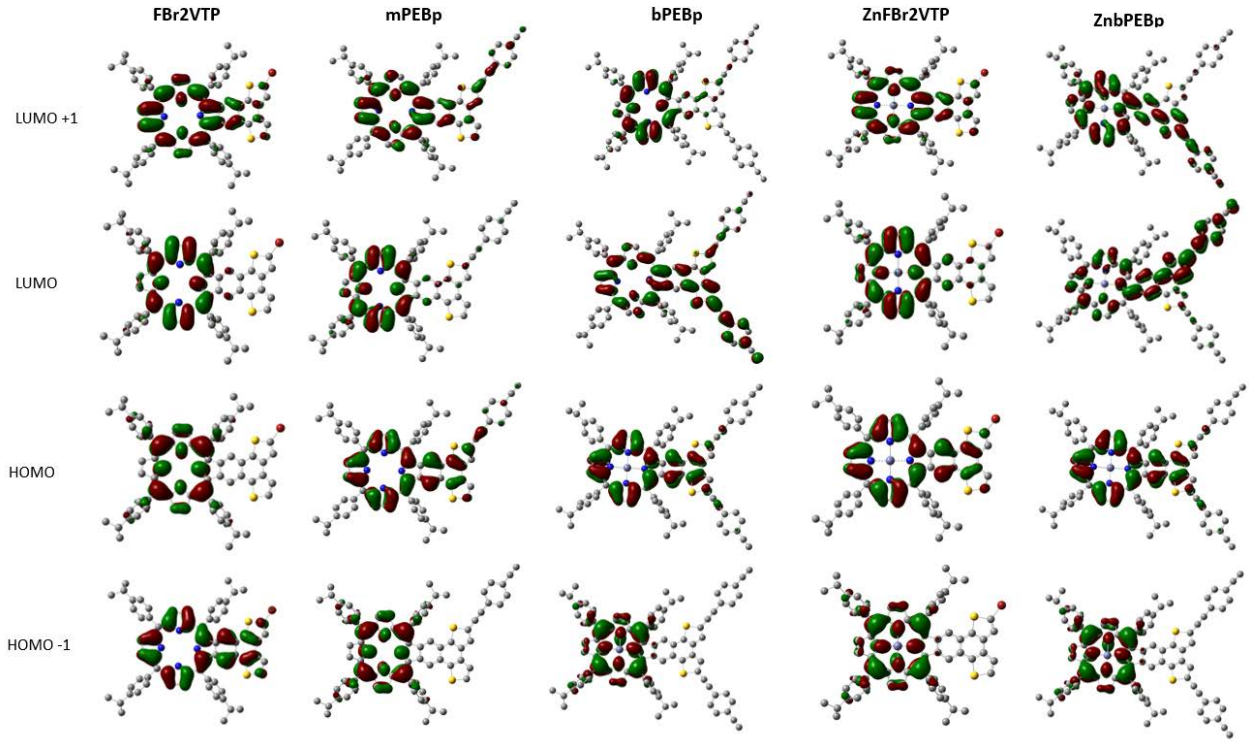

Figure 3.9: HOMO-1 to LUMO +1 isodensity surface for the synthesized monomers.

Minor differences exist in the energy level between the freebase and zinc-inserted monomers (Figure 3.10). **mPEBp** and **bPEBp** exhibit only a 0.01 eV energy difference. **FBr2VTP** does have a slightly higher energy level than that of its analogue **F2vtBr** in chapter 2 (a

difference of 0.02 eV). The insertion of zinc decreases the energy level by 0.03 eV between **FBr2VTP** and **ZnFBr2VTP** whereas **ZnbPEBp** and its freebase analogue have an energy difference of 0.05 eV.

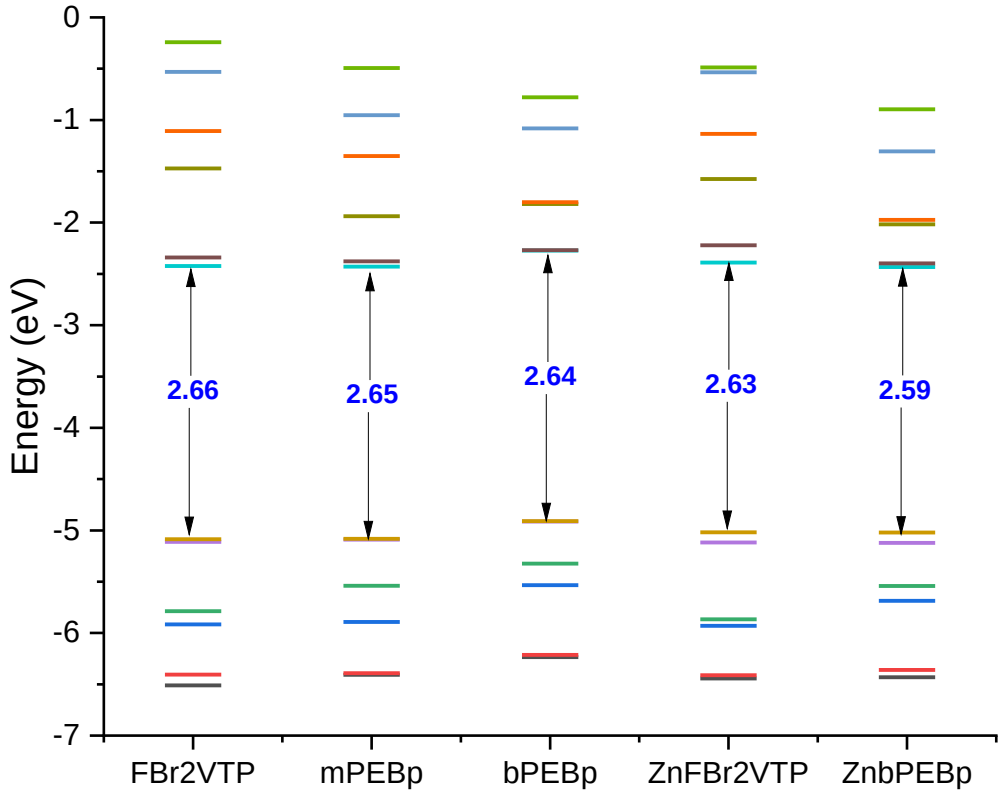

Figure 3.10: 10 HOMO-LUMO energy diagrams of monomers.

In Figure 3.11 we will look at and compare the isodensity surfaces of the freebase dimer and its zinc-inserted derivatives. Since we were looking at a porphyrin array and therefore looking for communication between the two porphyrins, it was decided that we would look at HOMO -5 to LUMO +5 for all the dimers. It is important to note that for Figure 3.11a-c, all the porphyrins were oriented the same exact way to make them easier to compare.

In the case of the freebase dimer, Figure 3.11a, isodensity is only on one porphyrin for HOMO and HOMO -1; however, the density is not focused on the same porphyrin which

suggests that there is some communication between the two porphyrins. The isodensity is located on the porphyrin in HOMO -3, but there is also isodensity on the benzene and thiophene rings as well. HOMO-2 predominantly shows isodensity on the bottom porphyrin and its extended rings with very minor isodensity present on the thiophene moiety of the other porphyrin. For HOMO-4 not much isodensity is found on the porphyrin core, instead it is primarily on the thiophene rings. In HOMO-5 isodensity occurs along the PEB-linker and into both porphyrins; however, one porphyrin does bear more isodensity than the other. The LUMO isodensity is like HOMO-4 in which the isodensity is predominantly on the benzene and thiophene rings of one porphyrin. However, unlike HOMO-4 it has isodensity reaching up onto the PEB linker. In LUMO +1 and LUMO+5 communication between the two porphyrin cores and along the PEB linker becomes apparent. LUMO+1 has more isodensity on both porphyrins compared to that of LUMO+5. LUMO+2 through LUMO+4 only shows isodensity on the two porphyrins and not the linker between them. In all three of these, one porphyrin core bears more of the isodensity than the other.

A)

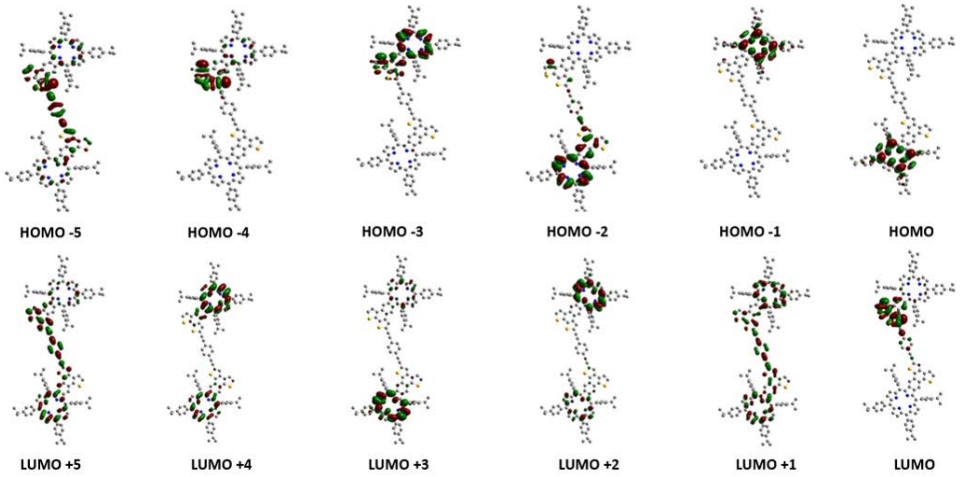

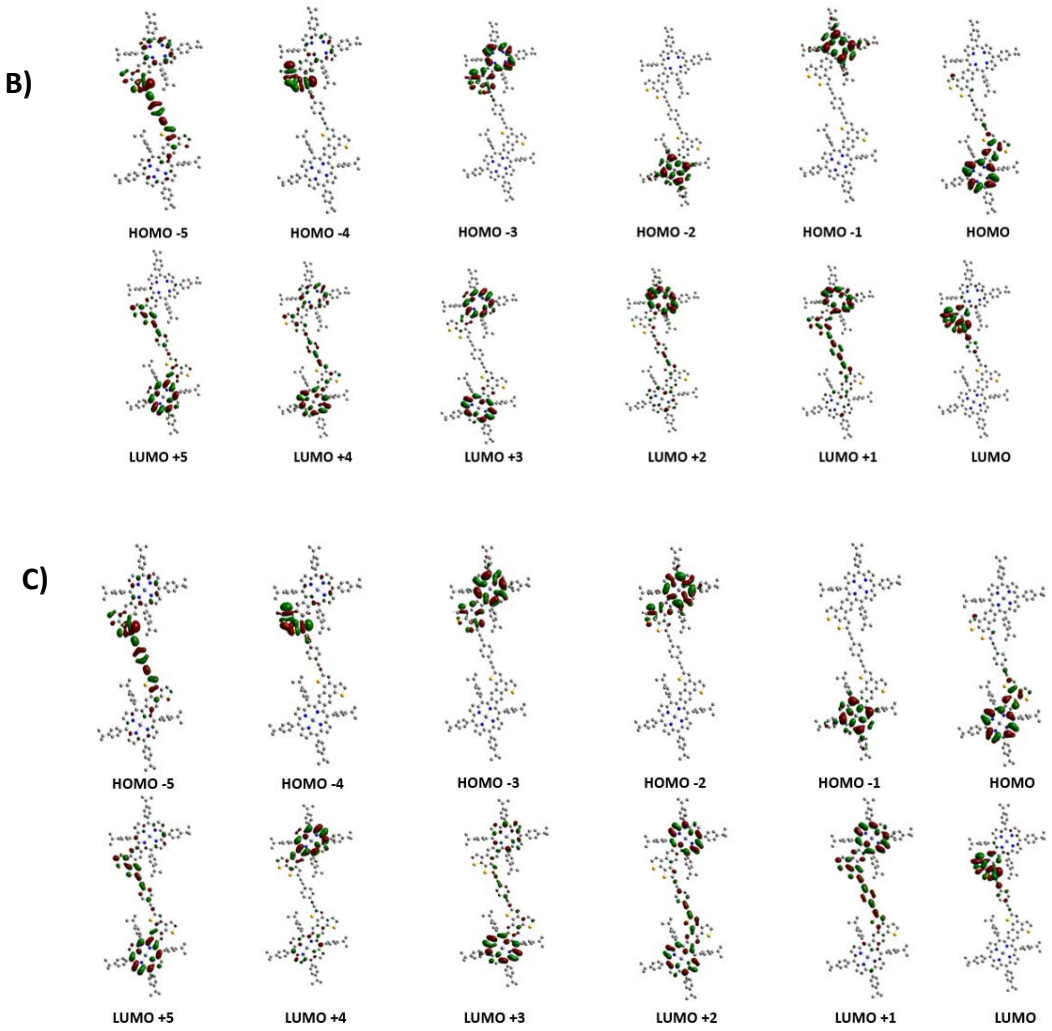

Figure 3.11: HOMO-LUMO orbital diagrams of Dimers: a) the freebase dimer; b) 1ZnD, and c) 2ZnD isodensity orbital surface diagrams.

In Figure 3.11b, for **1ZnD**, a similar trend to that of the free base dimer can be observed: there are two cases in which the isodensity is only on the porphyrin core (HOMO -1 and HOMO -2). However, it has the only case where it extends from the core onto the added rings (HOMO-3) but not the PEB linker and one in which it extends to not only to the rings fused to the porphyrin core, but also slightly onto the triple bond (HOMO). HOMO-4 has the majority of the isodensity onto the thiophene rings. In HOMO-5, the isodensity is mostly along the PEB linker and thiophene rings with very minor isodensity on the bottom porphyrin and more on the top

porphyrin. The isodensity in the LUMO resides along the benzene and thiophene rings fused to the porphyrin core with minimal density creeping onto the diethnylbenzene linker. Complete isodensity on the PEB linker is clearly shown in LUMO+1 and LUMO+4 and partial density is displayed in LUMO+2 and LUMO+5. In the case of LUMO+1 there is more isodensity present on PEB linker and on the top porphyrin; there is very minor isodensity present on the bottom porphyrin. For LUMO+4 it is flipped, there is more isodensity present on the bottom porphyrin that there is on the top. As compared to that of LUMO+1, LUMO+4 shows more electron density on the porphyrins. LUMO +2 shows mino isodensity on the bottom half of the PEB linker and minor density on the bottom porphyrin. The remaining density shown is localized on the top porphyrin's core. LUMO +5 shows isodensity along the bottom porphyrin and minor electron density in the PEB linker (towards the top porphyrin). However, unlike in LUMO +1 and LUMO +4, the isodensity is present on the porphyrin core; it is present on the thiophene rings of the top porphyrin. In LUMO +3, both porphyrins display isodensity, but none is present along the diethnylbenzene linker.

Figure 3.11c shows the **2ZnD** isodensity orbital surface diagrams. The isodensity is present exclusively on the bottom porphyrin in HOMO-1 and not the thiophene rings or PEB linker. HOMO-2 and HOMO-3 show isodensity along the top porphyrin and out to the thiophene rings, with more isodensity present in HOMO-3. Isodensity is also present on the porphyrin core and on the thiophene rings in the HOMO (bottom porphyrin instead), but unlike HOMO-2 and HOMO-3 there is minor isodensity on one of the other porphyrin's (top) thiophene ring as well. HOMO-4 shows isodensity predominantly along the thiophene rings and minor density on the top porphyrin core. The majority of the isodensity is present on the PEB

linker and the thiophene rings in HOMO-5 with very minor isodensity present on the bottom porphyrin and a bit more present on the top porphyrin core. On the other hand, the majority of the isodensity for LUMOs is found on the benzene and thiophene rings with some occurring on the p-diethnylbenzene linker. Isodensity occurs on the PEB linker in LUMO+1, LUMO+2, LUMO+3, and LUMO+5 as well. Specifically, minor isodensity is present on the linker in LUMO+3 and a partial heavy density present in LUMO+2 and LUMO+5. LUMO+1 experience complete isodensity coverage of the PEB linker. In LUMO+2 there seems to be equal isodensity present on both porphyrins, whereas LUMO+3 and LUMO+5 have more isodensity observed on one porphyrin than on the other. In the case of LUMO +4 the isodensity resides on both porphyrins with more density present on the top porphyrin and not as much present on the bottom.

When we compare the three dimers to each other we can see that all three exhibit similar trends in the HOMO-4, HOMO and LUMO with very minor variations. Furthermore, similar trends are observable within the (e.g isodensity on two porphyrins and not the linker or on one porphyrin and the linker) remaining HOMO and LUMO isodensity plots. However, where, and how those trends showed up depended on the porphyrin being studied. In the case of the freebase dimer, there are two instances in which isodensity only occurred on the porphyrin core. For **1ZnD** and **2ZnD** there is only one case of isodensity being displayed only on the porphyrin core. These data suggest that the communication pathway between the two porphyrins is similar in the porphyrin array regardless of the addition of zinc.

The HOMO-LUMO energy gap of freebase dimer (2.58 eV) is shorter than that of the monomers by $\leq$0.10 eV. However, it has a slightly larger energy gap than either of its zinc-inserted analogues, which suggests that the two porphyrins are communicating within the array

and lowering the energy gap in comparison to the monomers. **1ZnD** has an energy gap of 0.04 eV narrower compared to the freebase dimer and **2ZnD** has an energy gap of 0.02 eV narrower compared to the freebase dimer.

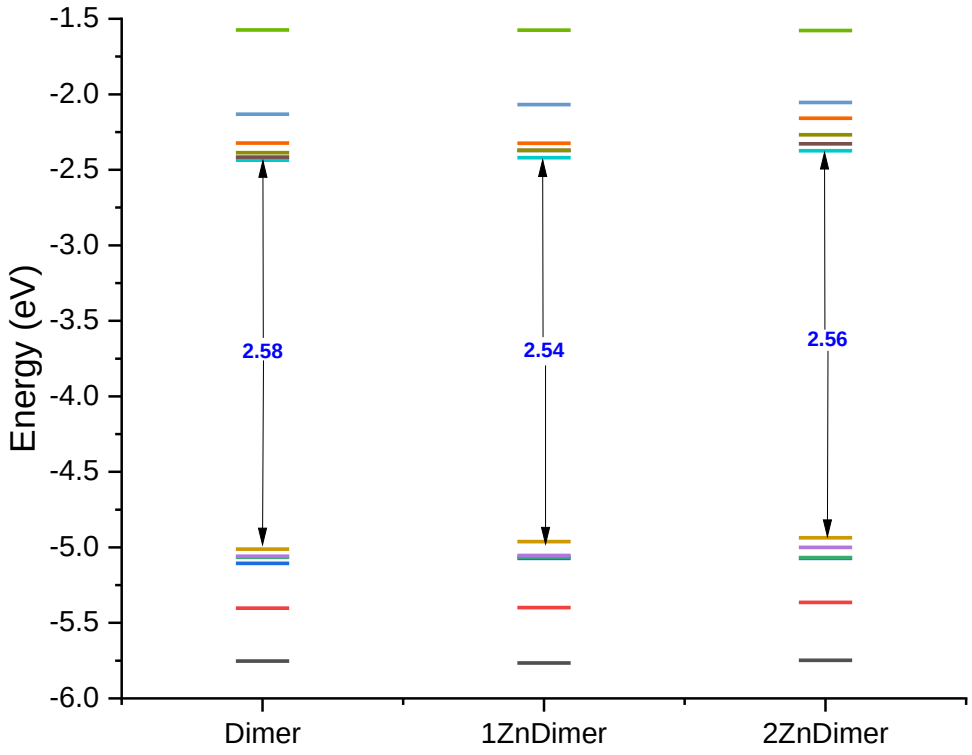

Figure 3.12: HOMO-LUMO energy diagram of Dimers

It was attempted to obtain isodensity surfaces for the trimer molecules, however, molecular orbitals have not been able to be generated using the DFT method mentioned earlier in this section. After discussion with our collaborator Dr. Khetrapal at the University of North Texas, it was determined that for an unknown reason data to build an isodensity surface was missing although the energy-level diagram information was present. Computational orbital diagrams for the trimer will be performed in the future.

The freebase trimer has a narrower HOMO-LUMO energy gap (2.53 eV) compared to any of the monomers (difference of $\leq$0.15 eV) and by a lesser margin, the dimers. In terms of

the freebase dimer there was an energy difference of 0.05 eV when compared to the trimer but only a 0.01 eV difference compared to **1ZnD**. The energy gap of the freebase trimer, **1ZnT** and **3ZnT** show very similar HOMO-LUMO energy gaps (2.53 eV). As a result, the one-thousandth decimal place was included. **2ZnT** experiences the smallest energy gap at 2.48 eV.

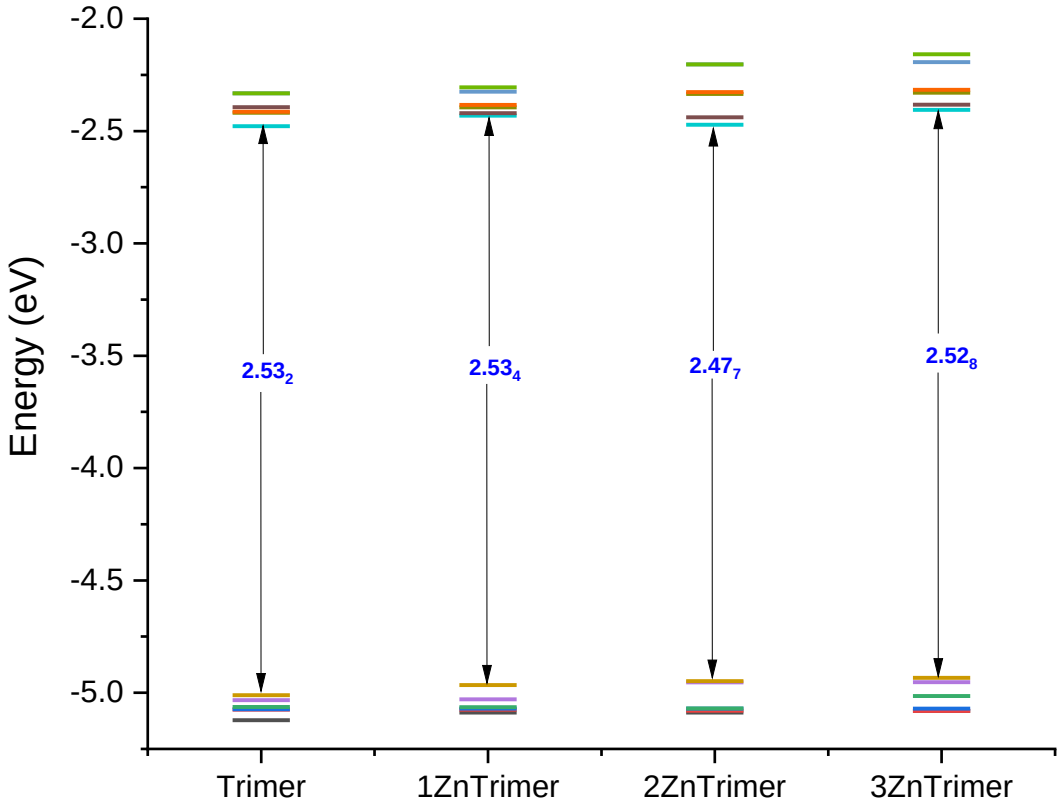

Figure 3.13: HOMO-LUMO energy diagram of Trimers

3.4.2 TDDFT Studies

TDDFT calculations for the synthesized porphyrins were performed, and the orbital transitions and oscillator strengths were obtained. For the monomers only three excited states were resolved; however, for the dimer and trimers six excited states were resolved based on the DFT isodensity plots. A complete oscillator table (tables 1-13) for each of the synthesized compounds could be found in the experimental section 3.7.4.

HOMO-1/LUMO (599 nm, 51%) and HOMO/ LUMO (562 nm, 53%) account for the primary transition of **FBr2VTP** corresponding to the Q bands followed by HOMO/LUMO+1 (599 nm, 48%) and HOMO-1/ LUMO+1 (562 nm, 46 %). The Q bands of the zinc inserted analogue, **ZnFBr2VTP**, predominantly arise from the HOMO/LUMO (578 nm, 67%) and HOMO-1/LUMO (565 nm, 54%) transitions; HOMO/ LUMO+1 also contributes (45%) more for the Q band around 565 nm. **mPEBp** shows HOMO-1/LUMO (603 nm, 45%), HOMO-1/LUMO+1 (567 nm, 46%), HOMO/LUMO+1 (603 nm, 43%) and HOMO/LUMO (567 nm, 43%) as the main transitions contributing to the Q bands. **bPEBP** experiences almost equal contributions of HOMO-1/LUMO (46.5%) and HOMO/LUMO+1 (47%) for the Q band around 607 nm. For the Q band around 571 nm, more contribution comes from HOMO-1/LUMO+1 (53%) than from HOMO/LUMO (43%). For **ZnbPEBp**, the HOMO/LUMO transition contributes the most (65%) to the Q band near 586 nm while HOMO/LUMO+1 (57%) contributes more to the Q band around 579 nm.

For the dimers, multiple orbitals contribute to the percent probability around the Q band; more so than those of the monomers resulting in a smaller percent contribution for each. Q band around 605 nm of the freebase dimer has the highest percent probability (29%) coming from the HOMO-1/LUMO+2 transition followed by HOMO-3/ LUMO (16%) and HOMO/LUMO (12%). Q band around 602 experiences more contribution from HOMO-2/LUMO+3 (38%), followed by HOMO/ LUMO+1 (25%). HOMO-2/ LUMO+2 and HOMO-1/LUMO transitions equally contribute (22%) to the Q band at 572 nm. HOMO-2/ LUMO+1 (29%) and HOMO/LUMO+3 (28%) also contributes almost the same for Q band at 566 nm. **1ZnD** Q bands have their major contributions predominately from HOMO-2/ LUMO+2 (602 nm, 28% and 566 nm, 36%), HOMO-1/LUMO (602 nm, 27%), HOMO/LUMO+1 (578 nm, 42%), HOMO/LUMO+3

(569 nm, 22%) and HOMO-3/LUMO+1 (569 nm, 29%). **2ZnD** experiences contributions from HOMO/ LUMO (578 nm, 32%), HOMO/ LUMO+1 (574 nm, 38%), HOMO-2/LUMO (568 nm, 28%), and HOMO-3/ LUMO+1 (32%).

It is interesting to note the orbital contributions of the trimers begin to show larger contributions from a wider range (e.g HOMO-3 to LUMO+5). The freebase trimer shows major contributions to the Q band from HOMO-3/LUMO (608 nm, 39%), HOMO-2/LUMO+4 (602 nm, 25%), HOMO-4/ LUMO+5 (601 nm, 24%), and the HOMO/LUMO (579 nm, 36%) transitions. **1ZnT** has the Q band major contributions coming from transitions: HOMO-3/LUMO+5 (601 nm, 20%), HOMO/LUMO+3 (582 nm, 44%), and HOMO/LUMO+2 (579 nm, 27%). **2ZnT** Q band contributions are a result of HOMO-3/LUMO (608 nm, 42%), HOMO-5/LUMO (580 nm, 37%), and HOMO-1/ LUMO+2 (573 nm, 33%) transitions. **3ZnT** showed most of the percent probability arising from HOMO/LUMO+1 (582 nm, 28%), HOMO/LUMO (579 nm, 35%), and HOMO-1/LUMO +3 (574 nm, 20%).

3.5 Aromaticity Studies

3.5.1 NICS [Small Molecule Comparisons to Chapter 2]

All NICS and AICD computational studies were performed with Gaussian16 [7] using the same parameters mentioned in Chapter 2 of this dissertation. The basis set used for NICS was GIAO B3LYP/6-31g(d,p) and all data was graphed on Origin software. AICD plots were calculated and plotted with the same basis set and program as mentioned in the previous chapter. As done in chapter 2, the NICS and AICD data were obtained for the small thiophene molecules without the porphyrin first. The two small molecules computationally modelled were the

mono-*p*-diethynylbenzene thiophene moiety (mPEBTh) and the bis-analogue (bPEBTh). In both cases, the Bq dummy atoms were placed from -5 to 5 Å at 0.2 Å intervals.

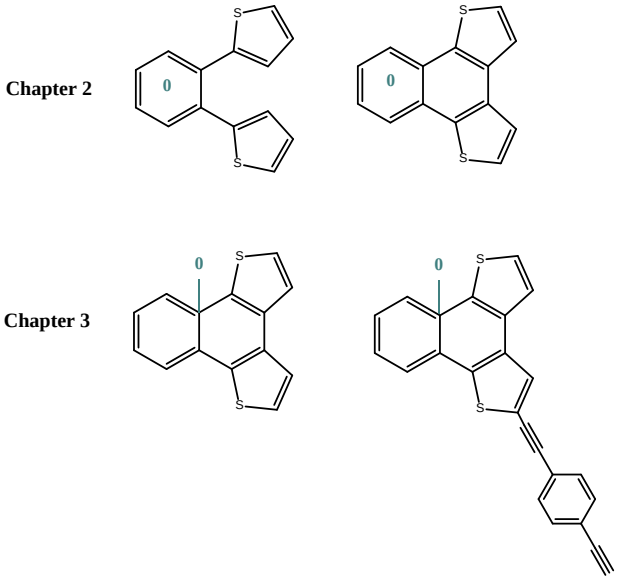

Figure 3.14: Comparison of chapter 2 and chapter 3 molecules and the placement of the dummy atom at 0 Å.

In this section we will discuss the two compounds and compare them to the small molecules in chapter 2. In the previous chapter there were no additional functional groups to consider and so the dummy atom at 0 Å was placed at the center of the benzene ring to better compare the unfused and the fused analogues. However, the dummy atom location for this chapter had to be adjusted to account for the placement of the PEB group on the molecule; therefore, the geometric center had been moved to the center of the naphthalene ring, for both the new molecules and **F2VT**, to get a better understanding of how that functional group affects the aromaticity. Not only will we compare the aromaticity based on the original placement of the dummy atoms in chapter 2 but also in whether there is a large difference in changing the origin point for chapter 3.

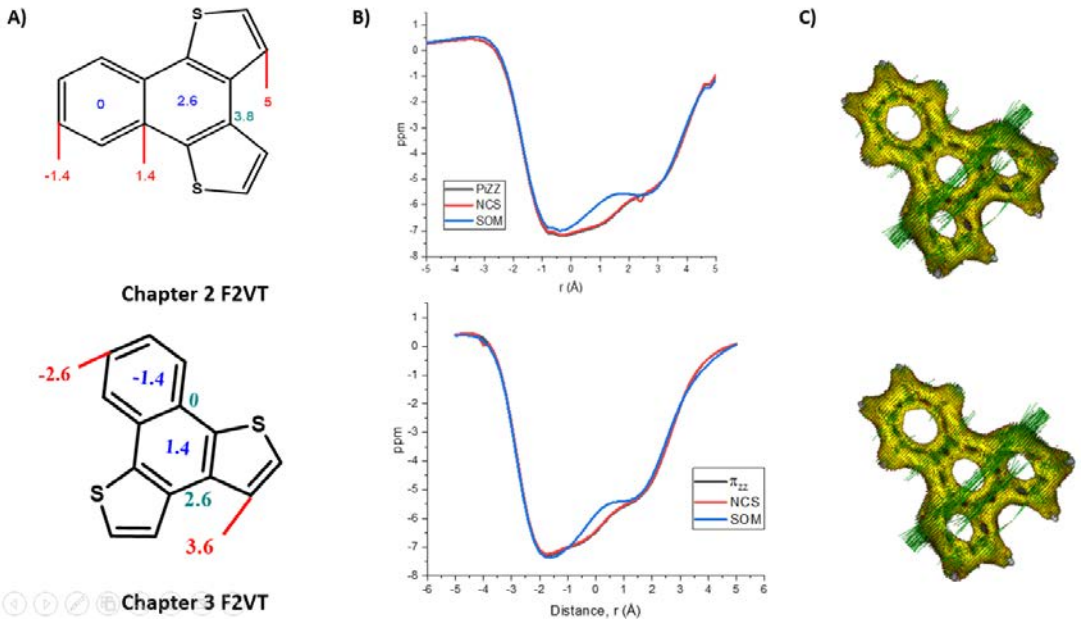

Figure 3.15: Aromaticity studies of small molecule F2VT; a) highlighted dummy atoms and specific distances; red indicates a dummy atom on the edge of a ring; blue indicates a dummy atom placed center of a ring and teal indicates a dummy atom over C-C bond; b) shows the plotted NICS$_{xscan}$ studies using all three methodologies; c) shows the AICD plots.

Figure 3.15a shows the location of the important dummy atoms for **F2VT** chapter 2 and chapter 3 datasets that were recorded; for all ppm values see table 13-14 in section 3.7.5 of the experimental section. The geometric center of chapter 3 **F2VT** ($NICS_{\pi zz}$ -6.47 ppm) data compared to that of chapter 2 **F2VT** ($NICS_{\pi zz}$ -6.47 ppm) has a very minimal difference of 0.011 ppm. However, as we get further away from the geometric center the difference in ppm between the two data sets becomes larger. The difference at the first benzene ring is 0.0646 ppm while the second benzene ring's difference is 0.39 ppm. The edge of the thiophene ring shows a difference of 0.0785 ppm. Despite the ppm values having some differences, it shows that the aromatic trend does not drastically change with the placement of the geometric center for similar molecules. The NICS plots for chapter 2 and chapter 3 **F2VT** display similar shapes, despite the geometric center being different. Both $\underline{\pi_{zz}}$ and NCS identical shapes for each;

however, chapter 2 has a small peak around 2.5 ppm which is not seen in chapter 3. The SOM data also shows a similar trend of increased and decreased aromaticity compared to the other two methods. In the case of chapter 3 **F2VT**, a marginal increase can be observed in aromaticity around -1.5 ppm and a decrease in aromaticity around 0-1 ppm. This is different from the **F2VT** SOM data in chapter 2 which shows a very mild decrease in aromaticity around -1 ppm and a very slight increase around 3 ppm. Overall, chapter 3's **F2VT** NICS data appears smoother and could be attributed to the placement of the geometric center being in the middle of two fused rings. As expected, the AICD plots, Figure 3.15c, for the structure are the same.

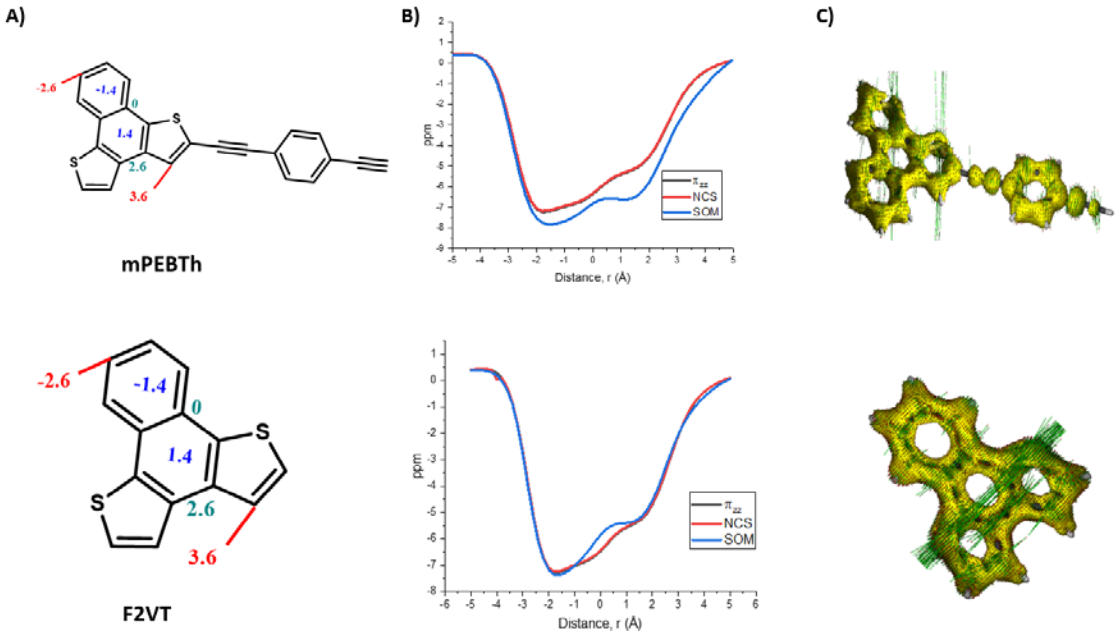

Figure 3.16: Aromaticity studies of small molecule mPEBTh. a) highlighted dummy atoms and specific distances for each molecule; red indicates a dummy atom on the edge of a ring; blue indicates a dummy atom placed center of a ring and teal indicates a dummy atom over C-C bond; b) shows the plotted $NICS_{xscan}$ studies using all three methodologies; c) shows the AICD plots.

For the NICS study of **mPEBTh**, all three NICS methodologies show a similar trend in which from -5 to -2.5 Å there is a gradual decrease from nonaromatic to weak aromatic character; this aromatic character remains from -2 to 3 Å before it begins to increase back to

nonaromatic character from 3 to 5 Å. Figure 3.16A shows the location of the important dummy atoms for **mPEBTh** that were recorded. Much like **F2VT** in chapter 2 and 3, the geometric center for **mPEBTh** *(*$\mathrm{NICS}_{\pi zz}$-6.36 ppm) show the second strongest aromatic character whereas the first benzene ring, located at -1.4 Å ($NICS_{\pi zz}$-7.13 ppm) shows the strongest. The second benzene ring, located at 1.4 Å, of **mPEBTh** ($NICS_{\pi zz}$ -5.20 ppm) exhibits the third highest aromatic character before it begins tapering off in nonaromatic character. The ppm values obtained from **mPEBTh** are lower than those obtained from the **F2VT** data obtained for chapter 2 and 3.

When comparing **mPEBTh** to **F2VT** NICS from chapter 2's graph, we can see that there is a very slight increase (1 Å difference) in aromatic character upon the addition of the PEB group. Furthermore, the aromatic character occurs earlier for **mPEBTh** (at -2.5 Å) than it did for chapter 2's **F2VT** NICS (-1 Å). The NICS_{SOM} data also shows more aromatic character for **mPEBTh** but overall, the shapes of the two graphs are comparable. This suggests that the addition of PEB only mildly affects the aromaticity of the small molecule.

The naptho-fused thiophene moieties exhibit a global current in the AICD plot in Figure Figure 3.16c. However, the PEB molecule seems to have isolated density on the ethylene bridge and benzene ring. While one of the ethyne linkers seems to exhibit minor inclusion within the benzene's aromaticity, the other one is excluded. This would indicate that the aromaticity may not be fully delocalized across the whole molecule but isolated between the two moieties. This could explain why the addition of the PEB group to the thiophene moiety seemed to slightly decrease the NICS ppm values. However, this does not necessarily mean that there is no global aromaticity at work or that the two groups do not communicate. **mPEBTh** AICD plot does show

full incorporation of the sulfur atoms into the overall global aromaticity very much like it does with **F2VT**.

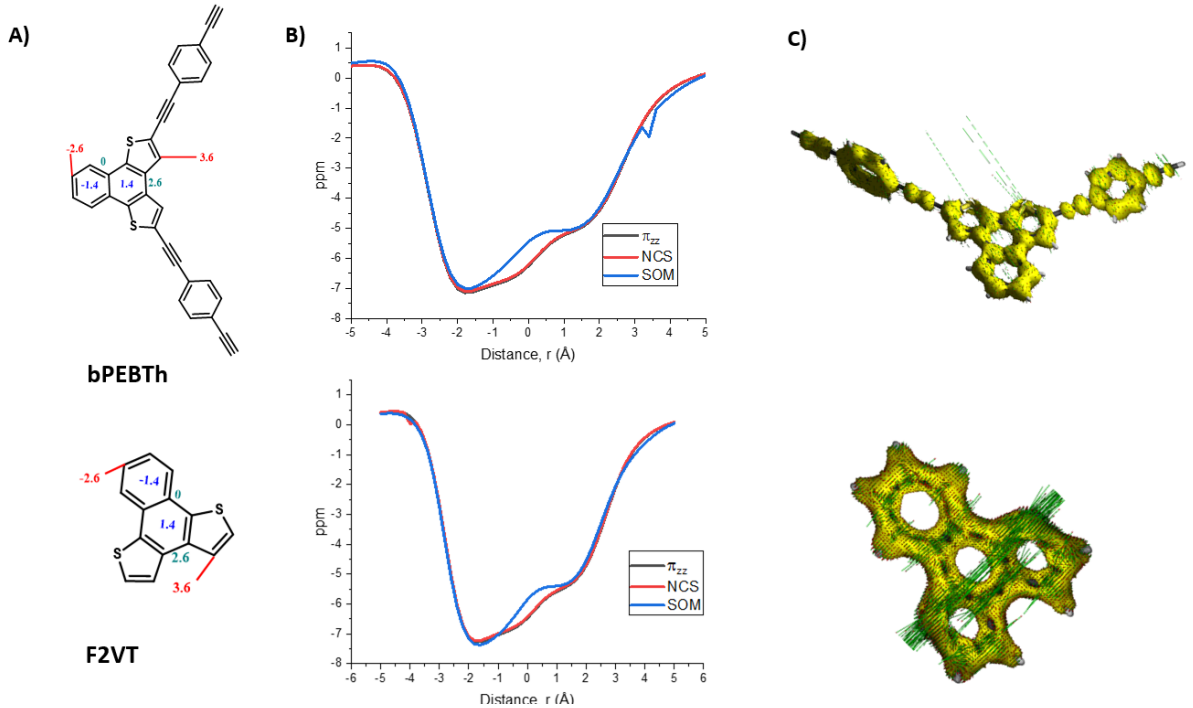

Figure 3.17: Aromaticity studies of small molecule bPEBTh; a) highlighted dummy atoms and specific distances; red indicates a dummy atom on the edge of a ring; blue indicates a dummy atom placed center of a ring and teal indicates a dummy atom over C-C bond; b) shows the plotted $NICS_{xscan}$ studies using all three methodologies; c) shows the AICD plots.

When comparing **bPEBTh** to **F2VT** NICS from chapter 2's graph, there is little change in the aromatic character and in the overall shape of the graph. All three NICS methodologies still show a similar trend in which from -5 to -2 Å there is a gradual decrease from nonaromatic to weak aromatic character; this aromatic character remains from -2 to 2 Å before it begins to increase back to nonaromatic character from 2 to 5 Å. The aromatic character does occur earlier for **bPEBTh** (at -2 Å) than it did for chapter 2's **F2VT** NICS (-1 Å) but at the same position (at -2 Å) for chapter 3's **F2VT**.

Figure 3.17a shows the location of the important dummy atoms for **mPEBTh** that were recorded. Again, repeated locations occur at -1.4, 0, 1.4, 2.6 Å for **bPEBTh** and **F2VT**. Similarly, to **mPEBTh** the different values that do occur are most likely due to the placement of the origin as mentioned previously. Once again, the ppm values only show a slight change for the same locations occurring on the two molecules. Much like **F2VT** and **mPEBTh** mentioned above, the geometric center for **bPEBTh** $NICS_{\pi zz}$-6.25 ppm) show the second strongest aromatic character whereas the first benzene ring, located at -1.4 Å ($NICS_{\pi zz}$-7.05 ppm) shows the strongest. The second benzene ring, located at 1.4 Å, of **mPEBTh** ($NICS_{\pi zz}$-5.03 ppm) exhibits the third highest aromatic character before it begins tapering off in nonaromatic character. The ppm values obtained from **bPEBTh** are lower than those obtained from **F2VT** and **mPEBTh**. This data further supports that the aromatic trend persists with similar molecules; it also suggests that the naphthalene ring is the dominant aromatic structure within the structure.

Similarly, the AICD plot in Figure 3.17c shows the naptho-fused thiophene moieties having a global current, however the PEB molecules still show to have the same isolated density on the ethyne linkers and benzene ring. As mentioned before this indicates that the aromaticity may not be fully delocalized across the whole molecule. Just like **mPEBTh** and **F2VT**, the sulfur atoms are also included in the current density.

NICS was not conducted on the monomers nor the dimer and trimer compounds within this report. There are two reasons for this: 1) upon the addition of PEB groups, although the overall structure is extended but not necessarily within the same plane 2) All dimers and trimers exhibit a similar computationally obtained geometry shown in Figure 3.18. As a result,

the ability to obtain accurate NICS-XY-scan data for **mPEBp, bPEBp, ZnPEBp**¸ and the dimer and trimer analogues would be difficult.

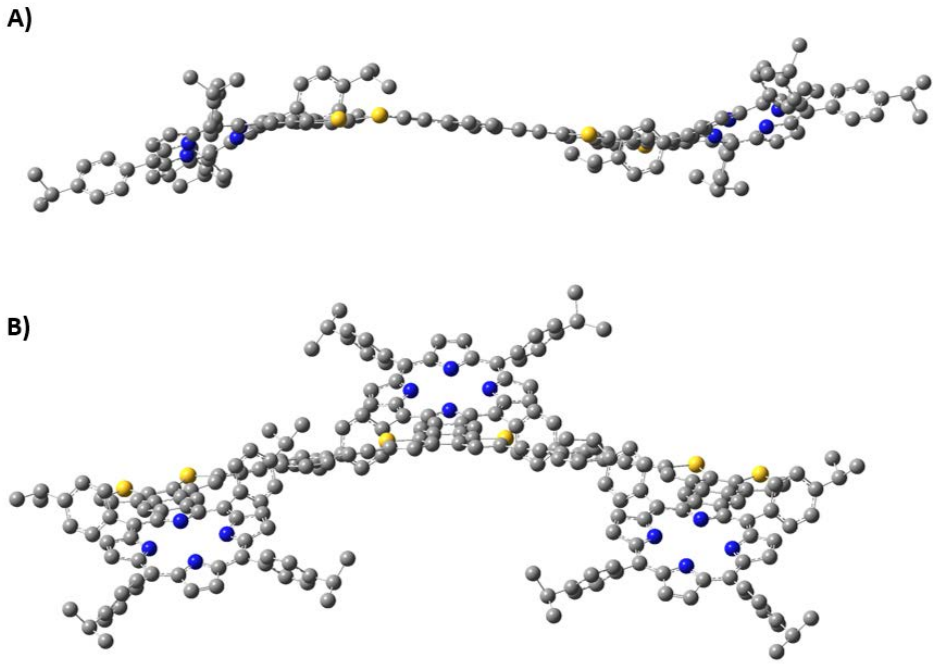

Figure 3.18: Computationally optimized geometry of a) dimer and b) trimer.

Based on the data obtained here and from the DFT, TDDFT, and the fluorescence data, global aromaticity is still possible and communication between molecules may still occur, most likely in the excited state. Therefore, future work on this would include both computational and experimental characterization.

3.5.2 AICD Studies

As mentioned earlier, an accurate NICS study would be difficult to obtain on the synthesized compounds due to geometric constraints. Instead, AICD computational studies were conducted to analyze the aromatic character of the synthesized compounds.

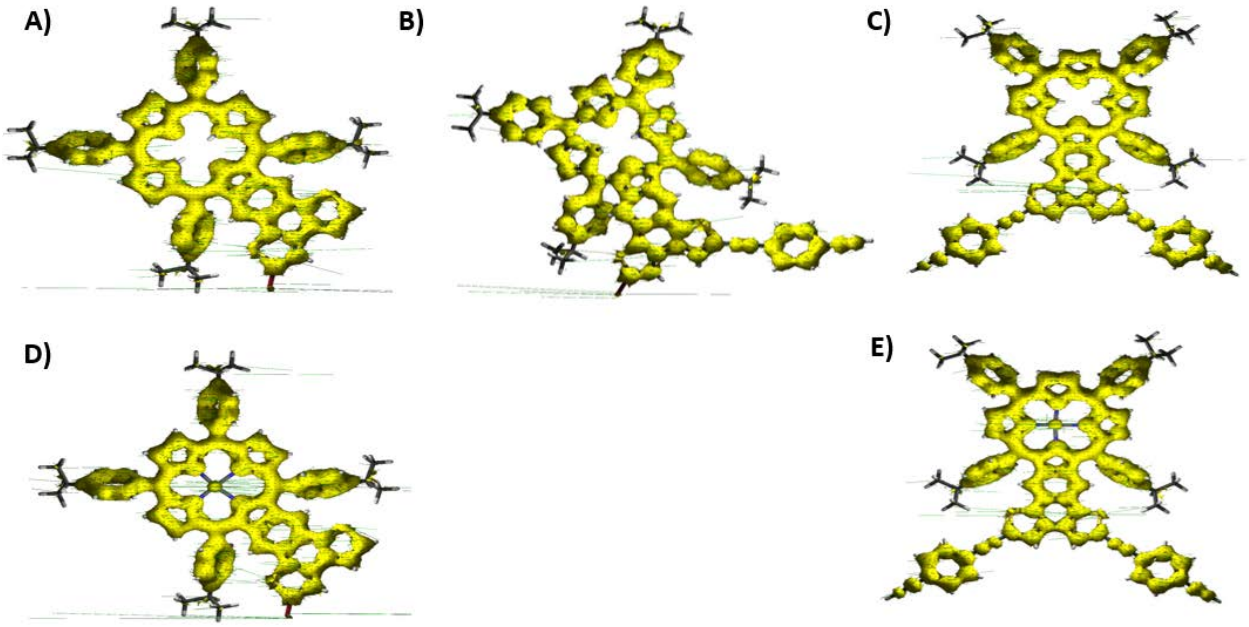

Figure 3.19: AICD of monomers. a) FBr2VTP, b) mPEBp, c) bPEBp, d) ZnBr2VTP, and e) ZnbPEBp.

As expected, all monomers show global aromaticity on the extended porphyrin core. Unlike the AICD in chapter 2, the sulfur atoms are incorporated into the global aromaticity for all the monomers. **FBr2VTP** (Figure 3.19a) and its zinc analogue (Figure 3.19d) show the naphthothiophenyl moiety being fully integrated into the global aromaticity while the bromine atom is excluded. Like the small molecules **mPEBTh** and **bPEBTh**, the PEB group added to **mPEBp** (Figure 3.19c), **bPEBp** (Figure 3.19d) and **ZnbPEBp** (Figure 3.19e) demonstrate a localized aromaticity in which they do not interact with the naphthodithiophenyl-fused porphyrin core. Unlike the small molecules, both ethyne linkers and the benzene ring appear to have isolated densities present. In these porphyrins, the thiophenes show some density indicating their participation in the global aromaticity. The naphthodithiophenyl-fused porphyrins with two PEB groups attached show more density on the thiophene rings compared to their mono-PEB counterpart. This indicates that the PEB groups do nominally contribute to the global aromaticity of the entire molecule.

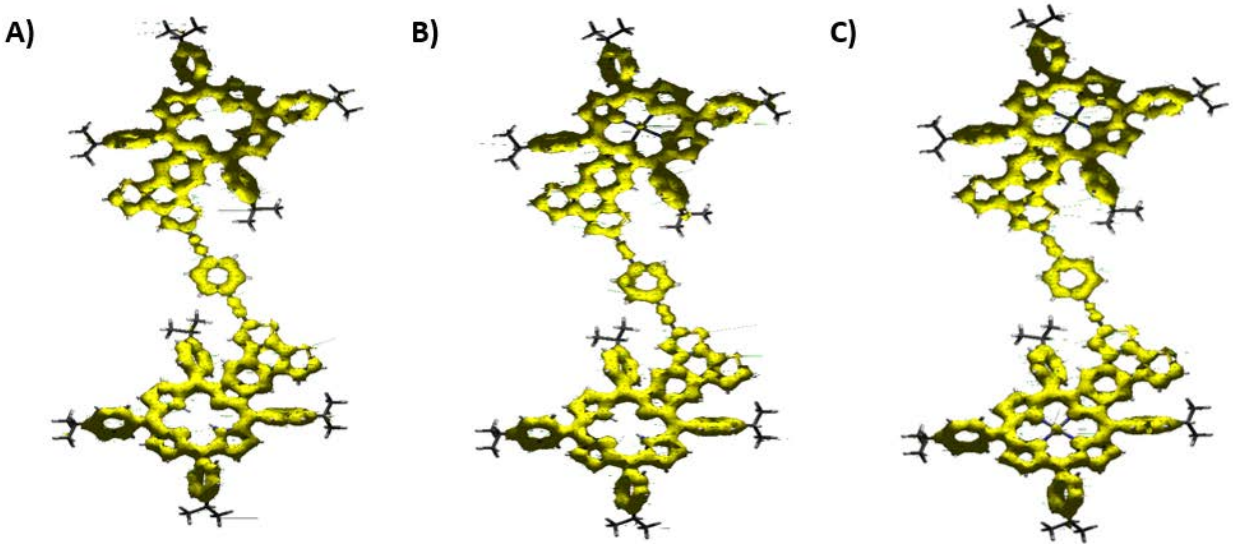

Figure 3.20: AICD of dimers a) freebase dimer, b) 1ZnD, and c) 2ZnD.

The dimer analogues show a similar trend – the porphyrin core is fully delocalized and the PEB linker mostly exhibits isolated density from the porphyrin. The sulfur atoms for all three porphyrins return to exhibiting little to no density as seen in chapter 2. However, there are differences within the PEB linker between three dimer analogues. The freebase dimer (Figure 3.20a) shows two globes of density on each side of the ethyne group; the one linking to the bottom porphyrin seems to have slight overlap of density within the middle of the ethyne group. We suspect that the globe shape reflects the "pulling" of current density from the attached groups, resulting in a node of weak current density within the two globe shapes.

1ZnD (Figure 3.20b) exhibits the same density placement as its freebase analogue except for the ethyne linking to the zinc inserted porphyrin which displays no globe shapes, but complete delocalization along the group. In the case of both porphyrins the ethyne groups do not demonstrate any interaction with the benzene moiety. This is not the case for **2ZnD** (Figure 3.20c) as the ethyne linker for the top porphyrin does show nominal interaction with the benzene ring. The shape of the density on this ethyne group resembles that of bottom ethyne

linkers in the dimer and **1ZnD** analogues. The bottom ethyne linker in **2ZnD** exhibits a distorted globe shape with minor density located near the benzene ring and most of the density facing towards the bottom zinc inserted porphyrin.

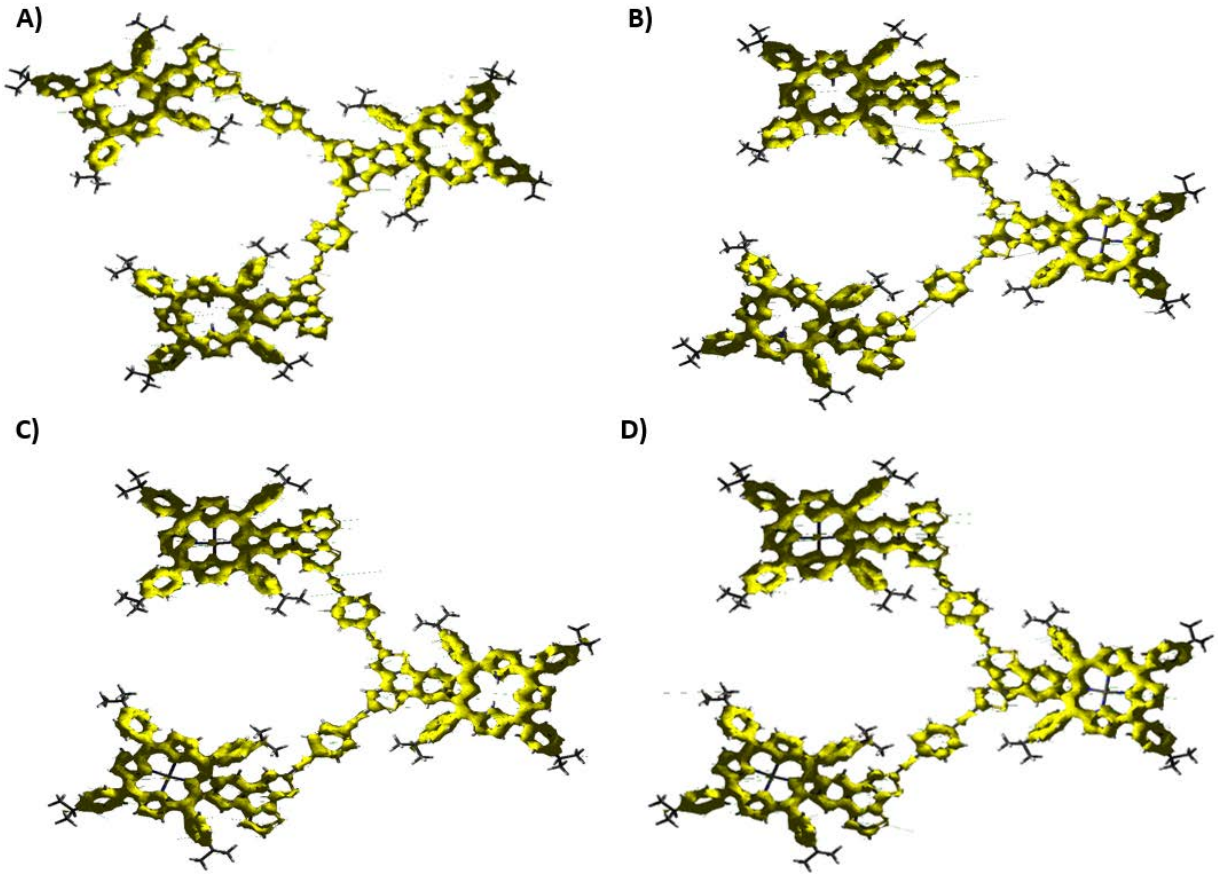

Figure 3.21: AICD of trimers a) freebase trimer, b) 1ZnT, c) 2ZnT, and d) 3ZnT.

Like the dimers, trimers exhibit a similar pattern to the current density. The porphyrins are fully covered apart from the sulfur atoms in the thiophene moiety. The PEB linkers also seem to mostly display localized aromaticity within itself but ultimately differ between each trimer. The top PEB group of freebase trimer (Figure 3.21a) exhibits a delocalized current not only with the benzene ring but also with the center porphyrin's thiophene moiety; there is little density on the second ethyne linker heading towards the top porphyrin and indicates some communication between these two porphyrins. Despite this, the top porphyrin and its upper

thiophene motif displays global aromaticity within itself with only mild density present on the thiophene ring connected to the ethyne linker. The bottom porphyrin within the trimer exhibits a global aromaticity. The PEB linker connecting it to the center porphyrin shows a similar trend to the previously mentioned porphyrins, namely the separation of density between the ethyne groups and benzene groups from each other and the porphyrin cores. The two ethyne groups display similar globe shape patterns to those discussed for the dimers.

Unlike its freebase analogue, **1ZnT** (Figure 3.21b) shows that there is no current density interaction between the PEB group, and the top or central zinc inserted porphyrin. All porphyrin moieties do display global aromaticity along the porphyrin core and to the thiophene moieties; with density excluded from the sulfur atoms only in the zinc inserted porphyrin. Both the ethyne linker heading from the top porphyrin to the central porphyrin and the ethyne group connected to the bottom porphyrin exhibit little current density. The remaining ethyne linkers exhibit either a globe shape at each end of the group or a uniform cylindrical shape. Regardless, a return to isolated density of the PEB groups within this compound is obvious, suggesting minimal to no communication between the three porphyrins.

2ZnT (Figure 3.22C) shows current density along all three of the porphyrin cores and through the thiophene rings with minor density on the sulfur atoms. The PEB linker between the top zinc inserted porphyrin and the central freebase porphyrin shows current density along the ethyne linker closest to the freebase porphyrin with the thiophene ring. The remaining ethyne linker and the benzene ring show the expected isolated current density. That is not the case for the second PEB linker in which the entire linker displays a current density with most of it showing towards the central freebase porphyrin.

3ZnT (Figure 3.21d) exhibits similar current density patterns to those of **1ZnT**. However, the ethyne groups exhibit more current density. The ethyne linkers in for the top and central porphyrin have a globe like shape whereas the ones connected to the bottom porphyrin have a more cylindrical shape. Although global aromaticity is present along the porphyrin core, the sulfur atoms in all three porphyrins still experience little to no current density.

3.6 Conclusion

In conclusion, we have synthesized a total of seven β,β'-π-extended porphyrin arrays. Specifically, we have synthesized three dimer and four trimer porphyrin arrays in which zinc was placed. Experimental characterization including UV-VIS and fluorescence spectroscopy, and computational modelling with DFT, TDDFT and AICD plots were performed. Although NICS plots were carried out for the small molecules, due to the nonplanar geometry of the arrays NICS-xscan was not able to be performed on the porphyrin oligomers. However, AICD conducted showed global and local current density on both the porphyrin core and the diethnylbenzene linkers. TDDFT calculations suggest that for the monomer and dimer compounds the primary transitions contributing to the Q bands are from HOMO -1 to LUMO +1 and variations therein. However, for the trimers, the primary transitions are composed o f a wider range of orbital contributions such as HOMO -5 to LUMO. To better understand these porphyrin arrays further characterization must be explored. We are currently working with our collaborator Dr. Francis D'Souza at the University of North Texas to perform other experimental characterizations such as transient absorption spectroscopy and cyclic voltammetry.

3.7 Experimental Section

3.7.1 General Information

All reagents, including solvents, not specified below was purchased from Millipore-Sigma, Matrix-Scientific, Ambeed, and Fisher and—excluding DMF which was dried through a commercially available purification system—was used without further purification. All porphyrin products underwent purification via recrystallization and column chromatography. All reactions were monitored with UV-VIS spectroscopy, thin-layer chromatography and crude ^{1}H NMR on a Varian 500 MHz NMR. The UV-VIS spectra were recorded with an Agilent Carry 5000 UV/VIS/NIR spectrometer with samples in CH_2Cl_2. All NMR spectra were recorded on a 500 MHz (^{1}H NMR)/126 MHz (^{13}C NMR) spectrometer with $CDCl_3$ used as an internal standard (δ = 7.26 and 77.0 ppm respectively).

3.7.2 Synthesis and Characterization

dPAp

Procedure: **F2vtBr** (0.0173 mmol), CuI (0.000694 mmol), and $PdCl_2(PPh_3)_2$ (0.000346 mmol), were added to a Schlenk flask and placed under vacuum for 30 minutes before

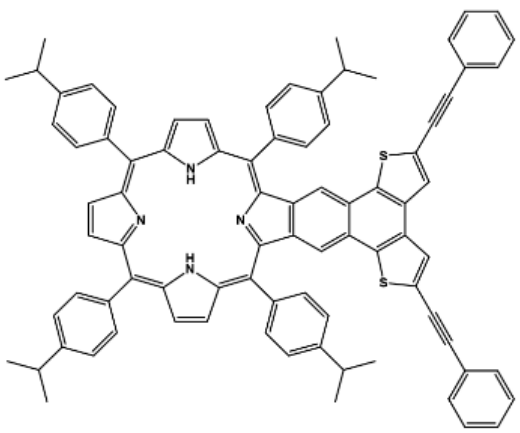

DMF/TEA (1:1 mixture) and phenylacetylene (0.01907 mmol) were added to the Schlenk flask under Ar. Solution was then heated to 40°C overnight. An aqueous work up with dichloromethane in brine, followed by deionized water was done and the resulting filtrate was recrystallized in dichloromethane and methanol.

$C_{84}H_{66}BrN_4S_2$; purple crystalline solid; yield 96%, ^{1}H NMR (500 MHz, cdcl$_3$) δ 8.89 (d, *J* = 4.9 Hz), 8.79 (d, *J* = 4.8 Hz), 8.70 (s), 8.21 (d, *J* = 7.7 Hz), 8.15 (d, *J* = 7.8 Hz), 8.11 (s), 7.82 (d, *J* = 7.7 Hz), 7.71 (s), 7.61 (d, *J* = 7.9 Hz), 7.56 (d, *J* = 4.8 Hz), 3.51—3.43 (m), 3.30—3.22 (m), 1.72 (s), 1.71 (s), 1.55 (s), 1.54 (s) , -2.36 (s).; ^{13}C NMR (500 MHz, $CDCl_3$) δ 139.43, 134.65, 133.72, 126.37, 125.25, 124.82, 123.02, 120.75, 77.27, 77.02, 76.77, 34.34, 34.13, 29.73, 24.42, 24.32, 1.04, UV/VIS (DCM): λ_{max}= 275, 313, 399, and 424, 449 (soret), 528, 561, 600, and 660 nm (Q bands).

Br2VTP

Procedure: **2VTP** (0.02 mmol) and recrystallized N-bromosuccinimide (0.02 mmol) was dissolved in $CHCl_2$ and sonicated for 30 sec before being quenched with triethylamine followed by an aqueous work up with deionized water. Recrystallize with dichloromethane and methanol (77% yield).

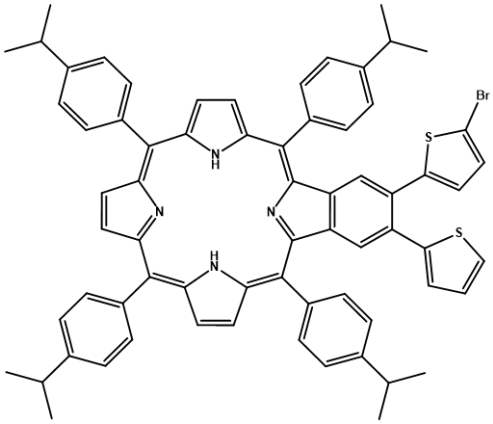

$C_{68}H_{59}BrN_4S_2$; purple crystalline solid; yield 74%,^{1}H NMR (500 MHz, cdcl$_3$) δ 8.90 (d, *J* = 4.9 Hz), 8.83 (d, *J* = 5.0 Hz), 8.72 (s), 8.13 (dd, *J* = 14.4, 7.9 Hz), 7.65 (s, *J* = 7.9 Hz), 7.61 (s, *J* = 7.9 Hz), 7.30 (s), 6.94 (dd, *J* = 5.1, 3.5 Hz), 6.80 (dd, *J* = 3.4, 1.1 Hz), 3.35—3.23 (m), 1.55 (s), 1.54 (s), 1.49 (s), 1.48 (s), -2.57 (s); ^{13}C NMR (500 MHz, $CDCl_3$) δ 149.22, 143.75, 139.82, 139.39, 134.67, 133.62, 127.12, 126.69, 125.95, 125.84, 124.81, 77.27, 77.01, 76.76, 34.29, 34.12, 29.72, 24.30.UV/VIS (DCM): λ_{max}=436, 484, 524, 600, and 654 nm (Q bands).

FBr2VTP

Procedure: **Br2VTP** (0.039 mmol) was dissolved in dry CH_2Cl_2. Ferric chloride (0.799 mmol) was dissolved in 1 mL nitromethane and added to the reaction solution slowly. It was allowed to react at room temperature for 15 min. Triethylamine was added to quench the reaction and was followed by an aqueous work up with deionized water. Recrystallized with dichloromethane and methanol (86% yield).

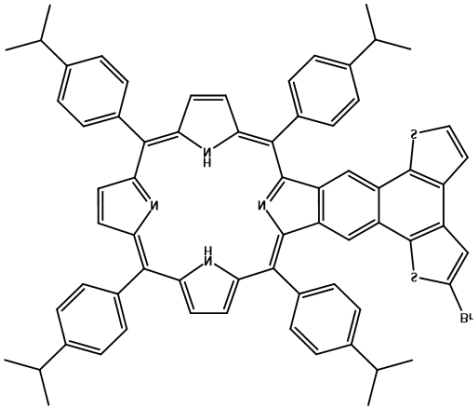

$C_{68}H_{57}BrN_4S_2$; purple crystalline solid; yield: 86%, ^{1}H NMR (500 MHz, cdcl$_3$) δ 8.90 (d, *J* = 4.9 Hz), 8.80 (d, *J* = 5.0 Hz), 8.71 (s), 8.22 (d, *J* = 8.0 Hz), 8.16 (d, *J* = 8.0 Hz), 8.12 (s), 7.83 (d, *J* = 7.9 Hz), 7.72 (d, *J* = 5.2 Hz), 7.62 (d, *J* = 4.1 Hz), 7.57 (d, *J* = 5.2 Hz), 3.50—3.39 (m), 3.33—3.20 (m), 1.73 (s), 1.72 (s), 1.55 (d, *J* = 2.1 Hz), -2.37 (s); ^{13}C NMR (500 MHz, $CDCl_3$) δ 149.15, 148.22, 139.87, 139.42, 134.64, 133.72, 133.31, 126.36, 125.24, 124.81, 123.01, 120.74, 79.41, 77.01, 76.76, 34.34, 34.12, 29.72, 24.41, 24.31, 0.01. UV/VIS (DCM): λ_{max}= 449, 529, 565, 605 and 661 nm (Q bands).

mPEBp

Procedure: **FBr-2VTP** (0.0307 mmol), CuI (0.000614 mmol), and $PdCl_2(PPh_3)_2$ (0.00122 mmol), and 1,4-diethynylbenzene (0.0307 mmol) were added to a Schlenk flask and placed under vacuum for 30 minutes before DMF/TEA (1:1 mixture). Solution was then heated to 40°C overnight. An aqueous work up with dichloromethane in brine, followed by deionized water was done and the resulting filtrate was recrystallized in dichloromethane and methanol.

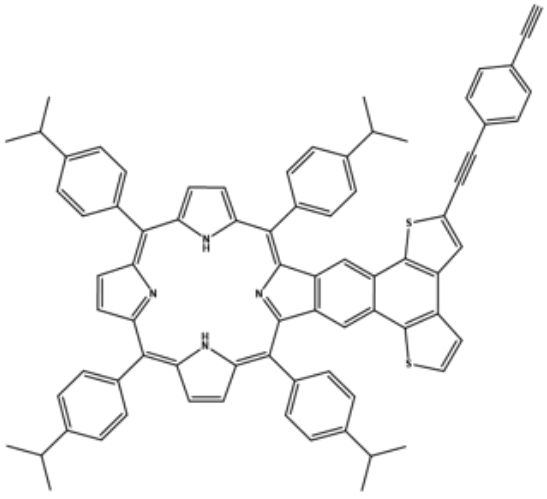

$C_{78}H_{62}N_4S_2$; purple crystalline solid; yield 80%; ^{1}H NMR (500 MHz, cdcl$_3$) δ 8.89 (d, *J* = 4.9 Hz), 8.79 (d, *J* = 4.8 Hz), 8.71 (s), 8.20 (d, *J* = 7.9 Hz), 8.15 (d, *J* = 7.9 Hz), 8.09 (s), 7.80 (d, *J* = 7.9 Hz), 7.65 (t, *J* = 5.8 Hz), 7.61 (d, *J* = 7.9 Hz), 7.53 (d, *J* = 5.1 Hz), 3.49—3.38 (m), 3.32—3.22 (m), 1.71 (s, 2H), 1.70 (s), 1.56 (s), 1.54 (s), -2.38 (s); ^{13}C NMR (500 MHz, $CDCl_3$) δ 149.28, 148.37, 140.01, 139.58, 136.93, 134.79, 133.86, 133.40, 127.31, 126.49, 125.37, 125.33, 124.96, 123.11, 121.50, 120.87, 116.61, 77.61, 77.41, 77.16, 76.91, 34.47, 34.27, 24.55, 24.46, 1.18, 0.16. UV/VIS (DCM): λ_{max}= 449, 528, 566, 606 and 658 nm.

bPEBp

Procedure: **F2vtBr** (0.0260 mmol), CuI (0.00104 mmol), and $PdCl_2(PPh_3)_2$ (0.000520 mmol), and 1,4-diethynylbenzene (0.130 mmol) were added to a Schlenk flask and placed under

vacuum for 24 minutes before DMF/TEA (1:1 mixture) was added to the Schlenk flask under Ar. Solution was then heated to 40°C overnight. A plug in 1:1 cyclohexane/CH_2Cl_2 was run and followed up by an aqueous work up with dichloromethane in brine, followed by deionized water was done and the resulting filtrate was recrystallized in dichloromethane and methanol.

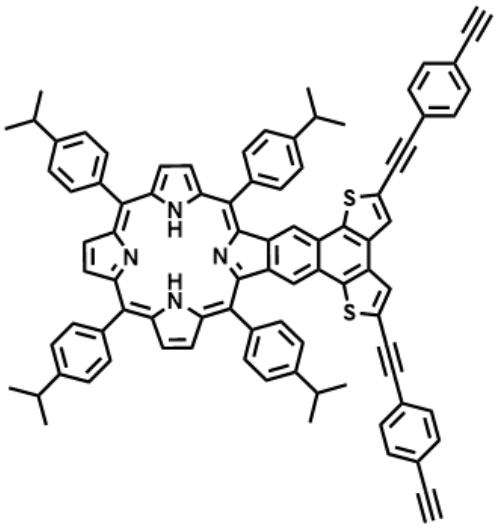

$C_{88}H_{66}BrN_4S_2$; purple crystalline solid; yield 90%, ^{1}H NMR (500 MHz, cdcl$_3$) δ 8.91 (d, *J* = 4.9 Hz), 8.81 (d, *J* = 4.8 Hz), 8.72 (s), 8.22 (d, *J* = 7.7 Hz), 8.17 (d, *J* = 7.8 Hz), 8.11 (s), 7.82 (d, *J* = 7.7 Hz), 7.63 (d, *J* = 7.8 Hz), 7.55 (d, *J* = 4.7 Hz), 3.50—3.39 (m), 3.31—3.20 (m), 1.73 (s), 1.72 (s), 1.57 (s), 1.56 (s), -2.37 (s); ^{13}C NMR (500 MHz, $CDCl_3$) δ 149.14, 148.22, 139.86, 139.43, 136.79, 134.65, 133.72, 133.38, 133.26, 127.77, 127.16, 126.35, 125.23, 125.19, 124.81, 122.97, 121.36, 120.72, 116.47, 77.27, 77.02, 76.76, 34.33, 34.13, 29.73, 24.41, 24.31, 1.04.UV/VIS (DCM): λ_{max}= 425 (shoulder), 449, 531, 565, 605, and 664 nm.

Dimer

Procedure: **FBr2VTP** (0.0133 mmol), mono-*p*-diethynylbenzene (0.0133 mmol), CuI (0.000535 mmol), and $PdCl_2(PPh_3)_2$ (0.00267 mmol) were added to a Schlenk flask and placed under vacuum for 15 minutes before DMF/TEA (1:1 mixture). Solution was then heated to 40°C overnight. An aqueous work up with dichloromethane in brine, followed by deionized water was done and the resulting filtrate was recrystallized in dichloromethane and methanol.

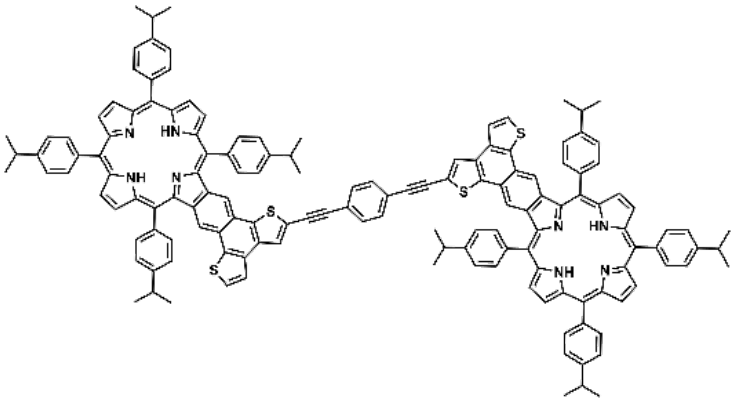

$C_{146}H_{118}N_8S_4$; purple crystalline solid; yield 89%; ^{1}H NMR (500 MHz, cdcl$_3$) δ 8.89 (d, *J* = 4.9 Hz), 8.79 (d, *J* = 4.9 Hz), 8.70 (s), 8.21 (d, *J* = 7.9 Hz), 8.15 (d, *J* = 8.0 Hz), 8.11 (s), 7.81 (d, *J* = 7.9 Hz), 7.71 (d, *J* = 5.0 Hz), 7.61 (d, *J* = 7.9 Hz), 7.56 (d, *J* = 5.1 Hz), 3.52—3.44 (m), 3.31—3.22 (m), 1.72 (s, 2H), 1.71 (s), 1.55 (s), 1.54 (s), -2.38 (s); ^{13}C NMR (500 MHz, $CDCl_3$) δ 149.30, 148.36, 140.01, 139.57, 136.97, 134.79, 133.86, 133.45, 126.51, 125.40, 124.95, 123.16, 121.52, 120.89, 116.62, 34.48, 34.27, 24.55, 24.46, 1.18, 0.15; UV/VIS (DCM): λ_{max}= 450 nm (Soret), 528, 568, 607 and 636 nm (Q bands).

Trimer

Procedure: **FBr2VTP** (0.0241 mmol), bis-*p*-diethynylbenzene (0.0121 mmol), CuI (0.000482 mmol), and $PdCl_2(PPh_3)_2$ (0.000241 mmol) were added to a Schlenk flask and placed under vacuum for 15 minutes before DMF/TEA (1:1 mixture). Solution was then heated to 40°C overnight. An aqueous work up with dichloromethane in brine, followed by deionized water was done and the resulting filtrate was recrystallized in dichloromethane and methanol.

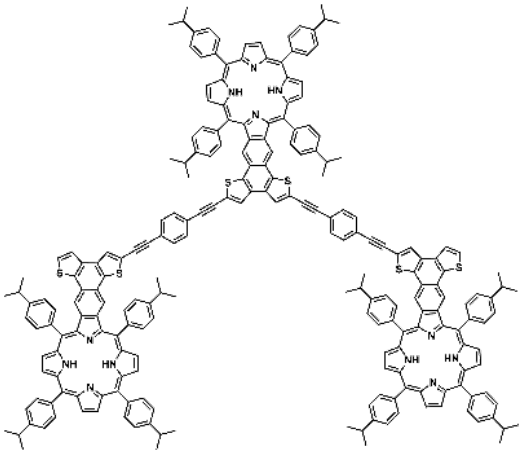

$C_{224}H_{178}N_{12}S_6$; purple crystalline solid; yield: 95%, ^{1}H NMR (500 MHz, cdcl$_3$) δ 8.89 (d, *J* = 4.9 Hz), 8.79 (d, *J* = 4.9 Hz), 8.71 (s), 8.20 (d, *J* = 7.9 Hz), 8.15 (d, *J* = 7.9 Hz), 8.09 (s), 7.81 (d, *J* = 7.9 Hz), 7.67 (d, *J* = 5.1 Hz), 7.61 (d, *J* = 7.9 Hz), 7.53 (d, *J* = 5.1 Hz), 3.55—3.43 (m), 3.31—3.22 (m), 1.71 (s), 1.70 (s), 1.55 (s), 1.54 (s), -2.39 (s); ^{13}C NMR (500 MHz, $CDCl_3$) δ 149.14, 148.22, 139.86, 139.43, 136.80, 134.65, 133.72, 133.27, 127.16, 126.35, 125.23, 125.20, 124.82, 122.98, 121.36, 120.73, 116.47, 77.27, 77.02, 76.76, 34.33, 34.13, 29.73, 24.41, 24.32, 1.04, 0.02. UV/VIS (DCM): λ_{max}= 401 and 426 (right shoulders), 449 (soret), 529, 563, 605, and 659 nm (Q bands).

Zn-Inserted Compounds

All of the compounds below were obtained by dissolving 0.01 mmol of porphyrin and $Zn(OAc)_2$ (10 eq, 0.1 mmol) in 3:1 $CHCl_3$/MeOH and refluxing for 1h. MeOH was then added and the reaction mixture was placed in an ice bath to recrystallize to give the final products.

ZnFBr2VTP

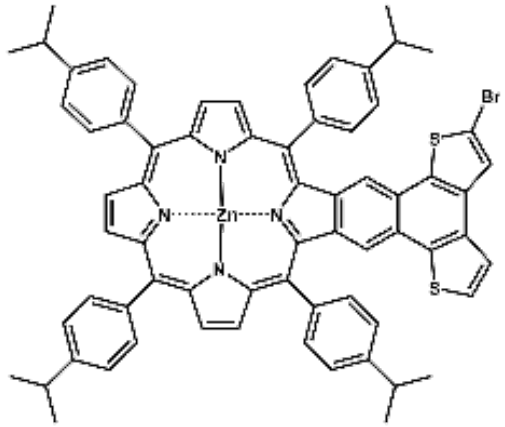

$C_{68}H_{55}N_4S_2BrZn$; purple crystalline solid; yield: 96%,^{1}H NMR (500 MHz, cdcl$_3$) δ 8.93 (d, *J* = 4.6 Hz), 8.84 (s), 8.77 (d, *J* = 4.6 Hz), 8.32 (s), 8.15 (dd, *J* = 18.0, 7.8 Hz), 7.81 (d, *J* = 7.8 Hz), 7.67 (d, *J* = 5.2 Hz), 7.59 (d, *J* = 7.7 Hz), 7.54 (d, *J* = 5.1 Hz), 3.51—3.42 (m), 3.36—3.24 (m), 1.73 (s), 1.72 (s), 1.54 (s); ^{13}C NMR (500 MHz, $CDCl_3$) δ 152.58, 149.60, 148.98, 148.53, 148.11, 146.57, 140.71, 140.22, 138.54, 136.79, 134.44, 133.37, 132.23, 131.07, 130.67, 126.39, 125.40, 125.28, 124.76, 123.23, 123.09, 121.06, 117.07, 34.47, 34.26, 24.56, 24.47, 1.18, 0.16.; UV/VIS (DCM): λ_{max}= 453 nm (Soret), 573 and 616 nm (Q bands).

ZnbPEBp

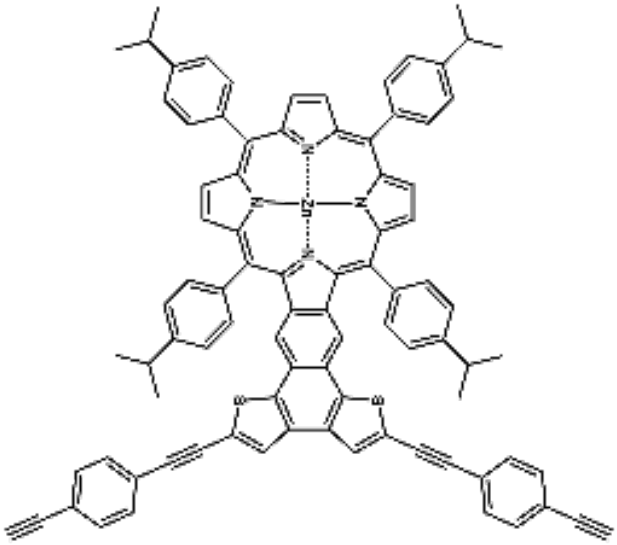

$C_{88}H_{64}N_4S_2Zn$; purple crystalline solid; yield: 89%, ^{1}H NMR (500 MHz, cdcl$_3$) δ 8.93 (d, *J* = 4.7 Hz), 8.84 (s), 8.78 (d, *J* = 4.6 Hz), 8.34 (s), 8.18 (d, *J* = 7.7 Hz), 8.13 (d, *J* = 7.7 Hz), 7.82 (d, *J* = 7.7 Hz), 7.71 (d, *J* = 5.1 Hz), 7.58 (dd, *J* = 14.2, 6.4 Hz), 3.53 – 3.47 (m), 3.30 – 3.22 (m), 1.74 (s), 1.72 (s), 1.56 (s), 1.54 (s); UV/VIS (DCM): λ_{max}= 453 nm (Soret), 575 and 617 (Q bands).

1ZnD

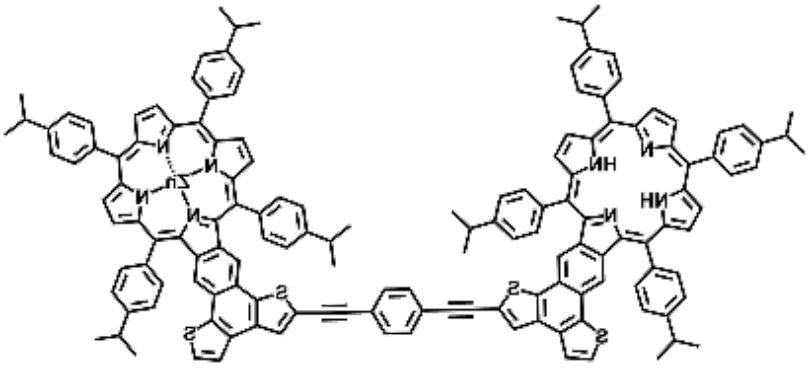

$C_{146}H_{114}N_8S_4Zn$; purple crystalline solid; yield: 92%, ^1H NMR (500 MHz, cdcl$_3$) δ 8.93 (d, *J* = 4.6 Hz), 8.89 (d, *J* = 4.8 Hz), 8.84 (s), 8.78 (dd, *J* = 11.2, 4.7 Hz), 8.70 (s), 8.31 (s), 8.20 (d, *J* = 7.9 Hz), 8.15 (dd, *J* = 15.9, 7.9 Hz), 8.09 (s), 7.82 (d, *J* = 1.9 Hz), 7.80 (s), 7.67 (dd, *J* = 10.4, 5.2 Hz), 7.60 (t, *J* = 7.6 Hz), 7.54 (d, *J* = 5.1 Hz), 3.50—3.41 (m), 3.36—3.24 (m),, 1.73 (s, 2H), 1.72 (s), 1.70 (s), 1.54 (s), -2.39 (s); ^{13}C NMR (500 MHz, $CDCl_3$) δ 134.79, 134.43, 133.86, 133.36, 126.49, 126.41, 125.37, 124.95, 124.76, 123.12, 77.41, 77.16, 76.90, 34.47, 34.26, 24.55, 24.46, 0.15; UV/VIS (DCM): λ_{max}= 451 nm (Soret), 528, 571, and 605 nm (Q bands).

2ZnD

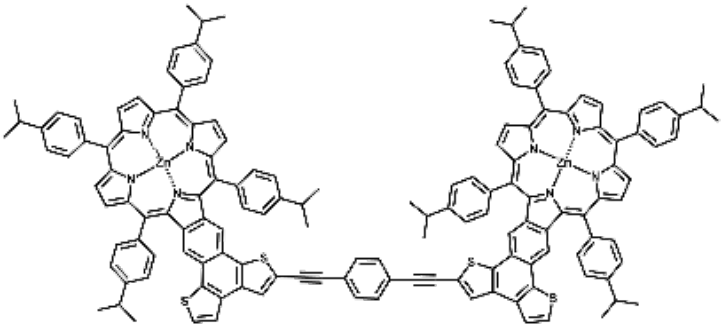

$C_{146}H_{112}N_8S_4Zn_2$; purple crystalline solid; yield: 95%, ^1H NMR (500 MHz, cdcl$_3$) δ 8.93 (d, *J* = 4.6 Hz), 8.84 (s), 8.77 (d, *J* = 4.6 Hz), 8.29 (s), 8.15 (dd, *J* = 12.2, 7.8 Hz), 7.81 (d, *J* = 7.7 Hz), 7.60 (d, *J* = 7.4 Hz), 7.49 (d, *J* = 5.0 Hz), 3.52—3.41 (m), 3.35—3.22 (m), 1.73 (s), 1.71 (s), 1.56 (s), 1.54 (s); ^{13}C NMR (500 MHz, $CDCl_3$) δ 152.45, 149.47, 148.85, 148.39, 147.98, 146.46, 140.54, 140.05, 138.37, 136.63, 134.29, 133.23, 133.15, 132.10, 130.94, 130.53, 126.26, 125.26, 125.14, 124.63, 123.11, 122.93, 120.93, 116.95, 77.26, 77.01, 76.76, 34.32, 34.11, 24.41, 24.32, 1.03; UV/VIS (DCM): λ_{max}= 451 nm (Soret), 530, 568, 608 and 658 nm (Q bands).

1ZnT

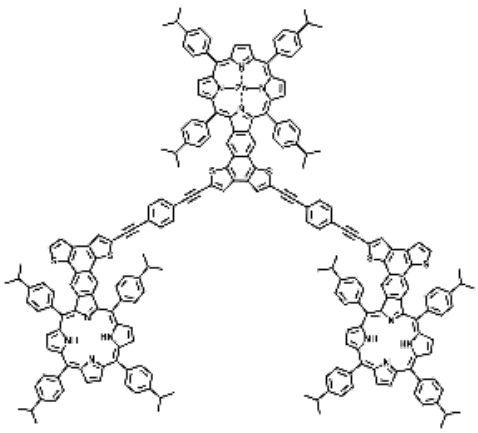

$C_{224}H_{176}N_{12}S_6Zn$; purple crystalline solid; yield: 80%, ^1H NMR (500 MHz, cdcl$_3$) δ 8.93 (d, *J* = 4.7 Hz), 8.89 (d, *J* = 5.0 Hz), 8.84 (s), 8.79 (d, *J* = 4.9 Hz), 8.77 (d, *J* = 4.7 Hz), 8.70 (s), 8.21 (d, *J* = 7.9 Hz), 8.15 (d, *J* = 8.0 Hz), 8.11 (s), 7.82 (d, *J* = 7.9 Hz), 7.72 (d, *J* = 5.2 Hz), 7.61 (d, *J* = 7.8 Hz), 7.56 (d, *J* = 5.1 Hz), 3.51—3.52 (m), 3.34—3.25 (m), 1.72 (s), 1.71 (s), 1.55 (s), 1.54 (s), -2.38 (s); ^{13}C NMR (500 MHz, $CDCl_3$) δ 149.47, 149.14, 148.57, 148.21, 139.86, 136.81, 134.64, 133.71, 133.29, 126.35, 124.80, 120.73, 116.47, 109.98, 34.33, 34.11, 24.40, 24.30; UV/VIS (DCM): λ_{max}= 452 nm (Soret), 529, 573 and 605 nm (Q bands).

2ZnT

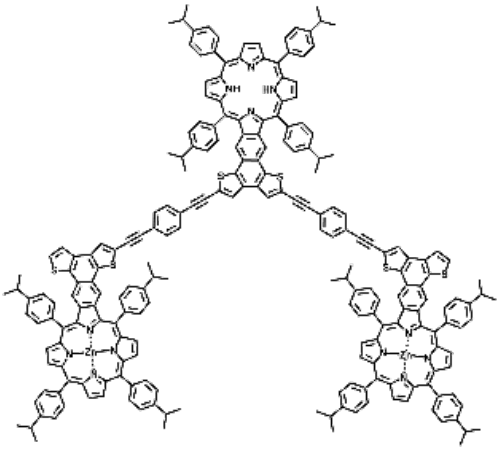

$C_{224}H_{174}N_{12}S_6Zn_2$; purple crystalline solid; yield: 82%, ^{1}H NMR (500 MHz, cdcl$_3$) δ 8.93 (d, *J* = 4.6 Hz), 8.89 (d, *J* = 4.9 Hz), 8.84 (s), 8.78 (dd, *J* = 9.6, 4.7 Hz), 8.70 (s), 8.32 (d, *J* = 3.6 Hz), 8.21 (d, *J* = 7.6 Hz), 8.15 (dd, *J* = 16.2, 8.2 Hz), 8.10 (s), 7.81 (d, *J* = 7.7 Hz), 7.64 – 7.58 (m), 7.54 (s), 3.52—3.41 (m), 3.33—3.21 (m), 1.73 (s), 1.72 (s), 1.70 (s), 1.54 (s), -2.39 (s); UV/VIS (DCM): λ_{max}= 452 nm (soret), 529, 573, and 609 nm (Q bands).

3ZnT

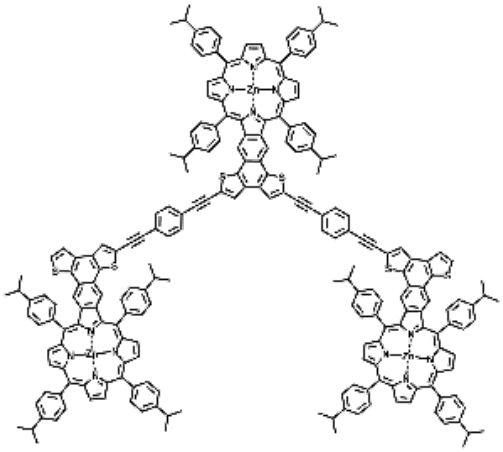

$C_{224}H_{172}N_{12}S_6Zn_3$; purple crystalline solid; yield: 90%, ^{1}H NMR (500 MHz, cdcl$_3$) δ 8.93 (d, *J* = 4.6 Hz), 8.84 (s), 8.77 (d, *J* = 4.6 Hz), 8.31 (s), 8.15 (dd, *J* = 16.7, 7.9 Hz), 7.81 (d, *J* = 7.9 Hz), 7.65 (d, *J* = 5.2 Hz), 7.60 (d, *J* = 7.9 Hz), 7.53 (d, *J* = 5.1 Hz), 3.50—3.39 (m), 3.34—3.23 (m), 1.73 (s), 1.72 (s), 1.56 (s), 1.54 (s); ^{13}C NMR (500 MHz, CDCl$_3$) δ 136.67, 134.28, 140.54, 140.04, 138.39, 152.46, 149.47, 148.86, 148.39, 147.98, 146.46, 133.22, 132.11, 130.94, 130.53, 126.27, 125.18, 124.62, 123.12, 116.96, 34.32, 34.11, 29.71, 24.41, 24.32; UV/VIS (DCM): λ_{max}= 452 nm (Soret), 578 and 611 nm (Q bands).

3.7.3 NMR Spectra

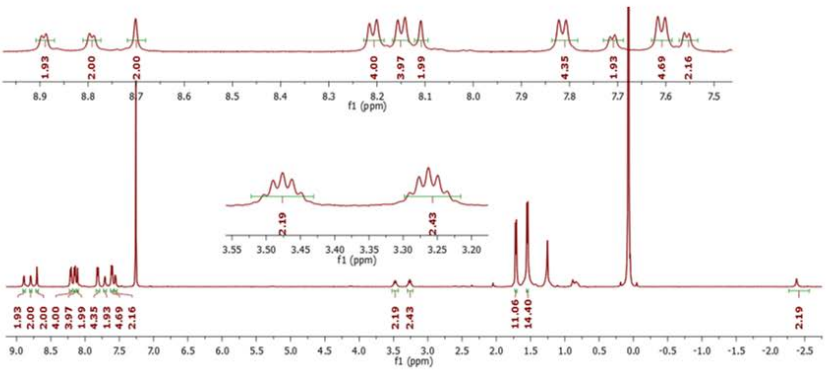

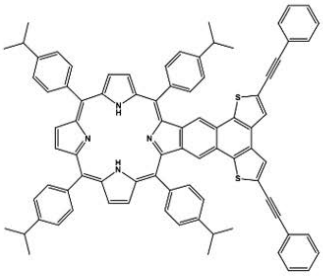

Figure 3.22: dPAp

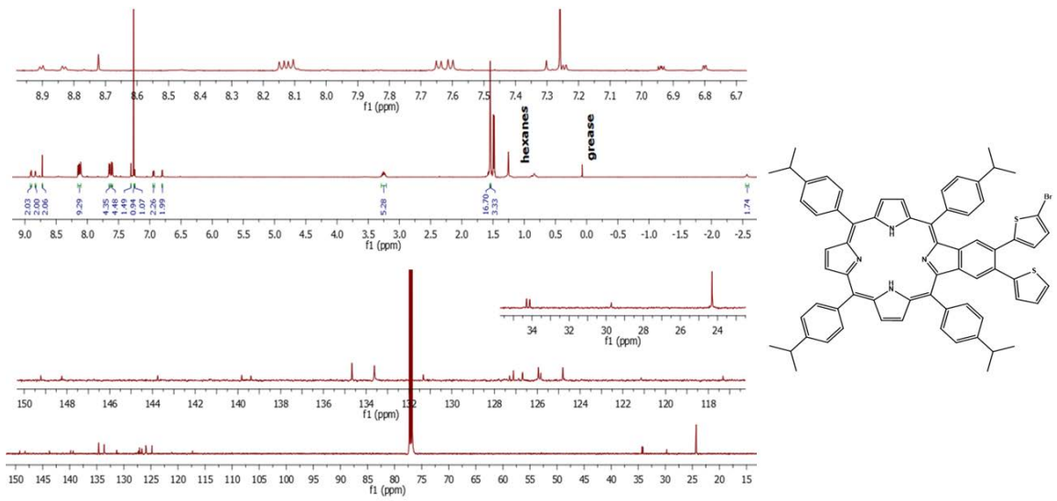

Figure 3.23: Br2VTP

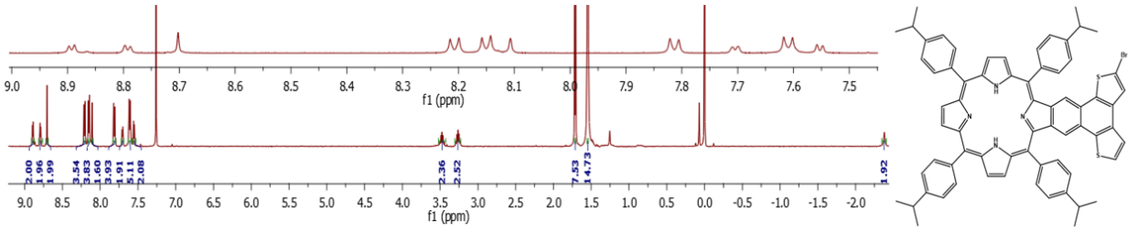

Figure 3.24: FBr2VTP

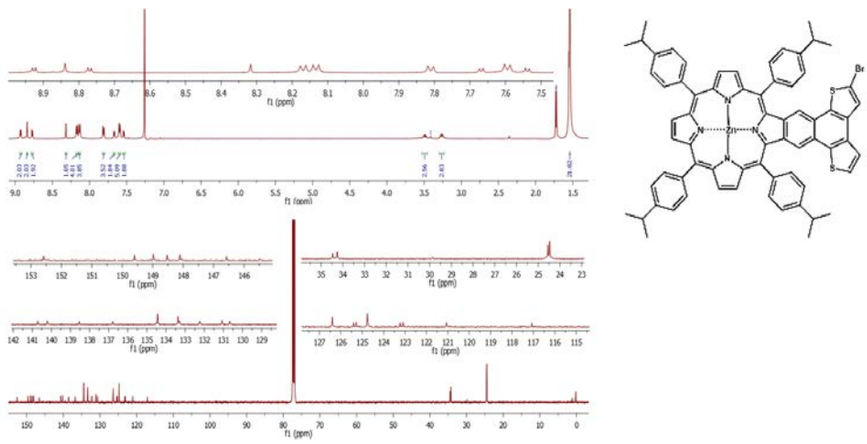

Figure 3.25: ZnFBr2VTP

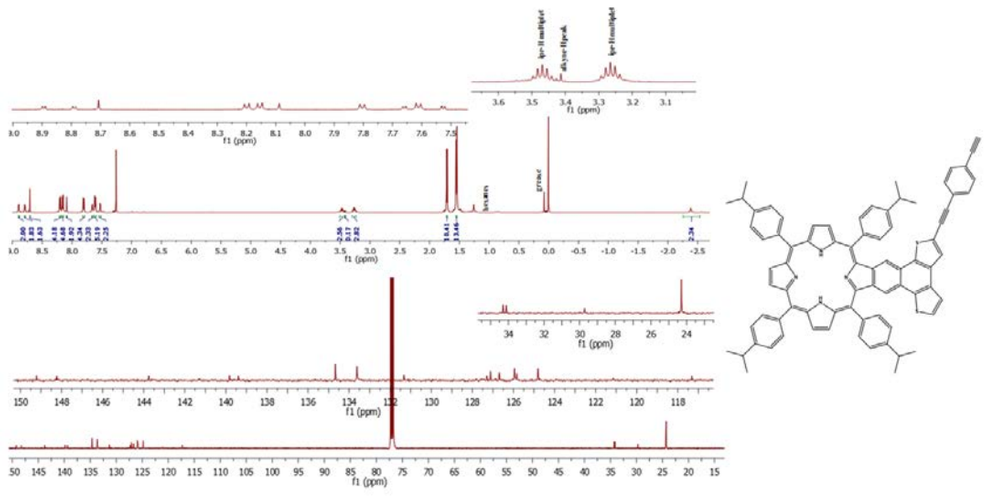

Figure 3.26: mPEBp

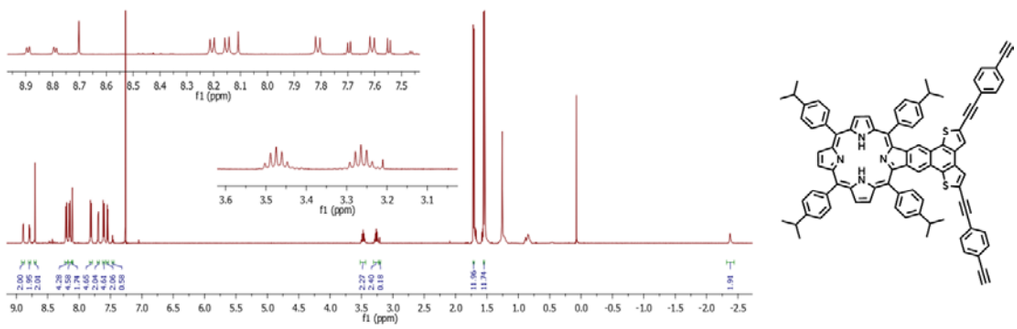

Figure 3.27: bPEBp

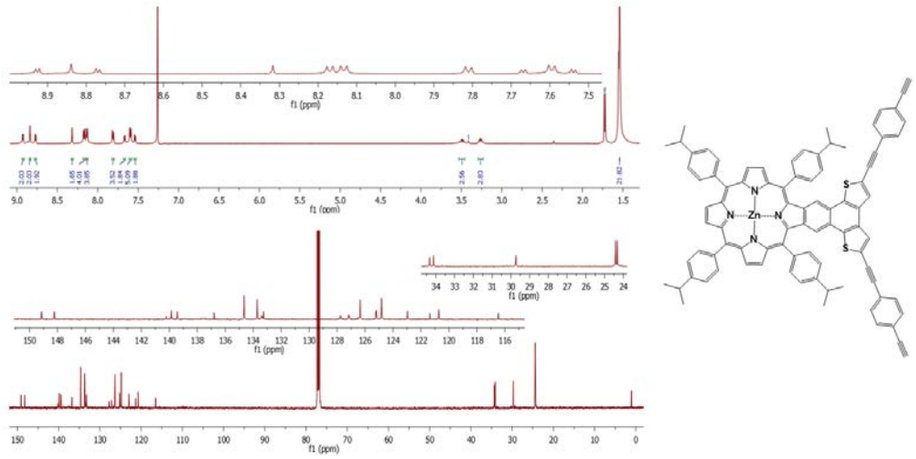

Figure 3.28: ZnbPEBp

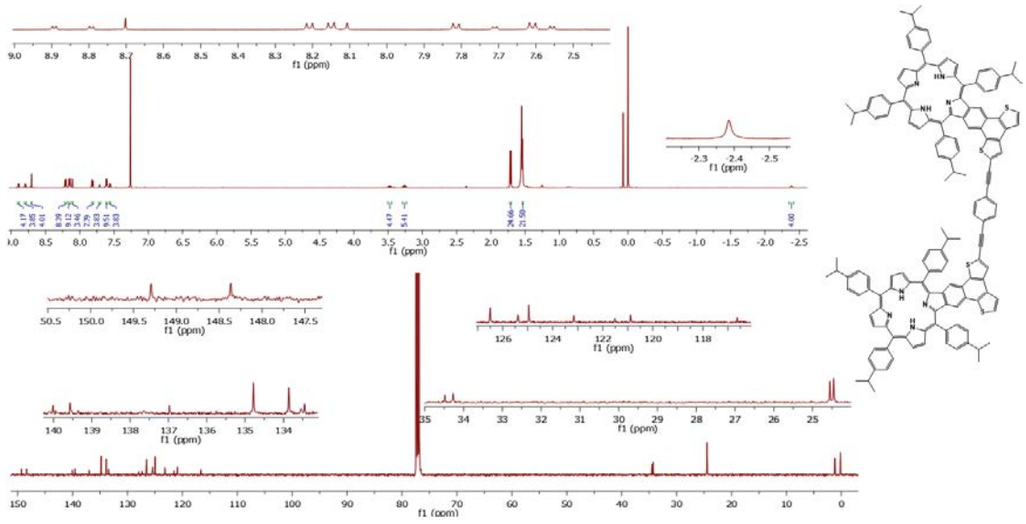

Figure 3.29: Dimer

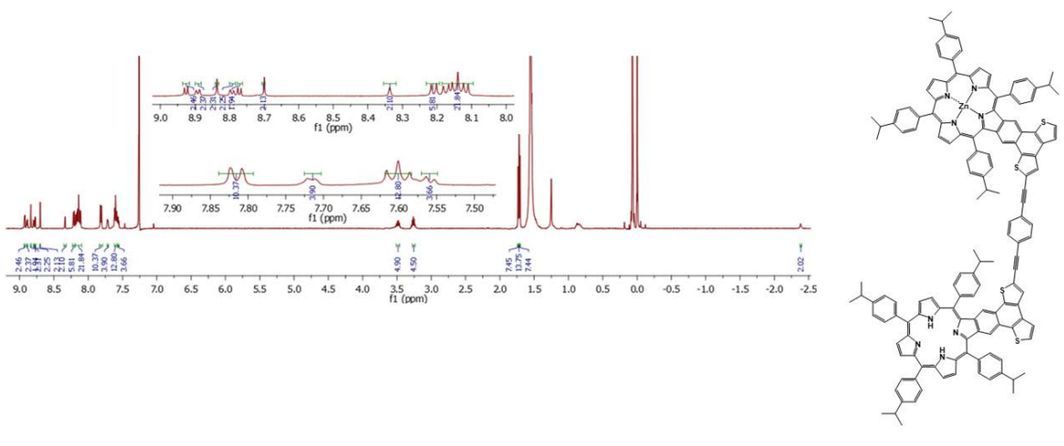

Figure 3.30: 1ZnD

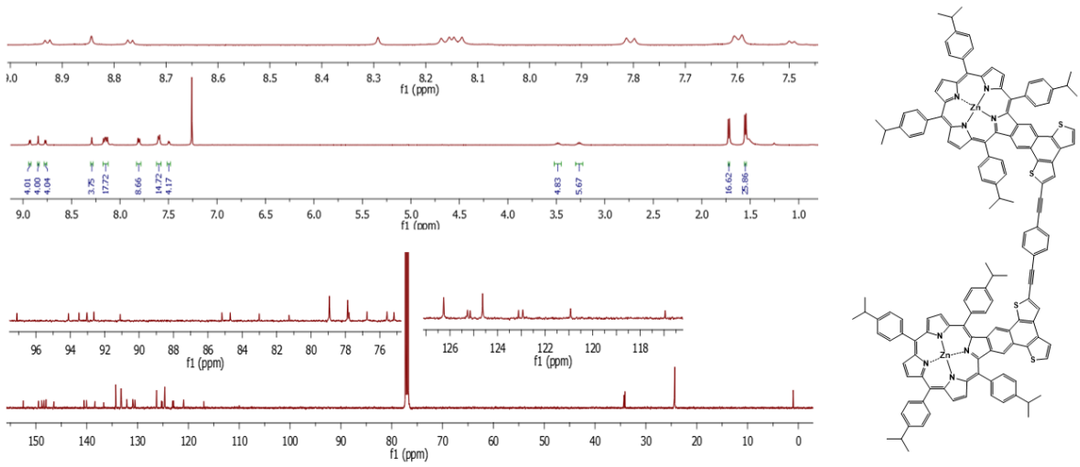

Figure 3.31: 2ZnD

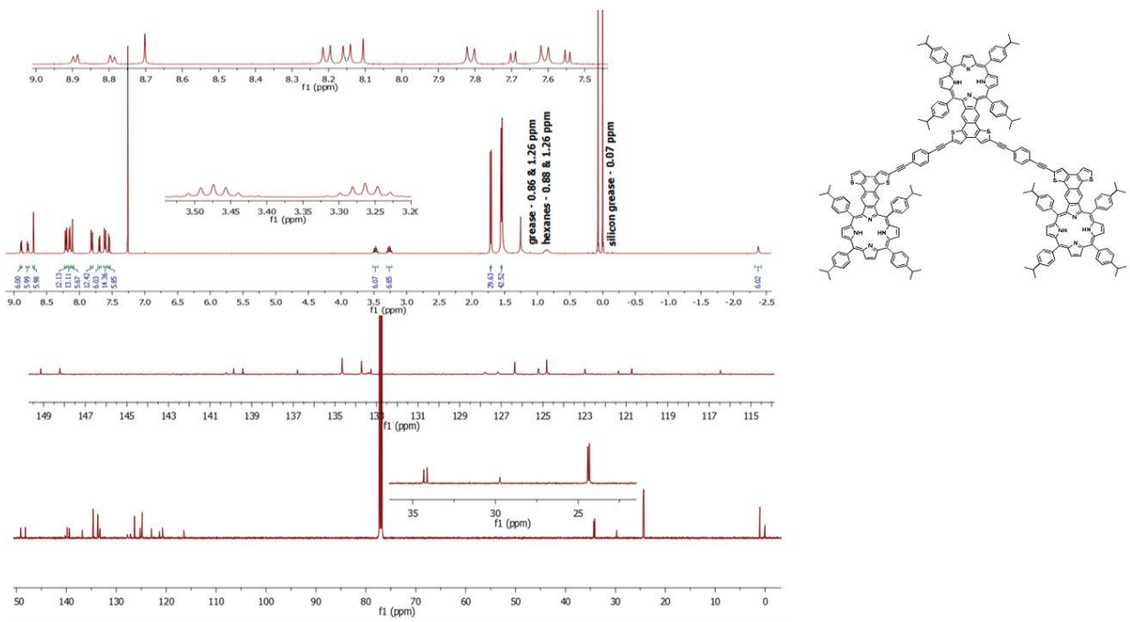

Figure 3.32: Trimer

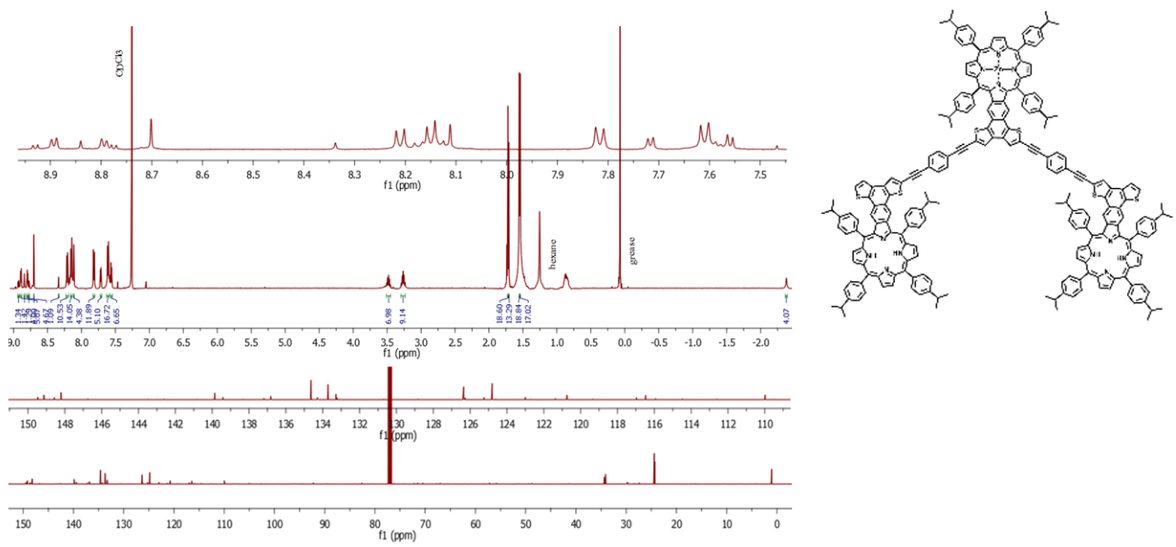

Figure 3.33: 2ZnT

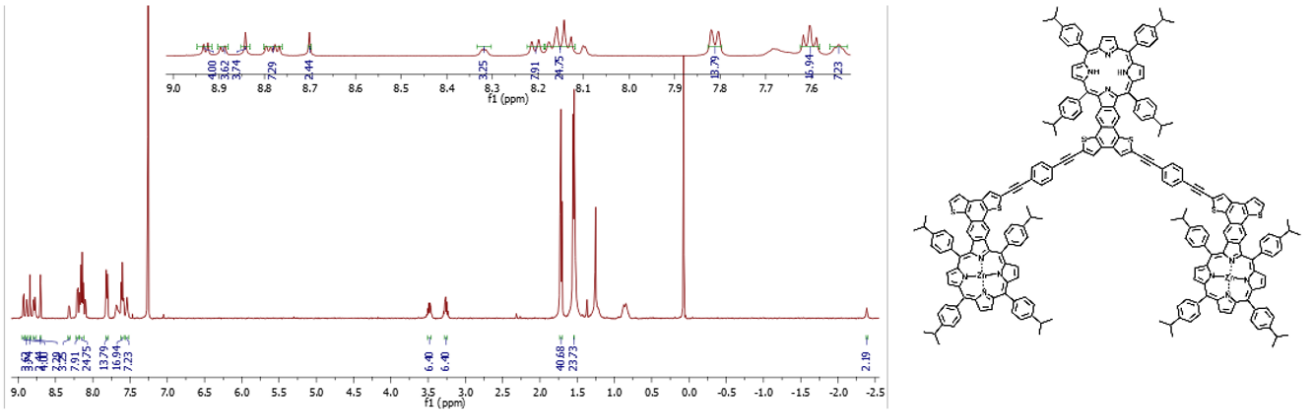

Figure 3.34: 2ZnT

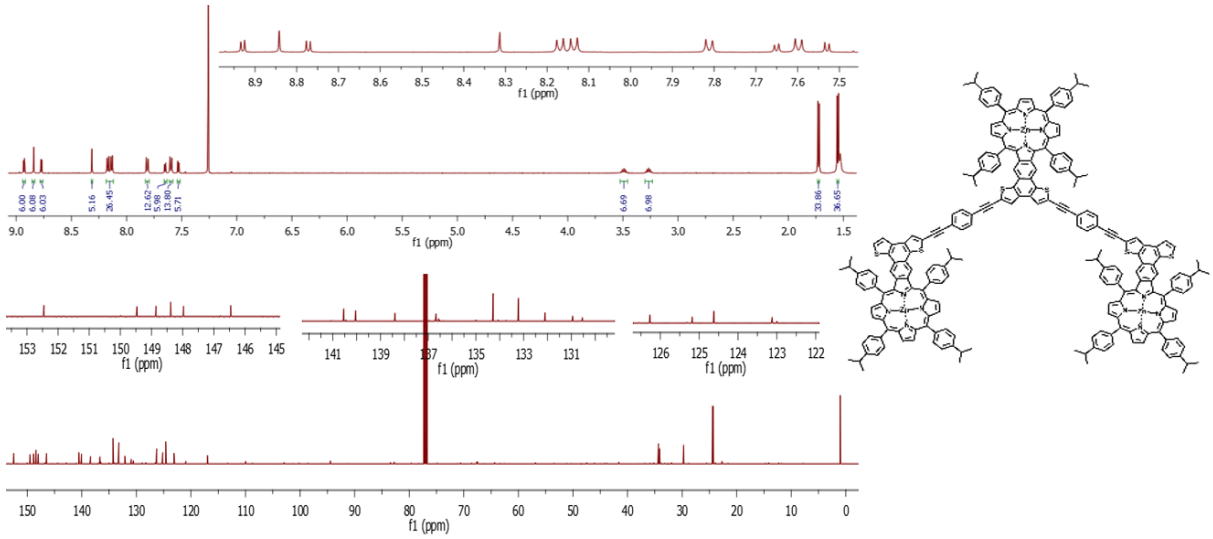

Figure 3.35: 3ZnT

3.7.4 Oscillator Tables

Table 3.1: FBr2VTP Oscillator Table

Excited State	FBr2VTP	Transition Energy (eV)	Wavelength (nm)	Oscillator Strength (f)	Orbital Transition		% Probability
1	Singlet-A	2.0712	599	0.0002	HOMO -1	LUMO	50.58%
					HOMO	LUMO +1	48.05%
2	Singlet-A	2.2076	562	0.0033	HOMO -1	LUMO +1	45.76%
					HOMO	LUMO	52.78%
3	Singlet-A	456	2.7182	1.7045	HOMO -3	LUMO	3.44%
					HOMO -3	LUMO +1	4.50%
					HOMO -2	LUMO +1	4.64%

Excited State	FBr2VTP	Transition Energy (eV)	Wavelength (nm)	Oscillator Strength (f)	Orbital Transition		% Probability
					HOMO -1	LUMO	13.13%
					HOMO -1	LUMO +1	33.51%
					HOMO	LUMO	25.56%
					HOMO	LUMO +2	11.67%

Table 3.2: ZnFBr2VTP Oscillator Table

Excited State	ZnFBr2VTP	Transition Energy (eV)	Wavelength (nm)	Oscillator Strength (f)	Orbital Transition		% Probability
1	Singlet-A	2.1466	578	0.0138	HOMO -1	LUMO +1	32.36%
					HOMO	LUMO	66.94%
2	Singlet-A	2.193	565	0.0011	HOMO -1	LUMO	53.68%
					HOMO	LUMO +1	44.98%
3	Singlet-A	2.7335	454	2.3337	HOMO -2	LUMO +1	3.46%
					HOMO -1	LUMO	38.27%
					HOMO	LUMO +1	49.90%

Table 3.3: mPEBp Oscillator Table

Excited State	mPEBp	Transition Energy (eV)	Wavelength (nm)	Oscillator Strength (f)	Orbital Transition		% Probability
1	Singlet-A	2.0576	603	0.0034	HOMO -1	LUMO	44.81%
					HOMO -1	LUMO +1	3.80%
					HOMO	LUMO	4.45%
					HOMO	LUMO +1	43.30%
2	Singlet-A	2.1875	567	0.0382	HOMO -1	LUMO	4.97%
					HOMO -1	LUMO +1	46.04%
					HOMO	LUMO	43.29%
					HOMO	LUMO +2	3.33%
3	Singlet-A	2.5526	486	1.951	HOMO -2	LUMO	5.45%
					HOMO -2	LUMO +1	9.88%
					HOMO -1	LUMO	10.80%
					HOMO -1	LUMO +1	27.88%
					HOMO -1	LUMO +2	10.05%
					HOMO	LUMO	24.05%
					HOMO	LUMO +1	7.99%

Table 3.4: bPEBp Oscillator Table

Excited State	bPEBp	Transition Energy (eV)	Wavelength (nm)	Oscillator Strength (f)	Orbital Transition		% Probability
1		2.0411	607	0.0037	HOMO -1	LUMO	46.50%

Excited State	bPEBp	Transition Energy (eV)	Wavelength (nm)	Oscillator Strength (f)	Orbital Transition		% Probability
	Singlet-A				HOMO	LUMO +1	47.36%
					HOMO	LUMO +2	3.35%
2	Singlet-A	2.1715	571	0.0608	HOMO -1	LUMO +1	52.96%
					HOMO	LUMO	43.07%
3	Singlet-A	2.5444	487	1.690	HOMO -3	LUMO+1	11.05%
					HOMO -1	LUMO +1	37.84%
					HOMO -1	LUMO +2	16.38%
					HOMO	LUMO	32.31%
4	Singlet-A	2.5952	478	0.023	HOMO -3	LUMO	8.95%
					HOMO -2	LUMO +1	10.05%
					HOMO -1	LUMO	32.64%
					HOMO -1	LUMO +3	5.23%
					HOMO	LUMO +1	32.29%
					HOMO	LUMO +2	8.60%
5	Singlet-A	2.725	455	0.4556	HOMO -2	LUMO +1	67.90%
					HOMO -1	LUMO +3	4.71%
					HOMO	LUMO +1	5.17%
					HOMO	LUMO +2	19.29%
6	Singlet-A	2.7335	454	0.1826	HOMO -2	LUMO	82.09%
					HOMO -1	LUMO +2	2.48%
					HOMO	LUMO +3	11.62%

Table 3.5: ZnbPEBp Oscillator Table

Excited State	ZnbPEBp	Transition Energy (eV)	Wavelength (nm)	Oscillator Strength (f)	Orbital Transition		% Probability
1	Singlet-A	2.1163	586	0	HOMO-1	LUMO +1	28.91%
					HOMO -1	LUMO +3	4.95%
					HOMO	LUMO	64.75%
2	Singlet-A	2.1425	579	0.1268	HOMO -1	LUMO	38.09%
					HOMO	LUMO +1	56.68%
					HOMO	LUMO +3	3.39%
3	Singlet-A	2.4446	507	2.0951	HOMO -3	LUMO +1	4.81%
					HOMO -1	LUMO	42.00%
					HOMO	LUMO+1	39.36%
					HOMO	LUMO+3	12.35%
4	Singlet-A	2.5472	487	0.0701	HOMO -3	LUMO	2.89%
					HOMO -2	LUMO +1	2.03%
					HOMO -1	LUMO +1	43.46%
					HOMO	LUMO	22.87%

Excited State	ZnbPEBp	Transition Energy (eV)	Wavelength (nm)	Oscillator Strength (f)	Orbital Transition		% Probability
					HOMO	LUMO +2	26.89%
5	Singlet-A	2.681	462	0.6923	HOMO -2	LUMO +1	6.71%
					HOMO -1	LUMO +1	20.61%
					HOMO -1	LUMO +3	19.42%
					HOMO	LUMO +2	49.16%
6	Singlet-A	2.7103	457	0.341	HOMO -2	LUMO	27.84%
					HOMO -2	LUMO +2	2.15%
					HOMO -1	LUMO	4.86%
					HOMO -1	LUMO +2	36.59%
					HOMO	LUMO +3	24.78%

Table 3.6: Dimer Oscillator Tables

Excited state	Dimer	Transition Energy (eV)	Wavelength (nm)	Oscillator Strength (f)	Orbital Transition		% Probability
1	Singlet-A	2.0502	605	0.0158	HOMO-3	LUMO	15.63%
					HOMO-3	LUMO +1	9.47%
					HOMO-3	LUMO +2	4.97%
					HOMO -1	LUMO	8.98%
					HOMO -1	LUMO +2	29.46%
					HOMO -1	LUMO +3	6.22%
					HOMO -1	LUMO +4	4.17%
					HOMO	LUMO	12.11%
					HOMO	LUMO +1	3.93%
2	Singlet-A	2.0587	602	0.0034	HOMO -4	LUMO +1	2.84%
					HOMO-3	LUMO	3.70%
					HOMO-3	LUMO +1	10.00%
					HOMO -2	LUMO +2	4.12%
					HOMO -2	LUMO +3	38.42%
					HOMO	LUMO	7.00%
					HOMO	LUMO +1	24.92%
3	Singlet-A	2.1687	572	0.2822	HOMO-3	LUMO	4.48%
					HOMO-3	LUMO +2	12.53%
					HOMO-3	LUMO +3	8.70%
					HOMO -2	LUMO +1	2.87%
					HOMO -1	LUMO	22.12%
					HOMO -1	LUMO +1	10.04%
					HOMO -1	LUMO +2	3.92%
					HOMO	LUMO	7.82%
					HOMO	LUMO +2	22.18%
4	Singlet-A	2.1898	566	0.0349	HOMO -4	LUMO +3	2.90%
					HOMO-3	LUMO	3.28%

Excited state	Dimer	Transition Energy (eV)	Wavelength (nm)	Oscillator Strength (f)	Orbital Transition		% Probability
					HOMO-3	LUMO +2	6.55%
					HOMO-3	LUMO +3	6.21%
					HOMO -2	LUMO	8.98%
					HOMO -2	LUMO +1	29.45%
					HOMO -2	LUMO +2	3.09%
					HOMO -1	LUMO	3.87%
					HOMO	LUMO +3	28.49%
5	Singlet-A	2.3463	528	2.8765	HOMO -4	LUMO	5.47%
					HOMO -4	LUMO +2	2.71%
					HOMO -2	LUMO +1	6.56%
					HOMO -1	LUMO	4.51%
					HOMO -1	LUMO +1	3.86%
					HOMO -1	LUMO +2	5.96%
					HOMO	LUMO	32.23%
					HOMO	LUMO +2	15.26%
					HOMO	LUMO +4	13.82%
6	Singlet-A	2.4747	501	0.2297	HOMO -4	LUMO +1	4.99%
					HOMO-3	LUMO	12.00%
					HOMO -1	LUMO	5.57%
					HOMO	LUMO	9.94%
					HOMO	LUMO +1	50.17%
					HOMO	LUMO +2	8.67%

Table 3.7: 1ZnD Oscillator Table

Excited state	1ZnD	Transition Energy (eV)	Wavelength (nm)	Oscillator Strength (f)	Orbital Transition		% Probability
1	Singlet-A	2.059	602	0.0043	HOMO -4	LUMO	3.73%
					HOMO-3	LUMO	8.86%
					HOMO -2	LUMO +1	10.72%
					HOMO -2	LUMO +2	27.80%
					HOMO -2	LUMO +3	5.98%
					HOMO -1	LUMO	27.20%
					HOMO	LUMO	10.50%
2	Singlet-A	2.1451	578	0.1278	HOMO-3	LUMO +1	3.03%
					HOMO-3	LUMO +3	13.59%
					HOMO-3	LUMO +4	7.67%
					HOMO -1	LUMO +2	7.08%
					HOMO -1	LUMO +3	6.32%
					HOMO	LUMO	3.16%
					HOMO	LUMO +1	42.20%
					HOMO	LUMO +2	11.74%

Excited state	1ZnD	Transition Energy (eV)	Wavelength (nm)	Oscillator Strength (f)	Orbital Transition		% Probability
3	Singlet-A	2.1785	562	0.1868	HOMO-3	LUMO +1	22.86%
					HOMO-3	LUMO +2	3.58%
					HOMO-3	LUMO +3	2.21%
					HOMO -2	LUMO	7.12%
					HOMO -1	LUMO +2	7.50%
					HOMO -1	LUMO +3	5.20%
					HOMO -1	LUMO +4	3.08%
					HOMO	LUMO +1	3.63%
					HOMO	LUMO +2	10.45%
					HOMO	LUMO +3	22.40%
					HOMO	LUMO +4	3.93%
4	Singlet-A	2.1909	566	0.019	HOMO-3	LUMO +2	14.59%
					HOMO -2	LUMO	35.92%
					HOMO -1	LUMO +1	18.61%
					HOMO -1	LUMO +2	6.85%
					HOMO	LUMO +2	3.70%
					HOMO	LUMO +3	9.04%
5	Singlet-A	2.3538	526	2.9699	HOMO -4	LUMO	2.24%
					HOMO -4	LUMO +1	4.45%
					HOMO-3	LUMO +2	2.57%
					HOMO-3	LUMO +3	6.67%
					HOMO -2	LUMO	8.52%
					HOMO -1	LUMO +1	13.28%
					HOMO -1	LUMO +2	2.28%
					HOMO	LUMO	12.01%
					HOMO	LUMO +1	14.96%
					HOMO	LUMO +2	4.81%
					HOMO	LUMO +3	9.14%
					HOMO	LUMO +4	9.03%
6	Singlet-A	2.4346	509	0.0978	HOMO -4	LUMO	2.84%
					HOMO -1	LUMO	4.49%
					HOMO	LUMO	69.14%
					HOMO	LUMO +1	11.96%

Table 3.8: 2ZnD Oscillator Table

Excited State	2ZnD	Transition Energy (eV)	Wavelength (nm)	Oscillator Strength (f)	Orbital Transition		% Probability
1	Singlet-A	2.1445	578	0.1591	HOMO -2	LUMO +2	16.28%
					HOMO -2	LUMO +3	4.59%
					HOMO -2	LUMO +4	5.65%
					HOMO -1	LUMO	17.21%

Excited State	2ZnD	Transition Energy (eV)	Wavelength (nm)	Oscillator Strength (f)	Orbital Transition		% Probability
					HOMO -1	LUMO +1	14.92%
					HOMO	LUMO	31.65%
2	Singlet-A	2.1589	574	0.0704	HOMO-3	LUMO +2	2.68%
					HOMO-3	LUMO +3	22.38%
					HOMO-3	LUMO +4	2.46%
					HOMO -1	LUMO	9.85%
					HOMO -1	LUMO +1	6.54%
					HOMO -1	LUMO +2	5.21%
					HOMO	LUMO	6.05%
					HOMO	LUMO +1	37.58%
3	Singlet-A	2.181	568	0.1119	HOMO -2	LUMO	28.41%
					HOMO -2	LUMO +1	11.69%
					HOMO -1	LUMO	3.39%
					HOMO -1	LUMO +2	13.06%
					HOMO -1	LUMO +3	6.69%
					HOMO -1	LUMO +4	3.88%
					HOMO	LUMO +2	20.80%
4	Singlet-A	2.2058	562	0.0576	HOMO-3	LUMO	10.82%
					HOMO-3	LUMO +1	31.58%
					HOMO-3	LUMO +2	4.06%
					HOMO -1	LUMO	2.61%
					HOMO -1	LUMO +2	3.44%
					HOMO -1	LUMO +3	8.66%
					HOMO -1	LUMO +4	2.09%
					HOMO	LUMO +2	3.09%
					HOMO	LUMO +3	25.28%
5	Singlet-A	2.3446	529	0.4633	HOMO -4	LUMO	5.48%
					HOMO-3	LUMO +1	5.59%
					HOMO -2	LUMO	3.98%
					HOMO -2	LUMO +1	2.46%
					HOMO -2	LUMO +2	4.65%
					HOMO -1	LUMO	2.17%
					HOMO -1	LUMO +1	3.80%
					HOMO	LUMO	31.43%
					HOMO	LUMO +2	19.27%
					HOMO	LUMO +4	10.43%
6	Singlet-A	2.4725	501	0.2526	HOMO -2	LUMO	5.83%
					HOMO -1	LUMO	48.17%
					HOMO -1	LUMO +2	4.84%
					HOMO -1	LUMO +3	6.11%
					HOMO	LUMO	2.78%
					HOMO	LUMO +1	20.84%

Table 3.9: Trimer Oscillator Table

Excited State	Trimer	Transition Energy (eV)	Wavelength (nm)	Oscillator Strength (f)	Orbital Transition		% Probability
1	Singlet-A	2.0379	608	0.0174	HOMO -5	LUMO +1	16.28%
					HOMO-3	LUMO	4.59%
					HOMO-3	LUMO +3	5.65%
					HOMO-3	LUMO +5	17.21%
					HOMO-3	LUMO +7	14.92%
					HOMO	LUMO +1	31.65%
2	Singlet-A	2.0585	602	0.0044	HOMO -6	LUMO +3	2.31%
					HOMO -5	LUMO +3	6.72%
					HOMO -2	LUMO +4	25.24%
					HOMO -2	LUMO +5	17.05%
					HOMO -1	LUMO +2	3.16%
					HOMO -1	LUMO +3	16.83%
					HOMO	LUMO +2	3.01%
					HOMO	LUMO +3	14.81%
3	Singlet-A	2.064	601	0.0053	HOMO -6	LUMO +2	2.31%
					HOMO -5	LUMO +2	7.22%
					HOMO -4	LUMO +4	17.22%
					HOMO -4	LUMO +5	23.80%
					HOMO -1	LUMO +2	20.46%
					HOMO -1	LUMO +3	3.56%
					HOMO	LUMO +2	11.15%
4	Singlet-A	2.1412	579	0.5598	HOMO -5	LUMO	22.05%
					HOMO -5	LUMO +5	2.62%
					HOMO-3	LUMO +1	27.61%
					HOMO	LUMO	35.83%
5	Singlet-A	2.1862	567	0.1239	HOMO -5	LUMO +4	5.89%
					HOMO -4	LUMO +2	3.14%
					HOMO -2	LUMO +2	5.95%
					HOMO -2	LUMO +3	31.04%
					HOMO -1	LUMO	5.33%
					HOMO -1	LUMO +4	4.73%
					HOMO -1	LUMO +5	13.63%
					HOMO	LUMO +4	15.79%
					HOMO	LUMO +5	2.77%
6	Singlet-A	2.194	565	0.0941	HOMO -5	LUMO	2.51%
					HOMO -5	LUMO +5	4.95%
					HOMO -4	LUMO +2	30.68%
					HOMO -4	LUMO +3	5.56%
					HOMO -2	LUMO +3	3.75%
					HOMO -1	LUMO +4	15.58%
					HOMO -1	LUMO +5	6.53%

Excited State	Trimer	Transition Energy (eV)	Wavelength (nm)	Oscillator Strength (f)	Orbital Transition		% Probability
					HOMO	LUMO +5	11.98%

Table 3.10: 1ZnT Oscillator Table

Excited State	1ZnT	Transition Energy (eV)	Wavelength (nm)	Oscillator Strength (f)	Orbital Transition		% Probability
1	Singlet-A	2.0379	608	0.0174	HOMO -5	LUMO +1	16.28%
					HOMO-3	LUMO	4.59%
					HOMO-3	LUMO +3	5.65%
					HOMO-3	LUMO +5	17.21%
					HOMO-3	LUMO +7	14.92%
					HOMO	LUMO +1	31.65%
2	Singlet-A	2.0585	602	0.0044	HOMO -6	LUMO +3	2.31%
					HOMO -5	LUMO +3	6.72%
					HOMO -2	LUMO +4	25.24%
					HOMO -2	LUMO +5	17.05%
					HOMO -1	LUMO +2	3.16%
					HOMO -1	LUMO +3	16.83%
					HOMO	LUMO +2	3.01%
					HOMO	LUMO +3	14.81%
3	Singlet-A	2.064	601	0.0053	HOMO -6	LUMO +2	2.31%
					HOMO -5	LUMO +2	7.22%
					HOMO -4	LUMO +4	17.22%
					HOMO -4	LUMO +5	23.80%
					HOMO -1	LUMO +2	20.46%
					HOMO -1	LUMO +3	3.56%
					HOMO	LUMO +2	11.15%
4	Singlet-A	2.1412	579	0.5598	HOMO -5	LUMO	22.05%
					HOMO -5	LUMO +5	2.62%
					HOMO-3	LUMO +1	27.61%
					HOMO	LUMO	35.83%
5	Singlet-A	2.1862	567	0.1239	HOMO -5	LUMO +4	5.89%
					HOMO -4	LUMO +2	3.14%
					HOMO -2	LUMO +2	5.95%
					HOMO -2	LUMO +3	31.04%
					HOMO -1	LUMO	5.33%
					HOMO -1	LUMO +4	4.73%
					HOMO -1	LUMO +5	13.63%
					HOMO	LUMO +4	15.79%
					HOMO	LUMO +5	2.77%
6		2.194	565	0.0941	HOMO -5	LUMO	2.51%

Excited State	1ZnT	Transition Energy (eV)	Wavelength (nm)	Oscillator Strength (f)	Orbital Transition		% Probability
	Singlet-A				HOMO -5	LUMO +5	4.95%
					HOMO -4	LUMO +2	30.68%
					HOMO -4	LUMO +3	5.56%
					HOMO -2	LUMO +3	3.75%
					HOMO -1	LUMO +4	15.58%
					HOMO -1	LUMO +5	6.53%
					HOMO	LUMO +5	11.98%

Table 3.11: 2ZnT Oscillator Table

Excited State	1ZnT	Transition Energy (eV)	Wavelength (nm)	Oscillator Strength (f)	Orbital Transition		% Probability
1	Singlet-A	2.0379	608	0.0174	HOMO -5	LUMO +1	16.28%
					HOMO-3	LUMO	4.59%
					HOMO-3	LUMO +3	5.65%
					HOMO-3	LUMO +5	17.21%
					HOMO-3	LUMO +7	14.92%
					HOMO	LUMO +1	31.65%
2	Singlet-A	2.0585	602	0.0044	HOMO -6	LUMO +3	2.31%
					HOMO -5	LUMO +3	6.72%
					HOMO -2	LUMO +4	25.24%
					HOMO -2	LUMO +5	17.05%
					HOMO -1	LUMO +2	3.16%
					HOMO -1	LUMO +3	16.83%
					HOMO	LUMO +2	3.01%
					HOMO	LUMO +3	14.81%
3	Singlet-A	2.064	601	0.0053	HOMO -6	LUMO +2	2.31%
					HOMO -5	LUMO +2	7.22%
					HOMO -4	LUMO +4	17.22%
					HOMO -4	LUMO +5	23.80%
					HOMO -1	LUMO +2	20.46%
					HOMO -1	LUMO +3	3.56%
					HOMO	LUMO +2	11.15%
4	Singlet-A	2.1412	579	0.5598	HOMO -5	LUMO	22.05%
					HOMO -5	LUMO +5	2.62%
					HOMO-3	LUMO +1	27.61%
					HOMO	LUMO	35.83%
5	Singlet-A	2.1862	567	0.1239	HOMO -5	LUMO +4	5.89%
					HOMO -4	LUMO +2	3.14%
					HOMO -2	LUMO +2	5.95%
					HOMO -2	LUMO +3	31.04%
					HOMO -1	LUMO	5.33%

Excited State	1ZnT	Transition Energy (eV)	Wavelength (nm)	Oscillator Strength (f)	Orbital Transition		% Probability
					HOMO -1	LUMO +4	4.73%
					HOMO -1	LUMO +5	13.63%
					HOMO	LUMO +4	15.79%
					HOMO	LUMO +5	2.77%
6	Singlet-A	2.194	565	0.0941	HOMO -5	LUMO	2.51%
					HOMO -5	LUMO +5	4.95%
					HOMO -4	LUMO +2	30.68%
					HOMO -4	LUMO +3	5.56%
					HOMO -2	LUMO +3	3.75%
					HOMO -1	LUMO +4	15.58%
					HOMO -1	LUMO +5	6.53%
					HOMO	LUMO +5	11.98%

Table 3.12: 3ZnT Oscillator Table

Excited State	3ZnT	Transition Energy (eV)	Wavelength (nm)	Oscillator Strength (f)	Orbital Transition		% Probability
1	Singlet-A	2.0379	608	0.0174	HOMO -5	LUMO +1	16.28%
					HOMO-3	LUMO	4.59%
					HOMO-3	LUMO +3	5.65%
					HOMO-3	LUMO +5	17.21%
					HOMO-3	LUMO +7	14.92%
					HOMO	LUMO +1	31.65%
2	Singlet-A	2.0585	602	0.0044	HOMO -6	LUMO +3	2.31%
					HOMO -5	LUMO +3	6.72%
					HOMO -2	LUMO +4	25.24%
					HOMO -2	LUMO +5	17.05%
					HOMO -1	LUMO +2	3.16%
					HOMO -1	LUMO +3	16.83%
					HOMO	LUMO +2	3.01%
					HOMO	LUMO +3	14.81%
3	Singlet-A	2.064	601	0.0053	HOMO -6	LUMO +2	2.31%
					HOMO -5	LUMO +2	7.22%
					HOMO -4	LUMO +4	17.22%
					HOMO -4	LUMO +5	23.80%
					HOMO -1	LUMO +2	20.46%
					HOMO -1	LUMO +3	3.56%
					HOMO	LUMO +2	11.15%
4	Singlet-A	2.1412	579	0.5598	HOMO -5	LUMO	22.05%
					HOMO -5	LUMO +5	2.62%
					HOMO-3	LUMO +1	27.61%
					HOMO	LUMO	35.83%

Excited State	3ZnT	Transition Energy (eV)	Wavelength (nm)	Oscillator Strength (f)	Orbital Transition		% Probability
5	Singlet-A	2.1862	567	0.1239	HOMO -5	LUMO +4	5.89%
					HOMO -4	LUMO +2	3.14%
					HOMO -2	LUMO +2	5.95%
					HOMO -2	LUMO +3	31.04%
					HOMO -1	LUMO	5.33%
					HOMO -1	LUMO +4	4.73%
					HOMO -1	LUMO +5	13.63%
					HOMO	LUMO +4	15.79%
					HOMO	LUMO +5	2.77%
6	Singlet-A	2.194	565	0.0941	HOMO -5	LUMO	2.51%
					HOMO -5	LUMO +5	4.95%
					HOMO -4	LUMO +2	30.68%
					HOMO -4	LUMO +3	5.56%
					HOMO -2	LUMO +3	3.75%
					HOMO -1	LUMO +4	15.58%
					HOMO -1	LUMO +5	6.53%
					HOMO	LUMO +5	11.98%

3.7.5 NICS-scan Distance Tables

Table 3.13: F2VT NICS with mPEBTh

Distance (Å)	mPEBTh			Distance (Å)	F2VT Chapter 3			Distance (Å)	F2VT Chapter 2		
	PiZZ	NCS	PiZZ		PiZZ	NCS	SOM		PiZZ	NCS	SOM
-2.6	-5.0661	-1.4	-5.3024	-2.6	-5.0797	-5.0435	-5.1629	-1.4	-5.3024	-5.2644	-5.1524
-1.4	-7.1322	0	-7.1434	-1.4	-7.208	-7.156	-7.3106	0	-7.1434	-7.0926	-6.8551
0	-6.3597	1.4	-6.4858	0	-6.4748	-6.4332	-5.8561	1.4	-6.4858	-6.4392	-5.6341
1.4	-5.2011	2.6	-5.5351	1.4	-5.3836	-5.3491	-5.2904	2.6	-5.5351	-5.4918	-5.6026
2.6	-3.1353	3.8	-3.632	2.6	-3.2412	-.32066	-3.0428	3.8	-3.632	-3.585	-3.443
3.6	-0.8512	5	-0.9617	3.6	-0.08832	-.8564	-0.2576	5	-0.9617	-0.9214	-1.1374

Table 3.14: F2VT NICS with bPEBTh

Distance (Å)	bPEBTh			Distance (Å)	F2VT Chapter 3			Distance (Å)	F2VT Chapter 2		
	PiZZ	NCS	PiZZ		PiZZ	NCS	SOM		PiZZ	NCS	SOM
-2.6	-5.0491	-5.0142	-4.9639	-2.6	-5.0797	-5.0435	-5.1629	-1.4	-5.3024	-5.2644	-5.1524
-1.4	-7.0578	-7.0113	-6.8942	-1.4	-7.208	-7.156	-7.3106	0	-7.1434	-7.0926	-6.8551
0	-6.2518	-6.2123	-5.4431	0	-6.4748	-6.4332	-5.8561	1.4	-6.4858	-6.4392	-5.6341
1.4	-5.0315	-4.9982	-4.9771	1.4	-5.3836	-5.3491	-5.2904	2.6	-5.5351	-5.4918	-5.6026
2.6	-3.0411	-3.0074	-2.960	2.6	-3.2412	-.32066	-3.0428	3.8	-3.632	-3.585	-3.443
3.6	-.8312	-.8054	-1.0433	3.6	-0.08832	-.8564	-0.2576	5	-0.9617	-0.9214	-1.1374

3.7.6 Normalized UV-Vis of Zinc-inserted Porphyrins

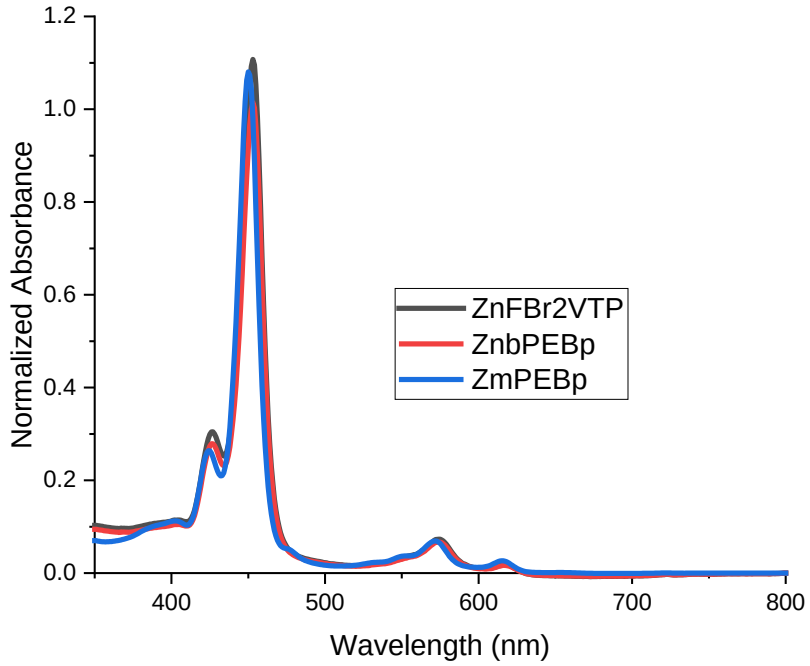

Figure 3.36: Normalized UV-VIS of Zinc inserted monomers.

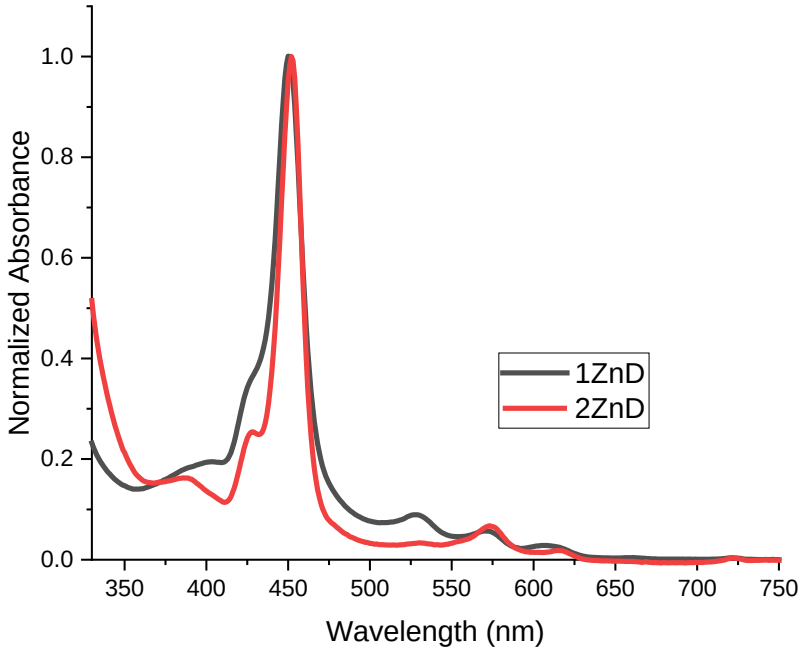

Figure 3.37: Normalized UV-VIS of Zinc inserted dimers.

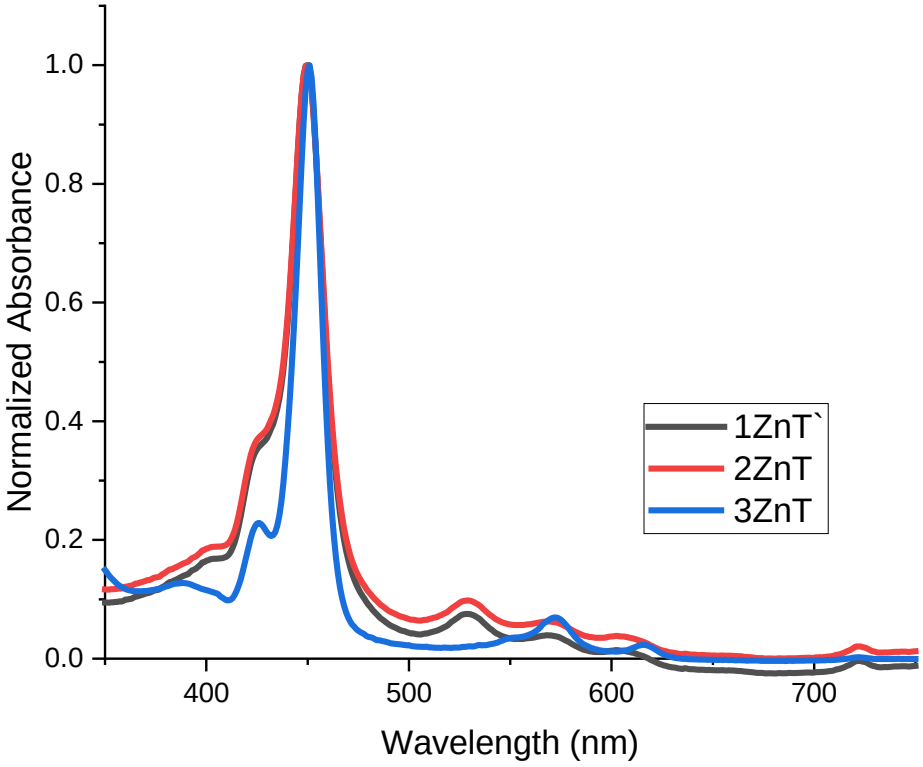

Figure 3.38: Normalized UV-VIS of Zinc inserted trimers.

3.7.7 FTIR Spectra

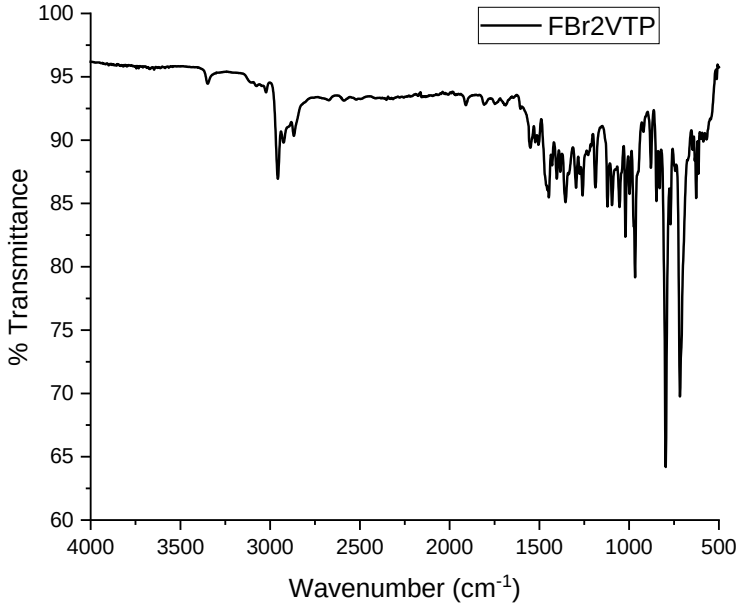

Figure 3.39: FBr2VTP

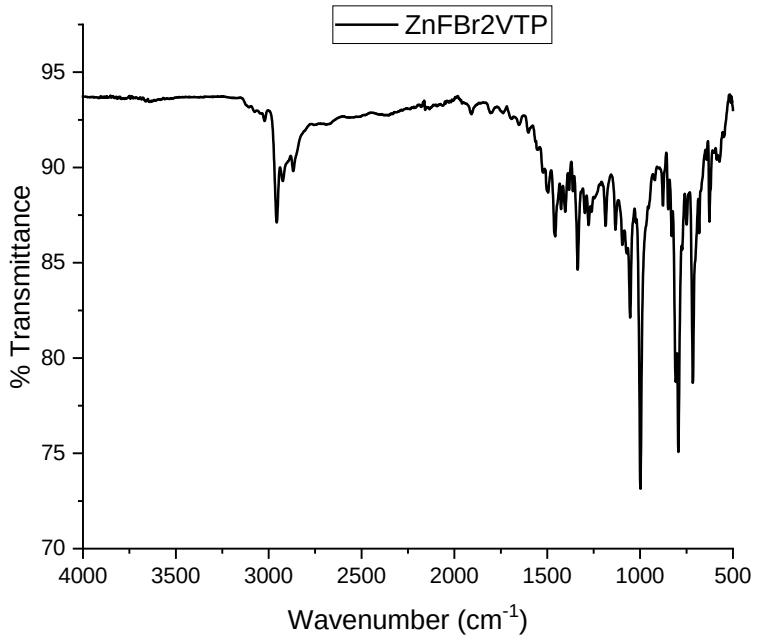

Figure 3.40: ZnFBr2VTP

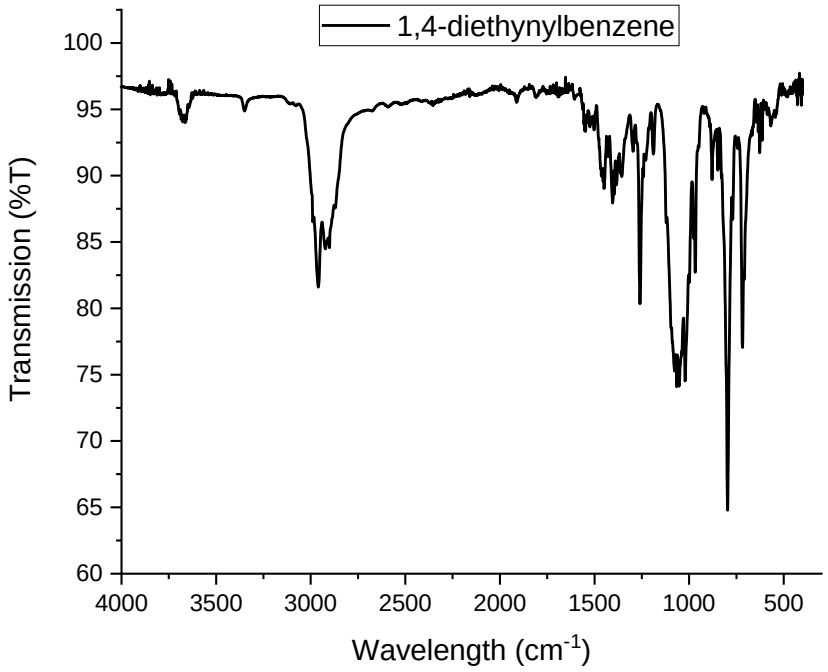

Figure 3.41: mPEBp

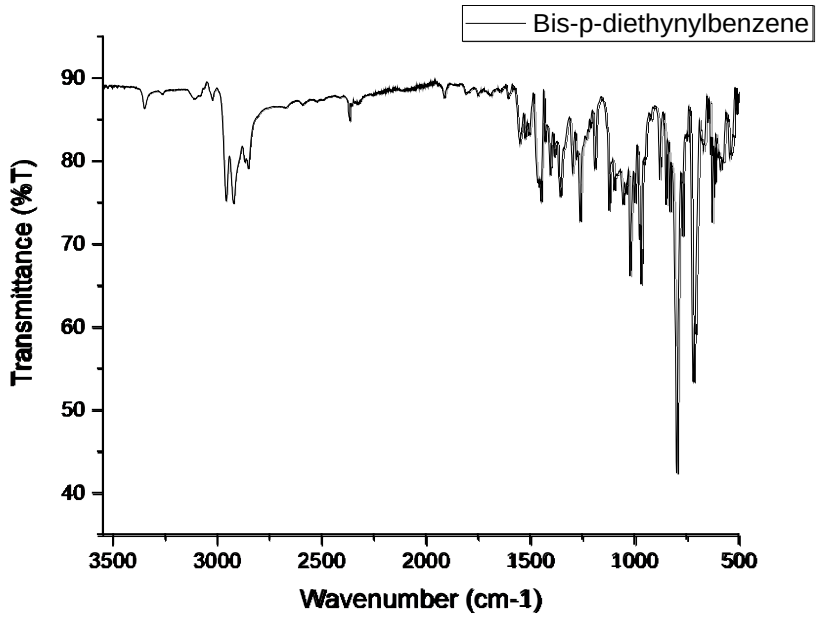

Figure 3.42: bPEBp

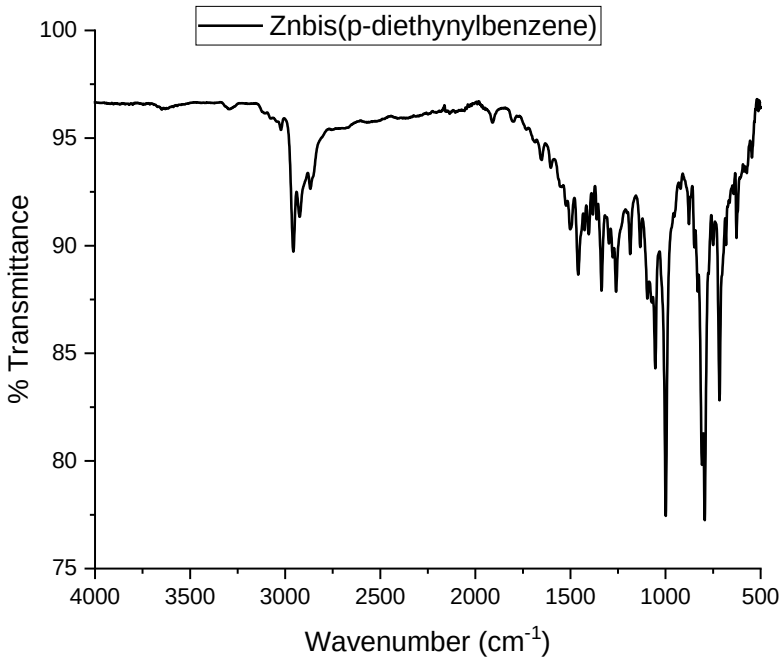

Figure 3.43: ZnbPEBp

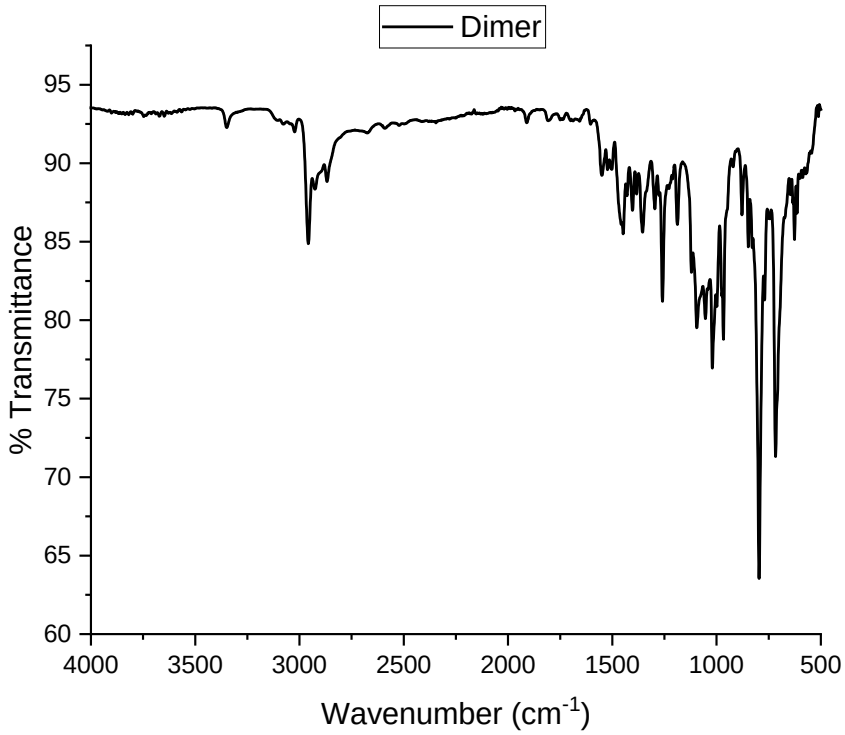

Figure 3.44: Dimer

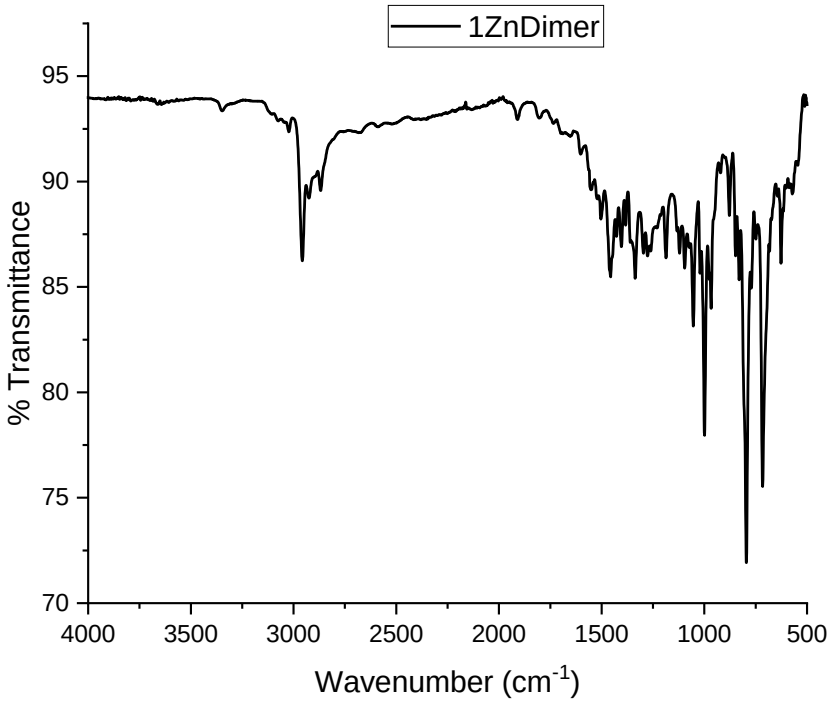

Figure 3.45: 1ZnD

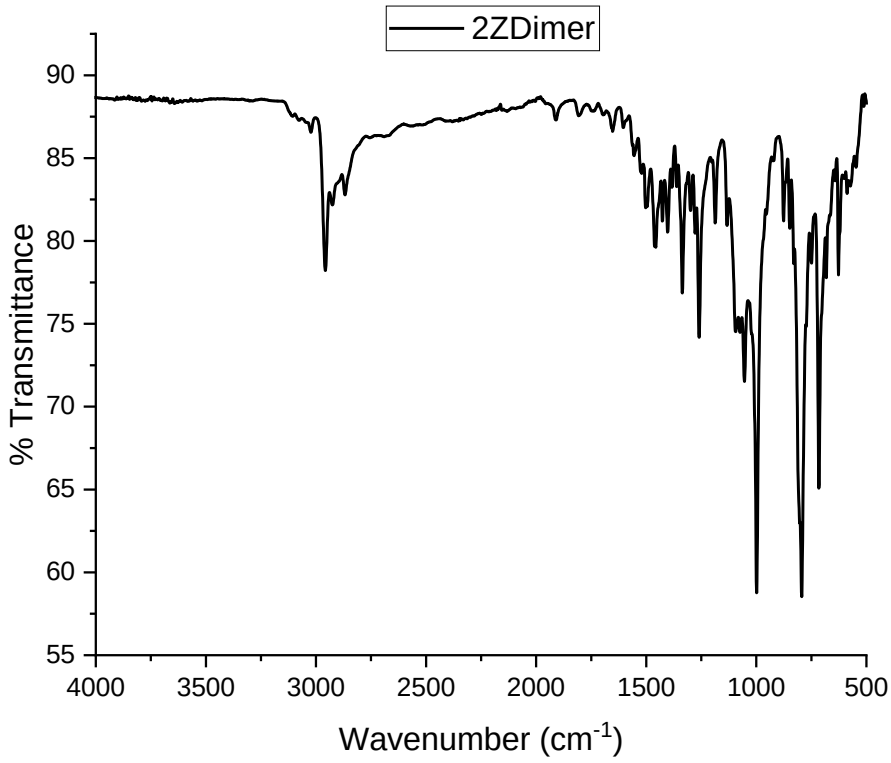

Figure 3.46: 2ZnD

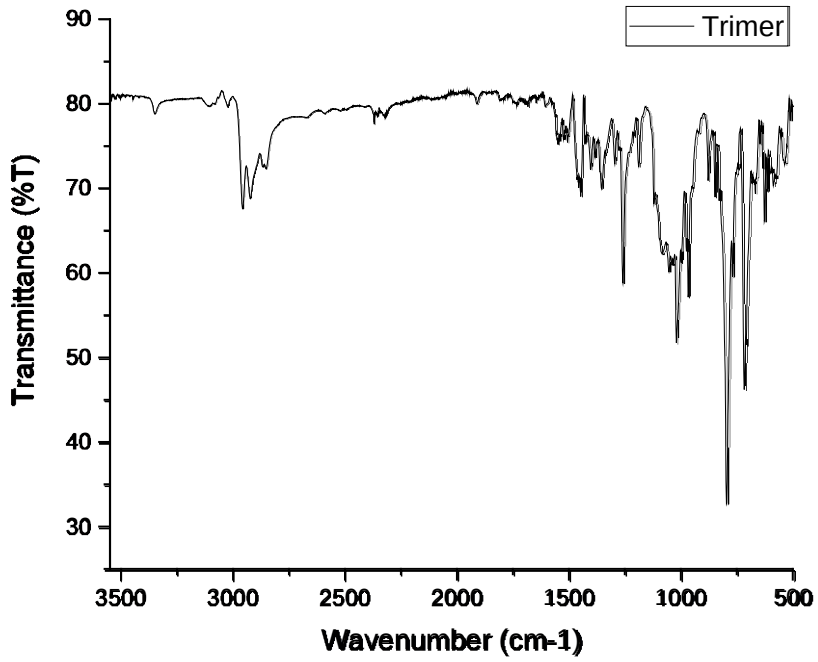

Figure 3.47: Trimer

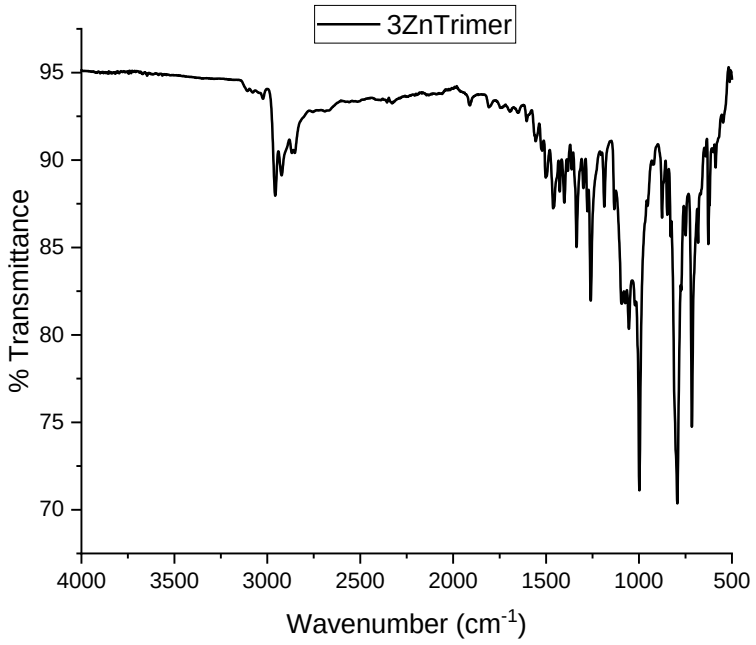

Figure 3.48: 3ZnTrimer

The FTIR spectra of 1ZnT and 2ZnT has not been done but will be in the future.

3.8 References

[1] a) Mohajer, F.; Heravi, M. M.; Zadsirjan, V.; Poormohammad, N. ***RSC Adv.***, 2021,**11**, pp 6885-6925; b) Gazvoda, M.; Virant, M.; Pinter, B.; Košmrlj, J. *Nat Commun* **9**, 4814 (2018); c) Cheng, J.; Sun, Y.; Wang, F.; Guo, M.; Xu, J.-H.; Pan, Y.; Zhang, Z; *J. Org. Chem.* 2004, 69, 16, pp 5428–5432; d) Urgaonkar, S.; Verkade, J. G. *J. Org. Chem.* 2004, 69, 17, pp 5752–5755; e) Li, J. H.; Liang, Y.; Xie, Y. X. *Journal of Organic Chemistry* **2005**, *70* (11), pp 4393–4396.

[2] Tanguy, L.; Hetru, O.; Langlois, A.; Harvey, P. D. *J. Org. Chem.* 2019, 84, 6, pp 3590–3594.

[3] Ali, H.; van Lier, J. E. *Tetrahedron* **1994**, *50* (41), pp 11933–11944.

[4] Hisaki, I.; Hiroto, S.; Kim, K. S.; Noh, S. B.; Kim, D.; Shinokubo, H.; Osuka, A. *Angewandte Chemie - International Edition* **2007**, *46* (27), pp 5125–5128.

[5] a) Morisue, M.; Kawanishi, M.; Ueno, I.; Nakamura, T.; Nabeshima, T.; Imamura, K.; Nozaki, K. *J. Phys. Chem. B* **2021**, *125*, 9295; b) Shultz, D. A.; Gwaltney, K. P.; Lee, H. *Journal of Organic Chemistry* **1998**, *63* (12), pp 4034–4038; c) Morisue, M.; Kawanishi, M.; Nakano, S. *J Polym Sci A Polym Chem* **2019**, *57* (24), pp 2457–2465.

[6] a) Arai, T.; Araki, K.; Maruo, N.; Sumida, Y.; Korosue, C.; Fukuma, K.; Kato, T.; Nishino, N. S. *New Journal of Chemistry* **2004**, *28* (9), pp 1151–1159; b) Tamaki, T.; Nosaka, T.; Ogawa, T. *Journal of Organic Chemistry* **2014**, *79* (22), pp 11029–11038; c) *Chem Lett* **2007**, *36* (9), pp 1112–1113.

[7] Gaussian 16, Revision C.01, Frisch, M. J.; Trucks, G. W.; Schlegel, H. B.; Scuseria, G. E.; Robb, M. A.; Cheeseman, J. R.; Scalmani, G.; Barone, V.; Petersson, G. A.; Nakatsuji, H.; Li, X.; Caricato, M.; Marenich, A. V.; Bloino, J.; Janesko, B. G.; Gomperts, R.; Mennucci, B.; Hratchian, H. P.; Ortiz, J. V.; Izmaylov, A. F.; Sonnenberg, J. L.; Williams-Young, D.; Ding, F.; Lipparini, F.; Egidi, F.; Goings, J.; Peng, B.; Petrone, A.; Henderson, T.; Ranasinghe, D.; Zakrzewski, V. G.; Gao, J.; Rega, N.; Zheng, G.; Liang, W.; Hada, M.; Ehara, M.; Toyota, K.; Fukuda, R.; Hasegawa, J.; Ishida, M.; Nakajima, T.; Honda, Y.; Kitao, O.; Nakai, H.; Vreven, T.; Throssell, K.; Montgomery, J. A., Jr.; Peralta, J. E.; Ogliaro, F.; Bearpark, M. J.; Heyd, J. J.; Brothers, E. N.; Kudin, K. N.; Staroverov, V. N.; Keith, T. A.; Kobayashi, R.; Normand, J.; Raghavachari, K.; Rendell, A. P.; Burant, J. C.; Iyengar, S. S.; Tomasi, J.; Cossi, M.; Millam, J. M.; Klene, M.; Adamo, C.; Cammi, R.; Ochterski, J. W.; Martin, R. L.; Morokuma, K.; Farkas, O.; Foresman, J. B.; Fox, D. J. Gaussian, Inc., Wallingford CT, 2016.

CHAPTER 4

EXPLORATION OF TRIPHENYLENE FUSED PORPHYRIN

4.1 Introduction

4.1.1 Polycyclic Aromatic Hydrocarbons (PAH)

Polycyclic aromatic hydrocarbons (PAH) [1] are a class of organic compounds which are comprised of multiple fused aromatic rings. These rings can have various sizes and have a propensity for π-π stacking. PAH comprised of only six-membered rings, e.g benzenoid PAH, are known to be alternant-PAH. Most PAH are planar because of adjacent carbon's having sigma bonds on the same plane which allows for the merging of sp^2 hybrid orbitals. As a result, most PAH are considered achiral.

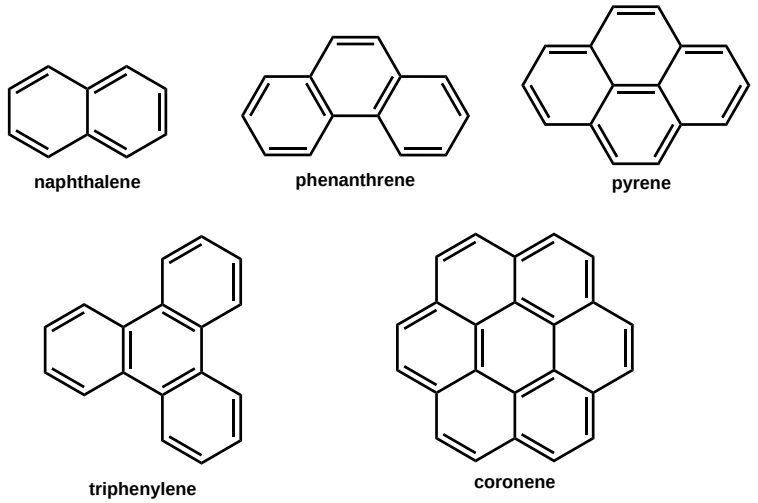

Figure 4.1: Examples of common PAH

However, some PAH can have a distortion from planarity due to repulsion and steric hinderance between hydrogen atoms like in the case of benzo[c]phenanthrene. [2] In the last twenty years, heteroatoms have been incorporated into PAH moieties which have offered even more applications in organic photovoltaics, biosensors, and organic semiconductors. [3]

4.1.2 Aromaticity and Reactivity of PAHs

Due to the variation in ring size, structure, and placement of the rings, PAH can have varying degrees of aromatic character. The aromatic character is defined by Clar's Sextet Rule. [4] This rule states that PAH which has the largest number of disjointed π-sextets, designated as a six-membered ring with a circle inside, will be more aromatic and will play a role in the molecule's characterization.

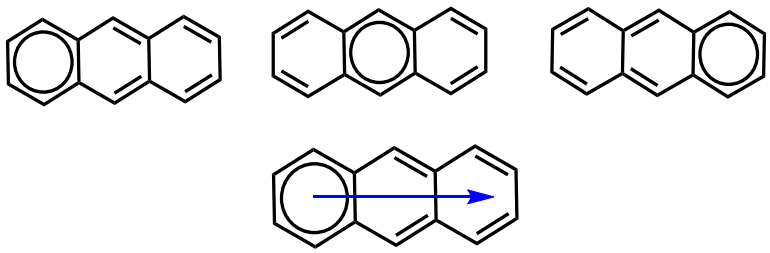

Figure 4.2: Clar's structure of anthracene; blue arrow indicates a migration of the sextet.

A good example to interpret a Clar's structure is anthracene in Figure 4.2. When scrutinizing all possible resonance structures of anthracene, it can be found that there will only be one π-sextet. However, the sextet migrates throughout the molecule, which is indicated by the structure on the bottom. In general, linear PAH like the acene family will experience the migration of the sextet and will not generate multiple π-sextets within the molecule. The main way of generating more π-sextets is the fusion of angular rings around the benzene moiety as seen in Figure 4.3.

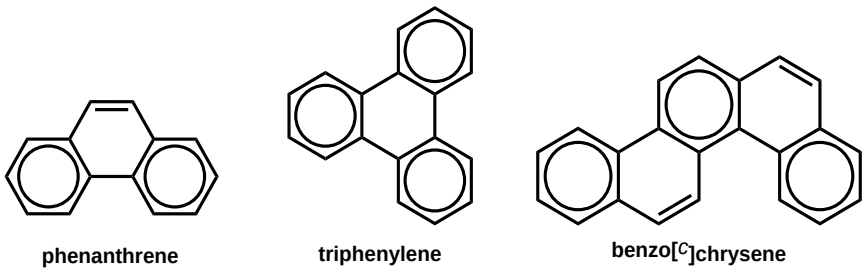

Figure 4.3: Examples of angularly fused PAHs.

It was found that molecules which have more π-sextets experience higher chemical stability (Figure 4.4). For example, anthracene only has one π-sextet, phenanthrene has two, and triphenylene has three π-sextet. When we look at the π-sextet migration we can see that the latter two have two and three π-sextet donating into the central ring respectively. This additional aromatic contribution increases the chemical stability of the molecule. This explains why acenes are so unstable compared to other PAH and why anthracene can undergo Diels-Alder reactions despite being aromatic while the other two have historically been inactive in Diels-Alder reaction. [1,5]

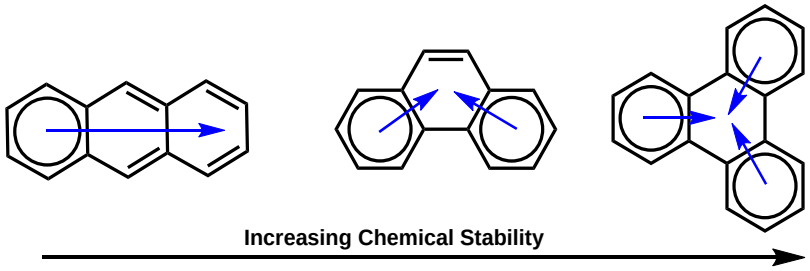

Figure 4.4: Clar's sextet rule demonstrates increased chemical stability.

Clar's sextet rule has been supported in both experimental and computational studies. [6] These studies show that the HOMO-LUMO gap is affected by the number of π-sextets within the molecule; the more π-sextet present, the larger the HOMO-LUMO gap is. Most PAH have HOMO-LUMO band gaps of >2.1 eV. [7] It has been theorized that the smaller number of π-sextets within a molecule would allow for more electron delocalization and decrease the energy gap. By understanding Clar's sextet rule, scientists have been able to rationalize the HOMO-LUMO band gap of various sized graphenes, predict properties of nanoribbons, and help determine ground states of biradical structures.

4.1.3 PAH-Fused Porphyrins

Due to the rich chemistry PAH offers, PAHs have been fused to a porphyrin core. [7] Porphyrins have been synthesized via thermal cyclodehydrogenation [8] and coupling reactions [9] with a variety of PAH including but not limited to naphthalene, benzene, azulene, and pyrene. [10] Porphyrins and PAH both have rich optical properties and when fused together broadening and shifting of both the porphyrin Soret and Q bands can be observed. Benzochlorins [9, 10, 11] have been a heavily studied PAH-porphyrin derivative that has been shown to disrupt the porphyrin ring's conjugation.

It is important to note that most PAH-fused porphyrins are metalated and involve electron donating groups like alkoxy groups. This is because metalation activates the porphyrin core and peripheral electron donating groups donate electron density into the aromatic system. Nickel (II) is the most common metal used in these PAH-fused porphyrins, but the metal deactivates the excited state through low-lying d-d states which limits optical properties. Furthermore, demetallation of Ni (II) from the porphyrin requires harsh conditions, often leading to low yields and decomposed byproducts.

In this chapter, previous work done on triphenylene-fused metal-inserted porphyrins will be discussed along with further attempts at functionalization. In particular, the failed attempts at Diels-Alder reactions and moderately successful attempts of intermolecular Scholl reactions will be discussed.

4.2 Triphenylene-Fused Porphyrin

4.2.1 Previous Work

Previous work [12], Scheme 4.1, has been done by our group in which a Ni-inserted 2,3-

dibromo-5,10,15,20-tetrakis(isopropylphenyl)porphyrin underwent a one-pot reaction in which a two-fold heck and 6π-cyclization reaction and aromatization occurs to generate a benzoporphyrin with methoxy groups attached to the peripheral benzene rings. Further functionalization was done via an intramolecular Scholl reaction which generated the first, and to our knowledge only, triphenylene-fused porphyrins.

Systematic naming of these porphyrins can be challenging in terms of identifying appropriate substituent and face locants, especially for the monobenzoporphyrin. As a result, the nickel inserted monobenzoporpyrin will be referred to **Ni3MSp** from here on out.

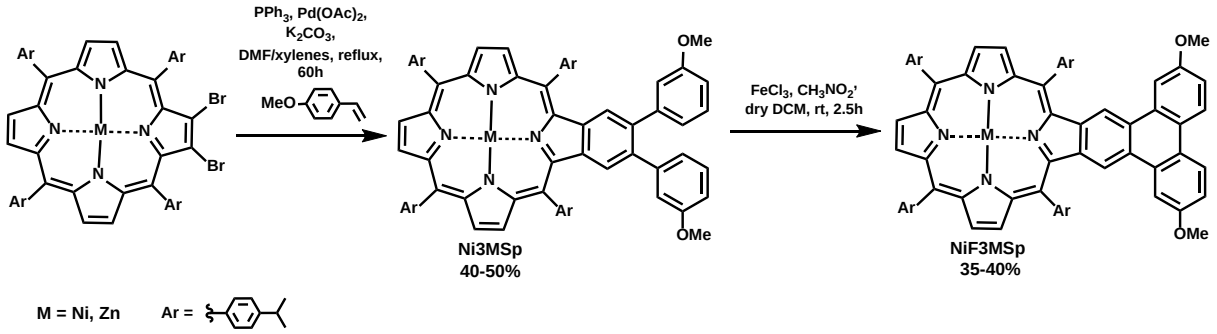

Scheme 4.1: Synthesis of Ni(II) 2,7-dimethoxytriphenylene-fused isopropyl porphyrin.

The intramolecular Scholl product is a bit easier to name as we have a common PAH fused to the porphyrin core. This means that we only need to assign the locants for the methoxy groups and obtain the name 2,7-dimethoxytriphenylene-fused (tetrakisisopropylphenyl)-porphyrin. But for the remainder of this dissertation, this porphyrin will be referred to as **NiF3MSp**.

With the success of the intramolecular Scholl reaction generating **NiF3MSp**, we decided to extend the porphyrin π-system further. However, instead of using 3-methoxystyrene as shown in Scheme 4.1 we used 3,4-dimethoxystyrene to generate a novel monobenzoporphyrins before following it up with an intramolecular Scholl reaction as the starting reagent (Scheme

4.2). This triphenylene-fused porphyrin then underwent an intermolecular Scholl reaction with 1,2-dimethoxybenzene.

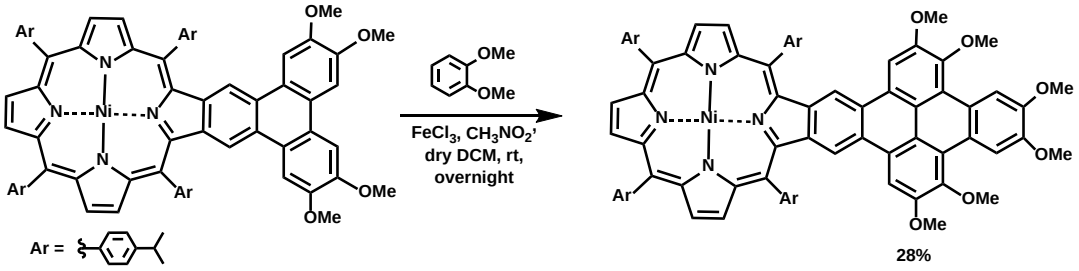

Scheme 4.2: Further extension of the porphyrin π-system of a triphenylene fused porphyrin.

No further functionalization has been done by our group, or others, since we published in 2011. We decided to revisit the **NiF3MSp** synthesis in Scheme 4.1 and attempted to further extend the π-system with other reagents which will be discussed in the following sections.

4.2.2 Current Synthesis

Using the same methodology, the freebase monobenzoporphyrins (**3MSp**) and its fused triphenylene (**F3MSp**) analogue were prepared (Scheme 4.3), which have not been reported in the literature.

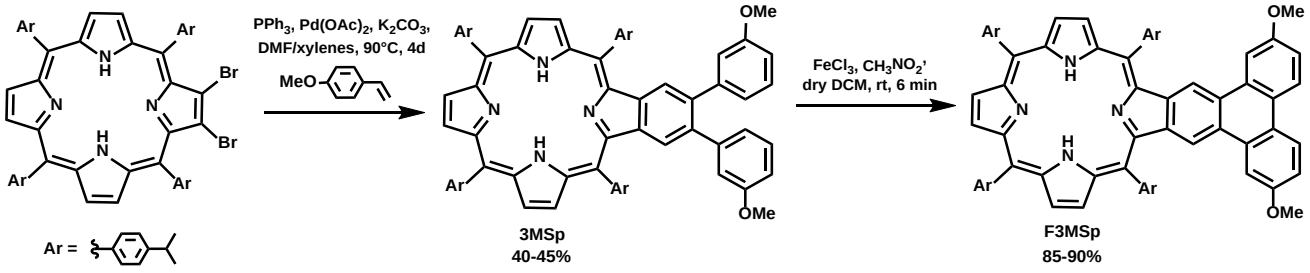

Scheme 4.3: Synthesis of 3MSp and F3MSp.

The UV-VIS absorption spectra of the freebase analogues can be compared with the previously reported **Ni3MSp** and **NiF3MSp** in Figure 4.5. The Soret band doesn't change between the freebase or nickel **3MSp** (433 nm) or **F3MSp** (447 nm) but the Q bands do change.

The freebase porphyrins display four Q bands while the metalated porphyrin display two. The specific wavelengths which these peaks appear can be found in the experimental section.

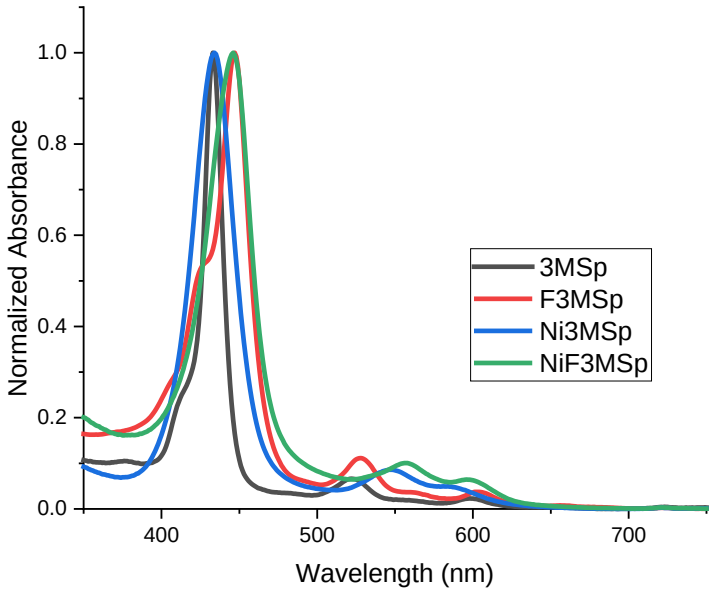

Figure 4.5: Normalized UV-VIS spectra of 3MSp and F3MSp and their nickel-inserted derivatives in dichloromethane.

Upon the completion of the intramolecular Scholl reaction, nickel was into the porphyrin core. However, an intermolecular Scholl reaction with **F3MSp** failed. This could be attributed to steric effects with the methoxy groups and the inherent aromaticity present in the isolated π-sextets present in the triphenylene moiety.

4.2.2.1 Diels-Alder Reactions

Our attempt at extending the π-system was first tried through a Diels-Alder reaction, Scheme 4.4, with various dienophiles. We wanted to see if the **NiF3MS** would undergo a Diels-Alder reaction; it was hypothesized that the combination of a metal activating the porphyrin and the presence of electron donating methoxy groups may facilitate a Diels-Alder reaction, even though triphenylene has been previously inert in these reactions.

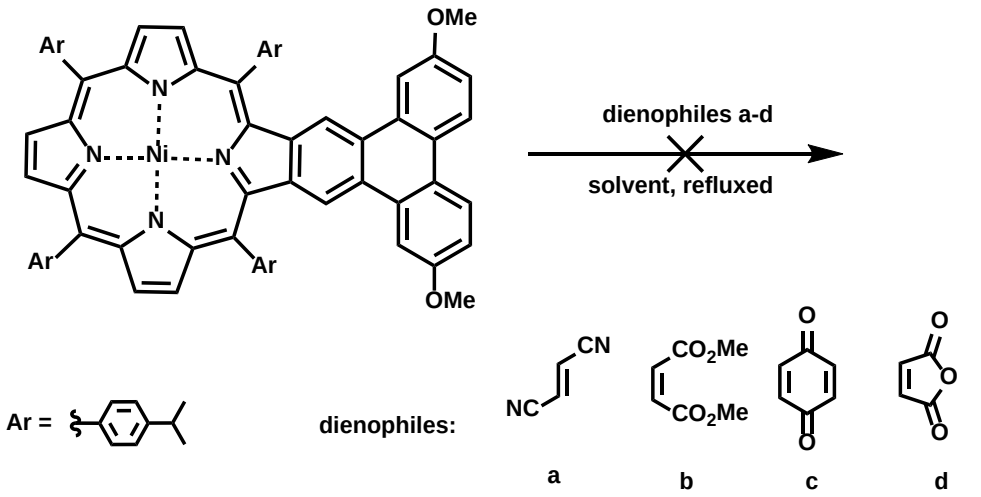

Scheme 4.4: Diels-Alder reaction with NiF3MSp; dienophiles b) and d) were also used as the solvent for that reaction with small amounts of toluene to dissolve the porphyrin; dienophiles a) and c) were conducted in dimethylformamide and xylenes respectively. All reactions were refluxed overnight and monitored by UV-VIS and TLC.

Maleic anhydride is known to be a strong and reactive dienophile which has reacted with perylene [1,3] in the past. Triphenylene has similar "bay regions" to those of perylene (Figure 4.6) and so it was theorized that the bay region of the triphenylene moiety in **F3MSp** may similarly undergo a Diels-Alder reaction.

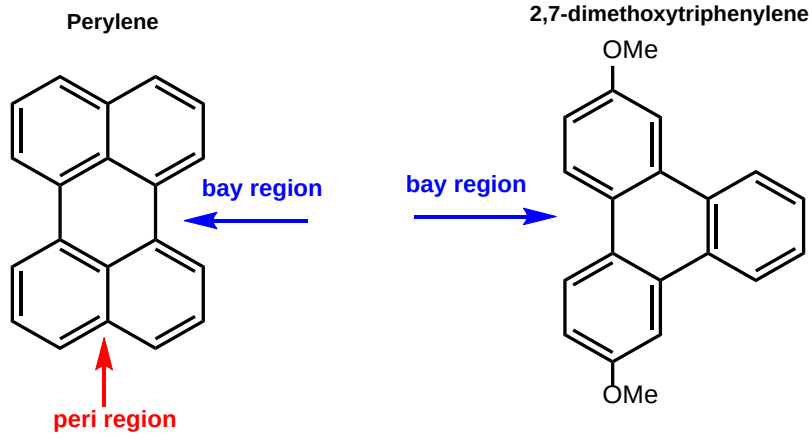

Figure 4.6: Bay regions of perylene and substituted-triphenylene.

However, the reaction did not proceed. Nor did it proceed with dimethyl malate, *p*-benzoquinone, or fumaronitrile. While monitoring the reactions through UV-VIS and TLC, no

changes were observed throughout the reaction timeframe. This perplexed us as literature has shown bay regions of some PAH can undergo a Diels-Alder reaction. To better understand why this reaction did not proceed, we need to refer to the π-sextets of these compounds.

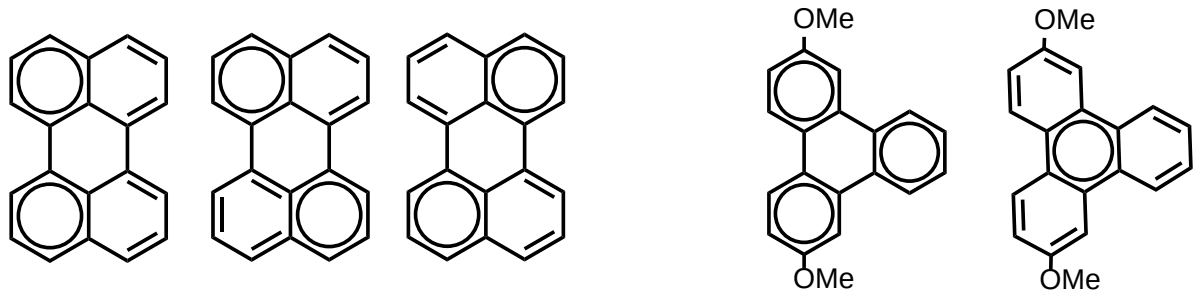

A. Perylene Clar Structures **B. Triphenylene Clar Structures**

Figure 4.7: Clar Structures of perylene and triphenylene.

As previously mentioned in section 4.1.2, the more Clar's sextets present within a PAH, the higher the compound's chemical stability. Regardless of how we draw the resonance structures for perylene, Figure 4.7, there are only two π-sextets. Considering the ability of perylene to undergo Diels-Alder reactions at the bay region it is also most likely that the resonance structure on the left is the contributing resonance structure during the Diels-Alder reaction. When we draw the resonance structures of triphenylene, we can get either one or three π-sextets; as Clar's rule states the compound with the most π-sextets are preferred, which suggests that the three π-sextets structure is the one to compare with. Triphenylene has a greater number of π-sextets and is therefore more chemically stable than perylene.

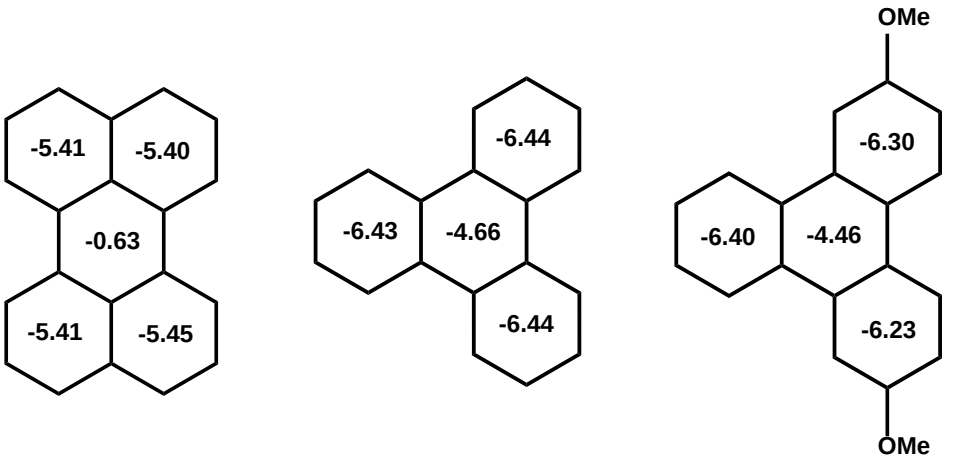

Figure 4.8: Individual ring NICS(1.7) ppm and total (ΣNICS(1.7) ppm) of perylene, triphenylene, and a 2,7-dimethoxytriphenylene. ΣNICS(1.7) is calculated by adding all the individual ring ppm's together within that molecule; NICS aromaticity studies were performed using the GIAO B3LYP/6-31G(d,p) basis set.

In fact, when we look at NICS studies in which the dummy atoms (Bq) are 1.7 Å above the plane of the molecule for each ring in the perylene and triphenylene (Figure 4.8) we see that triphenylene has a higher overall aromatic character, -24 compared to -22.3 respectively. The addition of two methoxy groups attached to the triphenylene position does reduce the aromatic character slightly; but the substituted triphenylene also has a higher aromatic character as well. This would support the statement that triphenylene is more chemically stable than perylene and help explain why the triphenylene moiety on the porphyrin did not undergo the Diels-Alder reaction.

4.2.2.2 Intermolecular Scholl Reactions

With the failure of the Diels-Alder reactions, we went back to the previously successful intermolecular Scholl reaction. Instead of using 1,2-dimethoxybenzene and four methoxy

groups on the triphenylene moiety, **NiF3MSp** was reacted with 1,4-dimethoxybenzene under the same conditions but varying equivalence of 1,4-dimethoxybenzene.

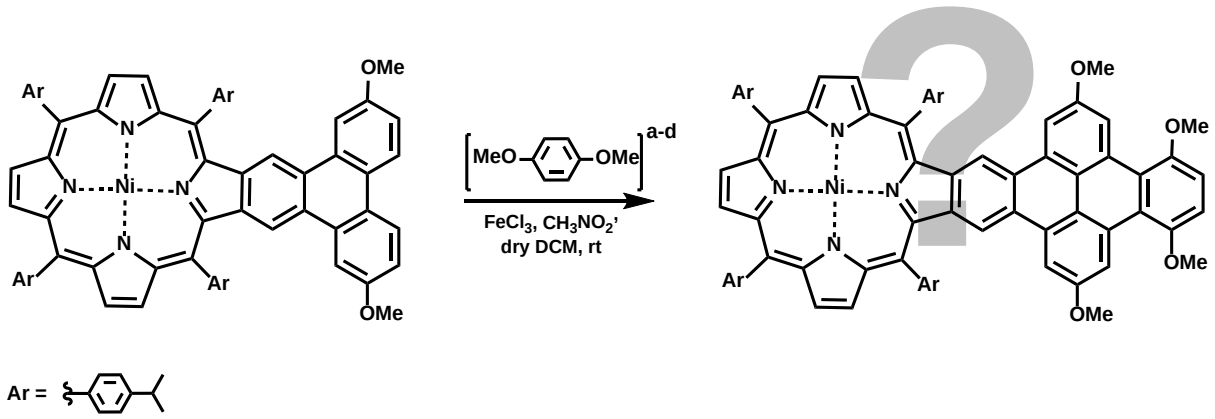

Scheme 4.5: Intermolecular Scholl reaction with NiF3MSp; attempts at the intermolecular Scholl reaction was done with: a) 2 eq 1,4-dimethoxybenzene, b) 4 eq 1,4-dimethoxybenzene, c) 20 eq 1,4-dimethoxybenzene, and d) slow addition of up to 5 eq of 1,4-dimethoxybenzene. Note that the product displayed was the targeted product. The question mark indicates that we are unsure of what the product(s) structure(s) are.

The first attempt at this intermolecular Scholl reaction was performed with 2 eq of 1,4-dimethoxybenzene (1,4-DMB) and 1 eq of **NiF3MSp**; however, this generated no change in the UV-VIS and minor changes in the TLC. These changes were attributed to the 1,4-DMB polymerizing with itself instead of the bay region on **NiF3MSp**. Therefore, more 1,4-DMB was added and a minor shift in the Soret was observed. Under the belief that perhaps a higher equivalence of 1,4-DMB is required for coupling to the triphenylene moiety, the next reaction had 4 eq of 1,4-DMB added at the start of the reaction. With this amount of 1,4-DMB there was no change in UV-VIS and minor changes in the TLC until more 1,4-DMB was added.

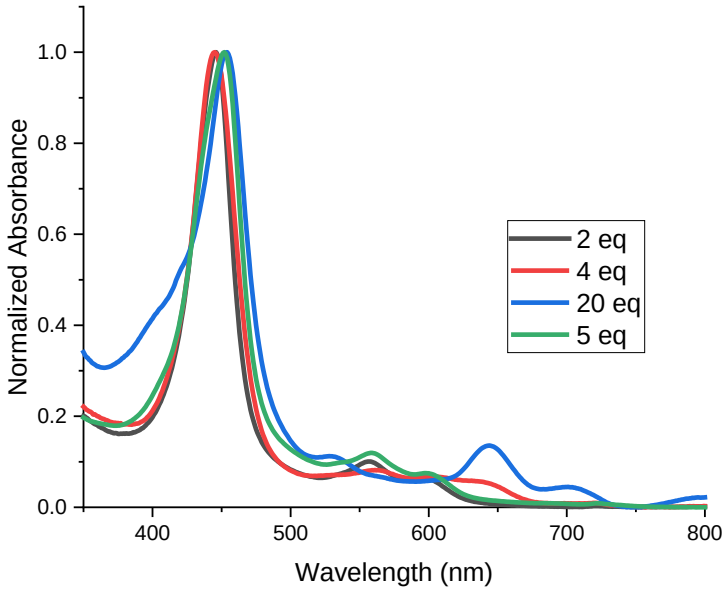

Figure 4.9: Normalized UV-VIS for intermolecular Scholl reaction with varying equivalents (2, 4, 5, and 20) of 1,4-dimethoxybenzene in dichloromethane.

Based on these results, there were two possible reason for the initial lack of reaction for the intermolecular Scholl reaction: 1) steric hinderance of the methoxy groups both on the triphenylene moiety and on 1,4-DMB which, in turn, limit the coupling of the two molecules or 2) the 1,4-DMB has a higher reactivity with itself than with the porphyrin and will be used up if added all at once. To test which scenario, we set up first step up a reaction with 20 eq 1,4-DMB and 1 eq **NiF3MSp**.This reaction was done to see if adding excess 1,4-DMB would force a coupling reaction between the small molecule and the triphenylene moiety. This would also ensure that even if the 1,4-DMB molecules reacted with each other there was still enough to react with the porphyrin. A red-shift in the Soret band was observed in the UV-VIS of the reaction mixture and multiple (7) spots were obtained when running a TLC in a 2:1 dichloromethane/hexanes solvent system. These spots were isolated by a Prep TLC using the same solvent system and a UV-VIS was taken which is shown in Figure 4.10 below. We can see that there are gradual differences in the B band of each of the products ranging from 452-458

nm. The Q bands drastically differ when looking at each of the products and most cases deviate from the expected two Q bands that come from metalation. In fact, the number of Q bands range from 2 – 4. This could indicate possible, although not very likely, demetallation of some of the porphyrin-based products. However, like most of the monomer attempts, the NMRs proved to be messy when ran in $CDCl_3$ but there was no N-H peak present which would indicate a freebase porphyrin; this suggests that demetallation of nickel did not occur.

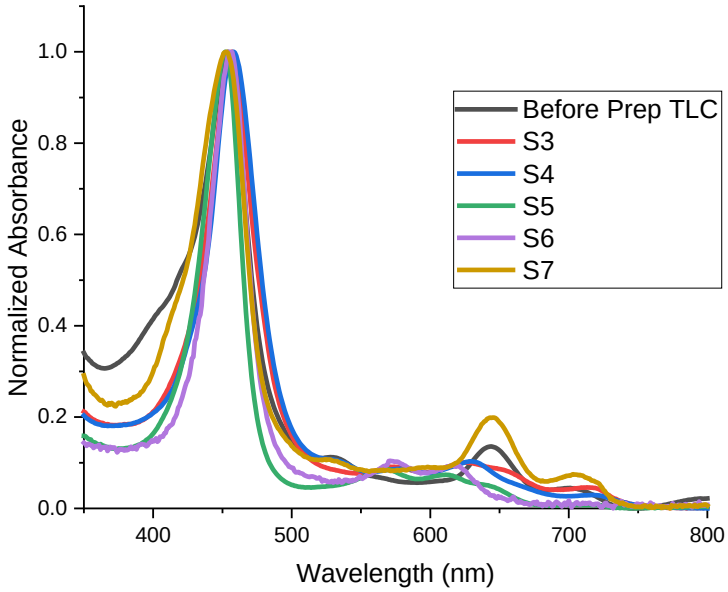

Figure 4.10: Normalized UV-VIS spectra for the 20 eq 1,4-DMB reaction and unidentified isolated products from the Prep TLC in dichloromethane.

These data suggest that something coupled to the porphyrin which resulted in a red-shift of the B band with higher equivalents of 1,4-DMB. However, this reaction also generated a complex mixture with undistinguishable products. When we look at the initial intermolecular Scholl attempts, we do note that adding 1,4-DMB in increments also can generate a bathochromatic shift in the Soret band. We then went back to the idea of a lower equivalence of 1,4-DMB and the reaction set up. In previous experiments all the starting materials were

added together, dissolved in dry dichloromethane, and the Ferric chloride solution was added and allowed to react overnight.

Instead of repeating these conditions, the 1,4-DMB and **NiF3MSp** were dissolved in dry dichloromethane and allowed to stir for 15 minutes shielded from light with aluminum foil before adding the Lewis acid. The reaction was then allowed to react overnight. These conditions provided the desired red shifting of the Soret band and produced less spots (3, two faint and one concentrated one) on the TLC in the same solvent system. These spots were easily separated through column chromatography. The first two spots were faint and did not produce a quantifiable amount. The major product (λ_{max}= 452 nm) was successfully isolated but the ^{1}H NMR spectra of this product was still messy. The identity of this product remains unclear and needs further investigation using single crystal X-ray crystallography.

The synthesis of a **NiF3MSp-dimer** was also attempted. This was done by increasing the equivalents of the porphyrin with only 1 eq of 1,4-DMB. This reaction generated similar results to the intermolecular Scholl reactions in that the B band shifts from the starting **NiF3MSp**.

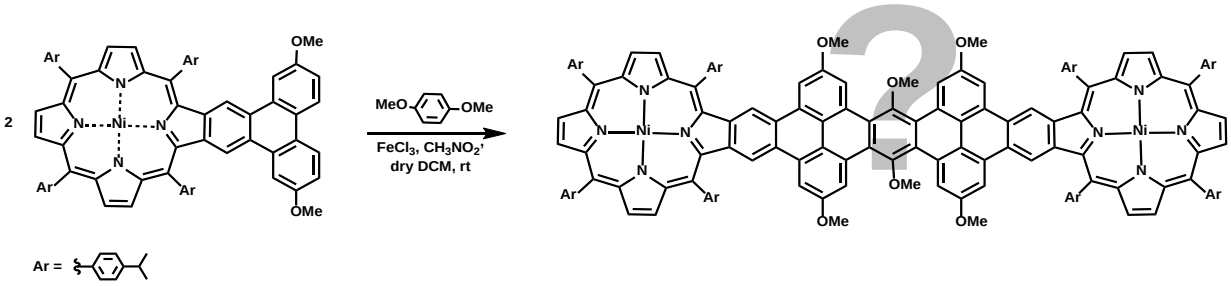

Scheme 4.6: Attempted synthesis of NiF3MSp-Dimer with 2 eq of NiF3MS and only 1 eq of 1,4-DMB. Note that the product displayed is the desired product. The question mark indicates that we are unsure of what the product(s) structure(s) are.

The UV-VIS spectra of the dimer before a Prep TLC is shown in Figure 4.11**,** along with two of the products (S3 and S4) that were isolated. Both products appear to be blue shifted

from the starting Soret band. The ^{1}H NMR spectra, found in the experimental section, of S3 and S4 show similar results as the monomer reactions, namely poor results when in $CDCl_3$ for product S4; although product S3 did give a spectrum that was cleaner in deuterated chloroform. As these reactions did proceed, they are not considered to be a failure—just a mystery that requires further study, hence the question mark on Scheme 4.5 and Scheme 4.6 product side.

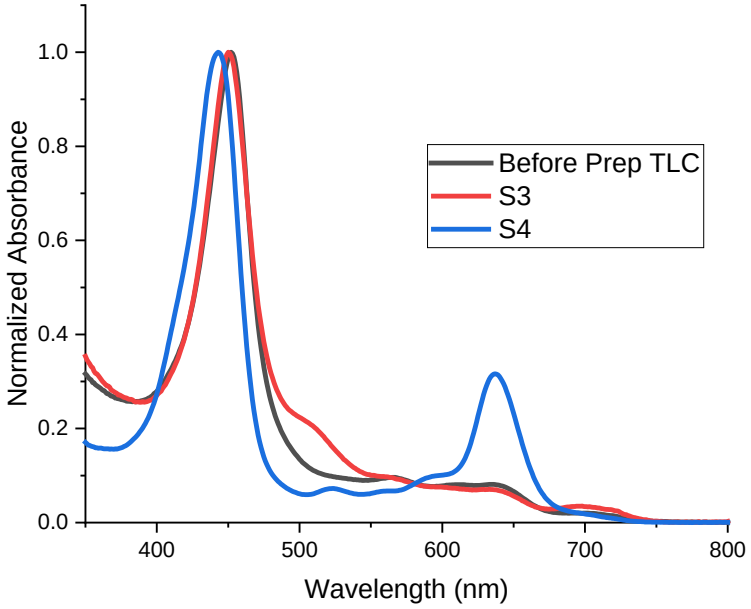

Figure 4.11: Normalized UV-VIS spectra of NiF3MSp-Dimer Scholl reaction solution and two unidentified products from Prep TLC.

Ultimately, we can infer three things from this work: 1) it is best to allow the reaction mixture to stir prior to the addition of the Lewis acid, 2) another deuterated solvent may be required for NMR characterization and 3) there is more work to be done to characterize these porphyrins.

4.2.3 Computational Studies

Although the optimization of the initial nickel inserted triphenylene-fused porphyrins

has been previously reported, computational studies on the freebase analogues were not. Therefore, the optimized structure of **3MSp** and **F3MSp** are included here. DFT calculations were also performed to determine the computational HOMO-LUMO band gap for **3MS**, **F3MSp**, **Ni3MSp**, and **NiF3MSp**. The DFT calculations were done using the B3LYP/6-31G(d,p) basis set and orbital images were rendered through Gaussian16. [13] Furthermore, NICS aromaticity studies were also carried out using the GIAO B3LYP/6-31G(d,p) basis set for the aforementioned porphyrins.

4.2.3.1 Geometry Optimization and DFT Calculations

Porphyrins are known to adopt various conformations depending on if and what type of metal is inserted into the porphyrin core. [14] Freebase and Zinc (II) inserted porphyrins tend to be planar because they are symmetrical. Depending on the size of the metal inserted the porphyrin core can be distorted. Common metals which cause distortion of the porphyrin core include nickel (II), cobalt (II)

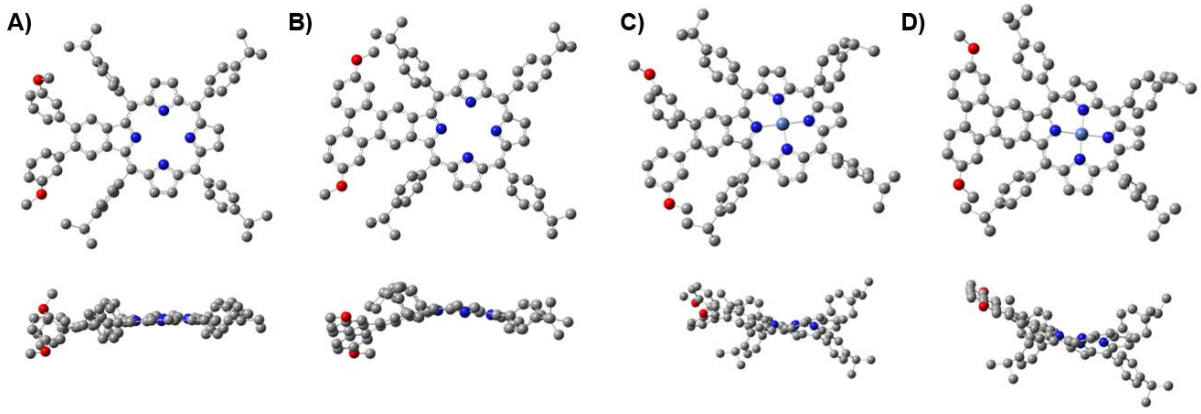

Figure 4.12: Geometry optimization. The top and side view of a) 3MSp, b) F3MSp, c) Ni3MSp, and d) NiF3MSp porphyrins. Note that hydrogens were omitted from these structures for clarity.

As a result, it is unsurprising to see that **3MSp** is planar in Figure 4.12. It's fused analog **F3MSp** does have a slight curvature of the core and the triphenylene moiety but is not distorted

like the geometries seen in both **Ni3MSp** and **NiF3MSp**. The insertion of nickel (II) forces the porphyrin core into a ruffled and out-of-plane shape whereas the freebase porphyrins remain mostly planar.

As mentioned previously, while DFT calculations had been done previously by our group in 2011, the HOMO-LUMO band gaps and the orbital diagrams of the freebase and nickel analogues of the triphenylene-fused porphyrins and their precursors were not reported. Therefore, in this section the HOMO -1 to LUMO +1 orbital diagrams (Figure 4.13) and the corresponding energy levels (Figure 4.14) will be discussed.

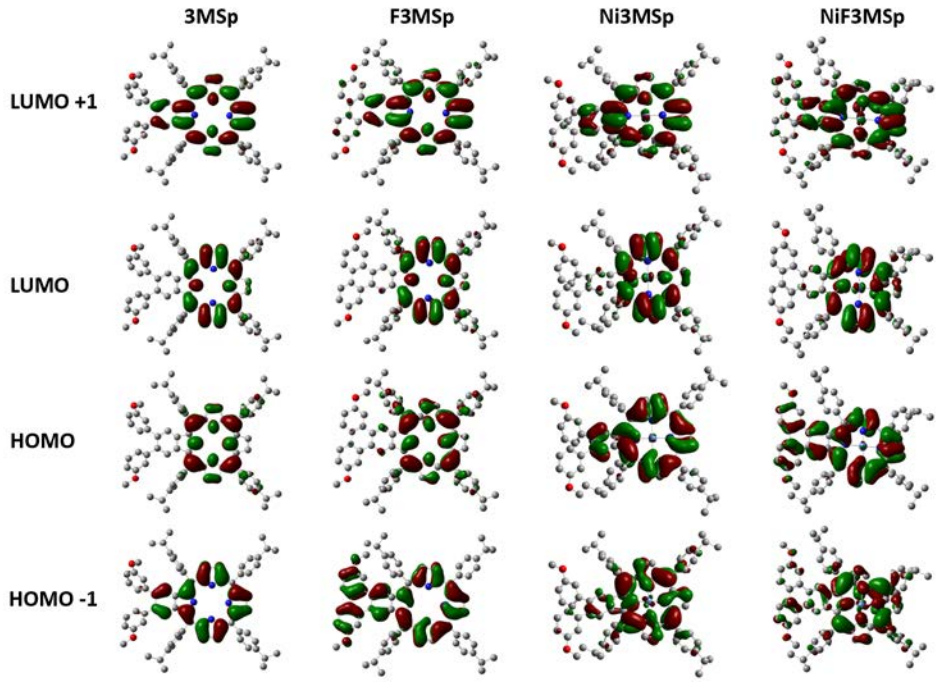

Figure 4.13: DFT HOMO -1 to LUMO +1 orbital diagrams for both the freebase and Ni (II) 3MSp and F3MSp.

The orbital diagrams of **3MSp** show that most of the electron density is on the porphyrin core. In both the HOMO -1 and the LUMO +1 the electron density is spread onto the benzene ring fused to the porphyrin core, but no electron density is located on the 3-methoxybenzene rings. This changes upon the fusion of these two rings. **F3MSp** does exhibit minor electron

density on the triphenylene moiety in both the HOMO and LUMO +1 orbitals and large amounts of electron density in the HOMO -2 orbital. The LUMO for this compound has the porphyrin core exhibiting the most electron density with only a minor part on the benzene fused ring.

Both nickel porphyrins adopted a ruffled shape which has affected how the electron density presents in the orbitals. **Ni3MSp** displays most of the electron density on the porphyrin core and the benzene ring directly fused to it in all but the LUMO orbital. Like its freebase counterpart, it doesn't show much electron density on the 3-methoxyphenyl rings attached. Whereas **NiF3MSp** displays electron density on the porphyrin core and throughout the triphenylene structure. The LUMO +1 orbital displays more electron density on the benzene ring than on the 3-methoxyphenyl rings. The HOMO -1 orbital shows roughly equal electron density placed upon the methoxyphenyl rings and the benzene ring. Whereas the HOMO orbital shows a large amount of electron density extending from the porphyrin core up to the methoxyphenyl rings. The LUMO of **NiF3MSp** however shows electron density predominantly on the porphyrin core and little anywhere elsewhere.

The energy gap between the HOMO and LUMO orbitals for each of the molecules is reported in Figure 4.14. It is apparent that the insertion of nickel into porphyrin increases the energy gap and that the fused triphenylene porphyrins have a lower energy gap than their precursors.

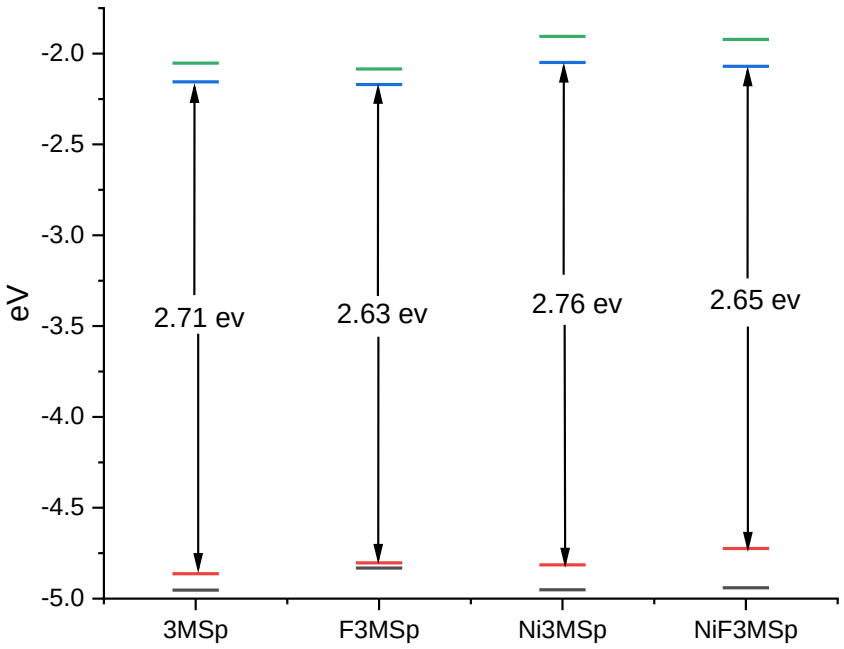

Figure 4.14: HOMO-LUMO energy diagram for both the freebase and Ni (II) 3MSp and F3MSp.

4.2.3.2 NICS(1.7) Studies

Due to the distortion of the Ni-inserted porphyrin cores and, in the case of the monobenzoporphyrins, lack of uniform planarity between the rings a NICS X-scan method was not used. The Bq atoms were placed at 1.7 Å away from the respective rings per Stanger's [15] method mentioned in Chapter 2. The dummy atoms were placed above the porphyrin core and along each ring that makes up the triphenylene moiety for both the fused and unfused porphyrins.

The individual ring currents are displayed in Figure 4.15. The insertion of nickel (II) drastically decreases the aromaticity of the porphyrin core as compared with its freebase porphyrin analogue. However, a and b of Figure 4.15 show the rings associated with the triphenylene moiety experience very little change in aromaticity in the monobenzoporphyrins, which is also observed in c and d of Figure 4.15 for the triphenylene-fused analogues.

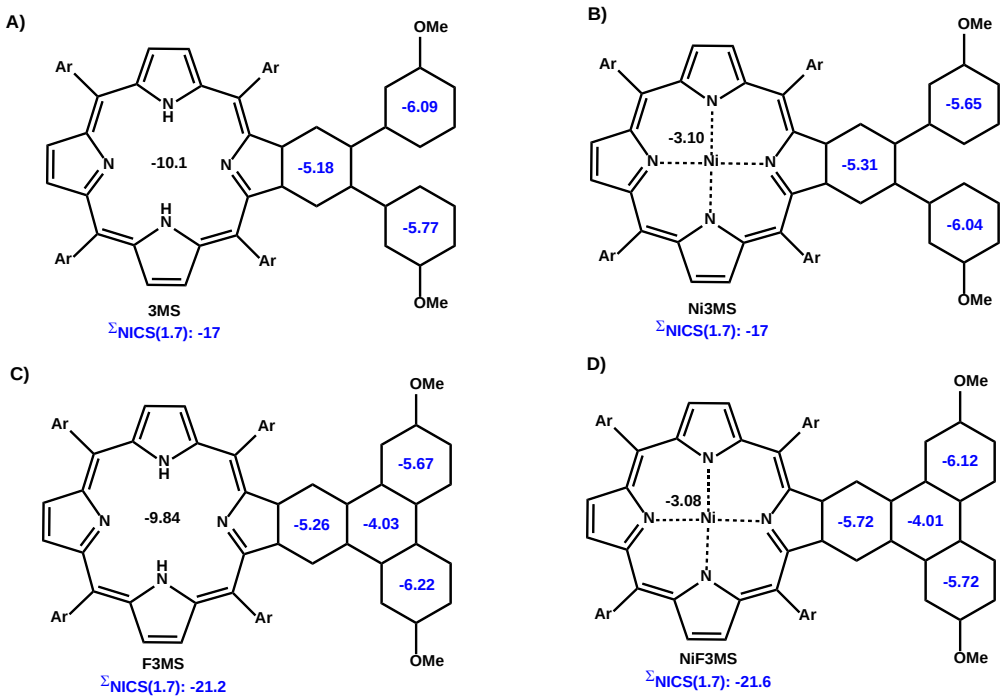

Figure 4.15: NICS(1.7) independent ring currents for a) 3MSp, b) Ni3MSp, c) F3MSp, and d) NiF3MSp.

This information allows for us to conclude that the fusion of a porphyrin to the triphenylene moiety only impacts the individual ring currents minimally—a difference of less than or approximately 1 ppm from the 2,7-dimethoxytriphenylene NICS values in Figure 4.8 from earlier. If we look at the total aromatic character, indicated in blue, of the rings of the *o*-terphenyl (a and b of Figure 4.15) and the triphenylene rings (c and d of Figure 4.15) we can see that the aromatic character doesn't change much regardless of nickel insertion. We only see an increase in aromatic character upon fusion of the *o*-terphenyl moiety into the triphenylene structure. This data supports the idea that the triphenylene structure fused to the porphyrin core maintains its three disjointed π-aromatic sextet which increases the chemical stability of the molecule.

4.3 Future Work and Conclusion

In conclusion, we revisited our initial **Ni3MSp** and **NiF3MSp** reported in 2011[11] and synthesized freebase analogues **3MSp** and **F3MSp**. Diels-Alder reaction conditions and intermolecular Scholl reactions were explored with **NiF3MSp** to extend the porphyrin π-system. The Diels-Alder reactions failed because of the inherent chemical stability present in triphenylene as explained by Clar's Rule and was supported by NICS(1.7) study of the small molecule triphenylene, substituted triphenylene, perylene, and freebase and nickel-inserted **F3MSp**. Intermolecular Scholl reactions yielded some results with varying equivalents of 1,4-dimethyoxybenzene so long it was either in excess or added in increments. These reactions generated multiple spots on analytical TLC and mostly poor ^{1}H NMR spectra were obtained in $CDCl_3$. Computational studies for the HOMO-LUMO energy gap, the orbital diagrams, and NICS(1.7) studies were also performed.

More work needs to be done in terms of characterizing the products from the intermolecular Scholl reactions of **NiF3MSp**. It cannot be guaranteed that ^{1}H NMR spectra of the isolated compounds without further purification will appear neat; this is because there are a multitude of potential products. This includes but not limited to various polymer derivatives of 1,4-dimethoxybenzene being fused to the porphyrin core, or multiple 1,4-dimethoxybenzene fused to the triphenylene rings or other places on the porphyrin. Examples of potential products are included in Figure 4.16. Furthermore, trying different deuterated NMR solvents is an important next step along with XRD and mass spectroscopy to help elucidate the structure of these compounds.

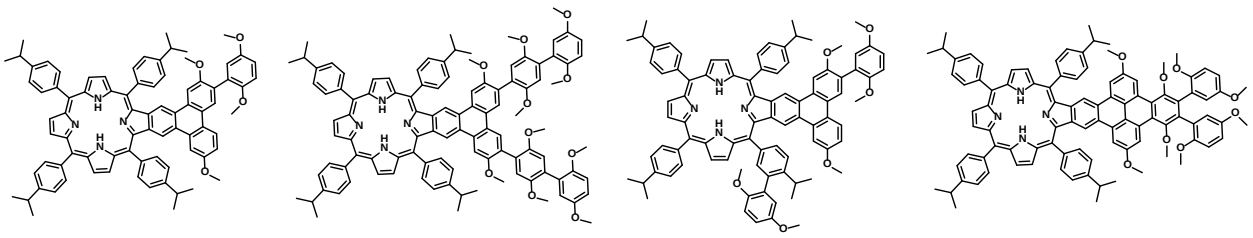

Figure 4.16: Examples of potential intermolecular Scholl reaction products.

A potential solution could be replacing the 3-methoxy groups with an electron withdrawing group on the nickel (II) triphenylene fused porphyrin. Alkoxy groups are known to be electron donating and therefore are ortho- and para-directors. However, the desired product for the intermolecular Scholl reactions is at the meta position. Replacing the methoxy groups with an electron withdrawing group may facilitate coupling at the meta-position; this group may also allow for a decrease in the aromatic character of the two rings and potentially allow for an inverse demand Diel-Alder reaction to occur with an electron rich dienophile. Specific details can be found in chapter 5.

4.4 Experimental Section

4.4.1 Synthesis

All reagents, including solvents, not specified below were purchased from Ambeed, Millipore-Sigma, Matrix-Scientific, and Fisher and—excluding dimethylformamide which was dried through a commercially available purification system—were used without further purification. All porphyrin products underwent purification on either a plug or column chromatography on silica gel. All reactions were monitored with UV-VIS absorption spectroscopy and analytical thin-layer chromatography.

3MSp

Procedure: Dibromoporphyrin (0.212 mmol), potassium carbonate (0.467 mmol), $Pd[OAc]_2$ (0.106 mmol), and triphenylphosphine (0.2763 mmol) were added to a Schlenk flask and placed under argon and dissolved in dimethylformamide/xylenes (10 mL). The 3-vinylanisole (2.12 mmol) was then added and the mixture was degassed by four freeze-pump-thaw cycles. The solution was heated at 90°C for four days. A silica plug with toluene was done to remove excess Pd^0 and polymer before the solvent was removed under vacuum; the desired product was collected and recrystallized using dichloromethane/methanol.

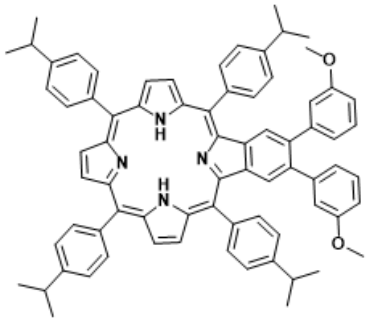

$C_{74}H_{68}N_4O_2$; purple; yield 43%, ^{1}H NMR (500 MHz, $CDCl_3$) δ, ppm 8.91 (d, *J* = 4.9 Hz), 8.84 (d, *J* = 3.8 Hz), 8.73 (s), 8.13 (dd, *J* = 11.3, 5.0 Hz), 7.61 (dd, *J* = 7.8, 6.1 Hz), 7.23 (d, *J* = 3.6 Hz), 7.13 (t, *J* = 7.9 Hz), 6.74 (d, *J* = 2.5 Hz), 6.72 (s), 6.70 (s), 6.56 – 6.55 (m), 3.57 (s), 3.23 (m), 1.55 (s), 1.54 (s), 1.43 (d, *J* = 6.8 Hz), -2.55 (s). UV/VIS (DCM): λ_{max}=433 nm (Soret) and 523, 557, 597, and 646 nm (Q bands).

F3MSp

Procedure: **3MSp** (0.146 mmol) was dissolved in dry CH_2Cl_2. Ferric chloride (1.46 mmol) was dissolved in 2 mL nitromethane and added to the solution under argon and stirred at room temperature for 6 min. MeOH was added to quench the reaction and the solution was washed with 10% $NaOH_{(aq)}$ and deionized water with dichloromethane. The organic layer was isolated, and the solvent removed by rotatory evaporation; the product was then recrystallized with dichloromethane/methanol.

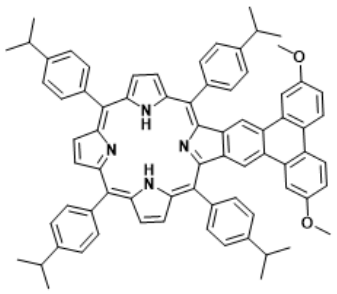

$C_{74}H_{66}N_4O_2$; purple; yield 90%, ^{1}H NMR (500 MHz, $CDCl_3$) δ, ppm 8.89 (d, *J* = 4.9 Hz), 8.76 (d, *J* = 4.9 Hz), 8.70 (d, *J* = 7.6 Hz), 8.37 (d, *J* = 8.8 Hz), 8.28 (d, *J* = 8.0 Hz), 8.15 (d, *J* = 8.0 Hz), 7.82 (d, *J* = 8.0 Hz), 7.57 (dd, *J* = 30.3, 10.8 Hz), 7.19 (d, *J* = 8.8 Hz, 1H), 4.01 (s), 3.53 – 3.40 (m), 3.36-3.20 (m), 1.55 (d, *J* = 5.9 Hz), -2.37 (s); UV/VIS (DCM): λ_{max}= 447 nm (Soret) and 528, 562, 604 and 654 nm (Q bands).

Ni3MSp and **NiF3MSp** were previously reported by our group. [12]

UV/VIS$_{Ni3MSp}$ (DCM): λ_{max}= 433 nm (Soret) and 548 and 587 nm (Q bands).

UV/VIS$_{NiF3MSp}$ (DCM): λ_{max}= 447 nm (Soret) and 558 and 559 nm (Q bands).

4.4.1.1 Diels-Alder Reaction

All Diels-Alder reaction procedures are split by the dienophile used.

Fumaronitrile

Procedure: **NiF3MSp** (0.015 mmol) and fumaronitrile (0.075 mmol) were added to a 50 mL round bottom flask and dissolved in 5 mL of nonpolar solvent (toluene and xylene in separate reactions). Argon was bubbled through the reaction solution before being refluxed overnight. No change was observed in the TLC or the UV-VIS; they remained similarly unchanged after an additional 2 days – an aqueous work up with 10% NaOH/deionized water and DCM were used and **NiF3MSp** was obtained after recrystallization with dichloromethane/methanol. Literature reported by Yates [16] suggested that Diels-Alder reactions could be accelerated with the use of the Lewis acid, $AlCl_3$. Therefore, another reaction with fumaronitrile was performed, using the same conditions but in dimethylformamide, 1 eq of $AlCl_3$ was added at the start of the reaction. No change in TLC or UV-VIS occurred, even when

the equivalents of $AlCl_3$ were increased to 5 equivalents. After work up, only **NiF3MSp** was recollected.

Maleic Anhydride

Procedure: **NiF3MSp** (0.014 mmol) was dissolved in 2 mL of toluene in a 50 mL round bottom flask and maleic anhydride (13.6 mmol) were added. The UV-VIS showed no change but the TLC (1:1 chloroform/ methanol solvent system) did display two spots. One of the spots were on the baseline of the TLC and one spot further up the TLC plate. Purification through a short silica plug revealed that the top spot was **NiF3MSp**. The baseline was only removed from the plug through acetone – this compound was insoluble in everything else; it is believed that this spot is a polymer product of homopolymerization of maleic anhydride and not a reaction product with the starting porphyrin. Another attempt at the reaction was done using 10 mL of dimethylformamide as the solvent; however, the reaction still did not proceed.

p-Benzoquinone

Procedure: Procedure: **NiF3MSp** (0.018 mmol) and p-benzoquinone (6.89 mmol) were dissolved in 10 mL of dimethylformamide in a 50 mL round bottom flask were added. Argon was bubbled through the reaction solution before being refluxed overnight. No change was observed in the TLC or the UV-VIS – an aqueous work up with 10% NaOH/deionized water and dichloromethane were used and **NiF3MSp** was obtained after recrystallization with dichloromethane/methanol.

Dimethyl Malate

Procedure: **NiF3MSp** (0.014 mmol) was dissolved in 2 mL of toluene in a 50 mL round bottom flask and dimethyl malate (27.9 mmol) were added. Argon was bubbled through the

reaction solution before being refluxed overnight. No change was observed in the TLC or the UV-VIS; they remained similarly unchanged after an additional day – an aqueous work up with 10% NaOH/deionized water and dichloromethane were used and **NiF3MSp** was obtained after recrystallization with dichloromethane/methanol.

We would like to note that even the addition of *p*-chloranil as a potential oxidant to induce aromatization of a Diels-Alder cycloadduct did not help the reaction proceed.

4.4.1.2 Intermolecular Scholl Reaction

Monomer

Procedure: NiF3MSp (0.0151 mmol) and 1,4-dimethoxybenzene (2 eq, 4 eq, 5 eq, and 20 eq) were dissolved in dry CH_2Cl_2. Ferric chloride (.151 mmol) was dissolved in 1mL nitromethane and added to the solution under argon and stirred at room temperature overnight. Reaction was monitored with TLC and UV-VIS. MeOH was added to quench the reaction and the solution was washed with 10% $NaOH_{(aq)}$ and deionized water with CH_2Cl_2. The organic layer was isolated, and the solvent removed by rotatory evaporation; the organic layer was then recrystallized with CH_2Cl_2/MeOH. For the reactions in which 2 eq and 4 eq of 1,4-dimethoxybenzene the starting NiF3MSp was obtained after recrystallization, not a new compound. New spots on the TLC and a UV-VIS shift only occurred upon the addition of more 1,4-dimethoxybenzene being added. For the reaction in which 20 eq of 1,4-dimethoxybenzene was used, multiple spots (5) were generated on the TLC and the B band was red shifted by 5 to 11 nm depending on the spot isolated. These spots were isolated and characterized to the best of our ability.

The mmol amount of 1,4-dimethoxybenzene required for each reaction is as follows: 0.0303 mmol, 0.121 mmol, 0.0758 mmol, and 0.303 mmol for 2 eq, 4 eq, 5 eq, and 20 eq respectively.

20 eq Prep TLC isolated S3

Molecular Formula is unknown; purple; ^{1}H NMR (500 MHz, cdcl$_3$) δ 10.02, 10.01, 9.99, 9.53, 9.52, 8.71, 8.68, 8.68, 8.67, 8.65, 8.64, 8.64, 8.63, 8.63, 8.62, 8.61, 8.42, 8.40, 8.38, 8.38, 8.37, 8.36, 8.32, 8.31, 7.99, 7.97, 7.96, 7.92, 7.92, 7.91, 7.91, 7.90, 7.89, 7.83, 7.81, 7.73, 7.73, 7.72, 7.69, 7.62, 7.60, 7.53, 7.51, 7.48, 7.47, 7.47, 7.43, 7.42, 7.39, 7.20, 7.20, 7.19, 7.18, 7.16, 7.15, 7.05, 6.97, 6.93, 6.91, 6.84, 6.68, 6.67, 6.60, 6.58, 6.55, 6.55, 6.54, 6.52, 6.45, 6.43, 6.33, 6.14, 6.12, 5.88, 5.68, 5.61, 5.50, 5.37, 4.08, 4.07, 4.05, 4.05, 4.04, 4.02, 3.99, 3.98, 3.97, 3.96, 3.94, 3.94, 3.93, 3.92, 3.91, 3.80, 3.79, 3.78, 3.77, 3.56, 3.55, 3.54, 3.49, 3.48, 3.48, 3.41, 3.39, 3.38, 3.36, 3.34, 3.31, 3.30, 3.23, 3.22, 3.20, 3.19, 3.17, 3.16, 3.15, 3.13, 3.04, 2.97, 1.65, 1.65, 1.64, 1.63, 1.63, 1.62, 1.60, 1.59, 1.58, 1.57, 1.56, 1.56, 1.56, 1.55, 1.54, 1.53, 1.49, 1.48, 1.47, 1.47, 1.46, 1.44, 1.43, 1.41, 1.40, 1.39, 1.38, 1.38, 1.37, 1.37, 1.36, 1.35, 1.33, 1.33, 1.32, 1.31, 1.30, 1.30, 1.29, 1.28, 1.27, 1.26; UV/VIS (DCM): λ_{max}= 457 nm (Soret) and 572, 628, 651 (Q bands).

20 eq Prep TLC isolated S4

Molecular Formula is unknown; purple; ^{1}H NMR (400 MHz, cdcl$_3$) δ 8.99, 8.77, 8.65, 8.64, 8.44, 8.43, 8.42, 8.41, 8.40, 8.39, 8.38, 8.37, 8.32, 8.31, 8.30, 8.28, 8.05, 8.04, 7.92, 7.92, 7.81, 7.80, 7.70, 7.69, 7.46, 7.06, 7.04, 7.02, 6.96, 6.95, 6.71, 6.71, 6.69, 6.68, 6.64, 6.64, 6.62, 6.61, 6.49, 6.48, 6.46, 6.45, 6.44, 6.28, 6.27, 6.23, 6.02, 5.97, 5.96, 4.37, 3.73, 3.72, 3.70, 3.64, 3.46, 3.35, 3.34, 3.30, 3.28, 3.21, 3.17, 3.13, 3.10, 3.06, 3.01, 2.88, 2.86, 2.81, 1.59, 1.58, 1.57, 1.56, 1.55, 1.46, 1.45, 1.43, 1.41, 1.37, 1.35, 1.34, 1.32, 1.28, 1.27, 1.26, 1.25, 1.25, 1.24, 1.23, 1.22, 1.17, 1.12, 1.10, 1.04, 1.02, 1.00, 0.53, 0.39.; UV/VIS (DCM): λ_{max}= 458 nm (Soret) and 534, 579, 632, 720 nm (Q bands).

20 eq Prep TLC isolated S5

Molecular Formula is unknown; green; There was not enough sample to get an NMR; UV/VIS (DCM): λ_{max}=452 nm (Soret) and 566, 609, and 648 nm (Q bands).

20 eq Prep TLC isolated S6

Molecular Formula is unknown; dark green; ^{1}H NMR (500 MHz, cdcl$_3$) δ 10.02, 8.15, 8.14, 7.74, 7.74, 7.66, 7.64, 7.48, 7.47, 7.45, 7.35, 7.33, 7.13, 7.10, 7.09, 7.09, 7.08, 7.07, 7.06, 7.05, 7.03, 7.01, 6.96, 6.94, 6.92, 6.71, 6.69, 6.68, 6.66, 6.65, 6.63, 6.61, 6.58, 6.57, 6.55, 6.55,

6.54, 6.50, 6.49, 6.45, 6.42, 6.14, 5.77, 5.74, 5.64, 5.64, 5.50, 5.43, 5.27, 5.25, 4.09, 4.06, 4.00, 3.99, 3.98, 3.95, 3.92, 3.84, 3.57, 3.55, 3.53, 3.52, 3.49, 3.32, 3.25, 3.19, 3.16, 3.14, 3.13, 3.12, 3.10, 3.05, 2.98, 2.97, 2.96, 2.95, 2.93, 2.91, 2.90, 1.65, 1.64, 1.59, 1.58, 1.56, 1.48, 1.47, 1.46, 1.44, 1.41, 1.39, 1.39, 1.38, 1.37, 1.37, 1.36, 1.36, 1.34, 1.33, 1.32, 1.31, 1.30, 1.29, 1.27, 1.21, 1.20, 1.19, 1.18.; UV/VIS (DCM): λ_{max}=454 nm (Soret) and 573 and 617 nm (Q bands).

20 eq Prep TLC isolated S7

Molecular Formula is unknown; bright green; ^{1}H NMR (500 MHz, $CDCl_3$) δ, ppm 8.90 – 8.87 (m), 8.86 (d, *J* = 5.0 Hz), 8.81 – 8.79 (m), 8.72 (s), 8.63 (s), 3.27 (m), 1.56 (s), 1.55 (d, *J* = 2.2 Hz), 1.53 (d, *J* = 2.4 Hz).; UV/VIS (DCM): λ_{max}=453 nm (Soret) and 528, 645, and 708 nm (Q bands).

Dimerization

Procedure: Procedure: NiF3MSp (0.0363 mmol) and 1,4-dimethoxybenzene (0.0181 mmol) were dissolved in dry dichloromethane. Ferric chloride (0.363 mmol) was dissolved in 1 mL nitromethane and added to the solution under argon and stirred at room temperature overnight. Reaction was monitored with TLC and UV-VIS. MeOH was added to quench the reaction and the solution was washed with 10% $NaOH_{(aq)}$ and deionized water with dichloromethane. The organic layer was isolated, and the solvent removed by rotatory evaporation; the organic layer was then recrystallized with dichloromethane/methanol.

Dimerization Prep TLC isolated S3

Molecular Formula is unknown; green; ^{1}H NMR (500 MHz, $CDCl_3$) δ, ppm 8.41 (d, *J* = 9.1 Hz, 1H), 8.29 (d, *J* = 4.8 Hz, 1H), 7.26 (s, 46H), 7.10 – 6.97 (m, 2H), 3.73 (s, *J* = 14.6 Hz, 2H), 3.02 (s, 2H), 2.90 – 2.75 (m, 3H), 1.61 – 1.52 (m, 8H), 1.52 – 0.76 (m, 72H), 1.02 (s, 18H), 1.02 (s, 18H), 0.51 (s, 9H), 0.39 (s, 4H); NMR integrates UV/VIS (DCM): λ_{max}= 450 nm (Soret) and 511, 563, 640, and 706 nm (Q bands).

Dimerization Prep TLC isolated S4

Molecular Formula is unknown; dark green; ^{1}H NMR (400 MHz, $CDCl_3$) δ, ppm 8.99, 8.77, 8.65, 8.64, 8.44, 8.43, 8.42, 8.41, 8.40, 8.39, 8.38, 8.37, 8.32, 8.31, 8.30, 8.28, 8.05, 8.04, 7.92, 7.92, 7.81, 7.80, 7.70, 7.69, 7.46, 7.26, 7.15, 7.13, 7.06, 7.04, 7.02, 6.96, 6.95, 6.71, 6.71, 6.69,

6.68, 6.64, 6.64, 6.62, 6.61, 6.49, 6.48, 6.46, 6.45, 6.44, 6.28, 6.27, 6.23, 6.02, 5.97, 5.96, 4.37, 3.73, 3.70, 3.64, 3.46, 3.35, 3.34, 3.30, 3.28, 3.21, 3.17, 3.13, 3.10, 3.06, 3.01, 2.88, 2.86, 2.81, 1.59, 1.58, 1.57, 1.56, 1.55, 1.46, 1.45, 1.43, 1.41, 1.37, 1.35, 1.34, 1.32, 1.28, 1.27, 1.26, 1.25, 1.25, 1.24, 1.23, 1.22, 1.17, 1.12, 1.10, 1.04, 1.02, 1.00, 0.53, 0.39, 0.36, 0.32, 0.29; UV/VIS (DCM): λ_{max}= 443 nm (Soret) and 523, 559, 593, and 637 nm (Q bands).

4.4.2 ^{1}H NMR Spectra

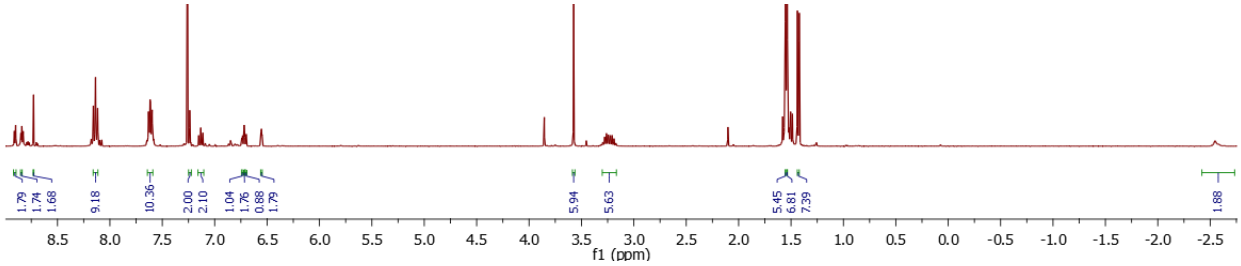

Figure 4.17: 3MSp– ^{1}H NMR (500 MHz, $CDCl_3$)

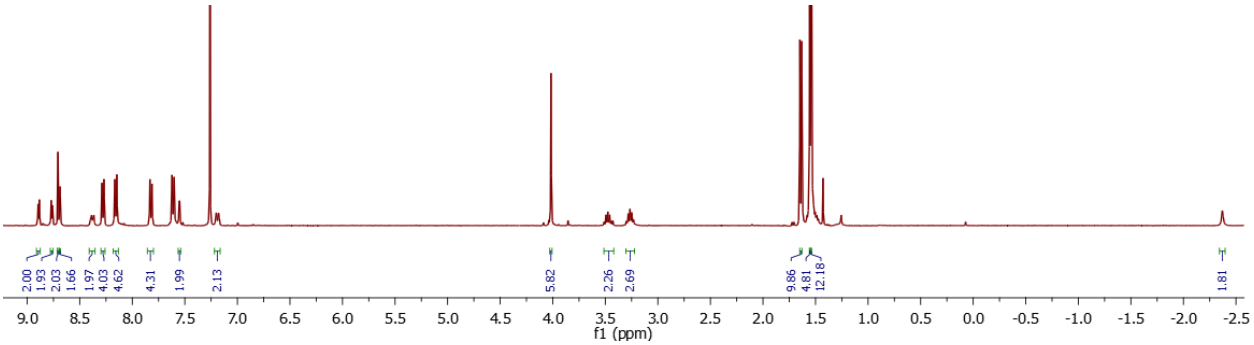

Figure 4.18: F3MSp– ^{1}H NMR (500 MHz, $CDCl_3$)

4.4.2.1 Monomer NMR Products

It is important to remember that these do not appear to be clean NMRs despite being isolated from Prep TLCs; these NMRs are included so that we can show what the NMR of these compounds look like in $CDCl_3$ and to show that we did not just recollect the starting **NiF3MSp**. Further characterization needs to be done to identify the structure of the isolated products. The NMR was analyzed to the best of our ability at the present time.

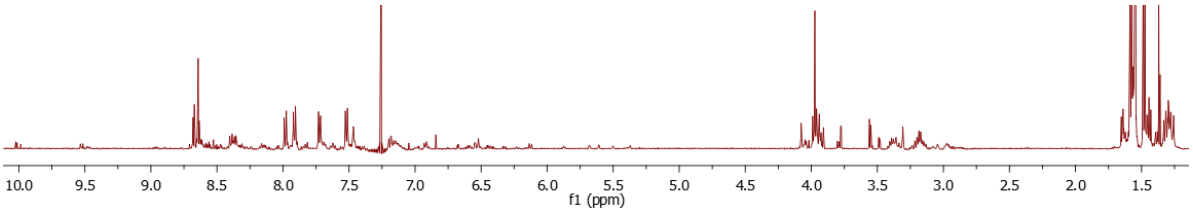

Figure 4.19: 20 eq Prep TLC isolated S3 – ^{1}H NMR (500 MHz, $CDCl_3$)

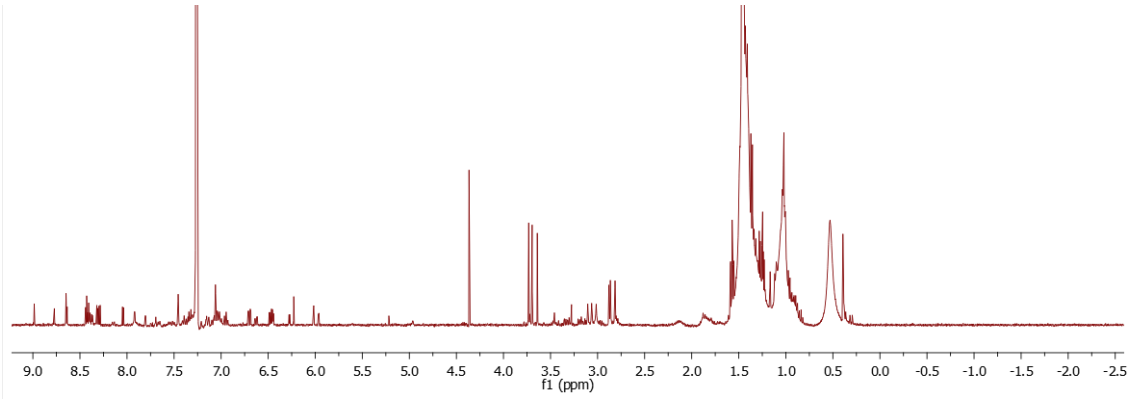

Figure 4.20: 20 eq Prep TLC isolated S4 – ^{1}H NMR (400 MHz, $CDCl_3$)

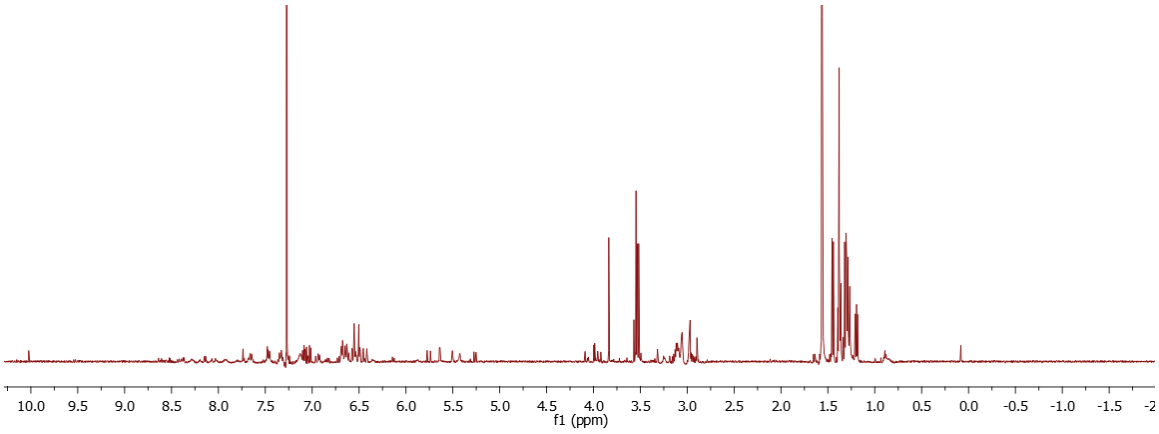

Figure 4.21: 20 eq Prep TLC isolated S6 – ^{1}H NMR (500 MHz, $CDCl_3$)

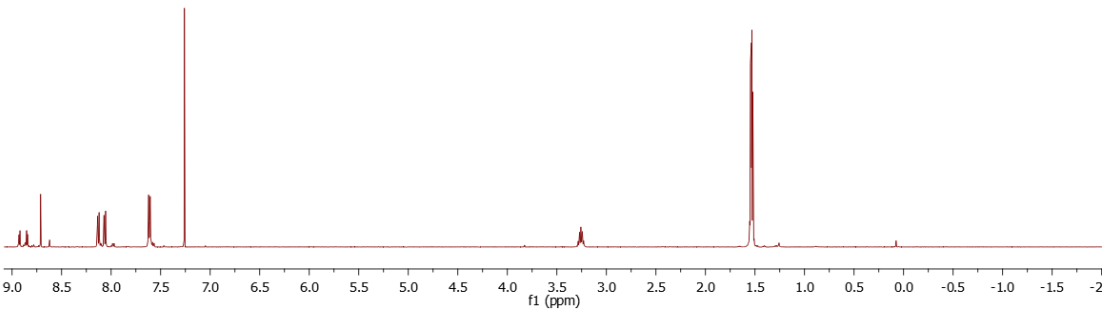

Figure 4.22: 20 eq Prep TLC isolated S7 – ^{1}H NMR (500 MHz, $CDCl_3$)

Common peaks attributed to the base porphyrin are the beta peaks between 9-8.5 ppm, multiplet peak around 3.25 ppm and the methyl peaks around 1.5 ppm. Integration was attempted with the assumption that the two doublet peaks around 9.0 ppm were beta-H of the porphyrin but integration of 2 (monomer) and 4 (dimer) did not yield an integration count that matched potential products and there did not appear to be any methoxy peaks present. Further analysis does need to be done.

4.4.2.2 Dimerization Product NMRs

It is important to remember that these do <u>not</u> appear to be clean NMRs despite being isolated from Prep TLCs; these NMRs are included so that we can show what the NMR of these compounds look like in $CDCl_3$ and to show that we did not just recollect the starting **NiF3MSp**. Further characterization needs to be done to identify the structure of the isolated products. The NMR was analyzed to the best of our ability at the present time.

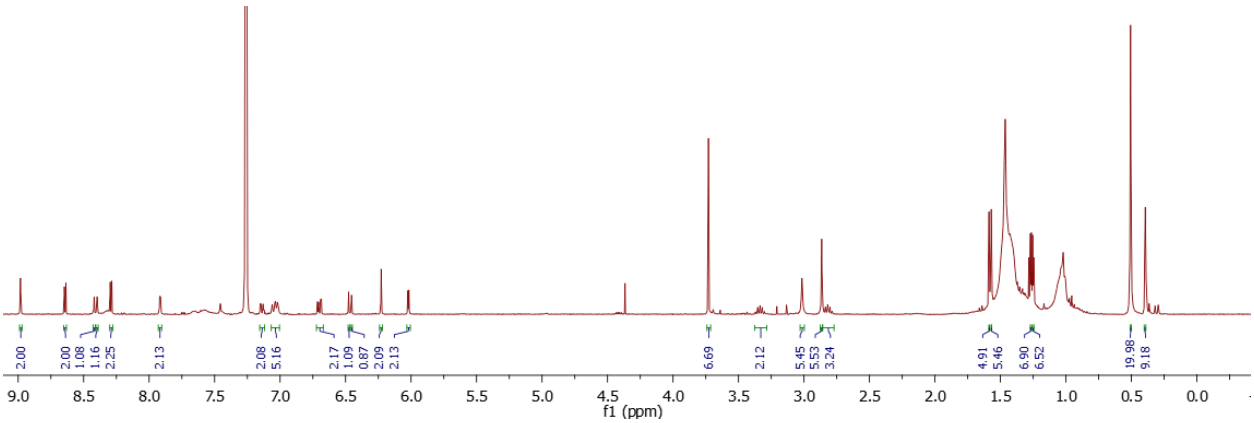

Figure 4.23: Prep TLC isolated S3 – ^{1}H NMR (400 MHz, $CDCl_3$)

Note the peak around 9 ppm was integrated to 2 based on the assumption that it's the singlet beta-H of the porphyrin core. We also see some multiplet peaks 2.8-3.45 ppm which could be attributed to the isopropyl-H peak. Based on these assumptions the integration

displayed in the NMR ends up being 102. However, in the experimental section, it is not integrated—this was done to report the general ppm and J-coupling value initially obtained. Integration to 102 was done to determine possible products based on porphyrin peaks. A potential product with the correct number of hydrogens can be seen below in Figure 4.24**.** However, the methoxy peaks (~3.75 ppm) do not integrate appropriately.

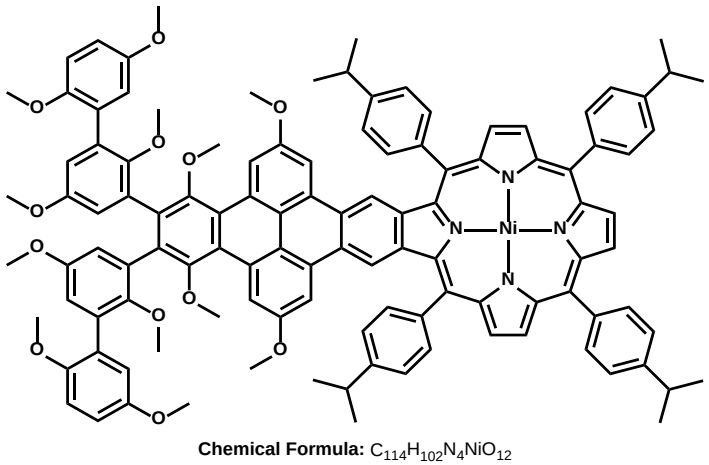

Figure 4.24: Potential structure of product S3 from the dimerization reaction.

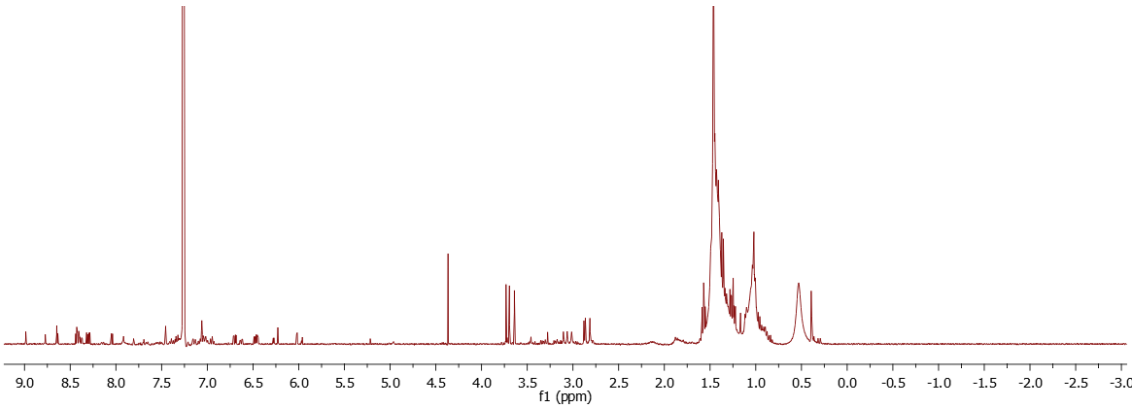

Figure 4.25: Prep TLC isolated S4 – ^{1}H NMR (500 MHz, $CDCl_3$)

4.4.3 UV-VIS

Note that all UV-VIS were done in dichloromethane; these spectra were displayed here to show that changes to the UV-VIS after the reaction did occur and generate different products

with different B and Q bands.

4.4.3.1 Monomer Product UV-VIS

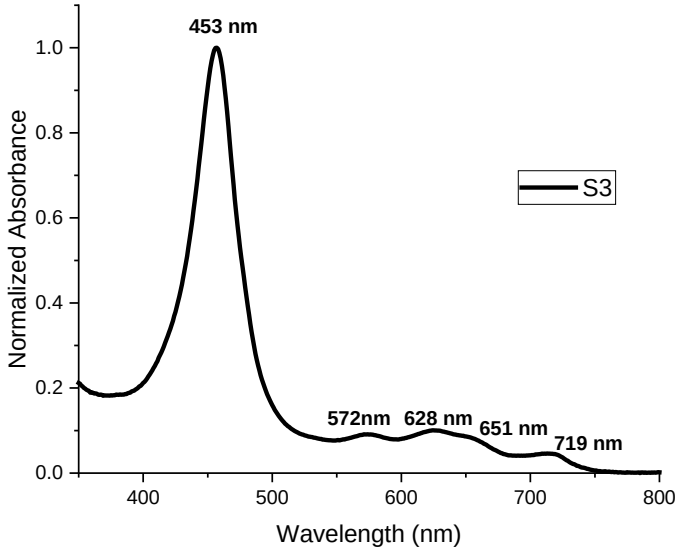

Figure 4.26: Isolated Product S3

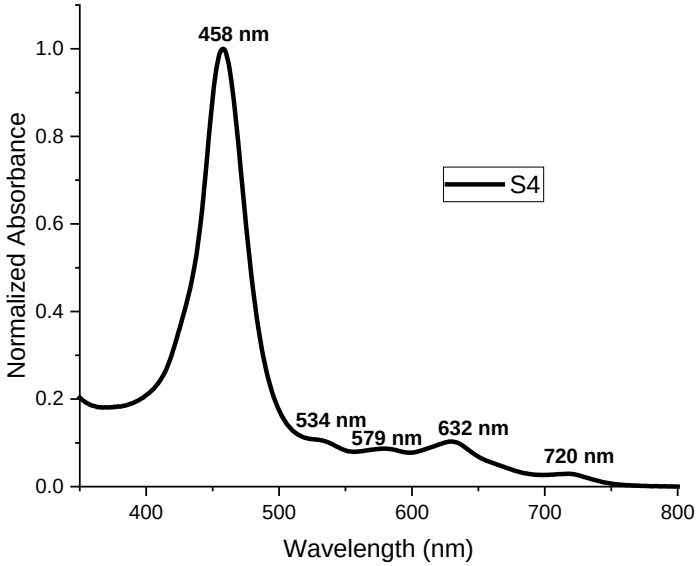

Figure 4.27: Isolated Product S4

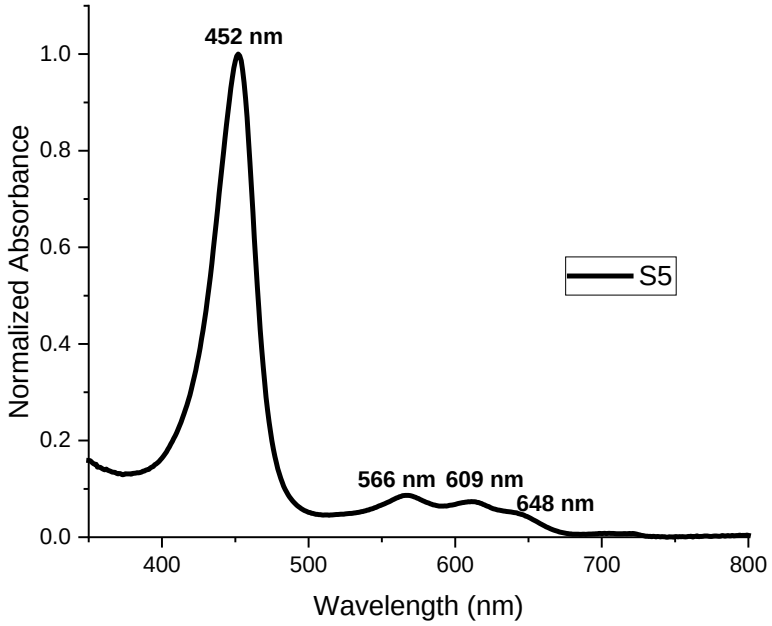

Figure 4.28: Isolated Product S5

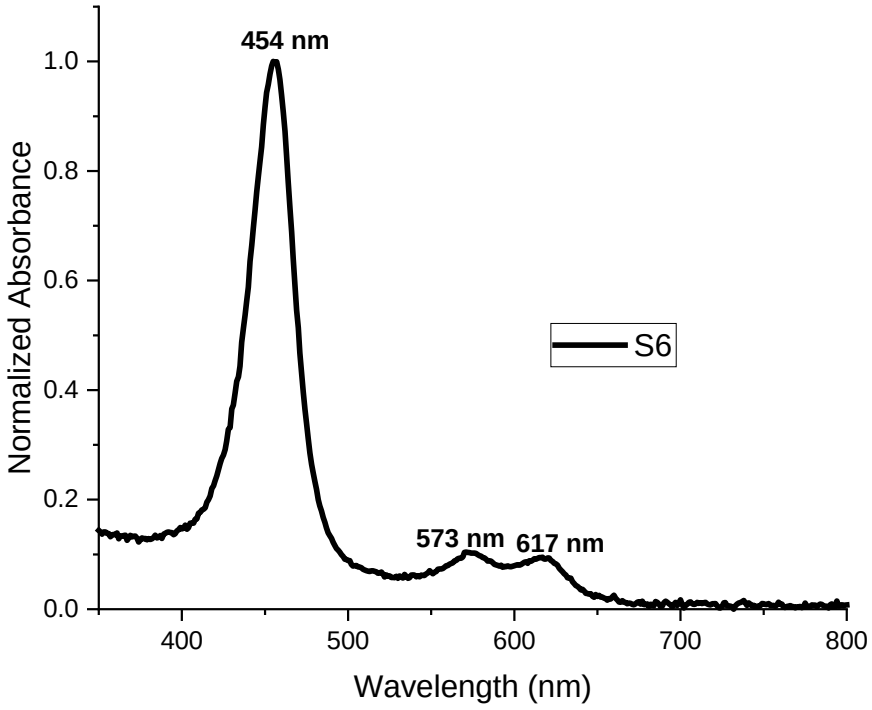

Figure 4.29: Isolated Product S6

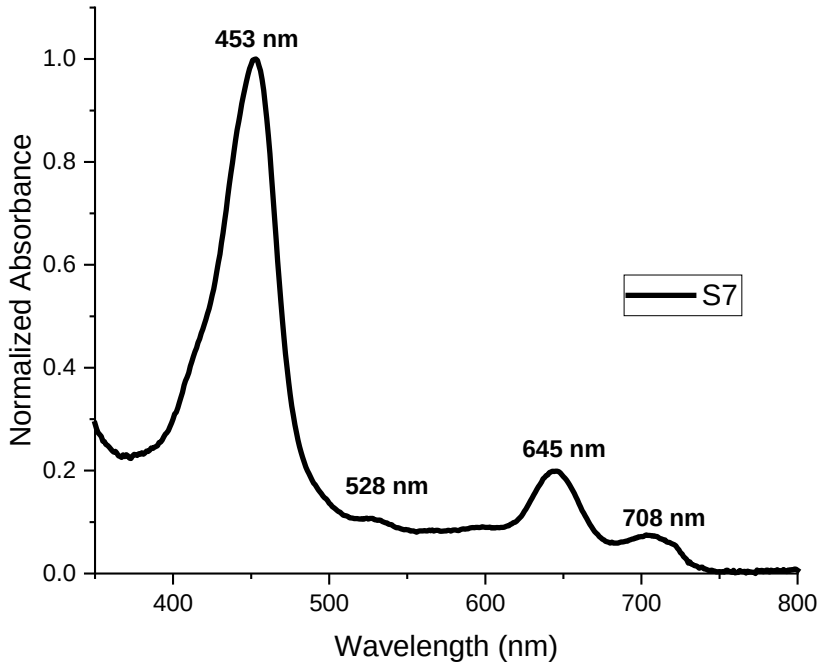

Figure 4.30 Isolated Product S7

4.4.3.2 Dimerization Product UV-VIS

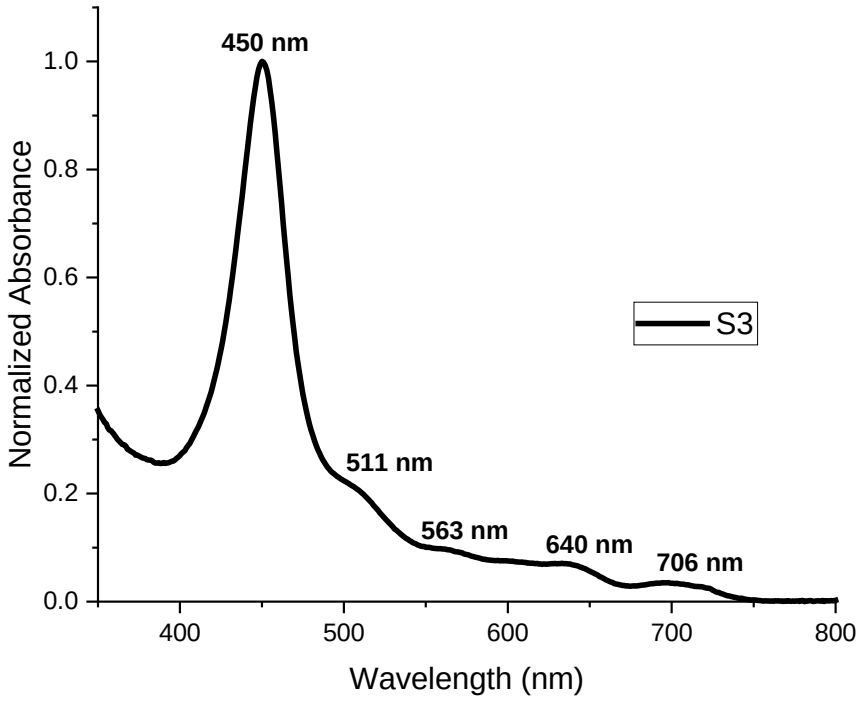

Figure 4.31: Isolated Product S3

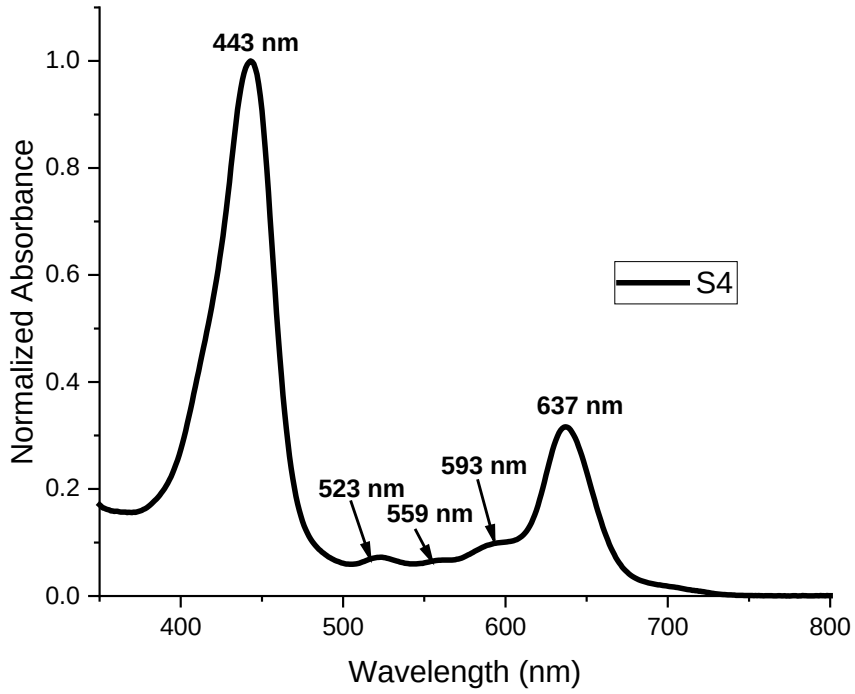

Figure 4.32: Isolated Product S4

4.5 References

[1] a) Kurpanik, A.; Matussek, M.; Szafraniec-Gorol, G.; Filapek, M.; Lodowski, P.; Marcol-Szumilas, B.; Ignasiak, W.; Małecki, J. G.; Machura, B.; Małecka, M.; Danikiewicz, W.; Pawlus, S.; Krompiec, S.; *Chemistry - A European Journal* **2020**, *26* (53), pp 12150–12157; b) Ruiz-Morales, Y. *Can. J. Chem.* **2009**, No. 87, pp 1280–1295; c) Kurpanik, A.; Matussek, M.; Lodowski, P.; Szafraniec-Gorol, G.; Krompiec, M.; Krompiec, S. *Molecules* **2020**, *25* (22), pp 34–37; d) Fort, E. H.; Donovan, P. M.; Scott, L. T. *J Am Chem Soc* **2009**, *131* (44), pp 16006–16007.

[2] Zhigalko, M. V.; Shishkin, O. V.; Gorb, L.; Leszczynski, J.; *J Mol Struct* **2004**, *693* (1–3), pp 153–159.

[3] a) Yang, M.; Zhou, H.; Li, Y.; Zhang, Q.; Li, J.; Zhang, C.; Zhou, C.; Yu, C. *J Mater Chem B* **2017**, *5* (32), pp 6572–6578; b) Lin, Y.; Zhan, X. *Acc Chem Res* **2016**, *49* (2), pp 175–183; c) Li, C.; Wonneberger, H. *Advanced Materials* **2012**, *24* (5), pp 613–636; d) Li, C.; Liu, M.; Pschirer, N. G.; Baumgarten, M.; Müllen, K. *Chem Rev* **2010**, *110* (11), pp 6817–6855; e) Huang, C.; Barlow, S.; Marder, S. R. *Journal of Organic Chemistry* **2011**, *76* (8), pp 2386–2407; f) Rao, K. V.; George, S. J. *Org Lett* **2010**, *12* (11), pp 2656–2659; g) Jiao, C.; Huang, K. W.; Guan, Z.; Xu, Q. H.; Wu, J. *Org Lett* **2010**, *12* (18), pp 4046–4049; h) Manning, S. J.; Bogen, W.; Kelly, L. A. *Journal of Organic Chemistry* **2011**, *76* (15), pp 6007–6013; i) Mahl, M.; Niyas, M. A.; Shoyama, K.; Würthner, F. *Nat Chem* **2022**, *14* (4),

pp 457–463; j) Zhou, C.; Li, W.; Chen, J.; Yang, M.; Li, Y.; Zhu, J.; Yu, C. *Analyst* **2014**, *139* (5), pp 1057–1062.

[4] a) Clar, E. Polycyclic Hydrocarbons; AP: London, 1964; b) Clar, E. The Aromatic Sextet, Wiley: New York, 1972, Vol. 101, p 1501; c) Clar, E.; Zander, M., *J. Chem. Soc*. 1957, pp 4616–4619; d) Solà, M. *Frontiers in Chemistry,* 1, 2013.

[5] Schmidt, W. Reactivity of Polycyclic Aromatic Hydrocarbons. 1. **1980**.

[6] a) Wassmann, T.; Seitsonen, A. P.; Saitta, A. M.; Lazzeri, M.; Mauri, F. *J Am Chem Soc* **2010**, *132* (10), pp 3440–3451; b) Misra, A.; Schmalz, T. G.; Klein, D. J. *Chem Inf Model* **2009**, *49* (12), pp 2670–2676; c) Strutyński, K.; Mateo-Alonso, A.; Melle-Franco, M. *Chemistry - A European Journal* **2020**, *26* (29), pp 6569–6575; d) Sun, Z.; Lee, S.; Park, K. H.; Zhu, X.; Zhang, W.; Zheng, B.; Hu, P.; Zeng, Z.; Das, S.; Li, Y.; Chi, C.; Li, R. W.; Huang, K. W.; Ding, J.; Kim, D.; Wu, J. *J Am Chem Soc* **2013**, *135* (48), pp 18229–18236; e) Portella, G.; Poater, J.; Solà, M. *J Phys Org Chem* **2005**, *18* (8), pp 785–791; f) Balaban, A. T.; Klein, D. J. *Journal of Physical Chemistry C* **2009**, *113* (44), pp 19123–19133; g) Houk, K. N.; Lee, P. S.; Nendel, M. *Journal of Organic Chemistry* **2001**, *66* (16), pp 5517–5521.

[7] a) Xu, Y.; Chu, Q.; Chen, D.; Fuentes, A. *Front Mech Eng* **2021**, *7*, 1–10; b) Böhme, T.; Simpson, C. D.; Müllen, K.; Rabe, J. P. *Chemistry - A European Journal* **2007**, *13* (26), pp 7349–7357; c) Hasobe, T. *Physical Chemistry Chemical Physics* **2010**, *12* (1), pp 44–57; d) Chen, T. A.; Liu, R. S. *Chemistry - A European Journal* **2011**, *17* (29), pp 8023–8027; e) Müller, M.; Kübel, C.; Müllen, K. *Chemistry - A European Journal* **1998**, *4* (11), pp 2099–2109; f) Watson, M. D.; Fechtenkötter, A.; Müllen, K. *Chem Rev* **2001**, *101* (5), pp 1267–1300; g) Dötz, F.; Brand, J. D.; Ito, S.; Gherghel, L.; Müllen, K. *J Am Chem Soc* **2000**, *122* (32), pp 7707–7717; h) Wu, J.; Pisula, W.; Müllen, K. *Chem Rev* **2007**, *107* (3), 718–747; i) Chen, T. A.; Liu, R. S. *Org Lett* **2011**, *13* (17), pp 4644–4647; j) Sun, Z.; Ye, Q.; Chi, C.; Wu, J. ***Chem. Soc. Rev.,*** 2012, 41, pp 7857—7889; k) Gutman, I.; Tomović, Ž.; Mü;llen, K.; Rabe, J. P. *Chem Phys Lett* **2004**, *397* (4–6), pp 412–416.

[8] Pijeat, J.; Chaussy, L.; Simoës, R.; Isopi, J.; Lauret, J. S.; Paolucci, F.; Marcaccio, M.; Campidelli, S. *ChemistryOpen* **2021**, *10* (10), pp 997–1003.

[9] a) Gutman, I.; Tomović, Ž.; Mü;llen, K.; Rabe, J. P. *Chemical Communications* **2009**, No. 9, pp 1028–1030; b) Yamane, O.; Sugiura, K. I.; Miyasaka, H.; Nakamura, K.; Fujimoto, T.; Nakamura, K.; Kaneda, T.; Sakata, Y.; Yamashita, M. *Chem Lett* **2004**, *33* (1), pp 40–41; c) Davis, N. K. S.; Thompson, A. L.; Anderson, H. L. *Org Lett* **2010**, *12* (9), pp 2124–2127; d) Davis, N. K. S.; Thompson, A. L.; Anderson, H. L. *J Am Chem Soc* **2011**, *133* (1), pp 30–31; e) Hasobe, T. *Physical Chemistry Chemical Physics* **2012**, *14* (46), pp 15975–15987; f) Arnold, B. D. P.; Gaete-holmes, R.; Johnson, A. W.; Smith, A. R. P.; Geoffrey, A. *J. Chem. Soc., Perkin Trans. 1* **1978**, 1660–1670; h) Kurotobi, K.; Kim, K. S.; Noh, S. B.; Kim, D.; Osuka, A. *Angewandte Chemie - International Edition* **2006**, *45* (24), pp 3944–3947.

[10] a) Richeter, S.; Jeandon, C.; Kyritsakas, N.; Ruppert, R.; Callot, H. J. *Journal of Organic Chemistry* **2003**, *68* (24), pp 9200–9208; b) Boyle, R. W.; Dolphin, D. *J. Chem. Soc., Chem. Commun.* **1994**, pp 2463–2464; c) Tsuda, A.; Furuta, H.; Osuka, A. *International Edition* **2000**, *39* (14), pp 2549–2552.

[11] a) Fukuda, T.; Makarova, E. A.; Luk'yanets, E. A.; Kobayashi, N. *Chemistry - A European Journal* **2004**, *10* (1), pp 117–133; b) Mettath, S.; Shibata, M.; Alderfer, J. L.; Senge, M. O.; Smith, K. M.; Rein, R.; Dougherty, T. J.; Pandey, R. K. *Journal of Organic Chemistry* **1998**, *63* (5), 1646–1656.

[12] Jiang, L.; Engle, J. T.; Sirk, L.; Hartley, C. S.; Ziegler, C. J.; Wang, H. *Journal of Organic Chemistry* **2011**, No. 8, pp 10–13.

[13] Gaussian 16, Revision C.01, Frisch, M. J.; Trucks, G. W.; Schlegel, H. B.; Scuseria, G. E.; Robb, M. A.; Cheeseman, J. R.; Scalmani, G.; Barone, V.; Petersson, G. A.; Nakatsuji, H.; Li, X.; Caricato, M.; Marenich, A. V.; Bloino, J.; Janesko, B. G.; Gomperts, R.; Mennucci, B.; Hratchian, H. P.; Ortiz, J. V.; Izmaylov, A. F.; Sonnenberg, J. L.; Williams-Young, D.; Ding, F.; Lipparini, F.; Egidi, F.; Goings, J.; Peng, B.; Petrone, A.; Henderson, T.; Ranasinghe, D.; Zakrzewski, V. G.; Gao, J.; Rega, N.; Zheng, G.; Liang, W.; Hada, M.; Ehara, M.; Toyota, K.; Fukuda, R.; Hasegawa, J.; Ishida, M.; Nakajima, T.; Honda, Y.; Kitao, O.; Nakai, H.; Vreven, T.; Throssell, K.; Montgomery, J. A., Jr.; Peralta, J. E.; Ogliaro, F.; Bearpark, M. J.; Heyd, J. J.; Brothers, E. N.; Kudin, K. N.; Staroverov, V. N.; Keith, T. A.; Kobayashi, R.; Normand, J.; Raghavachari, K.; Rendell, A. P.; Burant, J. C.; Iyengar, S. S.; Tomasi, J.; Cossi, M.; Millam, J. M.; Klene, M.; Adamo, C.; Cammi, R.; Ochterski, J. W.; Martin, R. L.; Morokuma, K.; Farkas, O.; Foresman, J. B.; Fox, D. J. Gaussian, Inc., Wallingford CT, 2016.

[14] Kingsbury, C. J.; Senge, M. O. *Coord Chem Rev* **2021**, *431*, 213760.

[15] a) Gershoni-Poranne, R.; Stanger, A. *Chemistry - A European Journal* **2014**, *20* (19), pp 5673–5688; b) Stanger, A. *Journal of Organic Chemistry* **2010**, *75* (7), pp 2281–2288.

[16] Yates, P.; Eaton P. *J. Am. Chem. Soc.* **1960**, *82* (16), pp 4436–4437.

CHAPTER 5

FUTURE WORKS AND CONCLUSION

5.1 Conclusion

A total of twenty-six new β,β'-π-extended porphyrins were synthesized and characterized in chapters 2 – 4 of this dissertation. These porphyrins were synthesized using the methodology developed in our laboratory [1] to extend one side of the porphyrin core which in turn extends the π-system of the porphyrin. NICS and AICD were used to characterize the aromaticity of the newly developed porphyrins. The NICS-scan method was employed for the first time on a porphyrin system which allowed for changes in aromatic character of the extended porphyrin to be observed.

In chapter 2, a total of eleven new β,β'-π-extended porphyrins were synthesized. The dithiophenyl-fused porphyrins were synthesized from a sequential reaction involving a Heck reaction, 6π-electron cyclization, and aromatization with vinylthiophenes (**2VTP** and **3VTP**). Bromination of the 5-position on the thiophene moiety of **2VTP** was done using a modified version of Aresenyan's[2] method and generated **2VTBr**. Scholl reactions were performed and generated the naphtho[1,2-*b*:3,4-*b'*]dithiophene-fused porphyrins (**F2VTP, F3VTP,** and **F2VTBr**). Zinc-inserted analogues of all but **F2VTP** were then prepared. In collaboration with Dr. Sergei Vinogradov at the University of Pennsylvania and Dr. Francis D'Souza at the University of North Texas, the fluorescence and fluorescence lifetimes of this new class of π-extended porphyrins were obtained. Crystal structures of **2VTP** and **3VTP** were obtained by Dr. Vladmir Nesterov at the University of North Texas. Computational aromaticity studies showed the effect of how the

position which the thiophene moiety is attached to the porphyrin core affects the aromatic character.

In chapter 3 a total of seven β,β'-π-extended porphyrin arrays were derived from naphthodithiophene-fused porphyrins reported in chapter 2 through a Sonogashira coupling reaction. Specifically, we have synthesized a freebase porphyrin dimer and trimer; zinc was then placed in dimer (**1ZnD** and **2ZnD**) and trimer (**1ZnT**, **2ZnT**, and **3ZnT**) porphyrin arrays. Additionally seven β,β'-π-extended porphyrin monomers were also synthesized through similar conditions reported in chapter 2 (**Br2VTP, FBr2VTP, ZnFBr2VTP**) and with a Sonogashira coupling reaction (**dPAp, mPEBp,** and **bPEBp**). A zinc inserted derivative of bPEBp was also done. Experimental characterization including UV-VIS and fluorescence spectroscopy have been done and further characterization is currently being carried out by our collaborator Dr. Francis D'Souza. Computational studies were also performed to evaluate the extent of the aromaticity, to obtain the HOMO-LUMO band gap, and to better understand the electronic properties of these new porphyrin oligomers.

In chapter 4 we revisited our previously reported triphenylene-fused porphyrin [3] and synthesized two freebase precursors (**3MSp** and **F3MSp**). Diels-Alder reactions with maleic anhydride, fumaronitrile, *p*-benzoquinone, and dimethyl malate were attempted with the triphenylene-fused porphyrin. Through NICS(1.7) studies we determined it was most likely a result of the chemical stability that triphenylene has; specifically the three π-sextets. An intermolecular Scholl reaction was also performed in an attempt to synthesize dimer and more-extended **NiF3MSp**. These reactions generated several products that were able to be isolated, but identification has proven difficult.

5.2 Future Works

The work presented in chapter 3 and chapter 4 of this dissertation still has some work that needs to be done. As mentioned earlier, further electrochemical and fluorescence studies of the porphyrin oligomers are currently being done by Dr. Francis D'Souza's group.

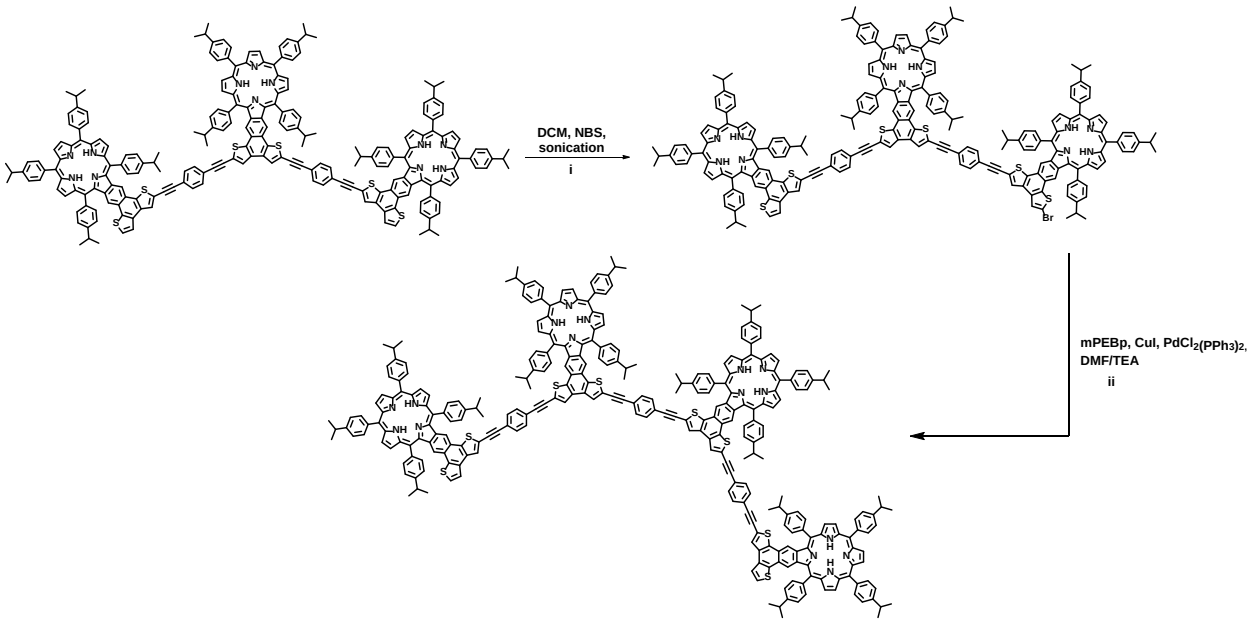

Scheme 5.1: Synthetic route for a porphyrin polymer derived from naphthodithiophene-fused porphyrins.

Although only dimer and trimer porphyrin arrays were designed and synthesized in this dissertation, extension of these arrays to create a porphyrin polymer is possible using a similar synthetic approach. Porphyrin polymers have applications in catalysis, in optoelectronics, and as sensors. [4] Scheme 5.1 provides a synthetic route for the porphyrin polymer through synthetic methods discussed in this dissertation. Since the 2- and 5- position of the thiophene ring is highly reactive, we theorize that bromination of these positions on both the dimer and trimer arrays should be viable. Once brominated, another Sonogashira coupling reaction could

be performed, which would allow us to control the length of the porphyrin polymer and potentially allow us to insert multiple metals into the porphyrin array (Figure 5.1).

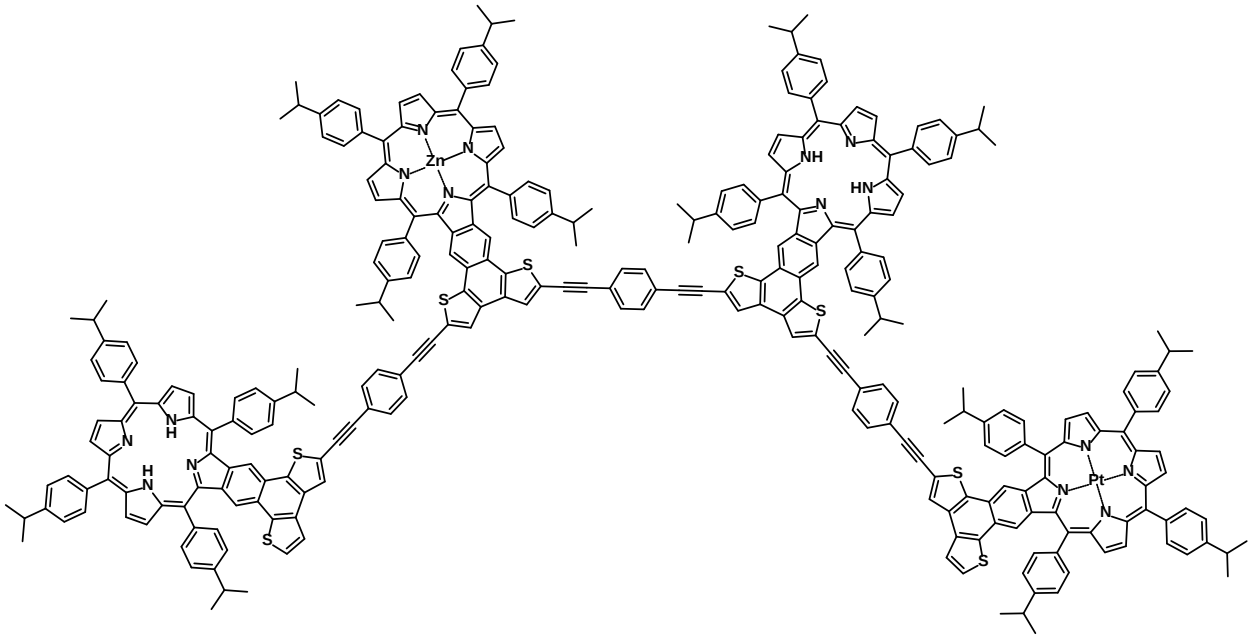

Figure 5.1: A porphyrin tetramer with zinc and platinum inserted.

Potential metals that could be inserted in a stepwise fashion includes platinum, nickel, manganese, cobalt, and iron. A similar approach could be done with the dimer. This synthetic methodology could potentially open the door for multi-metal porphyrin polymers which may generate interesting optoelectronic and catalytic properties.

The work in chapter 4 that needs to be done is far more extensive, but just as interesting as porphyrin polymers. Further work needs to be done in terms of characterization and identification of the products from the intermolecular Scholl. Work done by King [5] showed that in the presence of an electron donating group, Scholl reactions at the *meta*- position do not proceed. This suggests that any product isolated in chapter 4 must be *ortho*-substituted since the *para*-position is occupied by the methoxy group. However, there are some possible

directions that can be explored in the future (Scheme 5.2). One way we could do this is by using 4-methoxystyrene instead of 3-methoxystyrene.

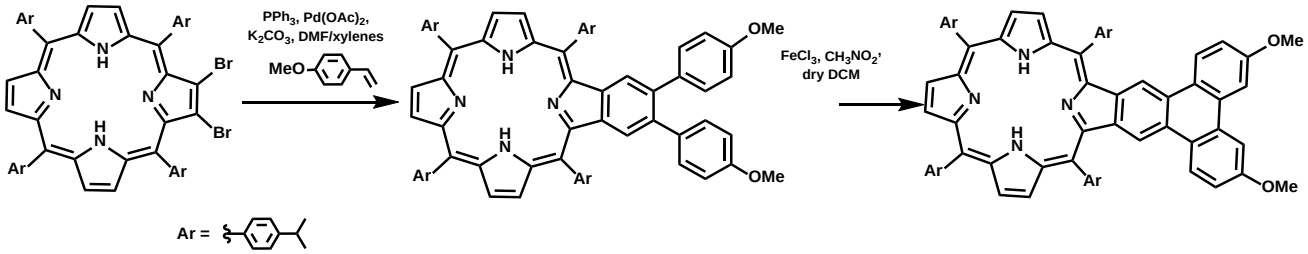

Scheme 5.2: Synthetic route for a nickel-inserted triphenylene fused porphyrin with 4-methoxystyrene.

Weakly electron-withdrawing groups like halides have been shown to couple aryl groups at the *meta*-position in hexabenzocorone. [6] Strong electron withdrawing such as cyano- and nitro- groups have not been found to work and therefore will not be explored. But a paper by Budniak [7] reported oxidative coupling between two 1-(trifluoromethyl)naphthalene in the presence of $Ag(SO_4)$. To successfully explore this option catalysts other than ferric chloride should be investigated. [8]

5.3 References

[1] Deshpande, R.; Jiang, L.; Schmidt, G.; Rakovan, J.; Wang, X.; Wheeler, K.; Wang, H. *Org Lett* **2009**, *11* (19), pp 4251–4253.

[2] Arsenyan, P.; Paegle, E.; Belyakov, S. *Tetrahedron Lett* **2010**, *51* (1), pp 205–208.

[3] Jiang, L.; Engle, J. T.; Sirk, L.; Hartley, C. S.; Ziegler, C. J.; Wang, H. *Journal of Organic Chemistry* **2011**, No. 8, pp 10–13.

[4] a) Ban, J.; Xu, S.; Pan, L. *J Mater Sci* **2021**, *56* (2), pp 1814–1826; b) Weyandt, E.; Leanza, L.; Capelli, R.; Pavan, G. M.; Vantomme, G.; Meijer, E. W. *Nat Commun* **2022**, *13* (1), pp 1–9; c) Lee, H.; Park, H.; Ryu, D. Y.; Jang, W. D. *Chem Soc Rev* **2023**, *52* (5), pp 1947–1974; d) Bansal, D.; Cardenas-Morcoso, D.; Boscher, N. *J Mater Chem A Mater* **2023**, pp 5188–5198.

[5] King, B. T.; Kroulík, J.; Robertson, C. R.; Rempala, P.; Hilton, C. L.; Korinek, J. D.; Gortari, L. M. *Journal of Organic Chemistry* **2007**, *72* (7), pp 2279–2288.

[6] a) Grzybowski, M.; Sadowski, B.; Butenschön, H.; Gryko, D. T. *Angewandte Chemie - International Edition* **2020**, *59* (8), pp 2998–3027; b) Nagase, M.; Kato, K.; Yagi, A.; Segawa, Y.; Itami, K. *Beilstein Journal of Organic Chemistry* **2020**, *16*, pp 391–397; c) Dodge, N. J.; Dodge, N. The Synthesis of Highly Substituted Aromatics and the Reaction of Alkene Pi Systems with Vinyl Cations, 2018.

[7] Budniak, A. K.; Masny, M.; Prezelj, K.; Grzeszkiewicz, M.; Gawraczyński, J.; Dobrzycki, Ł.; Cyrański, M. K.; Koźmiński, W.; Mazej, Z.; Fijałkowski, K. J.; Grochala, W.; Leszczyński, P. J. *New Journal of Chemistry* **2017**, *41* (19), pp 10742–10749.

[8] a) Stanojkovic, J.; William, R.; Zhang, Z.; Fernández, I.; Zhou, J.; Webster, R. D.; Stuparu, M. C. *Nat Commun* **2023**, *14* (1), pp 1–10; b) Beil, S. B.; Müller, T.; Sillart, S. B.; Franzmann, P.; Bomm, A.; Holtkamp, M.; Karst, U.; Schade, W.; Waldvogel, S. R. *Angewandte Chemie - International Edition* **2018**, *57* (9), pp 2450–2454; c) Schubert, M.; Leppin, J.; Wehming, K.; Schollmeyer, D.; Heinze, K.; Waldvogel, S. R. *Angewandte Chemie - International Edition* **2014**, *53* (9), pp 2494–2497; d) Waldvogel, S. R.; Trosiena, S. *Chemical Communications* **2012**, *48* (73), pp 9109–9119.

[9] a) Carboni, A.; Lindsey, V. J. Reactions of Tetrazines. *J, Am. Chem. Soc* **1959**, *81* (16), pp 553–4346; b) Oliveira, B. L.; Guo, Z.; Bernardes, G. J. L. *Chem Soc Rev* **2017**, *46* (16), pp 4895–4950.